

INFORMATION TO USERS

This manuscript has been reproduced from the microfilm master. UMI films the text directly from the original or copy submitted. Thus, some thesis and dissertation copies are in typewriter face, while others may be from any type of computer printer.

The quality of this reproduction is dependent upon the quality of the copy submitted. Broken or indistinct print, colored or poor quality illustrations and photographs, print bleedthrough, substandard margins, and improper alignment can adversely affect reproduction.

In the unlikely event that the author did not send UMI a complete manuscript and there are missing pages, these will be noted. Also, if unauthorized copyright material had to be removed, a note will indicate the deletion.

Oversize materials (e.g., maps, drawings, charts) are reproduced by sectioning the original, beginning at the upper left-hand corner and continuing from left to right in equal sections with small overlaps. Each original is also photographed in one exposure and is included in reduced form at the back of the book.

Photographs included in the original manuscript have been reproduced xerographically in this copy. Higher quality 6" x 9" black and white photographic prints are available for any photographs or illustrations appearing in this copy for an additional charge. Contact UMI directly to order.

UMI

A Bell & Howell Information Company
300 North Zeeb Road, Ann Arbor MI 48106-1346 USA
313/761-4700 800/521-0600

NOTE TO USERS

The original manuscript received by UMI contains pages with slanted print. Pages were microfilmed as received.

This reproduction is the best copy available

UMI

Multi - Metal Ion Exchange in Biosorption

Silke Schiewer

**Department of Chemical Engineering
McGill University, Montreal, Canada**



*A thesis submitted to the faculty of Graduate Studies and Research
in partial fulfillment of the requirements
of the degree of Doctor of Philosophy*

© Silke Schiewer, August 1996



National Library
of Canada

Acquisitions and
Bibliographic Services

395 Wellington Street
Ottawa ON K1A 0N4
Canada

Bibliothèque nationale
du Canada

Acquisitions et
services bibliographiques

395, rue Wellington
Ottawa ON K1A 0N4
Canada

Your file Votre référence

Our file Notre référence

The author has granted a non-exclusive licence allowing the National Library of Canada to reproduce, loan, distribute or sell copies of this thesis in microform, paper or electronic formats.

The author retains ownership of the copyright in this thesis. Neither the thesis nor substantial extracts from it may be printed or otherwise reproduced without the author's permission.

L'auteur a accordé une licence non exclusive permettant à la Bibliothèque nationale du Canada de reproduire, prêter, distribuer ou vendre des copies de cette thèse sous la forme de microfiche/film, de reproduction sur papier ou sur format électronique.

L'auteur conserve la propriété du droit d'auteur qui protège cette thèse. Ni la thèse ni des extraits substantiels de celle-ci ne doivent être imprimés ou autrement reproduits sans son autorisation.

0-612-30375-6

Canada

This thesis is dedicated

to my parents

who always tried to explain the underlying reasons
and did not just say "that's the way it is and has to be"

...and this goes well with the motto of my high school biology teacher:

"daß ich erkenne was die Welt im Innersten zusammen hält"

(Goethe, Faust I)

loosely and unpoetically translated:

"to recognize what keeps the world together at the basic level"

But then again, as Socrates, I know that I don't know anything...

ABSTRACT

Biosorption, a process of passive metal binding to biomass, may be used for purification of metal bearing effluents. This work investigates the binding of heavy metal ions (Cd, Cu, Zn), light metal ions (Ca, Na) and protons to biomass of the brown alga *Sargassum*.

The mechanism of metal binding was confirmed to be ion exchange. A novel multi-component sorption isotherm model for cation binding was derived to aid in predicting the biosorption performance of the new biosorbent. This model considers chemical binding to free sites on the biomass and ion exchange (1:2 stoichiometry for divalent ions). It is based on chemical equilibrium constants and assumes competition of all cations for the same binding sites. Two main binding sites (carboxyl and sulfate) were characterized in terms of their respective quantities and pK_a . Only two model parameters had to be determined for each metal cation (binding constants) and one additional parameter for each binding site (site quantity).

The two-site model successfully described metal and proton binding at different pH in mono- and di-metal systems. It was possible to predict the complete equilibrium sorption state, residual metal concentration in solution and metal uptake by the biosorbent, from the known initial state for varying amounts of biomass and different initial pH values.

In order to account for the effect of ionic strength and electrostatic attraction, the above mentioned biosorption model was expanded by incorporating a version of the Donnan model and / or a Gouy-Chapman double layer model. The charge density of the biomass was characterized and intrinsic binding constants were derived. Correlations to account for biosorbent particle swelling were established. For the specific case of linear increase of swelling with the number of free sites, an explicit sorption isotherm equation was derived that includes the Donnan model in an easy-to use-way.

Using the parameters obtained from pH titrations at different ionic strength, it was possible to predict the effect of ionic strength on Cd binding. The influence of Ca on Cd binding was predicted from experiments with Cd and Ca, respectively, in mono-metal systems.

RÉSUMÉ

Le procédé de biosorption, permettant de lier passivement le métal à la biomasse, peut être utilisé pour la purification des effluents contenant des métaux. Ce travail étudie la liaison d'ions de métaux lourds (Cd, Cu, Zn) et légers (Ca, Na) et de protons à une biomasse de l'algue brune *Sargassum*.

Le mécanisme de liaison du métal a été confirmé comme relevant de l'échange d'ions. Un nouveau modèle multivariable d'isotherme de sorption pour la liaison des cations a été établi pour prédire la performance de biosorption du nouveau biosorbant. Ce modèle tient compte de la liaison chimique avec des sites vacants de la biomasse et de l'échange d'ions (stoechiométrie 1:2 pour les ions divalents). Il est basé sur les constantes d'équilibre chimique et suppose que tous les cations sont en compétition pour les mêmes sites de liaison. Deux principaux sites de liaison (carboxyle et sulfate) ont été caractérisés en terme de quantités respectives et pK_a . Deux paramètres seulement ont dû être déterminés pour chaque cation métallique dans ce modèle (constantes de liaison) et un paramètre additionnel pour chaque site de liaison (quantité de sites).

Le modèle à deux sites a décrit avec succès la liaison d'un métal ou d'un proton, à différents pH, dans des systèmes à un ou deux métaux. Il a été possible de prédire complètement l'état d'équilibre de sorption, la concentration en métal résiduel dans la solution et la capture du métal par le biosorbant, à partir de l'état initial connu pour différentes quantités de biomasse et différentes valeurs initiales du pH.

Afin de tenir compte de la force ionique et de l'attraction électrostatique, le modèle de biosorption décrit ci-dessus a été élargi en y intégrant une version du modèle de Donnan et/ou un modèle à double barrière de Gouy-Chapman. La densité de charge de la biomasse a été établie et les constantes de liaison intrinsèques ont été calculées. Des corrélations pour tenir compte du gonflement des particules de biosorbant ont été déterminées. Dans le cas spécifique d'un accroissement linéaire du gonflement avec le nombre de sites libres, une équation explicite de l'isotherme de sorption a été calculée, incluant le modèle de Donnan d'une manière simple à utiliser.

En utilisant les paramètres obtenus par des mesures de pH pour différentes forces ioniques, il a été possible de prédire l'effet de la force ionique sur la capture de Cd. L'influence de Ca sur la capture de Cd a été prédit d'après des expériences avec Cd et Ca, respectivement, dans des systèmes monométalliques.

ACKNOWLEDGMENTS

First of all: thanks to Felix without whom I would not have come here to Montreal, to my parents for encouraging me in this endeavor (even though it meant me being a long time away from home) and to the DAAD (German Academic Exchange Service) whose generous scholarship made it all possible.

Then, thanks to Montreal for making me feel at home here. More specifically, thanks to all the friendly staff in Chemical Engineering (especially Jean Dumont).

Special thanks go to the people in my research group, I appreciated discussing biosorption (and other things) with them. Last not least, thanks to Professor B. Volesky, my research supervisor, for leaving me the freedom to explore what I found interesting and for his helpful criticisms and suggestions.

TABLE OF CONTENTS

Abstract / Résumé.....	i
Acknowledgments.....	iii
Table of Contents.....	iv
List of Figures.....	ix
List of Tables.....	xi
Symbols and Abbreviations.....	xii
1 Introduction	1
1.1 Need for Heavy Metal Removal Processes	1
1.2 Possible Applications of Biosorption	3
1.3 Objectives of this work	5
2 Literature Review	7
2.1 Biosorption	7
2.1.1 Characteristics of Biosorption.....	7
2.1.1.1 Biomass Types.....	7
2.1.1.2 Temperature Effect.....	7
2.1.1.3 Presence of Anions (Ligands).....	8
2.1.1.4 Influence of pH.....	10
2.1.1.5 Presence of other Cations.....	12
2.1.1.6 Equilibration time.....	12
2.1.2 Mechanism of Biosorption.....	13
2.1.2.1 Classification of Binding Mechanisms.....	13
2.1.2.2 Binding Forces.....	16
2.1.2.3 Ion Exchange versus Adsorption.....	17
2.1.2.4 Chemical versus Physical Binding.....	18
2.1.2.5 Binding Sites.....	19
2.1.2.6 Surface Charge.....	20
2.1.2.7 Location of the Accumulated Metal.....	21

2.2	Properties of <i>Sargassum</i>	22
2.2.1	Occurrence and Structure of <i>Sargassum</i>	22
2.2.1.1	Occurrence.....	22
2.2.1.2	Structure.....	22
2.2.1.3	The Cell Wall in Brown Algae.....	22
2.2.1.4	Main Biomolecules.....	24
2.2.2	Mannitol.....	25
2.2.3	Laminaran.....	25
2.2.4	Cellulose.....	26
2.2.5	Fucoidan.....	27
2.2.5.1	Structure and Properties.....	27
2.2.5.2	More complex sulfated polysaccharides.....	28
2.2.5.3	Location and Quantities.....	28
2.2.6	Alginic Acid.....	29
2.2.6.1	Structure.....	29
2.2.6.2	Location and Quantities.....	30
2.2.6.3	Properties.....	31
2.3	Properties of Metal Ions	33
2.3.1	Affinity Sequence Trends.....	33
2.3.2	Factors Influencing the Binding Strength.....	35
2.3.3	The Concept of Hard and Soft Acids and Bases.....	38
2.4	Modeling	42
2.4.1	Langmuir and Freundlich Isotherms.....	42
2.4.1.1	pH effect.....	44
2.4.1.2	Competing Ions in Solution.....	45
2.4.2	Ion Exchange Constants.....	46
2.4.3	Models Including Ionic Strength Effects.....	48
2.5	Conclusions	51

3	Materials and Methods	52
3.1	Choice of Conditions.....	52
3.2	Sorbent Materials.....	53
3.3	Cation Binding Experiments.....	53
3.3.1	General Methodology.....	53
3.3.2	Specific Conditions.....	54
3.3.2.1	Mono-Metal Systems at different pH.....	54
3.3.2.2	Multi-Metal Systems at different pH.....	54
3.3.2.3	Experimental and Modeling Errors.....	54
3.3.2.4	Proton Binding at Different Ionic Strengths.....	54
3.3.2.5	Metal and Proton Binding at Different Ionic Strengths	55
3.3.3	Experiments at Constant Concentration.....	55
3.3.4	Calculation of the Equilibrium Cation Binding.....	56
3.4	Swelling Experiments.....	58
3.5	Electrophoretic Mobility Determination.....	58
4	Results and Discussion	59
4.1	Mono-Metal Systems at different pH values.....	59
4.1.1	Preliminary Experiments.....	60
4.1.2	Influence of pH on Sorption.....	61
4.1.3	Change of pH.....	61
4.1.4	Relationship between Proton Release and Metal Binding.....	64
4.1.5	Surface Charge.....	68
4.1.6	Titrations.....	70
4.1.7	Sorption Isotherm Model.....	72
4.1.8	Determination of the Model Parameters.....	74
4.1.9	Modeling of Experimental Data.....	75
4.1.10	Influence of pH: Comparison Model / Langmuir Approach.....	77
4.1.11	Prediction of the Desorption Equilibrium.....	81
4.1.12	Section Summary.....	83
4.2	Multi-Metal Systems at different pH values.....	84
4.2.1	Multi-Component Sorption Isotherm Model.....	85
4.2.1.1	Comparison to Other Isotherms.....	86
4.2.1.2	Two Site Version Applied for <i>Sargassum</i>	87
4.2.2	Reaction Stoichiometry.....	88

4.2.3	Equilibrium Constants.....	91
4.2.3.1	Modeling Errors.....	91
4.2.3.2	Comparison of Constants from 1- and 2-Metal Systems.....	92
4.2.3.3	Number of Constants, Predictive Power.....	93
4.2.4	Influence of Metal Ion Concentrations on Binding: 3D plots.....	93
4.2.4.1	Affinity Sequence.....	94
4.2.4.2	Plateau Phenomenon.....	94
4.2.4.3	Dominant Site Speciation.....	97
4.2.5	Influence of Metal Ion Concentrations on Binding: 2D plot.....	97
4.2.6	Influence of Metal Concentration Ratio on Metal Binding.....	98
4.2.6.1	Effect on Total Metal Binding.....	99
4.2.6.2	Effect on Relative Metal Binding.....	100
4.2.7	pH Titration in the Presence of Two Metals.....	101
4.2.8	Using the Model if some Metals have Different q_{\max}	102
4.2.9	Section Summary.....	105
4.3	Experimental and Modeling Errors.....	106
4.3.1	Determination of the Error in Metal Binding.....	107
4.3.2	Evaluation of the Calibration Error.....	107
4.3.3	Drift and Fluctuation.....	109
4.3.4	Dilution.....	109
4.3.5	Total Error for the Concentration.....	109
4.3.6	Total Error for the Metal Uptake.....	110
4.3.7	Error Limitation through Choice of Initial Concentration.....	111
4.3.8	Comparison of the Experimental Error against the Model Error..	113
4.3.9	Section Summary.....	116
4.4	Proton Binding at Different Ionic Strengths.....	117
4.4.1	General Model Equations.....	118
4.4.2	Equations for the Donnan Model (DO).....	120
4.4.3	Equations for the Gouy-Chapman (GC) Model.....	123
4.4.4	Equations for the Plot of f versus $(\text{pH} - \text{pNa})$	127
4.4.5	Titration Curves.....	128
4.4.6	Variation of Apparent p^{CHK}	130
4.4.7	Plot of f versus $(\text{pH}-\text{pNa})$	132
4.4.8	Physical Behavior of Biosorbents.....	133

4.4.9	Model Parameters and Errors.....	135
4.4.9.1	Types of Models.....	135
4.4.9.2	Determination of Model Parameters.....	136
4.4.10	Modeling the Effect of Ionic Strength.....	139
4.4.11	Modeling Titration Curves.....	141
4.4.12	Modeling the Variation of Apparent p^{CHK}	142
4.4.13	Modeling the Plot of f versus $(pH-pNa)$	143
4.4.14	Section Summary.....	146
4.5	Metal & Proton Binding at Different Ionic Strengths	147
4.5.1	Model.....	148
4.5.1.1	Reactions and Isotherms.....	148
4.5.1.2	Donnan Model.....	149
4.5.1.3	Swelling of <i>Sargassum</i> Particles.....	150
4.5.1.4	Combination of Isotherm and Donnan Models.....	152
4.5.2	Specific Particle Volume.....	154
4.5.3	Modeling the Swelling of the Particle.....	154
4.5.4	Cadmium and Proton Binding.....	156
4.5.5	Stoichiometry Plot.....	159
4.5.6	Model Parameters and Fit.....	161
4.5.7	Modeling the Cadmium and Proton Binding.....	163
4.5.8	Change of Apparent Binding Constant.....	165
4.5.9	Importance of the Na Concentration for Cd Binding.....	165
4.5.10	Binding of Calcium in Mono-Metal Systems.....	168
4.5.11	Influence of Ca on Cd Binding in Di-Metal Systems.....	170
4.5.12	Comparison with Ca Competition Results in the Literature.....	172
4.5.13	Comparison with Donnan Models in the Literature.....	173
4.5.14	Section Summary.....	175
5	Summary, Original Contributions and Recommendations	176
5.1	Summary.....	176
5.2	Original Contributions.....	178
5.3	Recommendations for Future Research.....	179
6	References	180

LIST OF FIGURES

Figure		Page
1.2.1	Flow sheet of possible biosorption application.....	4
2.1.1	Biosorption mechanisms.....	14
2.2.1	The <i>Sargassum</i> plant.....	23
2.2.2	The chemical structure of mannitol.....	25
2.2.3	The chemical structure of laminaran.....	26
2.2.4	The chemical structure of cellulose.....	27
2.2.5	The chemical structure of fucoidan.....	28
2.2.6	The chemical structure of alginate.....	30
2.2.7	The "egg box" model for cation binding in alginate.....	32
2.3.1	Ionic and covalent bond character for different metals.....	39
2.3.2	Binding strength parameter for different metals.....	39
4.1.1	Kinetics of Cd biosorption at pH 4.5.....	60
4.1.2	Biosorption isotherm for metal binding at pH 4.5 and 2.5.....	62
4.1.3	Biosorption isotherm for metal and proton binding at pH 3.0.....	65
4.1.4	Binding of heavy and light metal ions as well as protons.....	67
4.1.5	Electrophoretic mobility and the change in binding of Cd and H.....	69
4.1.6	Binding of Cu and H for titration of protonated <i>Sargassum</i> biomass...	70
4.1.7	Isotherms of Cd for different pH values at low concentrations.....	80
4.1.8	Cd release and the final pH during desorption with HCl.....	81

Note:

The figure titles listed here are shortened,

the complete titles are to be found below the respective figures.

The same applies for the table titles in section VI.

4.2.1	Investigation of the reaction order for binding of divalent ions	90
4.2.2	Two-metal (Cd+Zn) biosorption: data and interpolated surface.....	95
4.2.3	Two-metal (Cd+Zn) biosorption: data and model predictions.....	96
4.2.4	Biosorption of Cd and Cu by <i>Sargassum</i> biomass at pH 4.5.....	98
4.2.5	Metal binding for different total metal concentrations.....	99
4.2.6	Titration of <i>Sargassum</i> biomass in the presence of Cu and Zn.....	101
4.2.7	Competitive binding of metal ions and metal-ligand complexes.....	104
4.3.1	Components of error in Cd concentration determination	108
4.3.2	Influence of sample dilution on error in determining [Cd].....	110
4.3.3	Influence of $[Cd]_f$ and $[Cd]_i$ on the error in determining M_q	111
4.3.4	Necessary $[Cd]_i$ and S/L ratio for the limitation of errors.....	112
4.3.5	Influence of pH and S/L on error in determining Cd uptake.....	113
4.3.6	Comparison of experimental errors and deviations data points - model..	114
4.4.1	Calculation algorithm for experimentally determined variables.....	119
4.4.2	Calculation algorithm for the Donnan model.....	123
4.4.3	Calculation algorithm for the Gouy-Chapman model.....	126
4.4.4	Titration of <i>Sargassum</i> biomass at different ionic strengths.....	128
4.4.5	Titration of Na-alginate at different ionic strengths.....	129
4.4.6	Variations of apparent p^{CHK} for titration of <i>Sargassum</i>	130
4.4.7	Variations of apparent p^{CHK} for titration of Na-alginate.....	131
4.4.8	Plot of f versus (pH-pNa) for titration of <i>Sargassum</i>	132
4.4.9	Plot of f versus (pH-pNa) for titration Na-alginate.....	133
4.4.10	Proton binding by <i>Sargassum</i> as a function of ionic strength.....	139
4.4.11	Variation of the apparent p^{CHK} for <i>Sargassum</i> with pH.....	140
4.4.12	Modeling f as a function of (pH-pNa) for Na-alginate.....	144
4.5.1	Calculation algorithm for the extended Donnan model.....	151
4.5.2	Swelling of the <i>Sargassum</i> particle.....	155
4.5.3	Cadmium and proton binding at different ionic strength and pH.....	157
4.5.4	Investigation of the reaction stoichiometry for divalent metal binding...	159
4.5.5	Change of binding sites occupation with increasing metal concentration	164
4.5.6	Change of apparent binding constants for Cd binding	166
4.5.7	Importance of Na in Cd binding by <i>Sargassum</i> biomass.....	167
4.5.8	Calcium and proton binding at different ionic strength levels.....	169
4.5.9	Cadmium binding in the two-metal system Cd-Ca.....	171

LIST OF TABLES

Table		Page
1.1.1	Drinking water standards and discharge limits for heavy metals.....	2
2.1.1	pK _a values of inorganic acids and acidic groups in biomolecules.....	20
2.2.1	Major polysaccharides in brown algae.....	24
2.3.1	Parameters characterizing the binding strength of metals.....	37
4.1.1	Model parameters for the 1-site and the 2-site sorption models.....	76
4.1.2	Parameters for the Langmuir model and mean square errors.....	78
4.1.3	Variation of Langmuir sorption parameters with pH.....	79
4.2.1	Model parameters and deviations model predictions - binding data.....	92
4.3.1	Parameters for the function describing the error in determining [M].....	108
4.3.2	Experimental errors in the determination of metal ion binding.....	115
4.4.1	Parameters for polyelectrolyte models.....	137
4.4.2	Absolute mean square errors of model in % of ¹ C.....	142
4.4.3	The concentration factor $\lambda_p - 1 = Q / n$	143
4.5.1	Regressions for stoichiometry test.....	160
4.5.2	Model parameters for mono-metal systems with Cd.....	162

SYMBOLS & ABBREVIATIONS

Variables*		default units unless stated otherwise
A_m	specific surface area per dry weight	m^2 / g
t_B	total amount of binding sites B	$mmol / g$
t_C	total amount of binding sites C	$mmol / g$
EPM	electrophoretic mobility	$m^2 s^{-1} Volt^{-1}$
F	Faraday constant = 96.5	$coul / mmol$
f	degree of ionization of binding site	-
I	ionic strength	$mmol / L$
${}^{ij}K$	equilibrium constant (formation) site i, cation j	$L / mmol$
m	dry weight of biomass	g
n	factor varying between 1 ($Q \gg 1$) and 2 ($Q \ll 0$)	-
P	constant related to surface charge density	$g mmol^{-0.5} L^{-0.5}$
$p^{ij}K, pX$	$-\log$ of ${}^{ij}K$ (in L/mol) or of concentration (in mol/L)	-
pK_a	$-\log$ of acid dissociation constant	-
Q	$= B / (V_m I)$ dimensionless constant	-
${}^j q$	binding (or uptake) of ion j (covalent + electrostatic)	$mequiv / g$
q_{max}	maximum binding at high concentration	$mequiv / g$
R	ideal gas constant = $8.315 \cdot 10^{-3}$	$V coul / (mmol K)$
r	radius of ion	$\text{Å} = 10^{-10} m$
S/L	$= m / V$, solid to liquid ratio	g / L
t_S	total amount of binding sites S	$mmol / g$
T	temperature	K
V	volume of solution	L
V_m	specific cation binding volume per dry weight	L / g

* Note: Only those terms that occur repeatedly throughout the thesis are listed here. Those which are only used in one specific chapter are explained in the text.

Preface: Symbols and Abbreviations

V_m	specific total particle volume per dry weight	L / g
Y_p	fitting parameter for P	$L^{0.5} \text{ mmol}^{-0.5}$
Y_{pv}	= Y_p / Y_v fitting parameter	$g^{0.5} \text{ mmol}^{-0.5} L^{-0.5}$
Y_v	fitting parameter for V_m	mL / g or mL / mequiv
z_j	charge of species j	-
x	electronegativity	-
γ	activity coefficient	-
ϵ	dielectric constant, for water at 25 °C = $6.95 \cdot 10^{-10}$	coul / (V m)
$1/\kappa$	double layer thickness	m
λ	concentration factor	-
σ	surface charge density	coul / m ²
ϕ	electrical potential	V
[X]	concentration (of molecular species X)	mmol / L
[ΣM]	sum of the concentrations of all divalent cations	mmol / L

Molecular Species:

B, C, S	free binding sites: general, carboxyl, sulfate
BH, CH, SH	binding site (general, carboxyl, sulfate) occupied by H
$BM_{1/2}$, $CM_{1/2}$, $SM_{1/2}$	metal ion - biomass complexes
B_2M , C_2M	metal ion - biomass complexes
H	protons
L	ligand
M	metal ion
Na	sodium
X	any ionic species

Indices

Position

add	added	bottom right
app	apparent	bottom right
B, C, S	of binding site B, C, S	top left
BH, CH, SH	of protonated binding site	top left
BM, CM, SM	of site occupied by metal ion	top left
cryst	of ion in crystal	bottom right
d	distance from charged surface	bottom right
des	desorbed	bottom right
exch	of ion exchange	bottom right
f	final	bottom right
H	of protons	top left
H	of acid	bottom right
hyd	of hydrated ion	bottom right
i	initial	bottom right
M, Cd, Cu, Zn, Ca	of specifically bound metal ion	top left
Na	of sodium	top left
p	average in particle	bottom right
s	at charged surface	bottom right
t	total	top left
x	for ion x	bottom right

Model abbreviations

CHEM	with equilibrium constant for Na binding
DORI	Donnan model assuming rigid particle
DOSW	Donnan model assuming particle swelling
GCRI	Gouy-Chapman model assuming rigid particle
GCSW	Gouy-Chapman model assuming particle swelling

1 INTRODUCTION

1.1 Need for Heavy Metal Removal Processes

Metal ions in the environment are bio-magnified in the food chain and accumulated in tissues. Cd for example has a half life of 10 - 30 years in the human body. Therefore, their toxic effects are especially pronounced in animals of higher trophic levels such as humans. Cd is one of the most toxic heavy metals, causing kidney damage, bone disease and cancer. The other two heavy metals in this study, Cu and Zn, are less toxic but they are among the most widely used metals (after Fe and Al). The main uses of Cd are in electroplating, batteries and pigments. Cu is mainly employed in the electrical industry (for example wires) and brass production. The major applications of Zn are galvanization and production of brass and other alloys. Mine tailings and effluents from non-ferrous metal industry are the major discharge sources of these three metals (Moore and Ramamoorthy, 1984; pp. 30-39, 50-51, 79, 182-185).

In the past decades, efficient biological treatment systems for sewage have been installed in most industrial countries. In most cases, however, there is no specific treatment for heavy metal removal. While the heavy metal ions may be accumulated in the sludge of biological treatment steps (which leads to a purification of the liquid phase)(Tien and Huang, 1991), the resulting sludges may carry a heavy freight of toxic metal ions. This restricts the otherwise beneficial use of the sludge as a fertilizer in agriculture and rather demands its incineration or disposal in landfills. While the former presents air-pollution and/or ash disposal problems, the latter is undesirable in terms of land requirements and costs involved for safe long-term storage.

Therefore, it would be beneficial to devise separate pre-treatment facilities for the elimination of heavy metals from wastewater, ideally at the site of those plants which discharge significant amounts of heavy metal ions with their wastewater. Such *on site* treatment of waste streams contributing a load of heavy metals would be more efficient than treating the large volumes of mixed (municipal) wastewater in a general sewage plant. Additionally, it appears reasonable from a policy viewpoint that the one who causes metal pollution should be responsible for its elimination. While enterprises are presently obliged

to meet certain discharge standards, drinking water quality is usually not attained since such treatment would be prohibitively costly (see Table 1.1.1).

Table 1.1.1:
Drinking water standards and discharge limits for heavy metals

Metal	Drinking water standards	Discharge Limits	
	WHO (WHO, 1993) (mg/L)	Canada (EPS, 1977) (mg/L)	USA (UNEP, 1989) (mg/L)
Cd	0.003 ^a	1.5	0.1
Cu	2 ^b	1	3.3
Cr	0.05 ^b	1	2.8
Ni	0.02 ^a	2	4
Pb	0.01 ^a	1.5	0.6
Zn	3 ^c	2	2.6

^a maximum acceptable concentration for health reasons

^b provisional value for health reasons

^c limit for aesthetic / consumer oriented reasons

Natural metal recycling in the environment makes metal recovery the only effective way of preventing heavy metals from poisoning the environment. If a cost effective way of 'completely' eliminating heavy metals could be found, this goal could be attainable. Current research activity in the field attempts to evaluate whether biosorption may eventually provide such an effective and economical treatment process alternative.

1.2 Possible Applications of Biosorption

The term biosorption commonly refers to the passive binding of metal ions or radioactive elements by living or dead biomass. It has to be distinguished from bioaccumulation which is usually understood to be an active, metabolically mediated process occurring in living organisms.

It has been known for decades that different brown algae bind trace metal ions, achieving concentration factors (compared to the sea water) of 1000 or even more (Black and Mitchell, 1952). The focus in early studies has been exclusively on the toxicological aspects of biosorption.

Recently, however, efforts are being made to develop this process into a technique for the treatment of toxic metal-bearing industrial effluents or for the recovery of precious elements from the sea water or from processing solutions. The process of gold sorption by *Sargassum* has been patented and the immobilized biosorbents AlgaSORB and AMT-BIOCLAIM have been made commercially available (Kuyucak, 1990b).

Biosorption removal of toxic heavy metals is especially suited as a 'polishing' step because it is possible to reach drinking water quality of the treated water (initial concentrations for example 1- 100 mg / L, final concentration < 0.01 - 0.1 mg / L), especially in packed-bed flow-through applications. In order to prevent unnecessarily rapid exhaustion of the sorption capacity when the metal concentrations in the wastewater to be treated are high (> 100 mg/L), it may be desirable to use a different technique such as precipitation or electrolytic recovery for pre-treatment (UNEP, 1989, p. 29).

The metal laden biosorbent can be incinerated and/or stored in landfills, having a rather small volume (compared to the wastewater) due to the high concentration of metals in the sorbent, which means the biosorption process serves to reduce the waste volume. Alternatively and preferably, regeneration of the biosorbent material is possible by metal desorption with for example acids or salt solutions. The resulting highly concentrated metal solution can be processed by other techniques such as precipitation or electro-winning to remove / concentrate the metal. The latter process may also enable the recuperation of the metal. The overall achievement of biosorption (complete adsorption + desorption cycle) is to concentrate the metal solution, possibly by a factor of ~ 100 or more. The process of biosorption and regeneration of the sorbent is illustrated in Figure 1.2.1.

Compared to conventional "polishing" techniques such as ion-exchange, activated carbon treatment or membrane technologies (electro-dialysis, reverse osmosis), the advantage of biosorption is not only that it can be operated under a broad range of conditions (pH, temperature) but especially that it may be economically attractive due to the

cheap raw materials that can be used as biosorbents (Kuyucak, 1990b). These include waste products from other industries (for example fermentation byproducts) or naturally abundant biomass (for example ubiquitous marine algae). Recent studies show that for certain types of seaweed biomass virtually no pre-treatment may be necessary: untreated *Sargassum* biomass was successfully applied in packed bed biosorption of Cu (Kratochvil, 1995). This means that the sole costs of the seaweed-based biosorbent may be only those for collection, transportation and drying.

In order to evaluate the expected performance of biosorption for treating typical wastewaters it would be desirable to predict how much metal could be bound under different operating process conditions. Computerized process simulations could effectively and economically provide this relevant information which is essential for the engineering process design and scale-up.

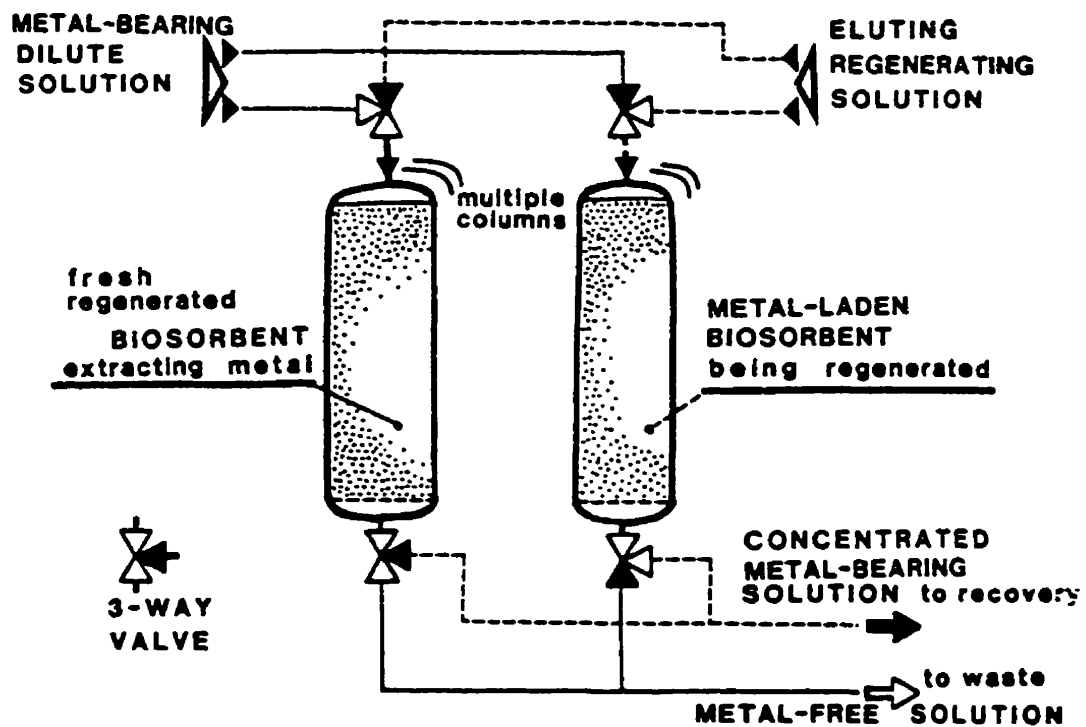


Figure 1.2.1 Flow sheet of possible biosorption application

(Volesky, 1990, p. 32)

1.3 Objectives of this work

This work focuses on modeling the biosorption binding equilibrium which is necessary as a prerequisite for all further work involving batch kinetic studies and column applications. In order to obtain a realistic model, it should conform with the binding mechanisms. Therefore the following aspects will be investigated in this work:

The metal binding mechanisms in *Sargassum* biomass will be identified.

- the stoichiometric amounts of ions exchanged are to be determined
- the relevance of electrostatic attraction in metal sequestration will be elucidated
- the main binding sites will be characterized in terms of their quantity and pK_a

The metal binding is to be quantified experimentally under varying conditions. The influence of the following parameters will be studied:

- Metal concentrations
- pH values
- Concentrations of other specifically bound cations
- Ionic strength values

The influence of the above-mentioned parameters on metal and proton binding will be modeled mathematically. The first model version is based on chemical equilibrium constants. The following steps are taken in the modeling:

- i Theory: formulation of suitable isotherm model
 - ii Determination of metal binding constants for isotherm model
 - iii Experimental verification of the model performance for proton binding at different metal concentrations as well as for predicting the effect of pH on metal binding and desorption in mono- or multi-metal systems
- Quantification of experimental and modeling error

An improvement of the model will be achieved by also including ionic strength effects. Similar to the above model, the individual steps are:

- i Theory: derivation of model equations for electrostatic effects
- ii Determination of intrinsic binding constants and the charge density including a characterization of the swelling behavior of *Sargassum* particles
- iii Quantification of the contribution of electrostatic binding to metal uptake
Experimental verification of the model performance for metal and proton binding at different ionic strengths

2 LITERATURE REVIEW

2.1 Biosorption

2.1.1 Characteristics of Biosorption

2.1.1.1 Biomass Types

A multitude of biomass types (Volesky and Holan, 1995), comprising fungal biomass (Kapoor and Viraraghavan, 1995), bacterial biomass (Mann, 1990), algae (Ferguson and Bubela, 1974; Holan and Volesky, 1994; Kuyucak and Volesky, 1990a), peat (Chen et al., 1990; Ho et al., 1995) etc. have been studied for their biosorption of metals. It was observed that not only the species but also the growth conditions such as the culture medium and the physiological state or age of the organism influence sorption performance (May, 1984, pp. 211-213; Tsezos, 1990). In several cases, the sorption by dead material proved to be more effective than that by living organisms (May, 1984, pp. 214-219; Tsezos, 1990). Marine brown algae have been found to be particularly effective in metal ion binding (Holan et al., 1993; Prasetyo, 1992), showing similar or better performance than industrial ion-exchange resins. Gold accumulation by the brown alga *Sargassum* can constitute up to 40 % of the alga's dry weight (Kuyucak and Volesky, 1989d). Further encouraging results with this sorbent material were obtained by Holan et al. (1993), Leusch et al. (1995) and Ramelow et al. (1992).

The particular amount of metal bound depends, however, not only on the chosen biosorbent but also on the type of metal ion, its concentration as well as on other physico-chemical factors (pH, ionic strength).

2.1.1.2 Temperature Effect

It was noted that the temperature can influence the sorption process. Kuyucak and Volesky (1989a) observed that the binding of Co by the brown alga *Ascophyllum nodosum* increased by 50 - 70 % when the temperature was raised from 4 to 23 °C. With further temperature increase to 40 °C the binding increased only slightly, whereas temperatures of 60 °C or more caused a change in the texture of the sorbent and a loss in the sorption capacity.

Simple physical sorption processes are generally exothermic, i.e. the equilibrium constant decreases with increasing temperature (Smith, 1981). This corresponds to the

observation of Haug and Smidsrod (1970) for exchange among alkaline earth metals in binding to alginate where the reaction was exothermic. For binding of Cu and release of alkaline earth metals, however, the reaction exhibited a positive enthalpy change (i.e. was endothermic), since the equilibrium constant rose with temperature. Haug and Smidsrod concluded that, since the enthalpy change was in this case unfavorable, the driving force must have been a large positive entropy change, possibly caused by a larger ordering effect of Cu (than Ca) upon the water molecules in the hydration sphere. This is illustrated by the following equation:

$$K = \exp\left(\frac{-\Delta G^\circ}{RT}\right) = \exp\left(\frac{-\Delta H^\circ + T\Delta S^\circ}{RT}\right) = \exp\left(\frac{-\Delta H^\circ}{RT}\right) \exp\left(\frac{\Delta S^\circ}{R}\right) \quad (1.1.1)$$

A rise in K with increasing T means that $\Delta H^\circ > 0$, i.e. that the reaction is endothermic. But since a reaction can only proceed when $\Delta G^\circ = \Delta H^\circ - T\Delta S^\circ < 0$, it follows that ΔS° must have been > 0 , i.e. the system's entropy must have increased.

Similar results were obtained by Weppen and Hornburg in calorimetric studies of the binding of divalent metal ions by potassium-saturated microbial biomass. The reactions were slightly endothermic and therefore driven by an increase in the entropy of the system. For most metals, the heat of reaction was constant, independent of the degree of site occupation. For Cu, however, the heat of reaction decreased with increasing degree of site occupation from 27 to 14 kJ/mol which may indicate the involvement of different binding sites or the formation of different types of Cu complexes with the biomass. For other heavy metals, the heat of reaction was between ~ 7-11 kJ/mol, for light metals between ~ 2.5-6 kJ/mol (Weppen and Hornburg, 1995).

Overall, however, the effect of temperature is small as compared to other influencing factors (Tsezos, 1990) (less than a factor of two in the study of Kuyucak and Volesky (1989a)). Greene and Darnall (1988) found that the distribution ratio (metal bound / metal in solution) for biosorption of Cd, Zn, Pb, Ni and Cu to *Spirulina* algae increased by only ~ 20% when the temperature was raised from 4 °C to 55 °C. Besides, possible application of biosorption is only reasonably to be expected in a rather narrow temperature range (~ 5 - 40 °C).

2.1.1.3 Presence of Anions (Ligands)

Theoretically, the presence of ligands (at levels which do not cause precipitation) can lead to (Tobin et al., 1987):

- 1) formation of complexes that have a higher affinity than the free metal ions to the sorbent, i.e. an enhancement of sorption;

- 2) formation of complexes that have a lower affinity than the free metal ions to the sorbent, i.e. a reduction of sorption;
- 3) interaction of anions with the biomass, changing the state of the active sites such that the binding is either enhanced or reduced.

There are no indications of the third kind of interaction reported in the biosorption literature. Additionally, these are unlikely to occur in brown algal biomass since the probable binding sites (negatively charged carboxyl and sulfate groups, see Section 2.2) are not expected to interact with anions such as sulfate, nitrate, etc.

It has been reported for sorption of Cu^{2+} and Ag^+ to inorganic oxide surfaces that metal binding at low pH was enhanced in the presence of certain ligands. Since the ligand itself was able to bind to the oxide and since a 1:1 stoichiometry of ligand and metal bound was noted, it was concluded that some metal complexes may bind more strongly than the respective free ions (Davis and Leckie, 1978). Negatively charged metal-EDTA complexes were bound to oxide surfaces (probably releasing OH^-), with sorption decreasing with increasing pH (Nowack et al., 1996).

Chen et al. (Chen et al., 1990) reports that up to 50 % of Cu binding by peat occurred as complexation of copper nitrate ($\text{Cu}(\text{NO}_3)_2$) with the binding sites. The remaining metal binding was due to ion exchange such that the overall charge neutrality was conserved. The data allow, however, also another interpretation: instead of up to half of the Cu being bound as $\text{Cu}(\text{NO}_3)_2$ and the other half as Cu^{2+} , up to 100 % could have been bound as $\text{Cu}(\text{NO}_3)^+$. Glaus et al. (Glaus et al., 1995) found that the binding of Co and uranyl (UO_2^{2+}) to humic substances could be modeled better when binding of metal-ligand (oxalate) complexes was included in the model.

In most cases of biosorption, however, metal binding tends to be reduced in the presence of ligands (exception: OH^-) (Greene et al., 1986a; Kuyucak and Volesky, 1989d; Tobin et al., 1987). This means that the biomass apparently has less affinity for many metal-ligand complexes than for free hydrated metal ions. Therefore, the influence of ligands in solution can be understood as a competition with the biomass for binding of the metal ions.

This effect is, however, not very pronounced unless these anions show a strong complexing power for the metal ions of interest (for example EDTA) (Ramelow et al., 1992; Tobin et al., 1987): Tobin et al. (1987) found that even by large excess (≥ 10 times) of the ligands glutamate, sulfate, phosphate, carbonate or chloride the maximum reduction of Cd binding to *Rhizopus arrhizus* biomass was only 21 %, while EDTA at only 1.5 times excess yielded a ~ 100 % inhibition of metal binding. The addition of 0.1 % EDTA

resulted in > 90 % reduction of binding for most cases of Cd, Cu, Zn and Pb biosorption by seaweeds (also *Sargassum*) (Ramelow et al., 1992).

Since significant concentrations of strong complexing agents are rare in typical metal-bearing industrial effluents, the effect of the presence of ligands is of secondary importance.

2.1.1.4 Influence of pH

Of great importance in sorption is the pH value of the solution. It is commonly agreed that the sorption of metal cations (Cd, Cu, Zn, Pb, Ni, Mn, Al, Co) increases with increasing pH (Darnall et al., 1986; Ferguson and Bubela, 1974; Greene et al., 1987; Holan et al., 1993; Kuyucak and Volesky, 1989a; Ramelow et al., 1992; Tsezos and Volesky, 1981). Only those metal ions which can occur as negatively charged complexes or that have a strong "b" character (i.e. tendency to form strong covalent bonds, see Section 2.3) such as Ag, Hg or Au (for example as tetrachloroaurate), may show either a decrease in binding with increasing pH or may have no significant pH effect at all (Greene et al., 1986a; Greene et al., 1987; Ramelow et al., 1992). There are three ways how the pH can influence metal biosorption:

First, the state of the active sites may be changed. When the binding groups are acidic, the availability of free sites depends on pH: at lower pH the active sites are protonated and therefore competition between protons and metal ions for the sorption site occurs (Greene et al., 1987; Tobin et al., 1984). At low enough pH, virtually all sites become protonated and complete desorption of the bound metal ions is possible (Aldor et al., 1995), which is why acid treatment is a method for metal elution and regeneration of the sorbent material. Decreasing the pH value by 2 units can in some cases result in a ~ 90 % reduction of metal binding (Aldor et al., 1995; Darnall et al., 1986; Ferguson and Bubela, 1974; Greene et al., 1987; Ramelow et al., 1992).

Second, extreme pH values, as they are employed in the regeneration (desorption) of the sorbent, may damage the structure of the biosorbent material. Microscopic observations have shown distorted cells; significant weight loss and decrease in the sorption capacity have been observed (Kuyucak and Volesky, 1989b).

Third, the speciation of the metal in solution is pH dependent. Whereas metals in aqueous solutions occur as hydrated cations in solvation shells when the pH is low, hydroxides may form at higher pH, especially for cations of high charge and small size (Baes and Mesmer, 1976, p. 397; Morel, 1983, p. 237-266; Stumm and Morgan, 1970, pp. 238-256). The formation of metal oxide and hydroxide complexes and precipitates is often called hydrolysis (i.e. decomposition or conversion by water)(Baes and Mesmer,

1976, pp. 1-7). The influence of pH dependent uranium solution speciation was suspected to be responsible for the variation of uranium binding with pH. While uranium occurs as UO_2^{2+} at pH 2, it is present as a negatively charged hydrolyzed species at pH 4 and above (Tsezos and Volesky, 1981). This can explain the lower sorption of uranium at low pH for anion exchange resins.

Adsorption depends not only on the attraction of the sorbate to the solid surface but also on its lyophobic behavior (Pagenkopf, 1978, pp. 161-167). This means, sorption increases with decreasing solubility (see Section 2.1.2). Since the solubility of many metal complexes in solution decreases with increasing pH, this provides an additional possible explanation why sorption increases with increasing pH. Especially in the narrow pH range where the metal ions are hydrolyzed, sorption is enhanced, so that even a charge reversal of the surface to positive values can occur (Pagenkopf, 1978, p. 228; Collins and Stotzky, 1992). Further possible explanations of increasing sorption with increasing pH are that hydrolyzed species have a lesser degree of hydration, i.e. less energy is necessary for removal or reorientation of the hydrated water molecules upon binding. Furthermore, OH shows affinity for some sorbents (Stumm and Morgan, 1970, pp. 474).

With further increase of pH the solubility of metal complexes decreases enough for precipitation to occur. Although precipitation may contribute to the overall removal of metals from solution (and therefore be desirable for metal removal applications), it renders the study of the biosorptive binding more difficult. For scientific purposes it is therefore recommendable to study biosorption at pH values where precipitation does not occur.

Furthermore, there is not only an influence of pH on biosorption but the reverse is also the case: the pH of the solution can be changed as a result of biosorption. An increase of pH during sorption was reported by Tsezos and Volesky (1981) who explained it as a process of reverse hydrolysis of the metal ion which released OH^- groups. Kuyucak and Volesky (1989a) claimed that the dissolution of cytoplasmic components or the release of carbonate ions from *Ascophyllum* biomass could perhaps be responsible for the observed increase in solution pH. It is, however, more likely that this was caused by a binding of the protons from solution during the course of a release of the ionic species that initially were present on the algal biomass (compare section 4.1.3). Holan et al.(1993) observed a decrease from pH 4.9 to pH 3.5 in sorption experiments with crosslinked *A. nodosum*, without giving an explanation for that phenomenon. Since the biomass was crosslinked under acidic conditions, it appears probable that an excess of protons was released. Crist et al. (1981) observed a decrease of pH during sorption which was explained by proton release. The freshwater algae used had been washed at pH 3 - 3.5 for partial protonation.

2.1.1.5 Presence of other Cations

Other sorbable ions in the solution may compete with the metal ion of interest for sorption sites. The binding of this metal ion is then decreased. The amount of inhibition depends on the binding strength of the respective ions to the biomass.

For example, Mg and Na are effective in competing with Zn for binding sites of green algae (90 % reduction of Zn binding at 200 mM NaCl or Mg(NO₃)₂), but they interfere less strongly with the binding of Pb or Cu (< 50 % reduction of Pb or Cu binding at 200 mM NaCl or Mg(NO₃)₂) (Ferguson and Bubela, 1974).

The inhibition by alkali metals (K, Na) of heavy metal ion binding to microbial biomass was much less pronounced than the inhibition by heavy metals (Zn, Cu, Fe) of uranium or radium binding (Tsezos, 1990).

For *Rhizopus arrhizus* biomass, the presence of uranium reduced the binding of Cd, Zn and Ag more strongly than vice versa; especially Ag was a weak competitor, but nevertheless its binding was unaffected by the presence of Na (Tobin, 1988).

In the sorption of Cd, Cu and Zn on formaldehyde-crosslinked biomass of the brown alga *Ascophyllum nodosum*, the presence of each ion reduced the binding of each other ion, with Zn being the weakest binding ion and Cu the most strongly binding one among those three cations (Chong and Volesky, 1995).

From the different literature sources it can be generally concluded that the light metals (alkaline and alkaline earth metals) bind less strongly than the heavy metal ions or radioactive elements. Therefore, the former do not strongly interfere with the binding of the latter. There are indications that among the heavy metals, Zn binds rather weakly and its binding is therefore more strongly affected by other ions.

In order to understand the reasons why some ions bind more strongly than others it is useful to look at the properties of different metals which are discussed in Section 2.3. Such knowledge can also serve to estimate how strongly an ion may bind that was not yet investigated. This knowledge serves as a basis to better understanding of the metal binding mechanism.

2.1.1.6 Equilibration time

In the literature it is reported that most of the sorption is completed in less than one hour. Greene et al. (1986b) observed that 90 % of the uranium binding by *Chlorella* was achieved in 10 minutes. Ninety percent of the equilibrium binding of Cd by *Ascophyllum nodosum* was reached in 30 min., the equilibrium was attained after ~ 300 min. (Volesky and Prasetyo, 1994). Recent investigations of Yang and Volesky showed that 50 % of the Cd desorption from *Sargassum* was achieved in less than three minutes and that the

equilibrium was reached in 30 minutes (Yang and Volesky, 1996). Since the actual chemical reaction of metal ion binding to aquatic particles (oxides and biological particles) is a fast phenomenon (Stumm et al., 1994, pp. 78-80; Hering and Morel, 1990, pp. 145-171), the mass transfer resistance determines the time necessary to reach equilibrium.

2.1.2 Mechanism of Biosorption

The effect of any of the above-mentioned influencing factors can be best quantitatively estimated when the mechanism of biosorption for different ions is known and when a mechanism-oriented mathematical model is used for predicting the effect of these factors.

2.1.2.1 Classification of Binding Mechanisms

The metal binding in biosorption has been attributed to a number of different sequestering mechanisms such as complexation, coordination, chelation, adsorption, ion exchange or micro-precipitation (as metal or metal complex) (Volesky, 1990). It is a recognized fact that a combination of several mechanisms, each functioning independently, can contribute to the overall metal uptake. In the studies of biosorption conducted so far very little attention has been paid to examination of a well defined metal uptake (by a specific mechanism) as opposed to the overall uptake where several types of sequestration may be taking place simultaneously. Systematic understanding of the metal uptake mechanisms and their relationships may greatly clarify the otherwise confusing broad definition of biosorption mechanisms in the literature.

For example, some mechanisms can be 'sub-mechanisms' of other 'overall' mechanisms. The claim of ion exchange metal binding mechanism for a specific system may not necessarily be contradictory of reports of chelation to be the relevant mechanism. The overall mechanism of ion exchange can be based on the 'sub-mechanism' of complexation. This means one complexed ion exchanges against another one.

A systematic presentation of the relationships between different mechanisms is compiled in Figure 2.1.1. The classification of bond types (bottom part of diagram) as described by Myers (Myers, 1991, pp. 39-67) was used as well as information on sorption processes from Westall (Westall, 1987, pp. 3-7) and Pagenkopf (Pagenkopf, 1978, p. 162).

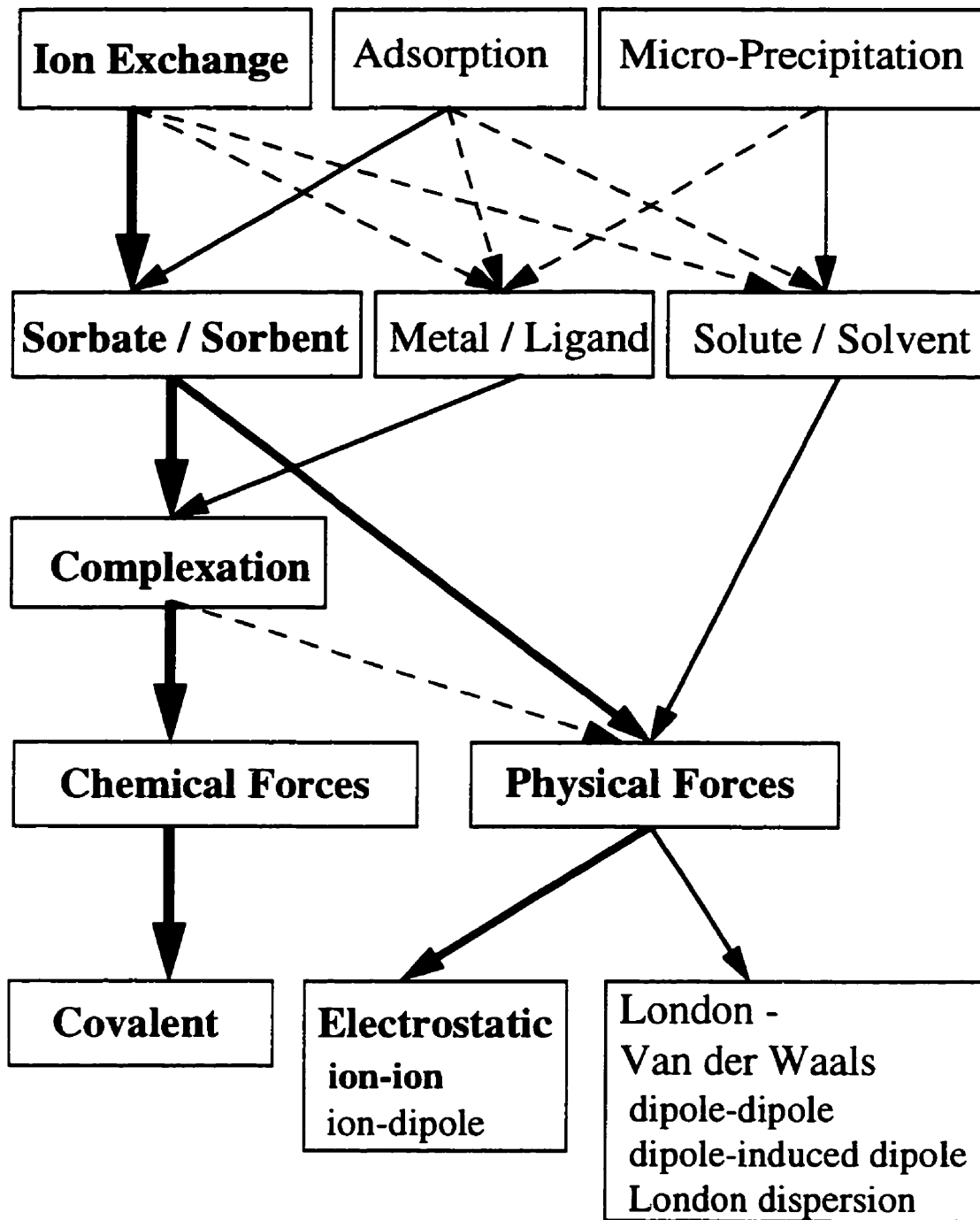


Figure 2.1.1 Biosorption mechanisms

Mechanisms probably important in biosorption by *Sargassum* biomass are printed bold.

Dashed lines indicate relations of secondary importance

In the context of this work, the term adsorption refers to binding of a solute (usually: metal cation) to 'free' sites which are previously not occupied by another cation. If the sites are initially occupied by another cation (regardless of the sub-mechanism, i.e. whether for example covalent or electrostatic binding is involved) and if this second ion is released upon the binding of the first ion, then the term ion exchange is used.

Micro-precipitation is the deposition of electrically neutral material (metal or metal salt) at the surface of the biomass and does not necessarily involve a bond between the biomass and the deposited layer. Micro-precipitation may, however, be facilitated by initial binding of metal ions to reactive sites of the biomass, which serves as a nucleation site for further precipitation (Mayers and Beveridge, 1989). This process is not limited to a monolayer (or saturation of sites): cells can accumulate several times their dry weight in metal (Macaskie et al., 1987; Macaskie et al., 1992). Micro-precipitation is based on interactions between the solute (dissolved solid) and the solvent and occurs when the local solubility is exceeded.

Ion-exchange and adsorption can be the result of three different interactions (which can act in combination): the main contribution for free metal ions (which are highly soluble in water) is usually attraction of the sorbate (metal ion) to the sorbent (biomass). In the case of binding of metal-ligand complexes or in the case of ligand exchange (where the metal ion in solution is complexed with a ligand which has to be released when the metal ion is bound to the biosorbent (Westall, 1987)), interactions between ligands and metal cations have to be taken into account. Additionally, hydrophobic (or generally: lyophobic) expulsion (which is an interaction between sorbate and solution) may also play a role (Pagenkopf, 1978, pp. 161-167; Westall, 1987, pp. 4-7), especially in the adsorption of organic dipoles and large organic ions because of their low affinity to the aqueous phase (Stumm and Morgan, 1970, pp. 450-454). Among inorganic ions, the less hydrated ones are more readily accumulated at the interface (Stumm and Morgan, 1970, pp. 450-454). The hydration effect is further discussed in Section 2.3.2.

Complexation plays an important role both in metal-ligand and in sorbate-sorbent interaction (Westall, 1987, pp. 4-7). A complex (also referred to as a coordination compound) is a poly-atomic molecule that consists of one or more (then: poly-nuclear complex) central atoms (usually metal cations) surrounded by ligands (other atoms or groups, usually of negative or neutral charge) that are attached to it. Complexes can be neutral or positively or negatively charged. The number of coordinating atoms (in the ligands) which are directly attached to the central atom is called coordination number and can be larger than the valence of the central atom (most common coordination numbers: 4 and 6, but 2 and 8 also occur frequently). If one ligand is attached to the central atom

through two or more coordinating atoms, then the complex is called chelate. The bonds between the central atom and the coordinated groups can arise from principal or auxiliary valence forces (Cahn and Dermer, 1979, p. 17; Fernelius, 1953, pp. 9-15).

2.1.2.2 Binding Forces

In general, the forces between atoms or molecules can be classified into chemical and physical ones. Chemical forces extend over very short distances (0.1 - 0.2 nm) (Myers, 1991, pp. 39). This type of bond is rather strong: Stumm and Morgan (1970, p. 447) reports an energy of $\gg 40$ kJ / mole, Myers (1991, p. 39) 150 - 900 kJ / mole, Smith (1981, p. 312) for chemi-sorption 20 - 400 kJ / mole and Pagenkopf (1978, p 162) 40-400 kJ / mol. Covalent bonds are formed by merging electron clouds such that a non-ionic molecule is formed. These bonds are directional (characteristic bond angles and lengths) and localized (Myers, 1991, p. 39).

Physical forces can be subdivided into electrostatic and London - van der Waals forces (Myers, 1991, p. 41). The energy of physi-sorption is reported as 2-20 kJ / mol and 20 - 40 kJ/mol by Smith (Smith, 1981, p. 311) and Pagenkopf (Pagenkopf, 1978, p. 162), respectively. In the resulting bonds, the electrons stay in their original systems. Electrostatic (or coulombic) forces between ions or between ions and dipoles extend over a long range and are the strongest among the physical bonds (Myers, 1991, p. 41) with energies $\gg 40$ kJ / mole (Stumm and Morgan, 1970, p. 447). The interaction is repulsive for ion charges of the same sign and attractive for unlike charges. The magnitude of the force is proportional to the charge of each ion and inversely proportional to the square of the distance between the ions.

London - van der Waals forces can be divided into three categories: dipole-dipole interactions (creating orientational energy), dipole-induced dipole interactions and the London dispersion force (Myers, 1991, p. 54). The first two are closely related to coulombic forces while the last one is of quantum-mechanical nature and acts over a long range of up to ~ 10 nm (Myers, 1991, pp. 54, 57-58). The energy of the dispersion force (8 - 40 kJ / mol) is larger than the one of orientational or induced dipole (or: polarization (Westall, 1987, p. 6)) energy (< 8 kJ / mol)(Stumm and Morgan, 1970, p. 447). An example of untypical strong (almost ionic) dipole interactions is hydrogen bonding (which may even display some covalent bond character). It occurs between molecules in which H is bound to a very electronegative atom such as O (for example in H₂O) (Russell, 1980, pp. 314-316).

The mechanisms and forces which are probably (as pointed out below) the most important ones in the case of metal binding by brown algal biomass are indicated in bold

type in Figure 2.1.1: ion-exchange (for which the driving force is the affinity of the sorbate (metal ion) to the sorbent (biomass)) based complexation by chemical covalent bonds, supported by physical electrostatic interactions between positively charged metal ions and negatively charged biomass.

2.1.2.3 Ion Exchange versus Adsorption

There have been some indications that ion exchange plays an important role in metal ion sorption by algal biomass. Kuyucak and Volesky (1989c) noted that the amount of ions (K, Na, Ca, Mg) released from the marine brown alga *Ascophyllum nodosum* was much more pronounced in metal (Co) bearing than in metal free solutions. A linear correlation between Ca release and Co uptake (2:3) was found when the biomass had been previously washed with CaCl and HCl. It was concluded that ion exchange was responsible for the metal binding (Kuyucak and Volesky, 1989c). If ion exchange was responsible, an exchange ratio of 1:1 should, however, be expected for two divalent ions such as Ca and Co. Since it can be expected that some sites would have been protonated due to the pre-treatment with a CaCl and HCl mixture and since some proton release was noticed, it would have been more appropriate to relate the Co binding to the sum of Ca and H released (everything in mequiv, not mol). This would have led to an exchange ratio much closer to 1:1.

Crist et al. (1990) included protons in the quantitative study of ions (Ca, Mg, H) released during metal (Cu) uptake by the freshwater alga *Vaucheria* and found that the amount of divalent metal ions taken up equaled the amount of other divalent ions plus protons released (in mequiv terms).

Treen et al. report that in column application of *Rhizopus* biosorbent two moles of protons were released for one mole of uranyl sequestered (Treen-Sears et al., 1984).

According to Chen et al., the Cu binding to peat at low metal concentrations was predominantly ion exchange (with H, Ca, Mg) while at higher concentrations binding of copper nitrate complexes occurred. The latter mechanism was dominant above 6 mM of Cu (Chen et al., 1990).

Literature observations regarding desorption can, in many cases, also be interpreted in terms of ion exchange. Such 'competitive' desorption can be achieved by acids (for example HCl, H₂SO₄) and / or salt solutions (for example CaCl₂) (Aldor et al., 1995; Kuyucak and Volesky, 1989b). In each case the cation (H, Ca) competes with the bound metal ion for the binding sites and replaces it if the concentration of the desorption agent is high enough. The effectiveness of desorption depends in this case on the binding strength of the added cation to the biosorbent. A different approach to desorption is the addition of

a complexing agent (for example EDTA, KSCN) (Kuyucak and Volesky, 1989b) which binds free metal ions and thereby lowers their concentration in solution to the extent that they are released from their binding sites on the solid. The 'driving force' is in this case the complexation of the metal ion. The efficiency of the desorption depends on the binding strength of the desorbed ion to the complexing ligand. Nevertheless, a charge balance of the sorbent particle has to be maintained, i.e. ion-exchange still occurs. That means some cation (for example the one that was added along with the complexing ligand, often Na) has to replace the desorbed ion at the binding sites, even if its affinity towards the binding sites is lower.

It appears reasonable that in many cases ion exchange rather than sorption to free sites is the relevant overall-mechanism for the binding of metal ions in biosorption. Since the overall charge of the biomass particle has to be neutral, any binding of one cation must be accompanied by either a stoichiometric release of other cations or by the binding of anions. Since the charge of algal biomass is negative (see below: section "Surface Charge"), it appears unlikely that free anions will be bound by the biomass. This means sorption of free cations is ruled out. If complexes in solution occur, double exchange of cations and anions or binding of the complex may take place. Generally, sorption of neutral (metal cation + anion) complexes would be possible. However, it is unlikely at the moderate pH and metal as well as ligand concentration under which many biosorption studies are conducted.

2.1.2.4 Chemical (Covalent) versus Physical (Electrostatic) Binding

The proportion of protons among the released species varied with the metal taken up (Crist et al., 1981; Haug and Smidsrod, 1970) and corresponded to the binding strength: more protons were released by the stronger binding ions. These authors concluded that in those cases where no protons were involved, as for most alkaline and alkaline earth metals, electrostatic attraction was the binding mechanism (Crist et al., 1988) whereas covalent binding occurred when protons were released (Crist et al., 1981).

It appears plausible that the number of protons released increases with the binding strength of the metal ion because it can more effectively compete with protons. Also, as a general rule, the force of electrostatic binding alone is weaker than binding with covalent contribution (especially since alkaline earth ions have a similar radius as many divalent heavy metal ions so that large differences in the binding strength are rather due to different amounts of covalent binding). However, it does not necessarily follow as a general rule that proton release indicates covalent binding: part of the protons (depending on the

relationship between pH and p^{BHK}) may also be bound by electrostatic attraction and therefore be easily replaceable by electrostatically bound ions (see Section 4.4).

2.1.2.5 Binding Sites

Which binding mechanism applies in any specific case depends of course largely on the type of biosorbent used and on the types of binding sites it contains. Biosorption has been attributed to different types of groups such as carboxylate, carbonyl, hydroxyl, amine, amide, imidazole, phosphate, thio and thioether groups (Greene et al., 1987).

Crist et al. proposed that carboxylate, sulfate and amino groups may be responsible for metal binding by freshwater algae (Crist et al., 1981). Indications for carboxyl and sulfate group participation were found by titration of marine algal biomass (Crist et al., 1992).

The chelating ability of polysaccharides from *Chlorella* was connected to their content of uronic acids. Their carboxyl groups would be negatively charged and could bind metal ions (Kaplan et al., 1987).

Tobin et al. (1984) concluded that in *Rhizopus arrhizus* fungal biomass at pH 4 carboxylate and phosphate groups offered the primary metal binding sites, supported by hydroxyl groups.

Greene et al. noticed a complete loss of available sulfhydryl groups (determined by polarimetric titration) after the binding of Au(III) to the freshwater alga *Chlorella*, thus giving evidence for the involvement of this group, but it could only account for a small amount of total gold binding. Cell modifications with succinic anhydride indicated the relevance of amine groups, since the sorption of tetrachloroaurate decreased by 50 % after their modification (Greene et al., 1986a).

The modification of carboxyl groups by esterification with acidic methanol resulted in a significant decrease in the binding of Cu and Al but a slight increase in Au binding by five different algae (Gardea-Torresdey et al., 1990). The decrease in sorption was more pronounced for Al, which as a hard metal is expected to bind preferably to hard sites such as carboxyl groups, whereas Cu as a softer metal may rather bind to nitrogen or sulfur containing groups (see Section 2.3.3 for an explanation of the "hard and soft acids and bases" principle). The binding of the negatively charged Au complex increased probably due to a decrease in the negative surface charge.

For brown algae it is assumed that alginates play a key role in metal ion binding (Kuyucak and Volesky, 1989c). Metal binding to alginate is further discussed in Section 2.2.6.

Fourest and Volesky (1996) investigated the binding of H, Cd and Pb by alginic acid and *Sargassum fluitans* biomass (same type as used in Sections 4.1 and 4.2 of this work) before and after modification of the carboxyl groups using acidic methanol or propylene oxide. A linear correlation between the binding capacity for Cd and the content of weak acidic groups (probably carboxylate) resulting from different degrees of blocking was noted. 48 h treatment with propylene oxide resulted in a ~ 90 % reduction of Cd binding and a ~ 80 % reduction of Pb binding as well as a 80 % reduction of titrable weak acidic (carboxylic) groups. This indicated that a majority of the metal was bound by carboxyl groups.

The maximum metal binding capacity of different algae was linearly correlated with their titer of weak acidic groups, with a stoichiometric relation between divalent metal bound and acidic titer of 0.36 to 0.5 mol/mol. This means that about two acidic sites are necessary per bound metal ion (Fourest and Volesky, 1997).

2.1.2.6 Surface Charge

The relevance of electrostatic attraction in biosorption depends on the types and amounts of sites present in the biomass and on whether they are ionized or occupied by protons or other ions. That, in turn, depends on the pH and on the pK_a of the respective group. Usually, a good agreement between the pK_a values of inorganic acids and their corresponding acidic groups in biomolecules exists, as evident from Table 2.1.1.

Table 2.1.1
pK_a values of inorganic acids and acidic groups in biomolecules

Inorganic Acid	pK _a	Acidic Group in Biomolecules	pK _a
sulfuric acid ^a	1.9	sulfate ^b	~1.5
phosphoric acid ^a	2.1, 7.2	phosphate ^c	2
benzoic acid ^a	4.2	carboxyl ^c	3-5
acetic acid ^a	4.8	carboxyl ^c	3-5
ammonium ^a	9.2	amine ^c	8-10
phenol ^a	10.0	phenolic OH ^c	10

^a Bower and Bates (1963, pp. 1.21-1.27)
^b Crist et al. (1992)
^c Buffle (1988, pp. 251, 323)

Amine groups are positively charged in their protonated form and neutral when deprotonated. Carboxyl, sulfate, and phosphate groups are neutral when protonated and negatively charged when deprotonated.

Greene et al. mentioned that the isoelectric point (i.e. where the overall charge is neutral) of the freshwater alga *Chlorella* is at pH 3. At lower pH, the positive charge (probably of amine groups) which leads to an attraction of anions, prevails, whereas at higher pH the negative charge (possibly of carboxyl groups) which attracts cations and repels anions, prevails (Greene et al., 1987).

Kuyucak and Volesky (1989a) noted that biomass of the marine brown alga *Ascophyllum nodosum* bears a negative charge whose magnitude sharply increased from pH 3 upward. It is likely that this surface charge originated from deprotonated carboxyl groups of the alginate in the cell wall.

2.1.2.7 Location of the Accumulated Metal

Knowledge pertaining to the location of metal uptake in the cell can provide some indication about the relevance of binding groups if it is correlated with information on which biomolecules occur in the respective parts of the cell. There have been indications that the cell wall plays an important role in metal ion biosorption by algal biomass.

Crist et al. (1988) measured protonation kinetics in whole cells for the freshwater algae *Vaucheria* and *Oedogonium* as well as in the supernatant (assumed to be cytoplasm) and sediment (assume to be cell walls) of ground cells. While the protonation in whole cells was initially fast (a few seconds) for a pH change from 3.5 to 4 and then slow (2 - 3 h), the cytoplasm fraction showed only the fast process and the cell wall both fast and slow binding. It was concluded that in whole cells a fast reaction in the cell wall was followed by a slow diffusion through the cell wall and a subsequent fast reaction in the cytoplasm.

Electron micrographs for Co binding by the brown alga *Ascophyllum nodosum* showed that the cell walls were the main location for Co binding, but at long reaction times and high concentrations Co was also found in the interior of the cell (Kuyucak and Volesky, 1989c).

For gold binding by the freshwater alga *Chlorella* electron micrographs also showed that binding occurred on the cell surface as well as in the interior (Greene et al., 1986a).

For better understanding of the relevant mechanisms in metal binding by brown algal biomass, detailed knowledge about the biomolecules and binding sites in these algae is necessary.

2.2 Properties of *Sargassum*

2.2.1 Occurrence and Structure of *Sargassum*

2.2.1.1 Occurrence

The marine alga *Sargassum* (family: Sargassaceae) belongs to the order of Fucales of the class of Phaeophyceae (brown algae) (Chapman, 1963, pp. 38-41; Lee, 1989, pp. 597-598). *Sargassum* grows either pelagic, i.e. floating on the ocean surface or attached in the littoral (tidal) and sub-tidal zone of the ocean shores (Lee, 1989, pp. 597-598). Generally, *Sargassum* inhabits warmer seas (Lee, 1989, pp. 597-598). It is the most conspicuous brown alga in tropical and subtropical waters (Bold and Wynne, 1985, p. 390). The species *S. natans* and *S. fluitans* occur as huge tangled floating masses in the Caribbean, the gulf of Mexico, the gulf stream and the Sargasso sea (Chapman, 1963, pp. 38-41; Lee, 1989, pp. 597-598).

2.2.1.2 Structure

The *Sargassum* plant is usually composed of one main axis with lateral branches which carry the leaves that are ~ 1.5 - 8 cm long and 2-8 mm wide. Air bladders (several mm diameter) are sometimes supported by small branchlets. The total size of the plant is a few decimeters (Chapman, 1963, pp. 38-41). An illustration of the *Sargassum* morphology is given in Figure 2.2.1.

The algal tissue consists of several layers of cells. Extra-cellular excreted polysaccharides, called mucilage, can form a layer (cuticle) around the cell tissue (Lee, 1989, pp. 586-589) which may serve to protect the plant from desiccation (South and Whittick, 1987, p. 127).

2.2.1.3 The Cell Wall in Brown Algae

The algal cell wall is composed of at least two different layers. The inner one consists of a fibrillar skeleton which provides the structural framework of the cell. The outer one is an amorphous embedding matrix (Lee, 1989, pp. 534-536; South and Whittick, 1987, pp. 27-28, 61-62). While the function of the fibrous layer is to provide mechanical strength, the amorphous part enhances rigidity, providing flexibility at the same time (Lobban et al., 1985, pp. 126-128). Additionally, this layer and the extra-cellular polysaccharides, some of which are hygroscopic, may prevent desiccation. These polymers also play a role in the control of ion and solute flow. It is known that they

function as ion exchangers (see also Sections 2.2.5 and 2.2.6) (Lobban et al., 1985, pp. 126-128; Mackie and Preston, 1974, p. 47; Percival and McDowell, 1967, pp. 22-23).

The fibrous skeleton of the algal cell wall is mostly insoluble (Kreger, 1962, p. 317) and it can be made up of cellulose, xylan (red and green algae) or mannan (red and green algae)(Lee, 1989, p. 10), as well as small amounts of alginic acid (Lobban et al., 1985, p. 125). For brown algae the main constituent is cellulose (Lee, 1989, p. 535) which is further described below. The fibers may be arranged randomly, longitudinal or transverse depending on the species (Mackie and Preston, 1974, pp. 43, 46; South and Whittick, 1987, pp. 60-62). There is indication that the matrix does not penetrate the fibers but is attached to them by hydrogen bonds (Mackie and Preston, 1974, p. 43). Although the matrix is amorphous it is probably far from being uniform (Lobban et al., 1985, pp. 125-126). For brown algae the main constituents of the cell wall matrix as well as of the extra-cellular polysaccharides are alginic acid and fucoidan(Lobban et al., 1985, pp. 125-126; Mackie and Preston, 1974, pp. 58, 63; South and Whittick, 1987, pp. 27-28).



Figure 2.2.1 The *Sargassum* plant (Taylor, 1960, p. 737)

2.2.1.4 Main Biomolecules

Polysaccharides make up a large portion (up to 65 %) of the dry weight of the algal cell (Volesky, 1970, p. 49). The major polysaccharides in brown algae are the storage products (energy reserves, most importantly laminaran) and mucilage as well as polysaccharide components of the cell wall (fucoidan, alginic acid) (O'Colla, 1962, p. 349; Percival and McDowell, 1967, p. 3). The content of these components varies not only between species but also with season, habitat, depth of immersion, plant part and state of development of the algal cells (Percival and McDowell, 1967, pp. 6-7).

The 5 major polysaccharides described below make up more than half of the dry weight of brown algae. The mucilage alone can already constitute 30 % of the alga's dry weight (Percival and McDowell, 1967, p. 13). The main features of these molecules are summarized in Table 2.2.1.

Table 2.2.1: Major polysaccharides in brown algae

Compound	Monomer	Groups	Function	% dry weight *
Mannitol	mannitol	CH ₂ OH, OH	storage	4-12 ^a
Laminaran	glucose	CH ₂ OH, OH	storage	~ 5 ^a
	mannitol	CH ₂ OH, OH		
Cellulose	glucose	CH ₂ OH, OH	cell wall	1-10 ^b , 4-6 ^c
Alginic acid	mannuronic acid	COOH, OH	cell wall, mucilage, cap around organelles	14 - 40 ^d , 10 - 25 ^c
	guluronic acid	COOH, OH		17, 33 ^a , 40 ^e
Fucoidan	fucose	CH ₃ , OH	cell wall, mucilage	5-20 ^{a f}
	ester sulfate	OSO ₃ ⁻		

* bold type indicates values obtained for *Sargassum*

a (Chapman, 1980)

b (Percival and McDowell, 1967)

c (Kreger, 1962)

d (Percival and McDowell, 1967)

e (Fourest and Volesky, 1996)

f (O'Colla, 1962)

Only alginic acid and fucoidan possess large amounts of groups (carboxyl, sulfate) that can be deprotonated and that are likely to be responsible for metal sorption. This corresponds to a more general statement by Buffle (1988, p. 156) according to which the functional groups in marine algae, other than OH groups, are the carboxyl groups of alginate and the

carboxyl and sulfate groups of fucoidan. Similarly, Crist et al. (1992) proposed that the active molecular entities in biosorption by marine algae are carboxyl and sulfate groups. The fact that alginic acid and fucoidan occur mainly in the cell wall and as extra-cellular polysaccharides corresponds to the observation (Section 2.1.2.7) that most of the bound metal ions were located in the cell wall.

2.2.2 Mannitol

Mannitol is a monomeric sugar alcohol ($C_6H_{14}O_6$) (Chapman, 1980, pp. 229-232; Lobban et al., 1985, pp. 123-124). It is the first accumulation product of photosynthesis, water soluble and has osmo-regulatory properties (Lee, 1989, pp. 536-537; Percival and McDowell, 1967, p. 8).

Mannitol occurs in all brown algae (Percival and McDowell, 1967, p. 5) and can constitute up to 30 % of their dry weight (Chapman, 1980, p. 229-232). The mannitol content in different *Sargassum* species was determined as 4 - 12 % respectively. The chemical structure of mannitol is illustrated in Figure 2.2.2.

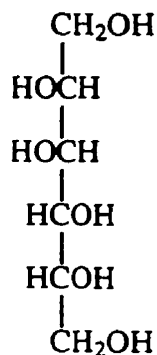


Figure 2.2.2 The chemical structure of mannitol after (Dean, 1985, p. 7.477).

2.2.3 Laminaran

Laminaran is a β - 1,3 (1,6) glucan which means that it is composed of glucose monomers (Lewin, 1974, p. 9; Lobban et al., 1985, p. 123). There are two types of laminaran chains, the G chains which are composed exclusively of glucose and the M chains, which have a mannitol end-group on C1 (Lobban et al., 1985, p. 123). About 3 % of the chains, which generally have a length of about 20 monomers, are terminated by mannitol (Chapman, 1980, pp. 226-229). The structure of laminaran is represented in Figure 2.2.3.

Due to its smaller osmotic effect as compared to mannitol, laminaran is the long-term storage product (Lee, 1989, p. 536; Lobban et al., 1985, p. 123).

Laminaran can contribute up to 30 % to the dry weight of brown algae but it has not been found in all species (Chapman, 1980, pp. 226-229; Volesky, 1970, p. 50). The laminaran content of *S. muticum* was determined as 4.6 % which is about an average value for brown algae (Chapman, 1980, pp. 226-229).

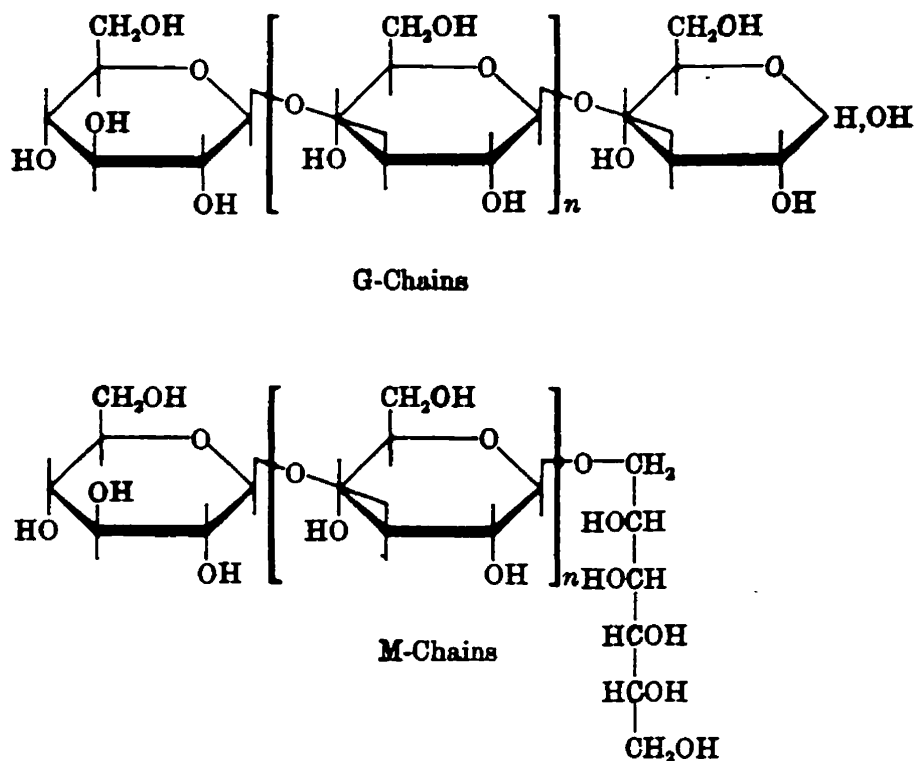


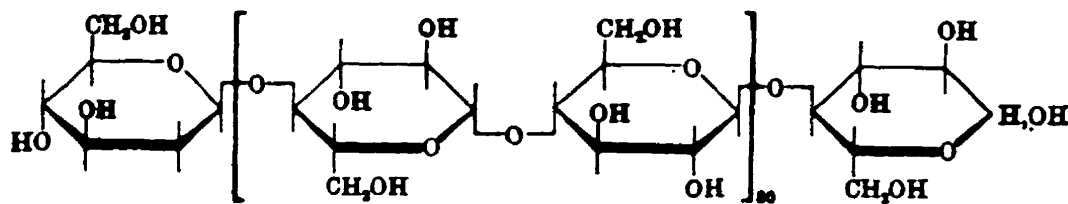
Figure 2.2.3

The chemical structure of laminaran (Percival and McDowell, 1967, pp. 56)

2.2.4 Cellulose

Cellulose is a polymer composed of β -1,4 D glucose (Lee, 1989, p. 10; Percival and McDowell, 1967, p. 84) (see Figure 2.2.4). It occurs mainly in the cell wall. Cellulose is fibrillar and uncharged (Lobban et al., 1985, p. 125) and not likely to contribute significantly to cation sorption.

In brown algae cellulose may constitute 4 - 6 % (Kreger, 1962, p. 318) or 1 - 10 % (Percival and McDowell, 1967, p. 86) of the dry weight, with a higher fraction in the stipe. Within the cell wall of brown algae the mass fraction of cellulose is 2 - 20 % (Kreger, 1962, p. 331). The contents for two members of the fucales, *Ascophyllum* and *Laminaria*, was determined to be 7 % and 20 %, respectively (Dodge, 1973, pp. 43-45).

**Figure 2.2.4**

The chemical structure of cellulose (Percival and McDowell, 1967, pp. 86)

2.2.5 Fucoidan

2.2.5.1 Structure and Properties

Fucoidan is a branched polysaccharide sulfate ester with L- fucose building blocks which are predominantly 1,2 linked with some 1,3 and 1,4 links (Lobban et al., 1985, pp. 124-129; Mackie and Preston, 1974, p. 72; O'Colla, 1962, pp. 349-350) (see Figure 2.2.5). The sulfate ester is mostly on C4, with 10 % sulfate on C2 and C3 (O'Colla, 1962, pp. 349-350).

The sulfate esters constitute ~ 40 % of the polymer mass, fucose ~ 60 % (Percival and McDowell, 1967, p. 157). The molecule may occur as a calcium salt, with Ca contributing less than 10 % to the weight (Chapman, 1980, pp. 232-233).

Fucoidan is described as viscous, water soluble and hygroscopic (Chapman, 1980, pp. 232-233; Lobban et al., 1985, p. 127; Percival and McDowell, 1967, pp. 157, 163-164). There are indications that sulfated polysaccharides like fucoidan can contribute to metal ion binding. Since sulfate groups are negatively charged they are expected to bind cations (Lobban et al., 1985, p. 127). Ca binding to sulfate groups of fucoidan has been noted by Chapman (Chapman, 1980, pp. 232-233). The sorption of Pb and Cd to sulfate groups in algal polysaccharides has been described by Veroy et al. The metal ion binding capacity of the sulfated polysaccharide carrageenan was correlated to the degree of sulfatation. The binding was believed to be mainly due to electrostatic attraction between the sulfate ester groups and the metal cation, possibly with involvement of hydroxyl groups (Veroy et al., 1980). The ability of fucoidan for ion-exchange with polyvalent metal ions was demonstrated by Paskins-Hurlburt et al. (1976) as well as by

Haug and Smidsrod (1970). Kloareg et al. (1986) described the poly-anion properties of fucoidan which has a similar charge density as alginates. There were indications that cation binding by fucoidan is purely electrostatic and does not show the selectivity as alginate.

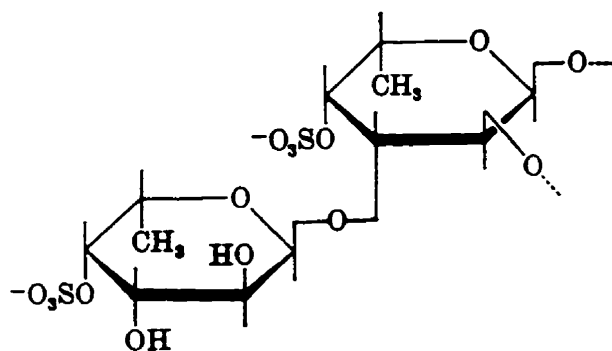


Figure 2.2.5

The chemical structure of fucoidan (Percival and McDowell, 1967, p. 161)

2.2.5.2 More Complex Sulfated Polysaccharides

The presence of galactose in the fucoidan of *Ascophyllum* has been reported with a ratio fucose : galactose : ester sulfate = 8:1:9 (O'Colla, 1962, p. 350). Beside galactose, xylose, uronic acids, arabinose, glucose and glucuronic acid have also been detected in the fucoidan *Ascophyllum* (Chapman, 1980, pp. 232-233; Mackie and Preston, 1974, p. 72). Therefore it may be more appropriate to speak of a family of compounds rather than of one fucoidan (Chapman, 1980, pp. 232-233). A similarly complex composition was observed in *Sargassum* (Mackie and Preston, 1974, p. 72). It was proposed that the poly-uronides form a backbone with branching molecules of fucose, xylose and sulfate. The name ascophyllan has been used for compounds that contain fucose, sulfate and uronic acids or other molecules. It has been reported that an ascophyllan contained 25% fucose, 13% NaSO₄, 19% Na uronate, 26% xylose and 12% protein (Percival and McDowell, 1967, p. 176).

2.2.5.3 Location and Quantities

Fucoidan occurs in the cell wall matrix as well as in the intercellular mucilage (Chapman, 1980, pp. 232-233; Percival and McDowell, 1967, p. 157).

Brown algae may contain up to 16 % of fucoidan (Volesky, 1970, pp. 55-56). The content of fucoidan in the fucales *Ascophyllum*, *Laminaria*, *Fucus* has been determined as

5 - 20 % (Chapman, 1980, p. 232; O'Colla, 1962, p. 349). Rock weeds and littoral species generally contain larger fucoidan quantities than sublittoral ones (Chapman, 1980, p. 232). This corresponds to the protective properties of fucoidan against desiccation. Fourest and Volesky (1996) determined the total number of sulfate groups in *Sargassum fluitans* biomass (of the type that was used in Section 4.1 and 4.2 of this study) as 0.27 mequiv/g. This corresponds to a fucoidan content of 6.5 % of the dry weight if it is assumed that 40 % of the fucoidan consists of sulfate.

2.2.6 Alginic Acid

2.2.6.1 Structure

Alginic acid consists of β - 1,4 D-mannuronic and L-guluronic acid (Chapman, 1980, pp. 194-196; Lewin, 1974, p. 58) (see Figure 2.2.6). Parts of the polymer are composed exclusively of mannuronic acid residues (M)_n, others of guluronic acid residues (G)_n and a third type of alternating building blocks (MG)_n. The length of each segment is 20 - 30 monomers (Percival and McDowell, 1967, p. 106), and the total chain length may be about 80 monomers (Chapman, 1980, pp. 194-196).

The ratio of mannuronic to guluronic acid depends on the algal species, age and on the plant part investigated (Haug et al., 1974; Percival and McDowell, 1967, pp. 109-111) and may vary between 0.5 and 2. For *Sargassum linifolium* it was determined to be 0.8 (or 0.6 including the correction factor of Haug) (Percival and McDowell, 1967, p. 110). For *Sargassum fluitans*, the ratio of mannuronic to guluronic acid was determined as 1.2 (Fourest and Volesky, 1997). There are indications that mannuronic acid occurs mainly in young cell walls and in the intercellular region, while guluronic acid dominates in older cell walls (Mackie and Preston, 1974, p. 58).

Guluronic acid chains are described as crystalline (Chapman, 1980, pp. 194-196) and as more rigid than mannuronic acid chains (Lobban et al., 1985, p. 127). It was postulated that mannuronic acid chains possess a higher rotational flexibility. Both uronic acids form twofold helices. The mannuronic acid polymers are arranged in flat ribbons with repetitive units spaced at 1.035 nm and are bound into sheets with hydrogen bonds. Guluronic acid chains in contrast form a rod and the repeating unit is 0.87 nm wide (Mackie and Preston, 1974, pp. 60-62).

The salts of alginic acid are called alginates. The Na, Li, K or Ca salts of mannuronic acid which are called mannurate form a three-fold helix with a repetition distance of 1.5 nm. The K or NH₄ salts of guluronic acid (gulurate) constitute a two-fold helix with a repetition distance of 0.87 nm (Mackie and Preston, 1974, pp. 60-61).

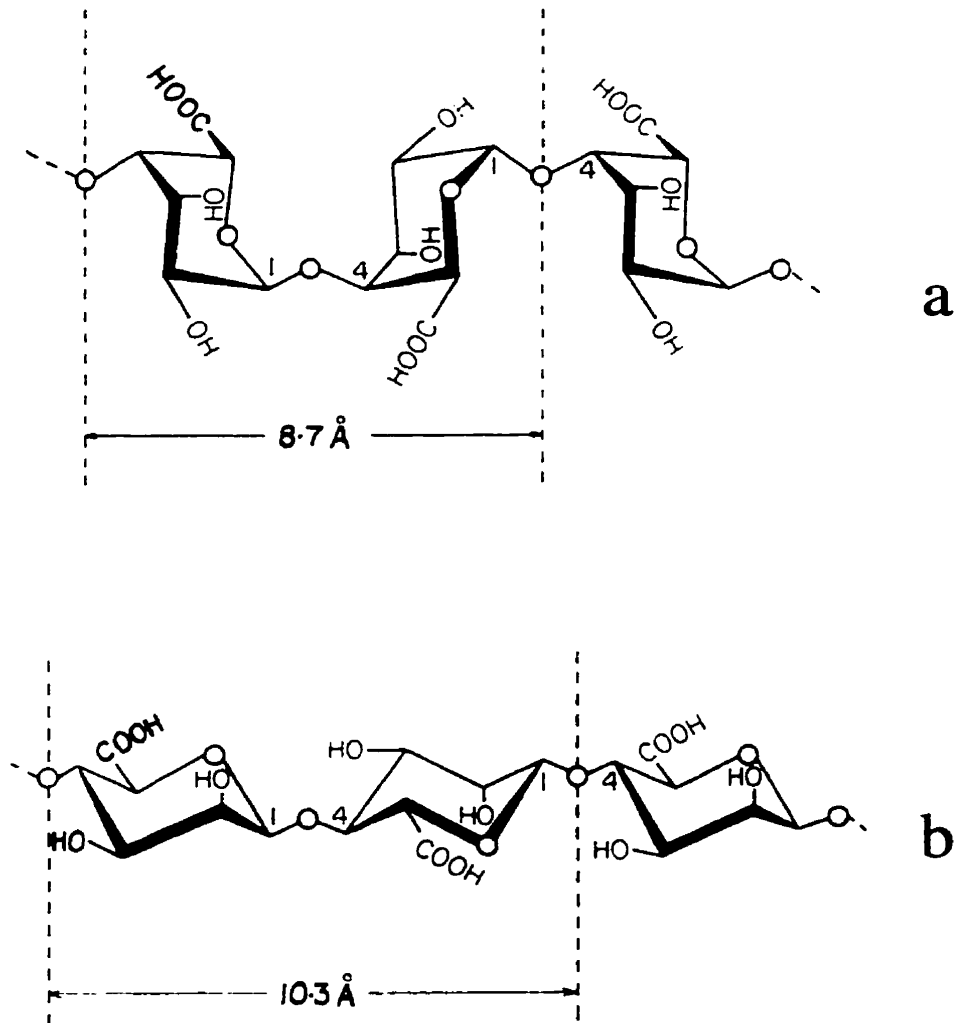


Figure 2.2.6

The chemical structure of alginic acid (Mackie and Preston, 1974)

a) guluronic acid; b) mannuronic acid.

2.2.6.2 Location and Quantities

Alginic acid occurs in both the cell wall matrix and in the mucilage or intercellular material (Chapman, 1980, p. 196; Mackie and Preston, 1974, p. 58). Additionally, organelles in the epidermal cell may be covered by a layer of alginic acid. This alginic acid cap may shield the chloroplast and nucleus from intense illumination (Lee, 1989, p. 587). According to Dodge, most of the cell is occupied by single-membrane bound vesicles containing alginic acid, fucoidan and polyphenols (Dodge, 1973, pp. 14-15).

Alginic acid is found in all brown algae (Percival and McDowell, 1967, p. 99) where it constitutes 10 - 40 % of the dry weight (Kreger, 1962, p. 320; Percival and McDowell, 1967, p. 99). The content for *Sargassum longifolium* was determined as 17 %, that for *S. wightii and tenerium* as 30 - 35 % (Chapman, 1980, p. 199). For the *Sargassum fluitans* biomass that was used in Section 4.1 and 4.2 of this work, the alginate content was determined by Fourest and Volesky (1996) as 40 % of the dry weight which corresponded to 2.25 mequiv/g .

2.2.6.3 Properties

The dissociation constants of mannuronic and guluronic acid monomers have been determined as $pK_a = 3.38$ and $pK_a = 3.65$, respectively, with similar pK_a values for the polymers (Haug, 1961a). While the salts of alginic acid with monovalent ions (alkali metals and ammonia) are soluble, the ones of divalent or polyvalent metal ions (except Mg) and the acid itself are insoluble (Percival and McDowell, 1967, pp. 114-117).

Schweiger (Schweiger, 1962) proposed that Ca binds with its primary valences to two neighboring carboxyl groups on one chain and coordinates with two (exception: Cd and Cu binding may involve only one (Schweiger, 1964)) hydroxyl group of one other monomer which may belong to a different chain. This formation would lead to crosslinking.

Two different types of binding for Ca have been described by Mackie and Preston (1974): for low Ca concentrations Ca binds to only one chain and OH groups are necessary for binding. At higher concentrations, however, Ca bridges between two chains. The binding depends on the presence of carboxyl groups and contiguous guluronic acid monomers (Mackie and Preston, 1974, p. 59).

Kohn (1975) argues that the minimum distance between two neighboring carboxyl groups on one chain is ~0.6 nm and that this is too large for Ca chelation. Kohn therefore proposes inter-molecular binding of divalent ions like Ca. This could explain a sharp drop of Ca activity with increasing linear charge density (after partial esterification) of the alginate gel which coincided with the observation of partial coagulation. Inter-molecular bonds would also offer the best geometric configuration for Ca binding to two carboxyl groups. This binding model is in accordance with the "egg box" model. A type of binding structure where divalent cations are bound in a zigzag configuration between two guluronic acid chains has been called the "egg box" model, (Grant et al., 1973; Morris et al., 1978). This is illustrated in Figure 2.2.7.

It is known that the salts of these acids engage in ion exchange (Haug and Smidsrod, 1965; Percival and McDowell, 1967, pp. 100, 118-119; Smidsrod and Haug, 1965).

The ion exchange-selectivity of alginate depends on the ratio of mannuronic to guluronic acid residues (Haug, 1961b; Haug and Smidsrod, 1965; Haug and Smidsrod, 1970). The selectivity in the exchange of Ca or other divalent ions against Na is higher for guluronic acid than for mannuronic acid (Haug and Smidsrod, 1965). The larger selectivity of guluronic acid can be explained by its zigzag structure as opposed to the flatter structure of mannuronic acid. The niches formed between two zigzag bands (see above: egg box model) represent a favorable molecular conformation for the binding of divalent ions (Lobban et al., 1985, p. 127). Additionally, guluronic acid generally has a higher selectivity among divalent metal ions with selectivity factors between 0.17 and 150. The selectivity of mannuronic acid for the same ions Ca, Mg, Cu, Sr, Ba, Co is smaller, the selectivity factors are between 1.1 and 12 (Haug and Smidsrod, 1970). The following section focuses on explaining the selectivity in cation binding.

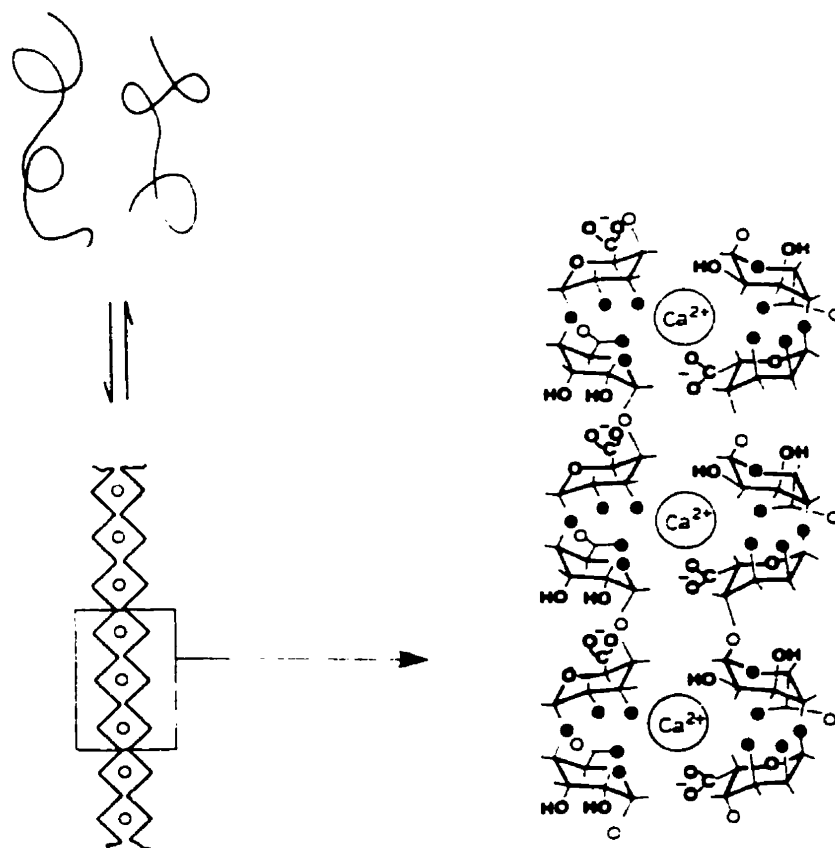


Figure 2.2.7:

The "egg box" model for cation binding in alginate (Thom et al., 1982).

Oxygen atoms involved in chelation are shown as filled circles.

2.3 Properties of Metal Ions

2.3.1 Affinity Sequence Trends

Studying metal ion binding to alginic acid from *Laminaria digitata*, Haug (1961b) reported that the amount of protons released into solution decreased in the order $\text{Pb} > \text{Cu} > \text{Cd} > \text{Ba} > \text{Sr} > \text{Ca} > \text{Co} > \text{Ni} > \text{Zn} > \text{Mn} > \text{Mg}$. This was explained by a better ability of strongly binding ions to compete with protons for organic binding sites. The affinity sequence for metal ion binding to alginate from *Laminaria digitata* followed a similar trend $\text{Cu} > \text{Ba} > \text{Ca} > \text{Co}$ (Haug and Smidsrod, 1965) and for binding of alkaline earth metals to poly-mannurate and poly-gulurate the binding strength decreased in the order $\text{Ba} > \text{Sr} > \text{Ca} > \text{Mg}$ (Haug and Smidsrod, 1970). According to Haug and Smidsrod, the preferential binding of the heavier ions could have been due to stereo-chemical effects, larger ions might better fit a binding site with two distant active groups. The amount of proton displacement by metal ions decreased in the order $\text{Pb} > \text{Cu} > \text{Ba} > \text{Sr} > \text{Ca} > \text{Cd} > \text{Zn} > \text{Ni} > \text{Mg} > \text{Co}$, Mn for poly-guluronic acid and in the order $\text{Pb} > \text{Cu} > \text{Cd} > \text{Ba} > \text{Ni} > \text{Sr} > \text{Ca} > \text{Mg} > \text{Zn}$, Co, Mn for mannuronic acid (Haug and Smidsrod, 1970). Again, the trend was concurrent with the one in binding strength.

Schweiger (1964) found a different order of complex stability for binding to alginate being $\text{Ba} > \text{Cd} > \text{Cu} > \text{Sr} > \text{Ni} > \text{Ca} > \text{Zn} > \text{Co} > \text{Mn} > \text{Mg}$ but still the binding of alkaline earth metal increased with their weight. For the elements Cu, Ni, Co, Mn of the third period an increase of binding strength with increasing atomic number was noticed.

In binding to fucoidan, the affinity sequence $\text{Pb} > \text{Ba} > \text{Cd} > \text{Sr} > \text{Cu} > \text{Fe} > \text{Co} > \text{Zn} > \text{Mg} > \text{Cr} > \text{Ni} > \text{Hg} > \text{Ca}$ was reported (Paskins-Hurlburt et al., 1976).

For *Rhizopus arrhizus* biomass, the maximum metal binding capacity decreased in the order $\text{UO}_2^{2+} > \text{Cr}^{3+} > \text{Pb} \sim \text{Ag}^+ > \text{Ba} > \text{La}^{3+} > \text{Zn} > \text{Hg} > \text{Cd} > \text{Cu} > \text{Mn}$. The metal binding capacity increased linearly with the crystal ionic radius, no correlation to the charge was noticed, except that the binding of alkaline metal ions was negligible (Tobin et al., 1984).

The observations of higher binding (both capacity and binding constant) with increasing ionic radii were interpreted as a consequence of the binding group conformation: assuming that binding groups are distant from each other, large ions could not only be easier dehydrated but also bind to several groups simultaneously (Tobin, 1986, pp. 110, 114, 119-120). This could explain the binding strength, however, it does not explain the higher binding capacity; quite the opposite: if several groups are involved in the binding of one large ion, the binding capacity of small ions, each binding to one site, could be higher.

Avery and Tobin found that the amount of proton displacement decreased in the order $\text{Cu} > \text{Cd} > \text{Zn} > \text{Mn} > \text{Sr}$. It was assumed by these authors that proton release occurred only when the metal was covalently bound and that the release of Ca and Mg indicated ionic binding. The ratio of $(\text{Mg} + \text{Ca})$ released per H^+ released was used as an index for the relative amount of ionic / covalent binding (Avery and Tobin, 1993). It was, however, not considered that, for example, Cu might bind covalently to a site from which Ca (that had been bound electrostatically) was released. This index should, therefore, not be used in a quantitative way.

Evans (1989) states that the affinity sequence in alkali metal binding to soil ($\text{Cs} > \text{Rb} > \text{K} > \text{Na} > \text{Li}$) reflects an increase in the hydrated radii of these ions; for divalent ions the binding strength to soil organic matter at pH 5.8 decreased in the order $\text{Hg} = \text{Pb} = \text{Cu} > \text{Cd} > \text{Zn} > \text{Ni} > \text{Co} > \text{Mn}$.

For freshwater algae Crist et al. observed a trend in binding strength $\text{Cu} > \text{Sr} > \text{Zn} > \text{Mg} > \text{Na}$ being similar to the one for proton replacement $\text{Cu} > \text{Zn} > \text{Mg} > \text{Sr} > \text{Na}$ and concluded that a trend from covalent to ionic bonding was responsible (Crist et al., 1981). As pointed out above (Section 2.1.2.4), however, electrostatic effects could have contributed to proton binding on the one hand and, on the other hand, covalent binding to sites previously occupied by light metals could be possible.

For binding of light metal ions to freshwater algae, the affinity sequence was $\text{Na} > \text{K} > \text{Li} > \text{Cs}$ and $\text{Mg} > \text{Ca} > \text{Ba} > \text{Sr}$. It was concluded that if the affinity between biomass and metals was high, the binding should increase with increasing charge density, i.e. with decreasing radius. If binding was weak, it would be controlled by dehydration energy and the larger ions would be preferably bound because they can be dehydrated more easily. The observed sequence which does not show clear preference for the large or smaller ions was interpreted as resulting from these opposite trends, indicating medium to strong bonds (Crist et al., 1988). It is questionable, however, whether the use of crystal ionic radii for characterizing the ionic binding of the hydrated ion is appropriate.

Leusch et al. determined the affinity sequence for untreated *Sargassum fluitans* as $\text{Pb} > \text{Cu} > \text{Ni} \sim \text{Cd} > \text{Zn}$ (Leusch et al., 1996). Fourest and Volesky (1996) observed that the binding capacity for divalent metal binding to *Sargassum* decreased in the order $\text{Pb} > \text{Cu} > \text{Cd} > \text{Zn} > \text{Ca}$ and related this to decreasing electronegativity. However, the binding strength, rather than the maximum binding capacity, should be influenced by the electronegativity. Possibly, the maximum binding was not reached under the conditions employed by these authors.

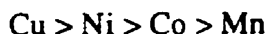
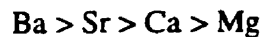
Conclusion

Generally, these binding strength trends (except for the work of Crist et al. (1988)) follow the pattern

for monovalent ions:



for divalent ions:



These basic trends will be explained in the following section. The three series for divalent ions are printed such that ions of similar binding strength are in one column (for example Ca ~ Ni ~ Zn), but no fixed relation between these series can be established. The sorbent material will determine whether for instance Cu or Cd is more strongly bound.

2.3.2 Factors Influencing the Binding Strength

Because they contribute to the free energy of binding of hydrated metal ions to biosorbent binding groups, the three factors that can determine the affinity of a metal ion are hydration effects, ionic (electrostatic) binding and covalent binding. Each will now be examined in detail:

1) Hydration Effects

A change in the orientation of the hydrated water molecules occurs in conjunction with electrostatic binding (Buffle, 1988, p. 59), but in such "outer sphere" complexes both partners retain their hydration spheres. Complete or partial dehydration takes place for "inner sphere" complexes resulting from covalent binding (Buffle, 1988, p. 195).

Both types of changes in the hydration state can occur more easily if the hydrated water molecules are not held strongly by the metal ion. Williams and Hale (1966, p. 276) showed that a good correlation between the ion hydration energy and the term z^2 / r_{cryst} exists. This is known as the Born equation. For estimating the strength of hydration, the radius of the non-hydrated cation should be used. This is usually taken as the ionic crystal radius (listed in Table 2.3.1).

Taking into account the hydration sphere, the effective hydrated radius is larger than the crystal ion radius. In general, the larger the hydration energy of an ion (i.e. the smaller the crystal radius) the larger the effective hydrated radius (Russell, 1980, p. 340-341). For alkali or alkaline earth metals, the hydrated radii and the ionic crystal radii follow opposite trends with respect to molar weight: crystal radii increase while hydrated radii

decrease with molar weight (see Table 2.3.1). It is difficult to quantify the radius of the hydrated ion, but some values have been compiled (Marcus and Kertes, 1969, pp. 28, 287-288).

According to Jain and Wagner (1980, p/ 198), hydration effects can be dominating when the electric field of the sorbent is weak (i.e. weak binding). In this case, larger ions (comparing crystal radii of ions of the same charge) that exert a smaller ordering influence on their hydrated water molecules (i.e. that are less strongly hydrated) are preferably accumulated at the interface.

2) Ionic (Electrostatic) Binding

If the binding groups are negatively charged, they can attract metal cations. The interaction is stronger the higher the charge density of both biosorbent and metal ion. If a strong electric field is present, electrostatic effects may become the dominant factor such that small ions which have a higher charge density are bound more strongly (Jain and Wagner, 1980, pp. 196-201). In the past, ionic crystal radii have been used in estimation of the ionic binding strength, also in aqueous solution (Buffle, 1988, pp. 60-61; Turner et al., 1981). However, since the cation retains its hydrated water molecules, the hydrated cation radius is more characteristic for electrostatic attraction (as opposed to hydration). According to Marcus and Kertes (Marcus and Kertes, 1969, p. 284), the selectivity increases with increasing charge and decreasing hydrated radius.

3) Covalent Binding

This type of bond involves sharing of the electrons. Therefore, the more similar the electronegativities of the metal ion and the coordinating atom of the ligand, the higher the covalent character of the bond (Dean, 1985, pp. 3-11). The selectivity (or binding strength) increases with increasing polarizability of the ion (i.e. softness, see Section 2.3.3) (Marcus and Kertes, 1969, p. 284).

Conclusion

Overall, the binding strength increases with

- increasing ionic radius and decreasing charge
(if binding is weak and largely due to hydration effects);
- decreasing hydrated radius and increasing charge
(if binding is intermediately strong and due to electrostatic effects);
- decreasing electronegativity difference
(if binding is strong and covalent).

Table 2.3.1 Parameters characterizing the binding strength of metals

Metal	z (-)	r_{cryst}^a (Å)	r_{hyd}^b (Å)	x^c (-)	$z^2/r_{\text{cryst}}^{d1}$ (1/Å)	z^2/r_{hyd}^{d2} (1/Å)	"b" type ^e (Å)	Δx^f (-)	ionic total ^g (-)	ξ^h (1/Å)
H	1	-	2.82	2.2	-	0.35	-	1.3	0.34	1.03
Li	1	0.76	3.82	1.0	1.32	0.26	1.61	2.5	0.79	0.33
Na	1	1.02	3.58	0.9	0.98	0.28	1.51	2.6	0.82	0.34
K	1	1.51	3.31	0.8	0.66	0.30	1.51	2.7	0.84	0.36
Rb	1	1.61	3.29	0.8	0.62	0.30	1.57	2.7	0.84	0.36
Cs	1	1.74	3.29	0.7	0.57	0.30	1.27	2.8	0.86	0.35
Mg	2	0.72	4.28	1.2	5.56	0.93	2.26	2.3	0.73	1.27
Ca	2	1.00	4.12	1.0	4.00	0.97	1.85	2.5	0.79	1.23
Sr	2	1.26	4.12	1.0	3.17	0.97	2.11	2.5	0.79	1.23
Ba	2	1.42	4.04	0.9	2.82	0.99	1.84	2.6	0.82	1.21
Mn	2	0.67	4.38	1.5	5.97	0.91	3.42	2.0	0.63	1.44
Co	2	0.65	4.23	1.8	6.15	0.95	4.86	1.7	0.51	1.84
Ni	2	0.69	4.04	1.8	5.80	0.99	4.99	1.7	0.51	1.92
Cu	2	0.73	4.19	2.0	5.48	0.95	6.32	1.5	0.43	2.22
Zn	2	0.74	4.30	1.6	5.41	0.93	4.07	1.9	0.59	1.56
Cd	2	0.95	4.26	1.7	4.21	0.94	5.20	1.8	0.56	1.69
Pb	2	1.19	4.01	1.8	3.36	1.00	6.61	1.7	0.51	1.94
Al	3	0.54	4.75	1.5	16.67	1.89	3.60	2.0	0.63	3.00
Ag	1	1.15	3.14	1.9	0.87	0.29	7.22	1.6	0.47	0.62

^a Shannon crystal radii (Evans, 1993, pp. 12.8-12.9)

^b Nightingale hydrated ion radii (Marcus and Kertes, 1969, p. 28)

^c Pauling electronegativity (Dean, 1985, pp. 3.11-3.12)

^d Parameter for hydration (1) or ionic bonding (2) strength
(Phillips and Williams, 1965, pp. 146-147, 159-164)

^e Parameter for covalent bond ("b") character $x^2(r_{\text{cryst}}+0.85)$
(Nieboer and McBryde, 1973)

^f Parameter for ionic bond character (Dean, 1985, p. 3.11)

^g Fraction of ionic bond character $1-\exp(-\Delta x^2/4)$ (Pauling, 1967, pp. 69-70)

^h Parameter for total binding strength $\xi = z^2/r_{\text{hyd}} / 1-\exp(-\Delta x^2/4)$

Since the first two criteria are almost opposed to each other, the affinity sequence can be reversed with changing electric field strength of the sorbent (Jain and Wagner, 1980, p. 196-201), except that the ionic and hydrated radii can exhibit opposite trends. Therefore, it is possible that for the alkaline and alkaline earth metals the affinity sequences $Cs > Rb > K > Na > Li$ and $Ba > Sr > Ca > Mg > Be$ which have been observed in industrial ion exchangers are due both to decreasing crystal and increasing ionic radius (Marcus and Kertes, 1969, pp. 287-288). A number of parameters have been introduced to quantify the ionic or covalent bond character, these are discussed in the following section.

2.3.3 The Concept of Hard and Soft Acids and Bases

In order to classify the behavior of metal ions, a division into so called hard and soft ions was introduced by Pearson (1963). Hard ions are characterized by predominantly electrostatic bonds where the entropy gain in the change of the orientation of the hydrated water molecules makes an important contribution to the free energy change ΔG (Buffle, 1988, p. 59). Hard ions have a weak polarizing power and retain their electrons strongly. Williams and Phillips used the charge density z^2/r (with z being the charge and r the cation radius) as a measure for the strength of ionic binding (Phillips and Williams, 1965, pp. 146-147, 159-164; Williams, 1960). Table 2.3.1 shows that the ionic binding strength of most divalent metal ions is similar and that it is higher than the one for monovalent ions. This is also illustrated in Figures 2.3.1 and 2.3.2.

The characteristics of hard ions resemble the ones of class "a" cations in the "a"- "b" categorization of metal ions. Type "a" ions form their strongest bonds with the first element of each group, "b" ions with the second or higher (Ahrland et al., 1958). Type "a" ions tend to form strong bonds with highly electronegative donors which are difficult to polarize (i.e. hard) (Bell, 1977, pp. 30-32). The difference between the electronegativity (x) of the metal ion and the one of oxygen has been used as a measure for "a" (i.e. ionic bond) character which increases with the square of the electronegativity difference $\Delta x^2 = ({}^Mx - {}^Ox)^2$ where Mx is the electronegativity of the metal and Ox the one of oxygen, respectively (Buffle, 1988, pp. 48-49). According to Pauling (1967, pp. 69-70), the ratio between ionic binding to the total binding strength is $1 - \exp(-\Delta x^2/2)$. Equal contributions of covalent and ionic binding occur when $1 - \exp(-\Delta x^2/2) = 0.5$. This is the case for $\Delta x = 1.7$. As seen in Table 2.3.1, the ionic bond character is larger than 70 % for alkaline (earth) metals and about 50 % for most heavy metals. Dean (1985, p. 3.11) describes a similar criterion: the ionic bond character increases with Δx and 100% ionic bonding occurs for $\Delta x > 2$ (according to Pauling's criterion the ionic bond character at $\Delta x = 2$ is 63%, not 100%).

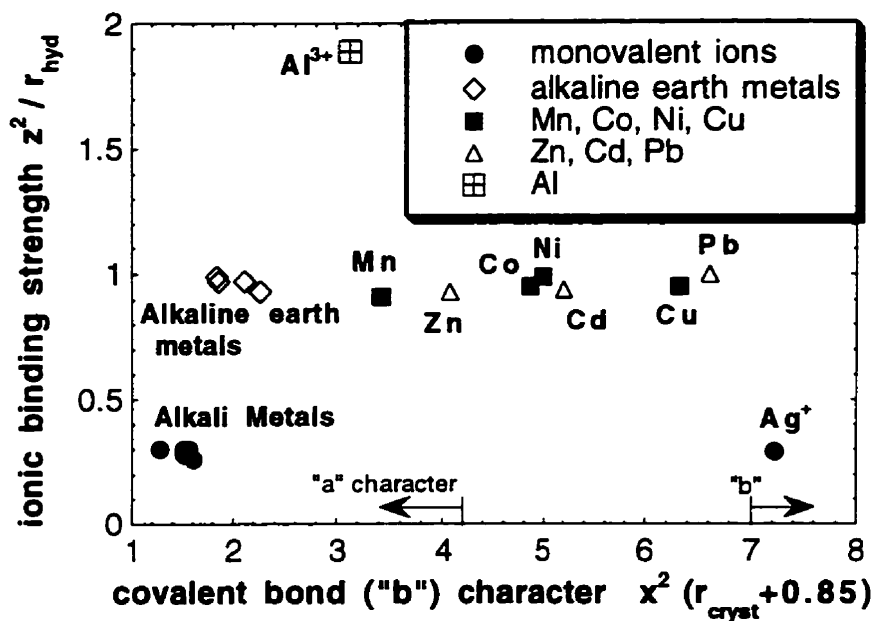


Figure 2.3.1 Ionic and covalent bond character for different metals

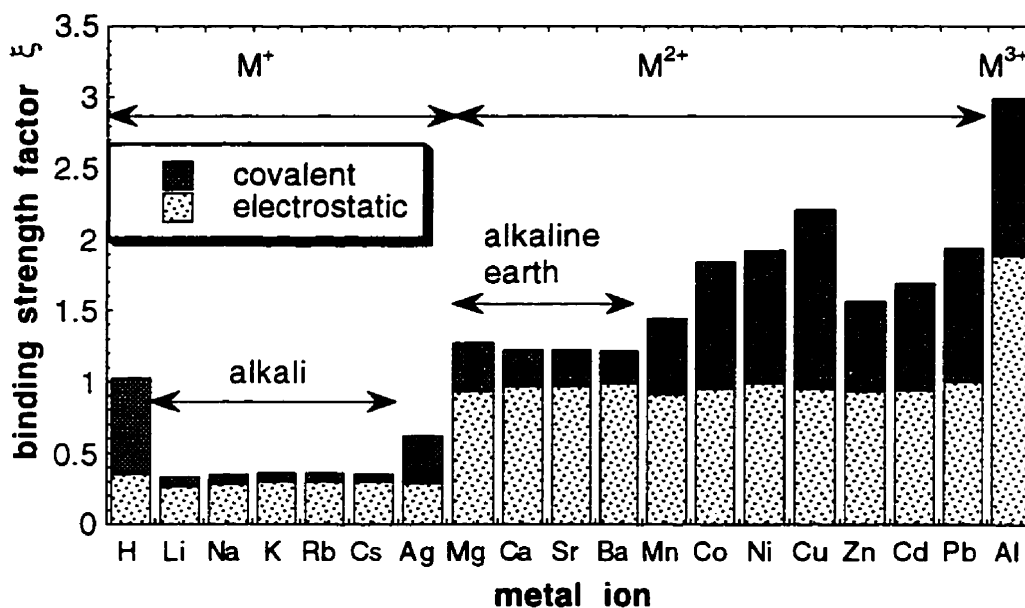


Figure 2.3.2 Binding strength parameter for different metals

Table 2.3.1 shows that the Δx criterion for purely ionic binding is fulfilled for alkaline and alkaline earth ions.

Soft ions participate in more covalent bonding where the free energy is mostly enthalpic (Buffle, 1988, p. 60). The characteristics of soft ions are opposite to the ones of hard ions, resulting in a reversed affinity sequence. The affinity sequence of soft or class "b" ions for ligands is $I > Br > Cl > F$ and $S > N > O$ (Nieboer and Richardson, 1980). A combined affinity sequence was described by Buffle: $S > I > Br > Cl \sim N > O > F$ (Buffle, 1988, p. 60). Therefore, the difference ΔK between the logarithms of the complexation constants ${}^F M K$ and ${}^{Cl} M K$ of a given metal M to F and Cl, respectively, has been introduced by Turner et al. to characterize softness which increases with decreasing $\Delta K = \log({}^F M K) - \log({}^{Cl} M K)$. Type "a" ions are characterized by $\Delta K < 2$, type "b" ions by $\Delta K > 2$; among the border elements, tendencies for "a" or "b" character are present for $\Delta K < 0$ or > 0 , respectively (Turner et al., 1981).

Nieboer and McBryde (1973) introduced the parameter $x^2 (r_{\text{cryst}} + 0.85 \text{ \AA})$ as a measure for the strength of "b" character or covalent bonding, where 0.85 \AA stands for the contribution of N or O donors to the bond distance. Type "a" ions are characterized by $x^2 (r_{\text{cryst}} + 0.85 \text{ \AA}) < -4.2$, type "b" ions are characterized by $x^2 (r_{\text{cryst}} + 0.85 \text{ \AA}) > -7$. Typical hard or class "a" ions are the alkaline and alkaline earth metals, transition elements up to class VI and for example Zn (Bell, 1977, pp. 31). As opposed to the original classification of Pearson, who considered Cd as a soft and H as a typical hard ion, these two are now regarded as borderline ions (Nieboer and Richardson, 1980). Table 2.3.1 and Figure 2.3.1 confirm that light metals and Mn can be classified as hard and most of the heavy metals listed as intermediate except for Zn which is just on the threshold to being hard and Ag which is soft.

For any donor (and especially for soft ones) the binding strength increases with cation softness (Buffle, 1988, p. 65). Soft cations form more stable complexes with soft donors (S, P or As) while hard cations prefer hard donors (F or O) (Pearson, 1963). N donors have intermediate characteristics. For O or N donor atoms, the Irving-Williams order of complex stability for divalent ions in the first series is: $Mn < Fe < Co < Ni < Cu > Zn$ (Bell, 1977, p 42-43). This can be explained by the electronegativity differences with respect to the donor atoms O or N.

Examples of hard ligands are carbonate, phosphate, sulfate or hydroxide ions (Bell, 1977, p. 32; Moore and Ramamoorthy, 1984, p. 82) as well as sulfate, carboxylate, alcohol or hydroxyl groups (Nieboer and Richardson, 1980, pp. 11-13). Soft ligands include sulfhydryl, thioether and amino groups.

The relevant parameters for different metals are listed in Table 2.3.1. The ionic binding parameter z^2 / r_{hyd} for different metal ions is plotted over the softness parameter x^2 ($r_{\text{cryst}} + 0.85 \text{ \AA}$) in Figure 2.3.1. Since the parameter z^2 / r_{hyd} expresses the ionic binding strength and the parameter $1 - \exp(-\Delta x^2/2)$ is supposed to characterize the relative contribution of ionic bonding to the total binding strength, one can obtain an indicator for the total binding strength by dividing z^2 / r_{hyd} over $(1 - \exp(-\Delta x^2/2))$. This parameter will be called ξ and it is listed in Table 2.3.1 as well as plotted in Figure 2.3.2 as the total height of the bar. The lower part represents the ionic, the upper part the covalent binding strength. The graph should, however, be used only for illustrative purposes rather than in a quantitative way because the exact magnitude of the contribution of ionic bonding is disputable. According to the Δx criterion, there is no covalent bonding for the light metals, while this plot, using Pauling's criterion, shows ~20 % covalent binding.

The binding trends summarized in Section 2.3.1 can now be explained: The tendency of stronger binding for the heavier elements in both the alkaline and alkaline earth metals can be explained as being due to lower charge density z^2 / r_{cryst} (i.e. weaker hydration) of the ions themselves and higher charge density z^2 / r_{hyd} of the hydrated ions (i.e. stronger electrostatic bonds) in the heavier elements of each series (see Table 2.3.1). Since these ions are "hard" there is little contribution of covalent bonding and therefore the electronegativity differences between them are irrelevant. The trend among the elements in the second period ($\text{Cu} > \text{Ni} > \text{Co} > \text{Mn}$) and the trend $\text{Pb} > \text{Cd} > \text{Zn}$ are probably mainly due to a decrease of the covalent binding (characterized by $x^2 (r_{\text{cryst}} + 0.85)$) but a decrease in the electrostatic binding (z^2 / r_{hyd}) (except for the relation between Ni and Cu) and increasing hydration strength (z^2 / r_{cryst}) (for all except Mn) may also contribute.

Since the binding trends in biosorption by algal biomass or its constituent molecules indicate that there is significant electrostatic and covalent binding, the model described in the next section focuses on these stronger interactions and neglects hydration effects which are weaker.

2.4 Modeling

For evaluating the feasibility and effectiveness of biosorption in wastewater treatment it is essential to make predictions of the sorption performance. This will also facilitate process design. Therefore it is necessary to develop appropriate mathematical models of biosorption.

The amount of metal, M , (or generally: sorbate) bound per mass of sorbent is called the binding (or: uptake) M_q . The binding is not only dependent on the sorbent material but also on the equilibrium concentration $[M]$ of the sorbate in solution and on other parameters such as pH and the equilibrium concentration of other ions in solution. The relationship between the equilibrium binding and the final concentration of an ion (at constant temperature) is depicted in a so-called isotherm plot of M_q versus $[M]$. With increasing metal concentration in solution its binding increases from zero to the maximum (for a typical example see Figure 4.1.2). It is desirable that a sorbent possesses a high capacity (maximum binding obtained at high equilibrium concentrations) and affinity (steep slope of isotherm curve at low equilibrium concentrations)

2.4.1 Langmuir and Freundlich Isotherms

Most mathematical biosorption models used in the literature describe simple Langmuir (Crist et al., 1988; Crist et al., 1992; Ferguson and Bubela, 1974; Holan et al., 1993; Holan and Volesky, 1994; Kuyucak and Volesky, 1989c) or Freundlich (Chen et al., 1990; Tsezos and Volesky, 1981; Tsezos, 1990) sorption isotherms, where the metal ion binding is determined as a function of the equilibrium concentration of that metal ion in the solution, without reference to pH or other ions in the same solution system.

The **Freundlich isotherm** (Freundlich, 1907) is originally of empirical nature but has later been interpreted as sorption to sites with an affinity distribution, i.e. it is assumed that the stronger binding sites are occupied first and that the binding strength decreases with increasing degree of site occupation. More specifically, the Freundlich isotherm is obtained when a log-normal affinity distribution (i.e. a normal distribution of $\log(K)$) is assumed (Smith, 1981, p. 319; Stumm, 1992, p. 95). The Freundlich isotherm is defined by the following expression:

$$M_q = k [M]^{1/n} \quad (\text{mmol/g}) \quad (2.4.1)$$

where k and n are empirically determined constants, with k being related to the maximum binding capacity and n related to the affinity or binding strength (Tsezos, 1990; Weber, 1985).

The **Langmuir isotherm** (Langmuir, 1918) is based on considering sorption as a chemical phenomenon. It is assumed that the forces exerted by chemically unsaturated surface atoms (total number of binding sites 'B) do not extend further than the diameter of one sorbed molecule and that therefore sorption is restricted to a monolayer. In the simplest case the following assumptions are made:

- all sorption sites are uniform (i.e. constant heat of adsorption);
- there is only one sorbate;
- one sorbate molecule reacts with one active site;
- there is no interaction between sorbed species.

The rate of adsorption is proportional to the rate constant of the forward reaction k_f , the number of free sites ($B = B - M_q$) and the number of sorbate molecules hitting the surface per unit time (i.e. proportional to their concentration $[M]$). Under the same conditions, the rate of desorption is proportional to the rate constant of the backward reaction k_b and the number of occupied sites M_q . The equilibrium is attained when the rate of adsorption equals the rate of desorption:

$$k_f B [M] = k_b M_q \quad (\text{mol / sec}) \quad (2.4.2)$$

With the equilibrium constant K (indicating the affinity for the sorbate) being defined as the ratio of ad- and de-sorption rates $K = k_f / k_b$ it follows:

$$M_q = \frac{B K [M]}{1 + K [M]} \quad (\text{mmol / g}) \quad (2.4.3)$$

Both Langmuir and Freundlich isotherms have been used to describe the equilibrium of metal biosorption. While it is possible to obtain good agreement between predictions of these isotherms and the experimentally determined metal binding, these simple equations have significant limitations: they cannot predict the effect of pH or of other ions in the solution.

2.4.1.1 pH Effect

Although the crucial role of protons in biosorption is generally known, it is usually neglected in the mathematical description of the process. The complex nature of biosorbent materials which may contain a multiplicity of binding groups makes the modeling of the pH effect in biosorption difficult. As a consequence, it has been a common practice to determine a separate isotherm (and a new set of parameters) for each pH value (for example (Ho et al., 1995; Huang et al., 1991b; Xue and Sigg, 1990)) or for each initial biomass saturation state (i.e. protonated or loaded for example with ions from the sea water). This has been necessary because the most frequently used Langmuir or Freundlich sorption models do not take into account the fact that metal ion biosorption is largely an ion exchange phenomenon. They do not allow the prediction of the remaining binding of those ions (for example protons or sodium) that were initially loaded onto the biosorbent, and neither do they incorporate the concentration of the exchanged species (for example protons) as a parameter. As a result, the conventional and tedious determination of the effects of these parameters has been necessary, normally not allowing any calculated predictions of the biosorbent performance.

A linear relationship between the consumption of base (which was assumed to be proportional to the charge of the biomass) and pH, as well as a linear relationship between Sr binding and pH was described by Crist et al. (1981). An attempt has been made, assuming a simplified linear relationship between the metal uptake and pH difference, to model the biosorptive binding of metal ions by a Freundlich isotherm, which was modified by a factor proportional to the pH difference (Votruba, 1994). This approach is only applicable within a rather limited pH range and can only be used as a purely empirical model which does not convey information about the real processes occurring, such as the involvement of different groups. The model used (Votruba, 1994) could not represent the change of proton binding in the presence of metal ions. In addition, no indication was given how well the model fitted the data it was based on.

Gonzales-Davila et al. (1995) described Cu binding to algal cells. Though protonation reactions for two acidic sites were considered in the derivation of the model, it was only used in a simplified form where pH, proton and metal binding constant were all lumped into one parameter for each of the sites. The resulting model was therefore a standard two site Langmuir isotherm.

The work of Huang et al. (1991a; 1991b) in which the binding of heavy metal ions to fungal biomass was investigated is one of the rare examples where a Langmuir model that includes H as one of the competing species was used. One or two (Huang et al., 1991b) binding sites are considered, with the two site model enabling a better fit of the

data. However, the model equations assume a 1:1 stoichiometry of metal binding and proton release although it was recognized that metal binding with a 1:2 stoichiometry probably occurs. Additionally, model predictions were only made using conditional (i.e. pH dependent) binding constants).

Recently, a modified Langmuir model that described competitive Cu and H binding to alginate was used by Jang et al. (1995b). The model accounted for Cu binding to two sites. The isotherm formulation chosen would, however, require iterative calculation of the uptake of each cation as a function of the binding of the other one.

Seki et al. (1990) developed a two site isotherm equation derived from a 2:1 proton-metal exchange constant. The model allows direct calculation of the metal binding as a function of the concentration ratio $[H]^2 / [M]$ but it does not account for free sites and it cannot easily be extended to include more species.

2.4.1.2 Competing Ions in Solution

Often, the prediction of sorption equilibria is complicated by the presence of several sorbed ions, requiring the use of multi-component isotherm equations. This is especially relevant when the sorption of one ion influences the binding of another, as the case when different ions compete for the same binding site. A variety of multi-component isotherms is presented in a recent review by Yu and Neretnieks (1990).

A multi-component Langmuir isotherm model for a 1:1 ratio of divalent metal ions to binding sites was used by Chong and Volesky (1995) for describing the competition of different heavy metal ions (Cd, Cu, Zn) for binding to *Ascophyllum nodosum* biomass that was crosslinked with formaldehyde.

A multi-component Langmuir isotherm model was also used by Trujillo et al. (1991) for the biosorption of several different metal ions to protonated peat moss beads. In both cases, however, biosorption was not regarded as an ion exchange process; the ions with which the biomass had originally been saturated were not considered.

Jang et al. (1995a) used a modified Langmuir type model that considered either 1:1 or 1:2 metal - binding site complexes for Cu and Co binding to alginate. The sorption isotherms were, however, not resolved for a calculation of the binding as a function of the concentrations. Iterative calculation of the binding of one metal as a function of the binding of the other one was necessary. Again, the exchanged species, in this case Na, was not considered in the model.

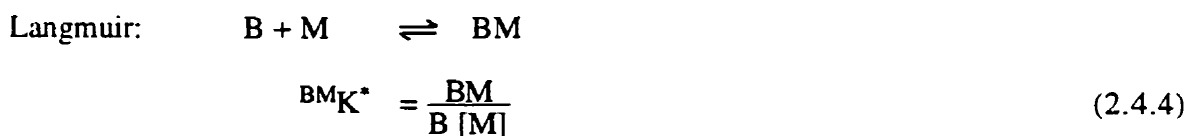
Complex systems (involving different cations and ligands) can (instead of using a multi-component isotherm) be modeled by incorporating binding constants for metal ion - biomass complexes into a computer program for the calculation of the chemical

equilibrium. Reviews of different computer programs for calculating the equilibrium speciation have been presented by Nordstrom and Ball (1984) and Pagenkopf (1978). These programs take acid / base reactions, coordination and dissolution / precipitation into account. Their use is advantageous if complexation in solution is expected or if final concentrations are to be predicted from the initial state. This approach was taken by Tobin et al. for predicting the influence of ligands (Tobin et al., 1987) and competing metal ions (Tobin, 1988) on the binding of UO_2^{2+} , La^{3+} , Pb^{2+} , Cd^{2+} , Ag^+ to the fungus *Rhizopus arrhizus*, using the equilibrium program REDEQL. After incorporating equilibrium constants for metal binding (corresponding to the Langmuir model), the model predictions in some cases showed good agreement with the observed behavior (Tobin et al., 1987; Tobin, 1988).

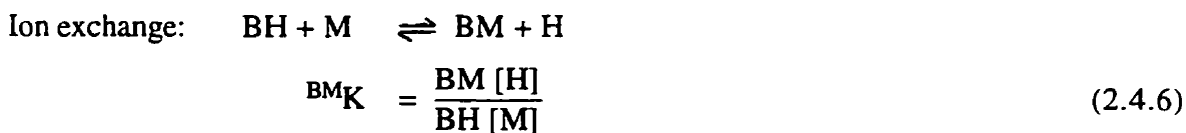
2.4.2 Ion-Exchange Constants

There have been indications (see Section 2.1.2.3) that ion-exchange is an important biosorption mechanism. Nevertheless, even some authors who noticed that biosorption was, in their case, an ion exchange process used simple sorption isotherms (Crist et al., 1992; Kuyucak and Volesky, 1989c). Only a few authors (Chen et al., 1990; Crist et al., 1981; Crist et al., 1994; Haug, 1961b; Haug and Smidsrod, 1970) draw the consequences of this observation and conclude that it is inadequate to assume only Langmuir or Freundlich type binding to free sites. Therefore, these authors used ion exchange models with equilibrium constants (so called ion-exchange constants or selectivity coefficients) that take into account the reversibility of the ion exchange reactions: the ion that is displaced into the solution can compete with the sorbed metal ion for the sites.

The Langmuir equation and the ion exchange constant for the binding of a metal ion M (for simplicity here a monovalent ion) replacing a proton H on a complexing site B are related as follows:



$$[{}^t\text{B}] = [\text{B}] + [\text{BM}] \quad (2.4.5)$$



$$[{}^t\text{B}] = [\text{BH}] + [\text{BM}] \quad (2.4.7)$$

$$\text{therefore: } \quad \text{BMK}^* = \text{BMK} / [\text{H}] \quad (2.4.8)$$

The difference between the two approaches is that the first one assumes that all sites are initially free and does not consider any reverse reaction of a displaced ion, in this case a proton, with the site. The second model assumes that all sites to which metal ions are sorbed are initially occupied, i.e. the number of free sites stays constant. Crist et al. (1994) compared the fit of the Langmuir sorption isotherm model and the one using ion exchange constants. The differences between the two models were especially pronounced at low metal ion concentrations because the reverse reaction involving the displaced ion is most noticeable if the concentration of the bound cation is low.

The ion exchange approach is probably somewhat closer to reality than the simple Langmuir model, but it is not completely satisfying either. While a constant number of free sites (in other words: the number of sites occupied by the bound ion is equal to the number of sites from which the exchanged ion is released so that $B = (B^1M) + (B^2M)$ can be assumed) may be a reasonable working assumption for a constant pH system, it may not hold for systems with changing pH values. According to Stumm and Morgan (1970, p. 488), the cation exchange capacity increases with increasing pH above the isoelectric point. Therefore, one cannot simply model the competitive binding of metals and protons by using only a metal-proton ion exchange constant. It is necessary to include at least one reaction where a cation reacts with a free site.

Treen et al. (1984) formulated a theoretical model that included metal ion and proton binding to the active sites. However, the model assumes a 1:1 exchange ratio between metal ions of any valence and protons, which is not likely the case. Also, it was only used as an empirical tool in a very limited version for the reaction of one metal ion with one or two sites. Constants were fitted arbitrarily without taking into account the number and nature of groups that were actually present on the biomass (Sears, 1986). One outcome of this approach is that the amount of sites postulated in order to fit the model for different metal ions varied from one metal ion to the other. No modeling of pH influence or proton binding has been attempted.

In the modeling of industrial ion exchangers, protons have been considered (Helfferich, 1962, pp. 79-93; Marcus and Kertes, 1969, pp. 345-351). However, these synthetic resins are chemically rather simple compounds that generally contain only one active group. Biosorbents, on the other hand, can be heterogeneous and contain different acidic groups active in metal ion binding. The p^{BHK} value, site quantity and metal ion binding constant must be known for each of these sites.

2.4.3 Models Including Ionic Strength Effects

Since Na is present in many industrial wastewaters, it is useful to be able to estimate the extent to which Na (or more generally: the ionic strength) interferes with the binding of heavy metal ions targeted by biosorption. In biosorption, no modeling of the effects of ionic strength and electrostatic attraction has been done until recently. Several models of ionic strength effects have, however, been published concerning metal binding to humic and fulvic acids. The physical characteristics of these molecules that are degradation products of organic matter are quite different from biosorbents such as *Sargassum*. Humic and fulvic acids are small water-soluble molecules. However, since these molecules contain carboxyl groups as one of their main functional groups (Gamble and Schnitzer, 1974) they may in some aspects be comparable to *Sargassum*.

Buffle (1988, p. 195-299) systematically describes possible models for complexation equilibria including site protonation, multiple sites and secondary effects like the influence of the electric field in polyelectrolytes on the local concentration.

The simplest approach to modeling the influence of Na in the biosorption system consists of the introduction of a binding constant for Na, as done by Westall et al. (1995) for the binding of H, Co and Na to humic acids (10 - 100 mM NaClO₄, pH 4.5 - 9.5, 4 discrete binding sites). A 1:1 binding stoichiometry for Co and Na to mono-protic sites was assumed. The modeling results were close to the experimental data, but the range of the Na concentration employed in the experiments was small and no general conclusions about the quality of the model can be made. The advantage of this approach is that it would easily be possible to derive a multi-component isotherm so that the binding of each species can be directly calculated (this is done in Section 4.4, equation (4.4.42)). Additionally, the Na binding constant can easily be incorporated into computer programs for the calculation of chemical equilibria in aqueous solutions, such as MINEQL+(Schecher, 1991). One disadvantage is, however, that the Na binding constant is purely empirical and does not reflect the electrostatic nature of the Na binding.

A second possibility is the use of the Donnan model (Donnan, 1911). An application of this approach for different charged polymers has been pioneered by Marinsky and coworkers (Marinsky, 1987) who established the use of Donnan models for interpreting protonation equilibria in organic polyelectrolytes including humic and fulvic substances (Ephraim et al., 1986a; Marinsky et al., 1982b; Marinsky and Ephraim, 1986) and alginic acid (Lin and Marinsky, 1993). The latter contribution involves an estimation of the water uptake (swelling) using osmotic coefficients from the literature which, unfortunately, was not verified with experimental results. Interactions with metals were included by the same research group (Marinsky et al., 1982a) (Cu and humic acids),

(Ephraim and Marinsky, 1986b) (Cu and fulvic acids) and (Lin, 1981) (Ca, Cd, Co, Ni, Zn and alginic acid). The relationships in different plots are discussed in terms of the Donnan model, but no model *predictions* of proton or metal binding under different conditions were made. Thus the model fit for that data set could not be judged.

Jang et al. (1990) also used a Donnan model for Cu binding to alginic acid which is considered as a separate phase. The data supported the model that considers competition of Cu and H for the same sites where Cu could be chelated.

Katchalsky et al. (1961) investigated Donnan equilibria in alginate gels and concluded that for divalent ions (for example Cu, Ca) that are complexed by the alginate (as opposed to monovalent ions (Na, K)) the concentration of free counter-ions is low.

Cabaniss and Shuman (1988) used Güntelberg activity coefficients to account for ionic strength effects and competition by alkaline earth metals on pH titrations and Cu binding in fulvic acids ($I = 5 - 100$ mM, $pH = 5 - 8$, 5 discrete binding sites), assuming that each fulvic acid molecule bears five negatively charged groups. This method is suited for rather small molecules and would not be appropriate for polyelectrolytes such as alginic acid or *Sargassum* biomass. The model includes binding to di-protic sites and a metal-proton exchange ratio of 1:2. It was expressed as an exchange constant or as an isotherm derived from this constant. The isotherm did not include a term for free sites. It was noticed that increasing ionic strength (Na) or the presence of Ca or Mg can reduce Cu binding.

A model that is suitable for both oligo- and polyelectrolytes was used by Bartschat et al. (1992) for modeling pH titrations and Cu binding ($I = 1 - 100$ mM, $pH = 4 - 9$, 3 binding sites) of humic acid molecules. Two of the sites were assumed to be di-protic and able to bind metal ions, one to be mono-protic and not to bind metals. The humic acid molecules are assumed to be penetrable or impenetrable spheres of two size classes (assuming that the total charge is proportional to the volume of the sphere). An equation that relates the concentration factor λ to the charge density per surface area, σ , (if impenetrable) or to the volumetric charge density (if penetrable), respectively, was used. For small λ the limiting case of simple charged molecules, and for large λ the limiting case of polyelectrolyte behavior is approximated. The model showed good agreement with the experimental data of these authors. The advantage of this approach is its generality concerning the size of the molecule. Therefore it is particularly suited for oligoelectrolytes which show a behavior intermediate between simple ions and polyelectrolyte gels. For alginate or *Sargassum*, however, this feature is not necessary since they could be considered as true polyelectrolytes. A disadvantage is, however, that the semiempirical correlation used by Bartschat et al. (1992) needs three fitting parameters for the electrostatic

effects for each of the two particle sizes. (As a comparison: the models used in the work presented here have only one fitting parameter instead of six). Moreover, the fitting parameters had to be determined individually for each ionic strength. This means that the effect of ionic strength was not predicted.

A Helmholtz model for the charged interface was used by Xue et al. (1988) for the binding of protons and heavy metal ions (Cu, Cd) to algal surfaces ($I = 10$ mM, $\text{pH} = 4 - 9$, 1 binding site). This model requires only one fitting parameter, the constant capacitance, for modeling the electrostatic effects. With a constant capacitance as in the model of Bartschat et al. (1992) it is, however, not possible to model ionic strength effects.

Another model which needs few fitting parameters has been employed by Tipping et al. (1988; 1993) for proton, Al, Cu, Mg and Ca binding to humic acids ($I = 1 - 1000$ mM, $\text{pH} = 3 - 11$, 8 binding sites of two general types). The advantage of this model is its economical way of using relatively few fitting parameters for the prediction of a wide range of experimental conditions. Only one or two parameters are needed in order to predict λ_s (at the charged surface) at different ionic strengths. Unfortunately, however, the equation used by Tipping et al. for the relationship between the concentration factor λ_s and the ionic strength is an empirical one.

De Wit et al. (1993) employed a Poisson-Boltzmann model for proton binding to humic substances ($I = 10 - 1000$ mM, $\text{pH} = 2 - 10$, 1 or 2 binding sites with affinity distribution). The advantages of this model are that it incorporates the effect of ionic strength on the concentration factor in a realistic manner and that it only needs one fitting parameter for electrostatic effects. Both for cylindrical and spherical impermeable particles, this fitting parameter is the particle radius. The assumption of small impermeable spheres or cylinders appears, however, to be not applicable to the large, penetrable particles investigated in the present study.

2.5 Conclusions

Quantitative knowledge of metal binding under different circumstances is necessary for feasibility studies and process design of biosorption as a treatment alternative for metal bearing wastewaters.

In ion-exchange processes, as biosorption by *Sargassum* may well be, the concentration of cations competing for the sorption sites is the most important factor influencing metal binding by a given biomass. If not only covalent binding but also electrostatic attraction play an important role in biosorption, even "hard" ions like Na (that are not specifically bound) can influence heavy metal binding (ionic strength effect), especially when "hard" chemical binding sites such as carboxyl groups are involved.

Biomass of some brown algae, specifically the genus *Sargassum*, has been proven to be an effective metal biosorbent. The major binding sites in the biomass of these brown algae are suspected to be the carboxyl groups of alginic acid and the sulfate groups of fucoidan which both occur in the cell wall and as extra-cellular polysaccharides. Since these groups are acidic, the availability of free ionized sites and also the surface charge depends on pH. Therefore, it is expected that metal binding increases with pH. If that proves to be the case, protons have to be considered as one of the competing species.

The influence of temperature and ligand concentration is probably of secondary importance unless strong complexing agents are present.

In most cases, biosorption has been modeled as sorption using simple Langmuir or Freundlich isotherm sorption models. For predicting the competition of cations for binding sites, using models based on ion-exchange constants would be more appropriate. Preferably, both ion exchange and binding to free sites should be considered, which has rarely been done.

The use of polyelectrolyte models to take electrostatic effects into account has been equally rare in metal biosorption work. In modeling of metal binding to humic and fulvic acids, the Donnan model as well as double layer models have been employed, setting a more sophisticated example for biosorption studies.

3

MATERIALS AND METHODS

3.1 Choice of conditions

The brown alga *Sargassum* was used as the biosorbent in this work because of its high metal binding capacity (Holan et al., 1993; Kuyucak and Volesky, 1989d; Ramelow et al., 1992). The biomass used in Sections 4.1 and 4.2 was crosslinked with formaldehyde because experiments with other brown algal biomass (*Ascophyllum nodosum*) had shown that crosslinked material was physically more stable and had a lower weight loss (leaching of soluble biomass components like alginate) during the sorption experiments compared to non-crosslinked biomass (Chong and Volesky, 1995; Holan et al., 1993). Recent investigations by Fourest and Volesky of alginate leaching from different non-crosslinked brown algae indicated the superior properties of *Sargassum*: due to the large molecular weight of alginic acid in *Sargassum*, its leaching was smaller than in other brown algae; virtually no alginate was released at $\text{pH} < 5$ (Fourest and Volesky, 1997). Therefore, the biomass used in Sections 4.4 and 4.5 of this work was not crosslinked.

The pH range for metal binding experiments in this study was pH 2 - 5 in order to prevent precipitation of Cu. Hydroxide (or oxide) formation becomes important for the ions Cd, Cu, Zn at pH 7, 5 and 5.5, respectively, and precipitation starts at pH 9-10, 6 and 8.5, respectively, (Baes and Mesmer, 1976, pp. 272-300, 410). Besides, strongly acidic or moderately alkaline conditions may damage the biosorbent material. In the pH range investigated in this study (pH 2 - 7) no serious damage is expected to occur.

The heavy metals were chosen because of their toxicity (Cd) or extensive use (Cu, Zn). The light metals (Ca, Na) were investigated because they are frequently present in natural waters (untreated algal biomass, for example, contains large amounts of these ions) and industrial wastewaters. Additionally, Na is frequently used in pH adjustments (NaOH) and therefore present in the biosorption experiments. Ca may be used in desorption and pre-treatment of the biomass and therefore occurs in biosorption applications.

Ligands were chosen such that little complex formation and no precipitation occurred (CdSO_4 and $\text{Cd}(\text{NO}_3)_2$, CuSO_4 , ZnSO_4 , $\text{Ca}(\text{NO}_3)_2$, NaNO_3).

3.2 Sorbent Materials

Beach-dried marine brown algal biomass of the genus *Sargassum* (Sections 4.1 and 4.2: collected in Naples, FL; Section 4.4 and 4.5: collected in Natal, Brazil), was ground (Section 4.1 and 4.2 in a homogenizer; Section 4.4 and 4.5 cut manually with a knife) and sieved.

Most of the biomass used in Section 4.1 and 4.2 (size fraction 0.84 - 1 mm) was crosslinked with formaldehyde following the procedure described by Leusch et al. (1995). The biomass used in Section 4.4 and 4.5 (size fraction 0.5 - 1.7 mm) was not crosslinked.

All biomass was washed in distilled de-ionized water and most of it (exception: some experiments with crude biomass in Section 4.1) was then washed in HCl for protonation (Section 4.1 and 4.2: 10 g crosslinked biomass / L, 0.1 N HCl; Section 4.4 and 4.5: 50 g biomass / L, twice in 1 N HCl) and then 10 times in the same volume of distilled de-ionized water, finally dried in an oven at 60 - 80 °C. Protonation of the biomass was performed to eliminate any other exchangeable ions that were present in the raw biomass, thereby enabling the study of a simple biosorption system, one involving only a known number of cations.

A stock solution of sodium alginate (Fisher) was prepared by dissolving 10 g of Na-alginate in 800 mL of distilled de-ionized water.

3.3 Cation Binding Experiments

3.3.1 General Methodology

For Sections 4.1 and 4.2 the sulfate salts $3\text{CdSO}_4 \cdot 8\text{H}_2\text{O}$ (Aesar), $\text{CuSO}_4 \cdot 5\text{H}_2\text{O}$ (ACP Chemicals) and $\text{ZnSO}_4 \cdot 7\text{H}_2\text{O}$ (J.T. Baker Chemical) were dissolved in distilled de-ionized H_2O . For Section 4.4 and 4.5 the nitrate salts NaNO_3 (Sigma), $\text{Cd}(\text{NO}_3)_2 \cdot 4\text{H}_2\text{O}$ (Fisher), $\text{Ca}(\text{NO}_3)_2 \cdot 4\text{H}_2\text{O}$ (Fisher) were used in order to avoid precipitation of CaSO_4 . Besides, Cd forms weaker complexes with nitrate than with sulfate.

Sargassum biomass (0.1 - 1 g, the higher sorbent masses were generally applied where small differences between initial and final metal concentration were expected (for example at low pH values) in order to avoid large experimental errors) or alginate (0.04 - 0.25 g of dry weight, only in Section 4.4) were contacted with 50 mL of solution (either distilled de-ionized water (for most pH titrations) or metal containing solutions of initial concentrations between 1 and 1000 ppm (for metal ion binding experiments)) in 125 mL Erlenmeyer flasks on a gyrotory shaker (New Brunswick Scientific, model G2) at 2 Hz for 6-12 h.

Different known amounts of 0.1 - 1 N acid (Sections 4.1 and 4.2: H₂SO₄ or HCl; Section 4.4 and 4.5: HNO₃) or base (NaOH) were added to the samples in order to achieve certain final pH values which were measured (Orion Ionalyser model 407A). Blanks, controls and duplicates were run as appropriate. Both initial and final metal ion concentrations ($[M]_i$, $[M]_f$) were determined by atomic absorption spectrometer (Thermo Jarrel Ash, model Smith-Hieftje II).

3.3.2 Specific Conditions

3.3.2.1 Mono-Metal Systems at different pH (Section 4.1)

Sulfate salts of Cd, Cu and Zn were used. The amount of biomass added was 0.1 g in each sample. No Na salt was added, Na was only present to the extent that NaOH was added for pH adjustment. For each of the three metals, experiments were performed at the three pH values 2.5, 3.0 and 4.5. The equilibrium concentrations of the metal ranged between ~ 0.01 and 10 mM, the initial concentrations were between 0.1 and 10 mM (~ 10 - 1000 ppm) for Cd and between 0.2 and 10 mM (~ 10 - 500 ppm) for Cu and Zn.

3.3.2.2 Multi-Metal Systems at different pH (Section 4.2)

As in the previous section, sulfate salts of the metals were used, the amount of biomass added was 0.1 g, no Na salt was added and the initial and final metal concentrations were in a similar range as for the mono-metal systems. The difference compared to the previous section was that the solution contained two different metals, in all three possible combinations of Cd, Cu and Zn. For each of the three metal combinations, the experiments were performed at the three pH values 2.5, 3 and 4.5. Each of those nine systems contained 9 (for pH 2.5 or pH 3) or 16 (for pH 4.5) data points.

3.3.2.3 Experimental and Modeling Errors (Section 4.3)

The evaluation of the experimental errors was performed for the data of mono- and multi-metal systems at different pH (Sections 4.1 and 4.2). No additional metal binding experiments were conducted. Though the error analysis was based on the data from Sections 4.1 and 4.2, the methodology and results can also be applied to Sections 4.4 and 4.5.

3.3.2.4 Proton Binding at Different Ionic Strengths (Section 4.4)

In this section, not only *Sargassum* biomass but also alginate was used. The amount of biomass added varied between 0.1 and 0.5 g (the latter usually for pH < 2.5-3 and also for the whole second series). In order to obtain a similar amount of binding sites when using

alginate as compared to *Sargassum*, the dry weight of the added alginate was ~ 40 % of the one added for *Sargassum* under comparable conditions (because about 40 % of the dry weight of *Sargassum* is alginate (Fourest and Volesky, 1996)). The initial concentration of NaNO_3 was zero for the first and second series, 100 mM for the third and 1000 for the fourth series of either *Sargassum* or alginate. Since different amounts of NaOH or HNO_3 were added for pH adjustment, the ionic strength varied from point to point. Therefore, the ionic strength at half-ionization of the acidic groups ($f=0.5$) is used to characterize the series and referred to in the discussion and in the figure captions. The titrations were performed between pH 2 (the estimation of the proton binding was very imprecise for lower pH values) and the endpoint of the titration of the carboxyl groups which was between pH 4.5 for high ionic strength and pH 6.5 for low ionic strength.

3.3.2.5 Metal and Proton Binding at Different Ionic Strengths (Section 4.5)

Nitrate salts of Cd and Ca were used with initial concentrations between about 5 and 1000 ppm (50 - 200 ppm for the two-metal system) and final concentrations between about 0.01 and 10 mM (~ 0.1 - 2 mM for the two-metal system). The amount of biomass added was either 0.1 g, 0.5 g (at pH 3 or $1 \text{ mM} < [\text{Ca}] < 5 \text{ mM}$) or 1 g (for $[\text{Ca}] > 5 \text{ mM}$). Experiments for Cd binding were conducted at pH 4.5 and pH 3, experiments with Ca alone and in the two-metal system Cd-Ca only at pH 4.5. For all of the above-mentioned conditions, two sets of experiments were performed, one where no NaNO_3 was added and one where the initial NaNO_3 concentration was 100 mM. Since the ionic strength varied from point to point due to different amounts of acid or base added, the two sets of experiments are referred to as low and high ionic strength.

3.3.3 Experiments at Constant Concentration

Some experiments were performed with $[\text{M}]_i \sim [\text{M}]_f$ (in the following, the final concentration is for simplicity referred to as $[\text{M}]$ without the subscript f) so that a desired final concentration was obtained. This was achieved by choosing a liquid volume of $\geq 1 \text{ L}$. Since the binding could not be determined from the concentration difference, the biomass was collected in a Buchner funnel, dried and the metal ions were desorbed in 50 mL (V_{des}) of 1 M HCl. After contacting overnight on a rotary shaker, the solution was filtered and analyzed for the metal concentration ($[\text{M}]_{\text{des}}$). A correction was made for metal in the specific volume (V_m) of the wet biomass and the adhering liquid after filtering:

$$M_q = [\text{M}]_{\text{des}} V_{\text{des}} / m - [\text{M}] V_m \quad (\text{mol/g}) \quad (3.3.1)$$

3.3.4 Calculation of the Equilibrium Cation Binding

For all of the models used, the equations for the conservation of mass for the molecular species C, S (carboxylic or sulfate binding sites), H, jM (j -th metal ion of charge z_j) and L (ligand, only necessary in Section 4.4 and 4.5, in this case NO_3) are:

$${}^tC = [C] + [CH] + \Sigma [C {}^jM_{1/z_j}] \quad (\text{mequiv/g}) \quad (3.3.2)$$

$$\text{for example: } {}^tC = [C] + [CH] + [C \text{Cd}_{0.5}] + [C \text{Ca}_{0.5}]$$

$${}^tS = [S] + [SH] + \Sigma [S {}^jM_{1/z_j}] \quad (\text{mequiv/g}) \quad (3.3.3)$$

$$\text{for example: } {}^tS = [S] + [SH] + [S \text{Cd}_{0.5}] + [S \text{Ca}_{0.5}]$$

$$\begin{aligned} {}^tH &= ([CH]_i + [SH]_i + [H_p]_i V_m) m + [H_{\text{add}}] V_{\text{add}} + [H]_i V_i \\ &= H_q m + [H] V \quad (\text{mmol}) \quad (3.3.4) \end{aligned}$$

$$\begin{aligned} {}^tM^{2+} &= 0.5 ([CM_{0.5}] + [SM_{0.5}] + [M_p] V_m) m + [M] V \\ &- 0.5 M_q + [M] V \quad (\text{mmol}) \quad (3.3.5) \end{aligned}$$

$$\begin{aligned} {}^tL &= [L_p]_i V_m m + [H_{\text{add}}] V_{H,\text{add}} + [NaL]_i V_i \\ &= [L_p] V_m m + [L] V \quad (\text{mmol}) \quad (3.3.6) \end{aligned}$$

CH is the amount of protonated C-sites, C the amount of free C-sites (analogous for S sites). V is the volume of the solution and m the mass of the sorbent. The total amounts (as different molecular species in solid and liquid phase) of each component (C, H, L) are indicated by the superscript "t". The subscript "i" denotes initial values, $[NaL]_i$ is for example the initial concentration of sodium salt in the solution before the biomass was added. The subscript "add" refers to the addition of acid (added volume $V_{H,\text{add}}$ or V_{add}) or base (added volume V_{add} , the concentration of the acid added for pH adjustment $[H_{\text{add}}]$ in equation (3.3.4) is assumed to be negative when base, not acid is added). $[H_p]_i$ and $[L_p]_i$ stand for excess acid initially present in the pores or cell of the biosorbent due to incomplete washing after protonation. For any ionic species "X", the concentrations $[X]$ without subscript are the ones in the bulk solution and $[X_p]$ is the average concentration of X in the particle (of the specific volume V_m).

The term proton binding, H_q , refers to the amount of protons bound to the sites that are considered to be involved in metal binding (i.e. carboxyl and sulfate groups). This means, for example, that the protons bound to phenolic groups are not included. H_q is defined as the sum of the covalently (as CH and SH) and electrostatically (as $[H_p] - [H]$) bound protons:

$${}^Hq = CH + SH + ([H_p] - [H]) V_m \quad (\text{mequiv / g}) \quad (3.3.7)$$

The change in the proton binding was calculated as the difference between the quantity of protons added ($[H]_{\text{add}} V_{\text{add}}$) for pH adjustment and the protons that accumulated in the solution ($[H] V - [H]_i V_i$). For pH near 7 an additional term for water dissociation may be added which was, however, negligible under the conditions of the study. The consumption or release of protons due to reactions in the aqueous phase is negligible because modeling with MINEQL+ (Schecher, 1991) showed that no hydrolyzed species occur up to pH 7 or even higher, except for Cu where precipitation may occur at around pH 5. The final proton binding in the experiments can be derived by solving equation (3.3.4) for Hq :

$${}^Hq = CH_i + SH_i + [H_p]_i V_m + \frac{[H_{\text{add}}]V_{\text{add}} + [H]_i V_i - [H] V}{m} \quad (\text{mequiv / g}) \quad (3.3.8)$$

When protonated biomass was used, it can be assumed that all sites are initially occupied by protons, i.e. the initial proton binding was equal to the total number of sorption sites ${}^B = {}^C + {}^S$.

$${}^Hq = {}^B + [H_p]_i V_m + \frac{[H_{\text{add}}]V_{\text{add}} + [H]_i V_i - [H] V}{m} \quad (\text{mequiv / g}) \quad (3.3.9)$$

In Sections 4.1 and 4.2 electrostatic binding was neglected, accordingly $[H_p]_i$ (or generally $[X_p]$) is assumed to be equal to the bulk concentration.

The binding of divalent metal ions is defined as the sum of the covalently (as $CM_{0.5}$ and $SM_{0.5}$) and electrostatically (as $[M_p] - [M]$) bound metal ions:

$${}^Mq = CM_{0.5} + SM_{0.5} + 2 ([M_p] - [M]) V_m \quad (\text{mequiv / g}) \quad (3.3.10)$$

The final binding of divalent metal ions in the experiments can be calculated from the mass balance for M (3.3.5):

$${}^Mq = {}^Mq_i + 2 \frac{[M]_i V_i - [M] V}{m} \quad (\text{mequiv / g}) \quad (3.3.11)$$

For the experimental data of this study, Mq_i was zero because the biomass was initially completely protonated (except for the desorption case in Section 4.1.11).

The concentration of ligand in solution can be calculated from equation (3.3.6)

$$L = \frac{([\text{NaL}]_i + 2 [\text{ML}_2]_i) V_i + [\text{H}_{\text{add}}] V_{\text{add}} + ([\text{L}_p]_i - [\text{L}_p]) V_m}{V} \quad (\text{mmol/L}) \quad (3.3.12)$$

This equation is only necessary for the calculation of the ionic strength in Section 4.4 and 4.5.

3.4 Swelling Experiments

In the swelling experiments, 0.25 or 0.5 g of *Sargassum* biomass and 10 mL of NaNO_3 solution (0 - 200 mM) were equilibrated overnight in 10 mL graduated cylinders after adding some HCl or NaOH as required for pH adjustment. After measuring the pH and the bed volume, the biomass was filtered off (using previously weighed Whatman #4 filter paper), weighed immediately, oven dried at 60 °C and weighed again after equilibrating at room atmosphere.

For the alginate as well as in regular metal binding experiments with *Sargassum*, the biomass was filtered off (using previously weighed Whatman #4 filter paper), weighed immediately, oven dried at 60 °C and weighed again after equilibrating at room atmosphere.

3.5 Electrophoretic Mobility Determination

For measurements of the electrophoretic mobility (EPM), the binding experiments were performed as usual except that more finely ground biomass was used. The pH was adjusted to different values. For each sample, 10 runs were performed on an electrophoresis apparatus (Rank Brothers). The time (t) of the particle to cross the distance $d = 100 \mu\text{m}$ was measured during each run. The average value (t') was used to calculate the electrophoretic mobility (particle velocity / potential gradient) for a cell length $\mathcal{L} = 7.13 \text{ cm}$ at an applied potential $U = 96 \text{ Volt}$:

$$\text{EPM} = \mathcal{L} d / (t' U) \quad (\text{m}^2 / \text{s V}) \quad (3.5.1)$$

4 RESULTS AND DISCUSSION

4.1 Mono-Metal Systems at different pH values

This section presents an approach to modeling the binding of heavy metal ions (Cd, Cu and Zn chosen as examples) and protons, as a function of metal ion concentration and pH, for a wide range of initial sorbent saturation states with the heavy metal ion and / or protons. The model presented here enables the prediction of the effect of protons as exchanged species on the metal ion binding. Although it has been recognized that the use of protonated biosorbent in sorption columns would tend to lower the pH (especially when applied in a column where pH adjustment is not easily performed) which in turn might adversely affect the sorption performance, this material was chosen for the present study because it enables one to study a simple sorption system with only one metal ion and protons. Using biosorbent initially saturated with other ions would introduce another species into the system since protons would always be present. Investigation of the proton-metal ion exchange is a prerequisite for further expansion of the model, considering also other ions.

The results presented in this section have in modified form been published in Schiewer and Volesky (1995a) and in Schiewer et al. (1995b).

4.1 Results and Discussion: Mono-Metal Systems at different pH values

4.1.1 Preliminary Experiments

In order to verify that 6-12 h are enough time to reach equilibrium, a preliminary kinetic experiment was performed for Cd binding, using untreated *Sargassum* biomass of a particle size between 0.5 and 0.8 mm. Cd is one of the largest of the investigated ions and may therefore be expected to have the lowest diffusion coefficient. The initial concentration was 0.74 mM (83 ppm) Cd and pH was manually adjusted to pH 4.5 with NaOH (note: due to the intermittent pH adjustment, the rate of binding may have been slower than in a system continuously at pH 4.5. The kinetic experiment was, however, representative of typical equilibrium metal binding experiments performed in this study in which the pH adjustment was sometimes done intermittently). The maximum time of the experiment was 200 min. As shown in Figure 4.0.1, 50 % of the final binding was already achieved after less than 20 min., 75 % after 50 min. In the last 100 min. the binding only changed by 5%. Therefore, it can be expected that the binding increases only very little after the first 3 hours. This corresponds to results from the literature described in section 2.1.1.6. In order to allow ample time for equilibration, 6-12 h were chosen as the duration of the experiments.

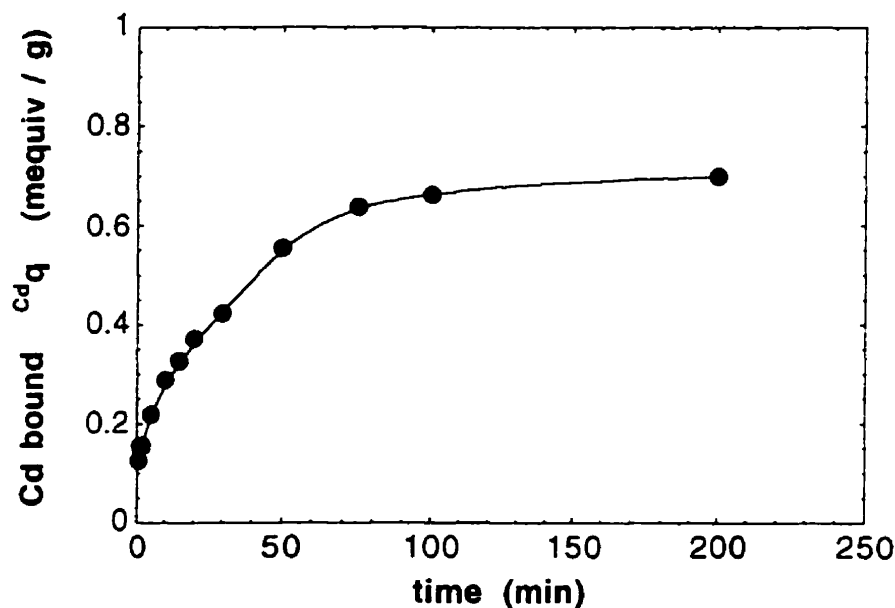


Figure 4.1.1 Kinetics of Cd biosorption at pH 4.5
using untreated *Sargassum* biomass of 0.5 - 0.8 mm particle size.

4.1.2 Influence of pH on Sorption

A trend of increasing metal ion binding with increasing pH could be observed for all three metal ions examined in this work as shown in Figure 4.1.2 for pH 4.5 and pH 2.5 and in Figure 4.1.3 for pH 3.0. The same trend was noted by other researchers as described in Section 2.1.1.4. The modeling results are discussed in sections 4.1.9 and 4.1.10.

Since Cd, Cu and Zn feature no hydrolyzed species at $\text{pH} \leq 4.5$, the pH influence on their binding by the biosorbent is an indication of the interaction of biomass active sites with protons. This means that protons and metal ions compete for the same binding sites, with more sites being available for metal ion sorption at higher pH values.

It has been recognized by Crist et al. (Crist et al., 1994) that the main effect of pH on metal ion binding consists of a reduction in the number of binding sites available with decreasing pH.

4.1.3 Change of pH

It was noticed in this work that the pH dropped from an initial value of about 4–5 to around 3 during sorption with protonated biomass, if no pH adjustment was undertaken. This means that proton release took place, because no reaction in the solution could account for the pH change. Raw, non-protonated biomass exhibited the reverse phenomenon: the pH rose from an initial pH of 3.5 (biomass and metal ion free solution, adjusted to pH 3.5 with HCl) to pH 6 after addition of the biomass (data not shown). After readjusting the pH to 3.5, a release of light metal ions that had been bound from the sea water (0.28 mequiv Ca, 0.32 mequiv Mg, 0.15 mequiv K and 0.22 mequiv Na) was measured. Since no reactions that involve protons should occur in the solution, the increase of pH must have been due to a binding of protons from the solution by the biomass. The observations, therefore, can be explained by an exchange between the light metal ions initially present and the protons. Since a higher ionic strength and also higher pH characterize sea water, it is plausible that the equilibrium in sea water is shifted toward the sorption of these light metal ions. On the other hand, in distilled water, the equilibrium tends toward lowering the amount of these sequestered metal ions, which are replaced by protons.

When formulating a model to describe the sorption behavior, it appears important to incorporate these differences in behavior which are due to the different initial states of the biomass. Otherwise, the sorption model for the equilibrium, which considers the final concentrations of the sorbed metal ions, is still valid only for a specific initial state reflecting the ion exchange capabilities of the biosorbent.

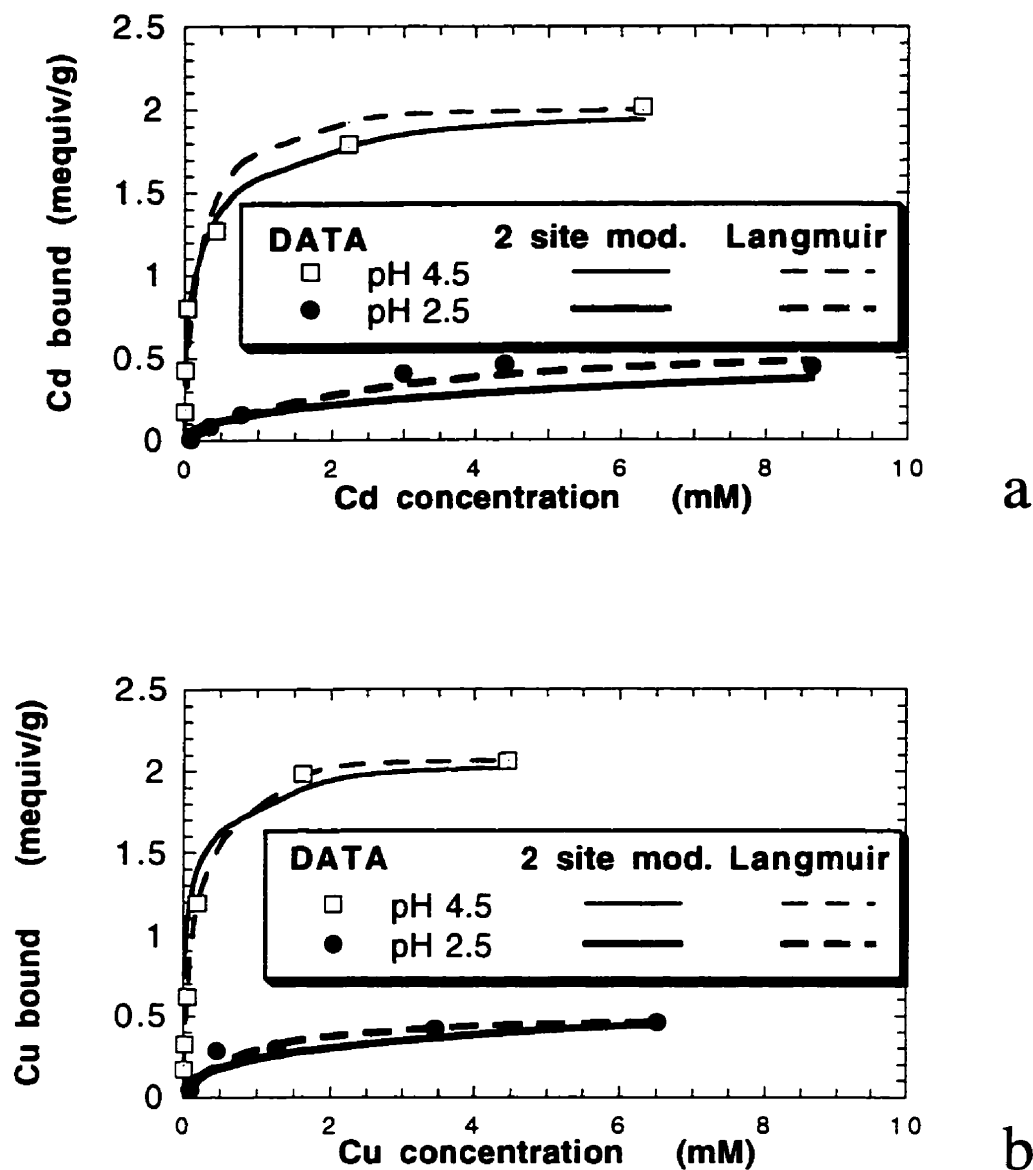


Figure 4.1.2: Biosorption isotherm for metal binding by protonated *Sargassum* biomass at pH 4.5 and 2.5.

- a) Cd binding: experimental data, the Langmuir isotherm model and the 2-site model;
- b) Cu binding: experimental data, the Langmuir isotherm model and the 2-site model;

4.1 Results and Discussion: Mono-Metal Systems at different pH values

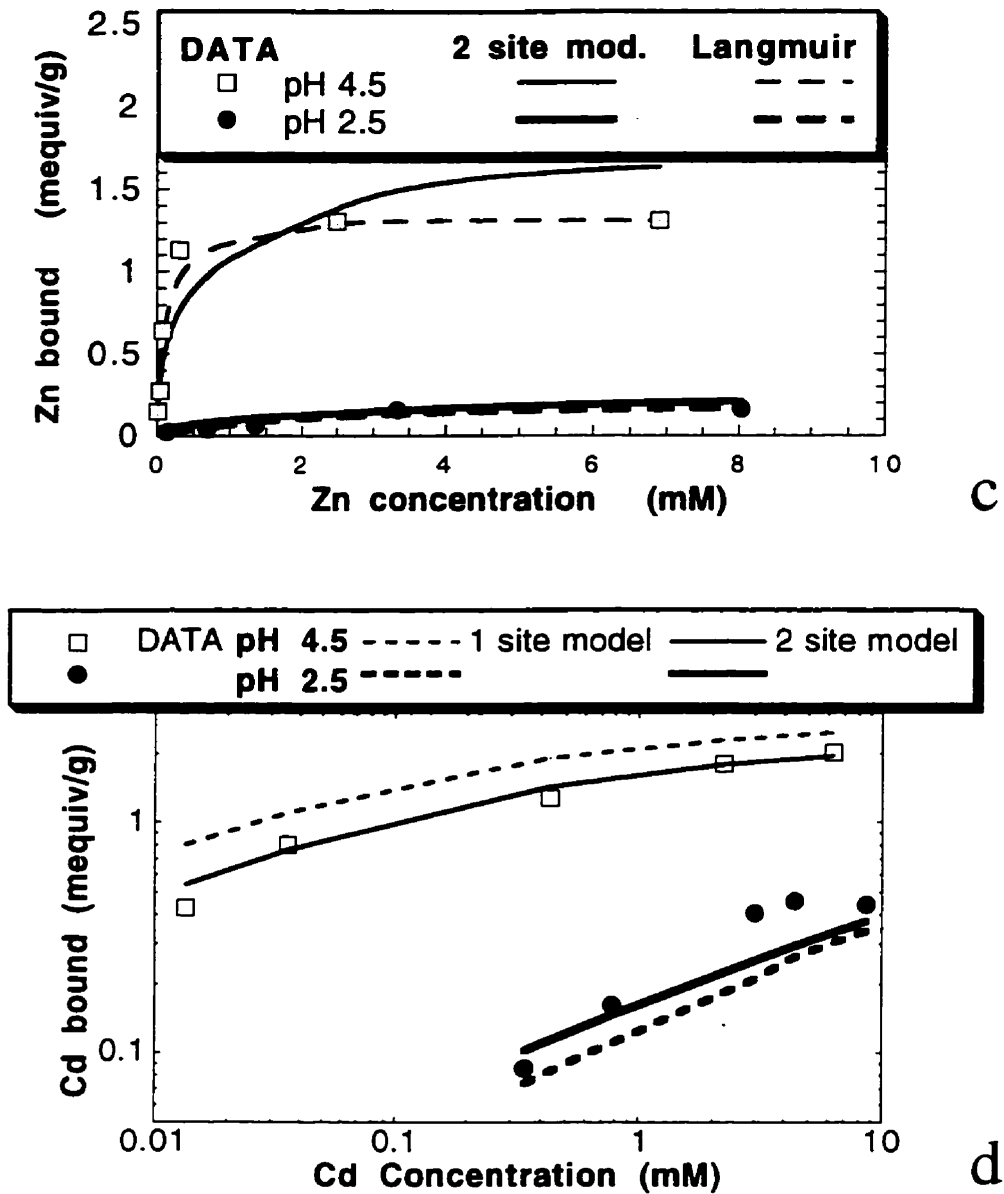


Figure 4.1.2: Biosorption isotherm for metal binding by protonated *Sargassum* biomass at pH 4.5 and 2.5.

- c) Zn binding: experimental data, the Langmuir isotherm model and the 2-site model;
- d) Cd binding: experimental data, the 1-site model and the 2-site model.

4.1.4 Relationship between Proton Release and Metal Binding

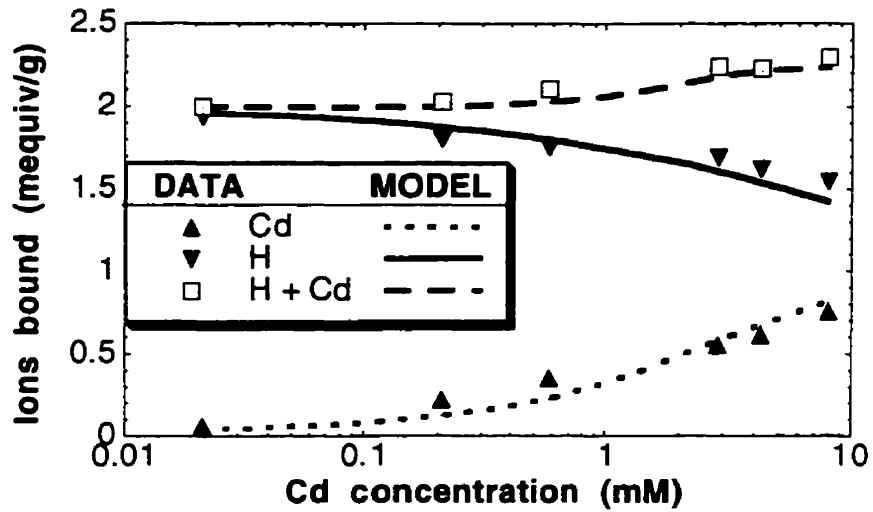
In order to examine whether heavy metal ion binding and corresponding proton release by protonated biomass can be modeled as an ion exchange process, the amount of protons remaining bound (equation (3.3.9)) after reaching the equilibrium binding of Cd, Cu or Zn at pH 2.5, 3, or 4.5, respectively, was quantified. The consumption or release of protons due to reactions in the aqueous phase is negligible because modeling with MINEQL+ (Schecher, 1991) showed that no hydrolyzed species occur until pH 7 or higher, except for Cu containing solutions where precipitation may begin at around pH 5.

The amount of proton and metal binding at increasing metal ion concentrations at pH 3 is plotted in Figure 4.1.3. It was observed that while proton binding decreases and metal ion binding increases with an increasing metal ion concentration, the total binding ($H_q + M_q$) on a charge basis (mequiv) stays approximately constant. This observation confirms that ion exchange does take place with a metal ion to proton ratio close to 1:2. The modeling of this phenomenon is discussed in section 4.1.9 and 4.1.10.

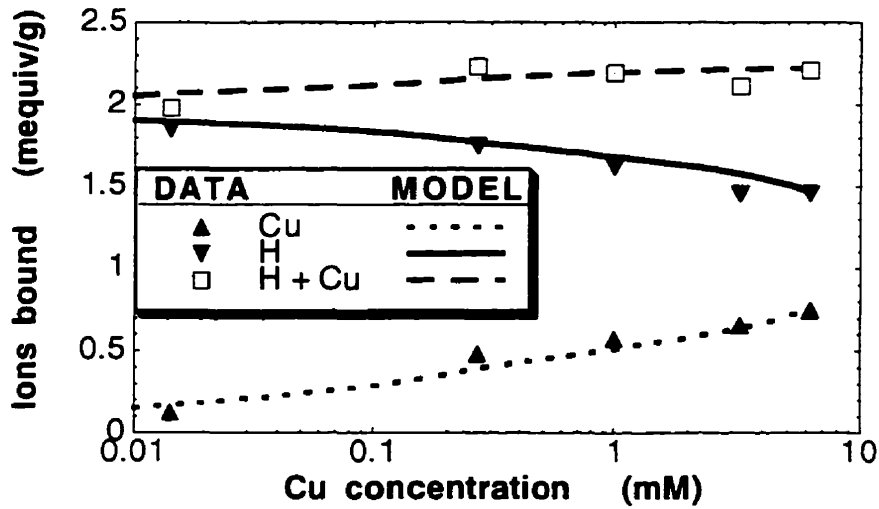
The same conclusion applies for sorption of metal ions by raw biomass, where the release of ions bound from the sea water (Na, Ca, K, Mg) is balanced by the binding of protons and heavy metal ions (Figure 4.1.4). The fact that the total cation binding by the untreated biomass (Figure 4.1.4) was higher than that of protonated biomass (Figure 4.1.2 and 4.1.3) may be due to a loss of binding sites during crosslinking and acid washing. Since the presented work focuses on the binding of heavy metals, the binding constants for Na, K, Mg, Ca were not determined and the data in Figure 4.1.4 were therefore not modeled.

If all biomass binding sites were initially protonated, it could be expected that any binding of a divalent ion would be associated with the release of exactly two protons. The experimental data, however, do not show such a perfect exchange behavior: a slight increase in the total binding ($H_q + M_q$) during metal sorption by protonated biomass was noticeable (Figure 4.1.3). The ratio of proton release to metal ion binding was slightly smaller than 2. This can be explained by the presence of a small number of groups which would be non-protonated at $pH \geq 3$ but which bound metal ions. In the biomass studied, these are likely to be sulfate groups which are strongly acidic. At pH 4.5 the increase of the total binding ($H_q + M_q$) with metal ion concentration was more pronounced: for example, it rose from 1.5 mequiv/g for $[Cd] = 0$ mmol/L to 2 mequiv/g for $[Cd] = 6$ mmol/L (Data not shown). This can be explained by the availability of a larger number of sites which were not protonated but ionized and/or occupied by other ions such as Na. Alginic acid is partially dissociated at pH 4.5.

4.1 Results and Discussion: Mono-Metal Systems at different pH values



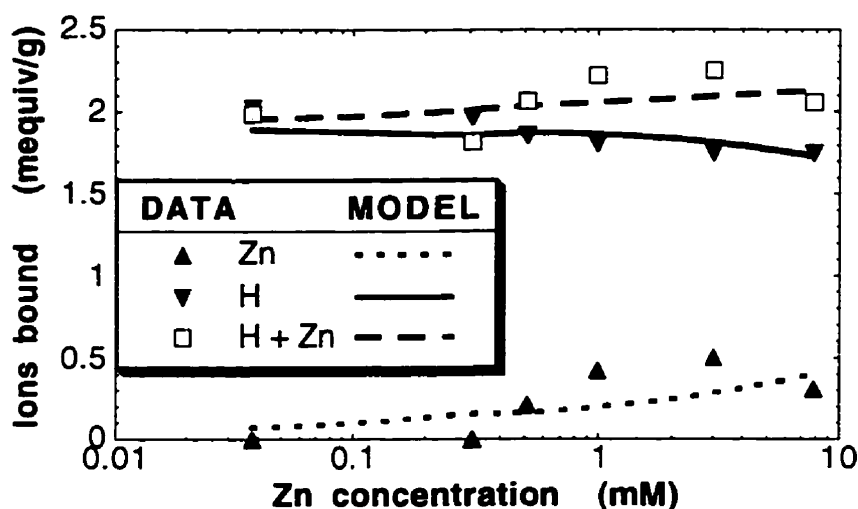
a



b

Figure 4.1.3: Biosorption isotherm for metal and proton binding by protonated *Sargassum* biomass at pH 3 (experimental data and the 2-site model).

- a) Cadmium and proton binding;
- b) Copper and proton binding;

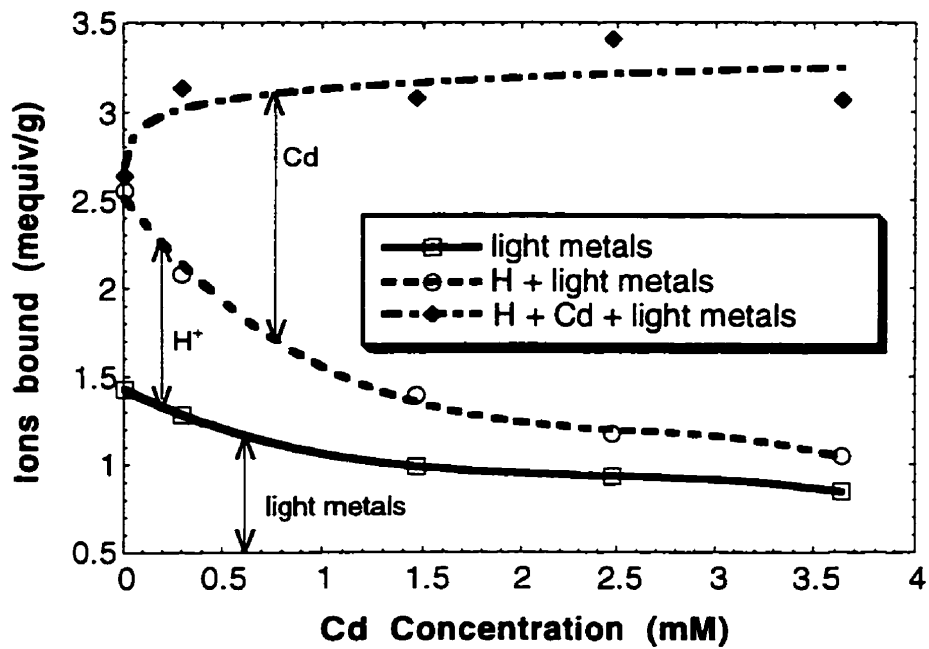


C

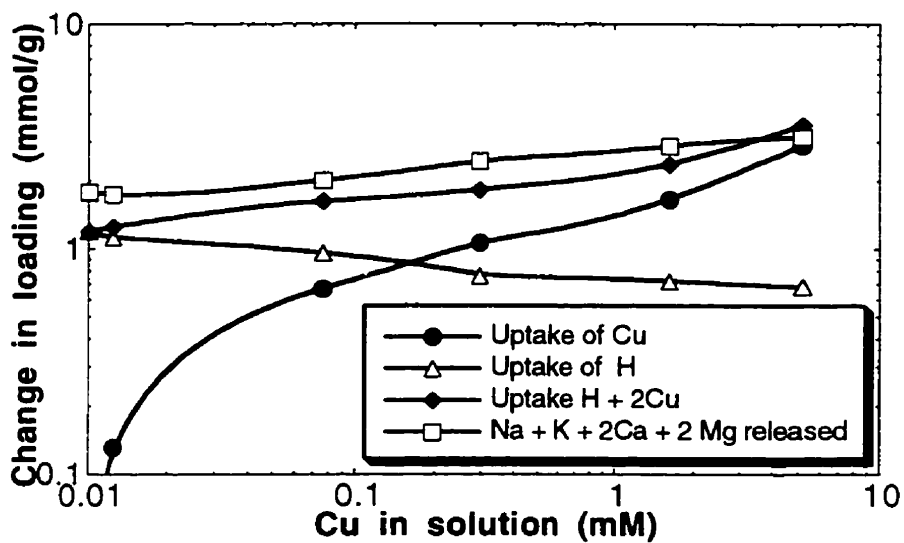
Figure 4.1.3: Biosorption isotherm for metal and proton binding by protonated *Sargassum* biomass at pH 3 (experimental data and the 2-site model).
 c) Zinc and proton binding.

The amount of protons displaced per metal ion sorbed has been reported to be less than 2. The proton release increased with increasing binding strength of the metal ion to freshwater algal biomass (Crist et al., 1981). There was no proton release during the binding of sodium, which was interpreted as pointing to electrostatic attraction as the sole sequestering mechanism. The contribution of covalent binding increased with the increasing ability to displace protons.

Crist et al. (1990) showed that the total charge of the released ions Ca, Mg and H equaled the charge of the metal ion taken up, demonstrating a perfect ion exchange behavior. This result was obtained for freshwater algae where no sulfate groups were present in their biomass. Therefore, no free groups contributed to sorption. Similar observations were made by Kuyucak and Volesky (1989c) for cobalt sorption by *A. nodosum*. Treen-Sears et al. (1984) reported that 2 protons were released for each uranyl ion sorbed by *Rhizopus arrhizus* in a flow-through packed biosorption bed.



a



b

Figure 4.1.4: Binding of heavy and light metal ions as well as protons by untreated *Sargassum* biomass

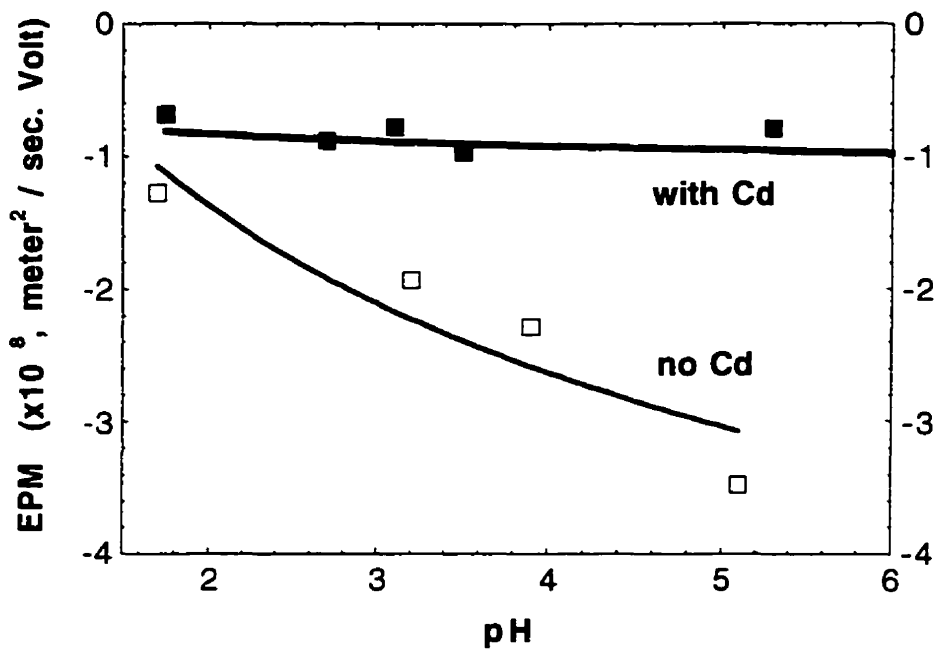
- a) as a function of the cadmium concentration;
 b) as a function of the copper concentration.

4.1.5 Surface Charge

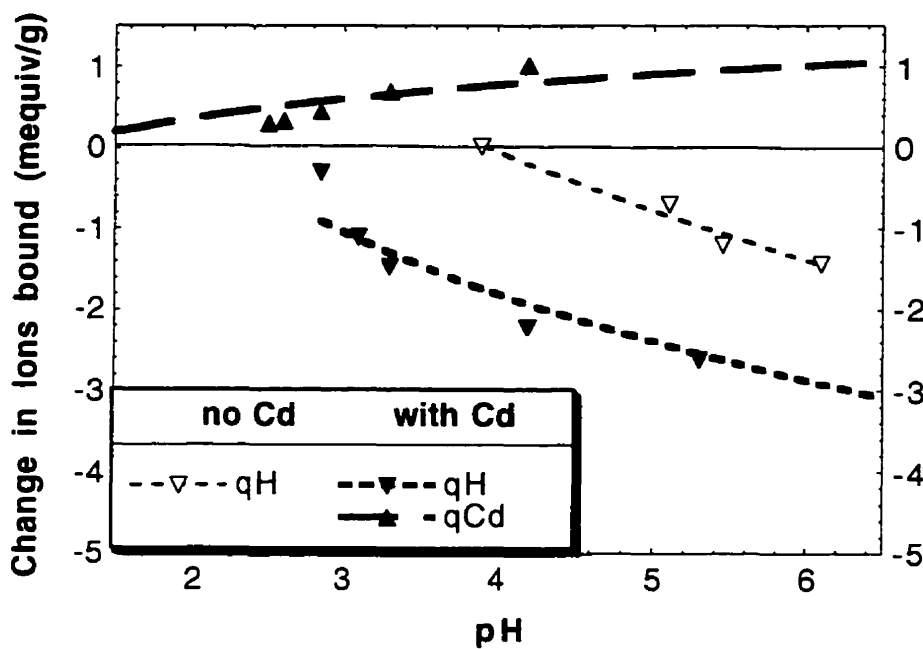
In order to investigate the effect of metal ion binding on the overall charge of the biomass, the electrophoretic mobility (EPM) was studied as a function of pH and metal ion concentration in solution (Figure 4.1.5). Between pH 2 and 6 the EPM, and therefore the charge of the biomass, was always negative, as the direction of the movement indicated. In the metal ion - free solution, the EPM decreased and the quantity of protons released increased with increasing pH. At higher concentrations of a heavy metal ion, however, the EPM remained constant at a small negative value while the metal ion binding increased, and the proton binding decreased with pH. The increase of the magnitude of the EPM with rising pH in a metal ion free solution can be explained by an increasing number of negatively charged deprotonated sites. The constancy of EPM as a function of pH in the presence of Cd indicated that the charge of the particle remained constant. This means that, at high metal ion concentrations, the charge of protons released with increasing pH equals the charge of metal ions taken up. Additionally, this indicates the importance of covalent binding in metal biosorption. Had the metal been bound only electrostatically (as *mobile* counter-ions) then a similar decrease of the EPM with increasing pH as in the case without metal would have been expected.

These results correlate with marine algal biomass findings of Kuyucak and Volesky (1989a) according to which a strong negative surface charge was present at pH 4-5. The magnitude of the surface charge decreased sharply when the pH was lowered to 3.

Collins and Stotzky (1992) found for bacteria and yeasts that with a higher pH (around 7) a surface charge reversal (to a positive charge) occurred in the presence of heavy metal ions (Cd, Cr, Cu, Ni, Zn) which did not take place in the presence of light metal ions (Na, Mg). This phenomenon was explained by a change in the solution speciation from the free hydrated ion to the still positively charged hydrolyzed species, which apparently was sorbed well. With a further increase in the pH, when the dominant hydrolyzed species in solution were neutral or negative, the sorption decreased, and a surface charge reversal back to negative values occurred. In the pH range investigated in this study, hydrolysis was negligible, and no such surface charge reversal could be observed.



a



b

Figure 4.1.5: Electrophoretic mobility and the change in binding of Cd and H by protonated *Sargassum* biomass as a function of pH (at a total Cd concentration of 0 or 3000 mg/L).

- a) electrophoretic mobility
- b) change in binding of Cd and H

4.1.6 Titrations

The curve representing the protonation state of the biomass during titration with 0.1 M NaOH in the metal ion free solution (Figure 4.1.6) showed an inflection at pH ~ 4.8. This indicated the presence of an acidic group with an apparent $pK_a \sim 4.8$, which constitutes approximately 2.0 mmoles per gram of biomass. This amount corresponds to the alginate content determined by Fourest and Volesky (1996) as described in section 2.2.6.2. The titration of protonated *Sargassum* biomass in the presence of 400 mg/L Cu (Figure 4.1.6) showed the protonation of the same number of sites (2.0 mequiv/g) as in the metal ion free solution. However, in the presence of metal ions, the inflection point shifted from pH 4.8 to pH 3.3. This indicated clearly the competition between metal ions and protons for the same binding sites. As these sites became occupied by metal ions, a higher proton concentration was needed to displace them and to achieve the same binding of protons, i.e. the apparent pK_a is lowered. The change in the metal ion binding with changing pH also equals approximately 2.0 mequiv/g. Therefore, it appears that all sites with the $pK_a = 4.8$ could be used for metal ion binding, with a ratio of 2 sites per divalent metal ion, thus conserving the charge of the biomass. This was further demonstrated by the mirror symmetry of the curves for the metal ion binding and proton release.

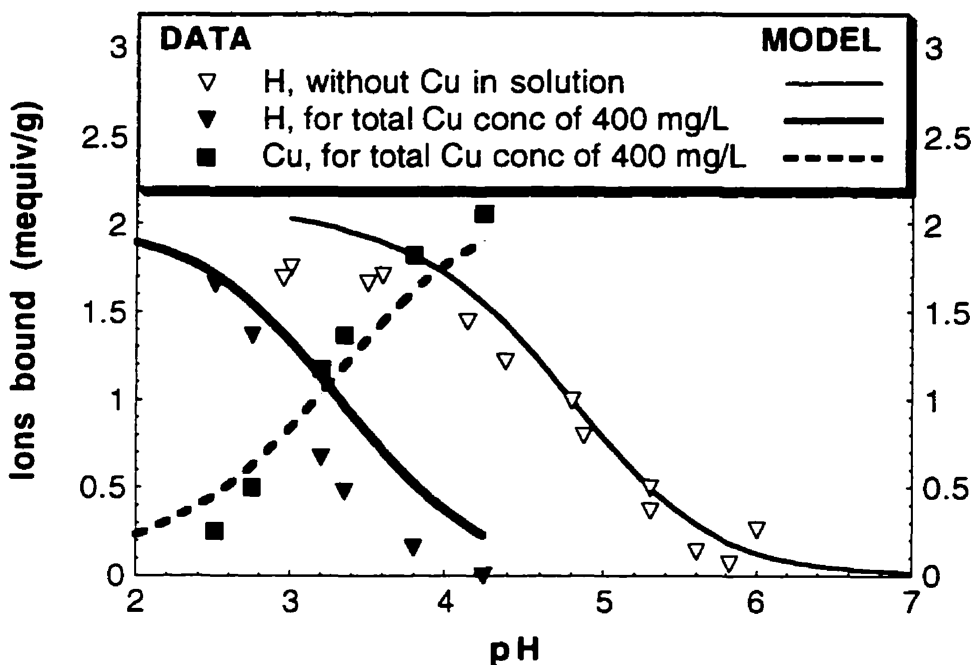


Figure 4.1.6:

Binding of Cu and H for titration of protonated *Sargassum* biomass
(total Cu concentration 0 or 400 mg/l; experimental data and 2 site model)

4.1 Results and Discussion: Mono-Metal Systems at different pH values

The curve for the metal ion binding does, however, not reach zero at pH 2. Again, this could be explained by metal ion binding to strong acidic groups which do not become protonated at pH 2 (the pH at which all carboxyl groups should be expected to be protonated). The proportion of this group was estimated from the biomass binding capacity at low pH to be 0.25 mequiv/g, as seen from the titration curve (Figure 4.1.6). In addition, this equals the amount of protons released when protonated biomass is equilibrated in distilled water, yielding pH 3.3 (Data not shown). An increase in proton concentration in solution by $10^{-3.3}$ mole/l corresponds to a decrease in proton binding by 0.25 mmol/g. At pH 3.3, strongly acidic sites should be mostly ionized. However, the degree of ionization of the weakly acidic groups (pK_a 4.8, 2 mequiv/g) was according to the model predictions only 0.06 mequiv/g (Data not shown). Therefore, the amount of protons released is predominately that which was bound to sulfate sites. The model for the titration curves is discussed in section 4.1.9 and 4.1.10.

The apparent $pK_a = 4.8$ exhibited in the titration of *Sargassum* biomass is in the range of carboxylic group pK_a 's. Crist et al. (1992) reported a pK_a between 5 and 7 for the carboxyl groups of marine algae. The pK_a of pure alginic acid is lower, however: 3.38 for mannuronic and 3.65 for guluronic acid, respectively (Haug, 1961a). Buffle (1988, pp. 251, 323) reported pK_a values between ~ 3 and 5 for carboxyl groups in different organic compounds. This deviation of the pK_a values in different compounds indicates the relevance of secondary effects such as different molecular environments or polyelectrolyte effects (see Section 4.4).

The involvement of carboxyl groups in metal binding by algal biomass has been reported in the literature. Gardea-Torresdey et al. (1990) observed that after the blocking of carboxyl groups of algal species by esterification, the binding capacity for Cu and Al decreased. This decrease was correlated to the degree of esterification. Recent results of Fourest and Volesky (1996) show that the blocking with propylene oxide of weakly acidic groups (pK_a near 5) in *Sargassum fluitans*, which are likely to be carboxyl groups, was 80 % effective and resulted in 80 -95 % reduction of the metal ion binding. This demonstrated the responsibility of weakly acidic groups for most of the metal ion binding.

The other, more strongly acidic group, which has a capacity of ~ 0.25 mequiv/g, is likely to be a sulfate group. Crist et al. (1992) reported the pK_a of biomass sulfate groups to be around 1.5. Fourest and Volesky (1996) determined the total number of sulfate groups in *Sargassum* as 0.27 mequiv/g. This is very close to the amount of strong acidic groups that was postulated from the titration and ion binding experiments (0.25 mequiv/g).

4.1.7 Sorption Isotherm Model

For quantitative description of biosorption, it would be very useful to develop a mathematical model capable of reflecting biosorption as a process that involves ion exchange between metal ions and protons as well as binding to non-protonated sites. Specifically, the influence of pH on the active sites has to be incorporated. In order to predict the final metal ion binding from the initial conditions, this model has to allow the calculation of the change of binding of the initially sorbed species.

A model is proposed in the present work that is simple and adequately accurate. It is capable of representing the relevant findings about the metal ion biosorption mechanism pertaining to marine brown algae materials. Theoretically, the modeling of adsorption could include terms for electrostatic attraction, specific chemical bonds (complexation of metal ions, acid base reactions) and solvation energies (Pagenkopf, 1978, pp. 224-226). Although it is likely that at least electrostatic attraction and chemical bonds contribute significantly to metal ion binding, both phenomena will for now be lumped into one constant. Since acid-base reactions which are not electrostatic play an important role, and since sorption is known to be specific, the choice is to express the binding in this first model version through overall chemical equilibrium constants. This is supported by the results for the EPM in the presence of Cu which clearly indicated significant covalent binding. Additionally, the number of apparently free sites is small compared to the total number of binding sites for $\text{pH} \leq 4.5$ and therefore the surface charge density (and thereby the electrical potential) may be small as well, especially since the charges are not concentrated on the particle surface but distributed throughout the particle volume. It has to be noticed, however, that these chemical equilibrium constants are not thermodynamically well defined and that they may deviate from constancy when the activity of an ion in the matrix differs from its activity in the bulk solution (Stumm and Morgan, 1970, pp. 489). For further improvement of the model, a separate term for electrostatic attraction will be considered in Section 4.4 and 4.5. Although this also is a simplification, it is assumed that the biomass contains 2 homogeneous groups which are solely responsible for the binding. From the experimental results for the *Sargassum* biosorbent, it follows that one site largely consists of carboxyl groups (in the following called group C), while the second group (called S) is a sulfate group (see above). One divalent metal ion reacts with two such monovalent groups. The reactions considered are:



4.1 Results and Discussion: Mono-Metal Systems at different pH values

$$K_{CH} = \frac{[CH]}{[C][H]} \quad (4.1.1b)$$



$$K_{SH} = \frac{[SH]}{[S][H]} \quad (4.1.2b)$$



$$K_{CM} = \frac{[CM_{0.5}]^2}{[C]^2 [M]} \quad (4.1.3b)$$



$$K_{SM} = \frac{[SM_{0.5}]^2}{[S]^2 [M]} \quad (4.1.4b)$$

The formulation $2 CM_{0.5}$ is chosen instead of C_2M in order to stress that, for desorption, 2 bonds between the metal ion and biomass have to be broken. The likelihood of the bonds to the two sites that chelate one divalent metal ion being broken at the same time is the square of the likelihood of one bond to one carboxyl group being broken. This is in turn proportional to the number of occupied sites. Therefore, a reaction order of two is expected for desorption of a metal ion that is chelated to two sites. This should occur in the case of specific competitive binding where not only electrostatic attraction but also complexation is relevant (Buffle, 1988, pp. 278-286). The formation constants can easily be transformed into ion exchange constants or selectivity coefficients by dividing equation (4.1.3) by the square of equation (4.1.1).

It is convenient to use explicit sorption isotherm equations where the binding of one species can be calculated from the final concentrations of all species directly. The above equations can be reformulated into modified multi-component Langmuir sorption isotherms as adapted from Hill (1977, pp. 173-177):

$$^m q = CM_{0.5} + SM_{0.5} = \frac{C \sqrt{K_{CM} [M]}}{1 + K_{CH} [H] + \sqrt{K_{CM} [M]}} + \frac{S \sqrt{K_{SM} [M]}}{1 + K_{SH} [H] + \sqrt{K_{SM} [M]}} \quad (\text{mequiv/g}) \quad (4.1.5)$$

4.1 Results and Discussion: Mono-Metal Systems at different pH values

$$q = CH + SH = \frac{C^{CH} K [H]}{1 + C^{CH} K [H] + \sqrt{C^{CM} K [M]}} + \frac{S^{SH} K [H]}{1 + S^{SH} K [H] + \sqrt{S^{SM} K [M]}} \quad (\text{mequiv/g}) \quad (4.1.6)$$

Although the mathematical form of these isotherm equations is similar to the one for Langmuir type adsorption of several competing metal ions to *free* sites (for example Chong and Volesky, 1995), a very different principle lies behind the formulation. In the present case, the isotherm describes *exchange* reactions, not a simple competition for free binding sites. The main difference is the consideration of the reverse reaction, which depends on the final concentration of the displaced ion (in this case the proton) in solution (or if pH is controlled it affects the amount of acid or base added), which in turn depends on the initial loading of the biomass with exchangeable species.

With the above equations it is possible to determine the equilibrium bindings of metal ions and protons as a function of the final pH and metal ion concentration. These parameters themselves are, however, not independent variables (although they are often treated as such in isotherm models, since they can be determined directly) but they depend on the initial loading of the sorbent, pH and concentrations.

In order to predict the complete final state of the sorption system (the cation concentrations in the solution, as well as adsorbed) from the known initial state, it is necessary to include the mass balances of all species ((3.3.2) - (3.3.5)) as additional equations. Since there is no explicit analytical solution to these equations, the calculations are conveniently done by mathematical equilibrium programs that perform the necessary iterations. In this case, the program MINEQL+ (Schecher, 1991) has been used for this purpose. The necessary input parameters are the total concentrations of all species (tH , tM , tC , tS) as well as the equilibrium constants.

4.1.8 Determination of the Model Parameters

The sorption model parameters that best fit the data were determined by applying the computer program MATLAB 4.2c, such that the average absolute error of the metal ion binding values for all experiments was minimized.

Three types of models were considered in the following:

- I a simple classical Langmuir model as described in section 2.4.1. This model assumes only one type of binding sites and that each divalent ion binds to one site.

4.1 Results and Discussion: Mono-Metal Systems at different pH values

All parameters (q_{\max} , K) are determined individually not only for each specific metal but also for each specific pH value.

- II a new type of one site model (equations 4.1.5 and 4.1.6 with ${}^tS = 0$, i.e. assuming no sulfate sites) that assumes that a divalent metal ion binds to two binding sites. For this one site model, two cases are distinguished:
- a) a new set of constants (tC , CHK , CMK) is determined for each metal ion
 - b) tC , CHK are determined once for all three metals, only CMK is determined individually for each metal ion

In either case, the constants are valid for all pH values and the average error of metal ion and proton binding was minimized, since the CHK values still had to be determined.

- III a new type of two-site model that also assumes that a divalent metal ion binds to two binding sites. The parameters tC , tS and CHK were fixed at those values obtained in the titration experiments. By this process, instabilities in the optimization process could be avoided that might occur if too many parameters are optimized simultaneously. SHK was assumed to be $10^{2.5}$ in order to fit the desorption data of Aldor et al. (1995). Using this approach, the parameters that characterize the biomass are the same for all three metal ions. Only CMK and SMK had to be determined for each metal. All parameters are valid for any pH value.

The parameters for the one-site model (IIa and IIb) and for the two-site model (III) are summarized in Table 4.1.1. The constants for the Langmuir model are listed in Table 4.1.2. The Langmuir model and the two site model are compared in section 4.1.10.

4.1.9 Modeling of Experimental Data

For the one-site model (Table 4.1.1, case IIa) it was possible to find parameters tC , CHK , CMK for each metal ion in such a way that the experimental data could be well represented. However, the values determined for CHK and tC were obtained by curve fitting, and they did not correspond to the values that were determined experimentally by titration (Figure 4.1.6). Furthermore, they were different for each metal ion, although the different metal ions should be using the same sites. When the same values for CHK , and tC are used for all 3 metal ions (Table 4.1.1, case IIb), the accuracy of the one-site model decreased. Specifically, the predictions of the one-site model were too high for pH 4.5 and too low for the low pH values (Figure 4.1.2d), because the availability of non-protonated, easily accessible S sites is not given in that model.

4.1 Results and Discussion: Mono-Metal Systems at different pH values

Table 4.1.1

Model parameters for the 1-site and the 2-site sorption models

Number of Sites	Metal	CHK [L/mol]	CMK [L/mol]	tC [mequiv/g]	SHK [L/mol]	SMK [L/mol]	tS [mequiv/g]	Std. Dev.* [mequiv/g]
1 site (case IIa)	Cd	$10^{4.0}$	$3.3 \cdot 10^3$	2.7	-	-	0	0.22
	Cu	$10^{5.3}$	$5.1 \cdot 10^5$	2.4	-	-	0	0.28
	Zn	$10^{3.9}$	$7.4 \cdot 10^2$	3	-	-	0	0.66
1 site (case IIb)	Cd	10^5	$2.0 \cdot 10^5$	2.7	-	-	0	0.28
	Cu	10^5	$2.9 \cdot 10^5$	2.7	-	-	0	0.34
	Zn	10^5	$4.5 \cdot 10^4$	2.7	-	-	0	0.34
2 sites (case III)	Cd	$10^{4.8}$	$8 \cdot 10^4$	2	$10^{2.5}$	$0.8 \cdot 10^3$	0.25	0.092
	Cu	$10^{4.8}$	$20 \cdot 10^4$	2	$10^{2.5}$	$3.7 \cdot 10^3$	0.25	0.22
	Zn	$10^{4.8}$	$1 \cdot 10^4$	2	$10^{2.5}$	$0.5 \cdot 10^3$	0.25	0.172

Initially protonated biomass of *Sargassum fluitans* was used.

Model parameters were determined from 5-6 experimental points for each pH (2.5, 3.0, 4.5) and metal (Cd, Cu, Zn).

* Standard deviations refer to M_q

Therefore, a two-site model should be used, especially if the behavior of different metal ions is to be described by the same model. The two-site model uses only 2 parameters, CMK and SMK to fit the metal ion and proton binding for each of the 3 different pH values (tC , CHK and tS were fixed at the values obtained by titration). Considering the relation between the variety of modeled conditions and the number of parameters, which does not allow for individual fitting of the data in one particular graph but demands that the data in all graphs of this section (4.1) are fitted by one set of constants, the fit is quite good (Table 4.1.1), both for the binding of the heavy metal ions at different pH values (Figure 4.1.2 and Figure 4.1.3) and for the binding of protons (Figure 4.1.3): the standard deviation of 0.16 mequiv/g (average for the three metals) corresponds

4.1 Results and Discussion: Mono-Metal Systems at different pH values

to 7 % of the maximum uptake. This is a similar magnitude as the experimental errors (Section 4.3). When judging the fit of the model it has to be kept in mind that the same set of parameters (Table 4.1.1) is used for modeling all figures in section 4.1. Especially for a heterogeneous biological material like *Sargassum* it can not be expected that a model fits all data equally well. Obviously, it is a simplifying assumption to represent the multitude of chemical compounds present in this material by two binding groups.

The fact that the trends in the titration curves are modeled well (Figure 4.1.6) shows that the pK's of weakly acidic groups do not differ widely. They can be approximated by a single pK value 4.8. It is therefore not necessary to use affinity spectra for the binding groups. It can also be seen from Figure 4.1.6 that the model can be extrapolated over the entire region of pH 2 to 6. Further improvement can be expected when electrostatic effects are included in the model (sections 4.4 and 4.5).

4.1.10 Influence of pH:

Comparison Model vs. Langmuir approach

A major advantage of the model presented here in contrast with simple isotherm models is that both the effect of pH on sorption as well as the change of pH during the sorption process or the required amount of acid or base for pH adjustment can be predicted. Neither the Langmuir nor the Freundlich isotherm model in their simple form include the pH value as one of the variables. If these modeling approaches are used, it is therefore not possible to predict changes in proton binding.

Also, the respective constants of those simple models have to vary with pH since binding changes with pH. To illustrate this by an example, the Langmuir constants that enabled the best fit for each of the series in Figure 4.1.2a-c are listed in Table 4.1.2. Both q_{\max} (corresponding to the number of sites tC) and K (related to the equilibrium constant) for the Langmuir model strongly increase with pH. Additionally, the number of binding sites, q_{\max} , determined by fitting the Langmuir model varies among the metals. At both pH values Zn has significantly lower q_{\max} than the other two metals. Consequently, a multi-component Langmuir model that accounts for competition among the ions for the same binding sites (i.e. that would have the same q_{\max} for all ions, such as the one used by Chong and Volesky (Chong and Volesky, 1995)) would also be expected to over-predict the Zn binding as the two-site model does. The constants for the simple Langmuir model whose predictions are depicted in Figure 4.1.2a-c were individually fitted to each of the isotherms in Figure 4.1.2a-c (so that for each set of 5-6 data points at constant pH two parameters are determined, i.e. a total of 18 parameters was determined in order to fit the binding of three metals at three pH values each).

4.1 Results and Discussion: Mono-Metal Systems at different pH values

For the two site model, on the other hand, the number of sites for metal binding was derived from a pH titration in the absence of metals (and not fitted to each isotherm) and the binding constants are independent of pH (for all data at different pH two parameters are necessary per cation and additionally two for the site quantities, adding up to a total of 10 parameters).

Summarizing the main differences between the two models one has to distinguish between some very different advantages, being the quality of fit versus the flexibility of the model (whether it can be applied to different conditions). The fit of the Langmuir model is generally better than for the two-site model (the absolute mean square errors expressed in % of the total binding capacity 'B are listed in Table 4.1.2). This occurs because the data of each isotherm have been individually fitted using a new set of constants. The main advantage of the two site model, on the other hand, is that it does not require the determination of a new set of parameters for each pH value, i.e. that it allows for the prediction of the influence of pH on metal binding. The Langmuir model can be used if isolated isotherm are to be described. The application of the two site model is recommendable when biosorption at different conditions shall be predicted.

Table 4.1.2 Parameters for the Langmuir model and absolute mean square errors expressed in percent of the total binding capacity

Metal pH	Cd		Cu		Zn	
	4.5	2.5	4.5	2.5	4.5	2.5
Langmuir parameters						
q_{\max} (mequiv/g)	2.04	0.62	2.12	0.51	1.33	0.21
K (L/mmol)	7.72	0.40	8.17	1.40	12.2	0.52
Error in % of 'B						
Langmuir	10.0	1.9	2.3	1.9	2.7	0.7
2-site model	4.8	4.5	16.8	2.4	8.1	1.3

In order to illustrate the extent to which the Langmuir parameters vary when biosorption over a broader pH range than in Figure 4.1.2 and Table 4.1.2 is considered, the Langmuir constants q_{\max} and K are summarized in Table 4.1.3 for pH 2-7. Since the

4.1 Results and Discussion: Mono-Metal Systems at different pH values

simple Langmuir model and the modified Langmuir model described in this work give different sorption isotherm shapes, the Langmuir parameters were determined such that the Langmuir sorption isotherm equals the predictions of the presented model both at $[M] = 0.1$ mmol/L (representing the initial slope region) and at $[M] = 10$ mmol/L (representing the maximum saturation region).

Note that although an accurate experimental determination of the Cu binding above pH 5 is not possible due to precipitation, the equilibrium relationship of equation (4.1.5) between free Cu^{2+} in solution and sorbed Cu is still valid. The respective reaction constants are unchanged, only the concentration of free ions in the solution is lowered due to precipitation. The Langmuir parameters in Table 4.1.3 have been derived by approximating equation (4.1.5), not the experimental data. Consequently, they are also valid at the higher pH values where they could not be determined experimentally.

Table 4.1.3 Variation of Langmuir sorption parameters with pH

METAL	pH	2	3	4	5	6	7
Cd	q_{\max} [mmol/g]	0.3	0.6	1.9	2.5	2.6	2.6
	$K \cdot q_{\max}$ [L/g]	1.1	1.5	5.0	14	17	18
Cu	q_{\max} [mmol/g]	0.3	0.9	2.2	2.6	2.7	2.7
	$K \cdot q_{\max}$ [L/g]	1.5	2.3	7.8	18	21	21
Zn	q_{\max} [mmol/g]	0.2	0.3	1.3	2.2	2.4	2.4
	$K \cdot q_{\max}$ [L/g]	0.7	1.0	2.8	9.1	13	13

Initially protonated biomass of *Sargassum fluitans* was used.

It is often stated in the literature that there is little difference between biosorption at pH 4 and 5 (Kuyucak and Volesky, 1989a; Tsezos and Volesky, 1981). Indeed, q_{\max} does not change much above pH 4.5. The product ($q_{\max} \cdot K$) which corresponds to the initial slope of the isotherm, however, increases up to about pH 6. This means that for

4.1 Results and Discussion: Mono-Metal Systems at different pH values

high metal ion concentrations pH 4.5 is already close to being optimal. For low metal ion concentrations, however, a significant increase in the metal ion binding can be achieved by raising the pH to 5.5 or 6 which is shown in Figure 4.1.7. The modeling exercise confirmed that sorption of Cd and Zn in the low concentration range can be optimized by increasing the pH to 6, where still no hydrolysis or precipitation occurs for these metal ions. For Cu, pH 4.5 can be maintained as optimal because of the danger of precipitation for $\text{pH} > 5$. When studying the biosorption process, it is essential to maintain pH values below the metal ion precipitation range in order to avoid its unpredictable effects on the metal ion removal from solution. However, under process conditions where the maximum metal ion removal is desired, precipitation may increase the overall metal ion removal efficiency which is reflected in the elevated overall process metal ion concentration ratio values achievable.

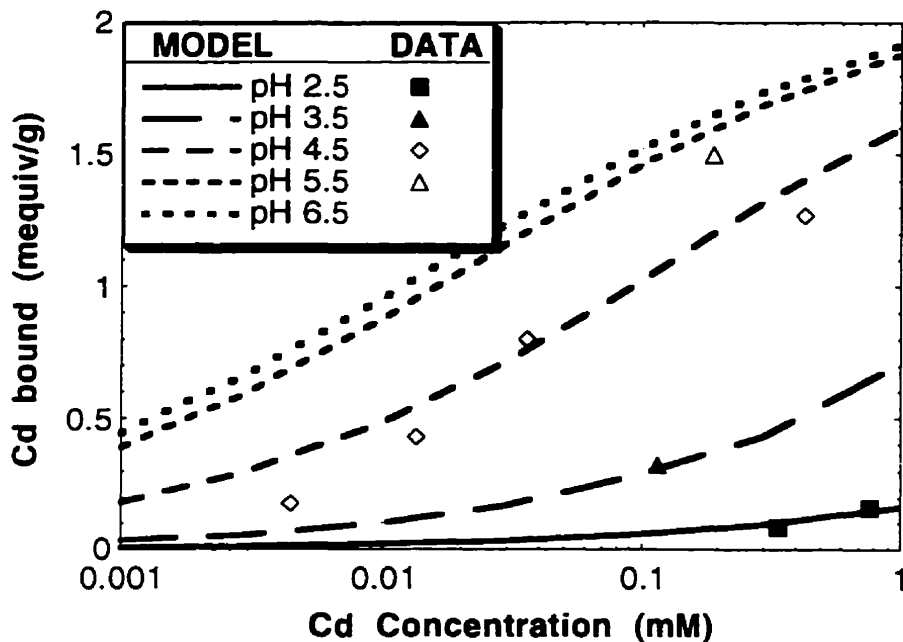


Figure 4.1.7: Isotherms of Cd for different pH values at low concentrations
(experimental data and the 2-site model).

4.1.11 Prediction of the Desorption Equilibrium

Modeling attempts of competitive metal ion desorption have been rare. Desorption is frequently achieved by acid washing, in which case it can be represented by the two site model. The description of the desorption efficiency is complicated by the use of a number of the following characteristic process parameters which are commonly employed: the solid-to-liquid ratio (S/L), the initial metal ion loading of the sorbent, the concentration of the desorbing acid, the equilibrium pH value, % of elution, the overall process concentration ratio, and types of eluants, biomass and metal ions (Kuyucak and Volesky, 1989b; Aldor et al., 1995).

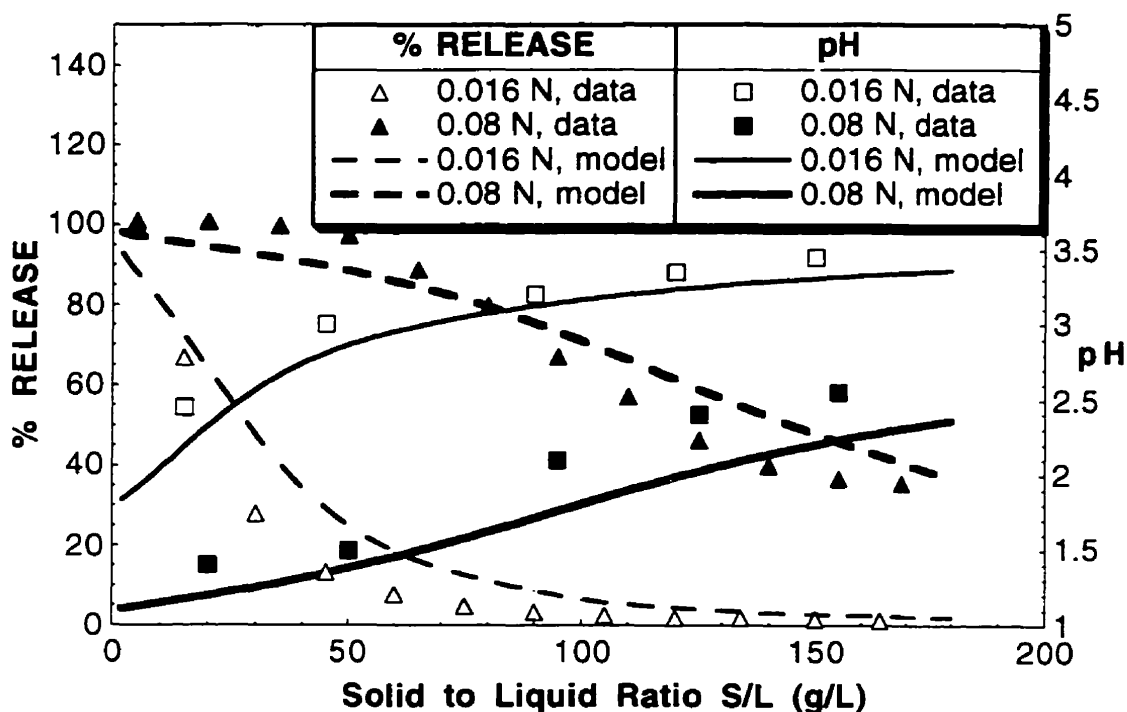


Figure 4.1.8: Cd release and the final pH during desorption with HCl as a function of the S/L ratio

(0.08 and 0.016 N HCl; initial Cd binding 33 mg/g; experimental data of Aldor (personal communication) and the 2-site model).

4.1 Results and Discussion: Mono-Metal Systems at different pH values

Given the type of biomass, the metal ion and the eluant (acid), it only is necessary to specify the CMK and SMK for the model developed here in order to describe the desorption behavior for any combination of independent parameters. All of the other parameters either are specific, arbitrarily chosen initial conditions, or dependent variables that can be calculated from the initial ones by using the model. For any biomass that can be described using this model, the complete desorption behavior is very conveniently characterized by 2 constants. Thus it is superfluous to mention the details concerning the initial and final conditions.

To calculate the parameters for the equilibrium state (pH, binding, concentrations) a model like MINEQL+ requires only the information concerning the equilibrium constants as well as the total concentrations expressed in mol/L, i.e. the total concentrations from equations (3.3.2) - (3.3.5) were divided by V (and multiplied by m for tC and tS).

An example of such desorption modeling is shown in Figure 4.1.8 for different initial acid concentrations and for solid-to-liquid ratios as independent variables.

The experimental points are from recent results by Aldor (personal communication). Since the initial proton binding was unknown, it was assumed that it was 1.4 mequiv/g, which is the value obtained from the model for $M_q = 0.296$ mmol/g at pH 3.8, as obtained by Aldor (personal communication). The model is able to predict the influence of S/L ratio and initial acid concentration on elution efficiency and final pH. Considering that this is the first time in biosorption that desorption has been modeled, the results are encouraging.

4.1.12 Section Summary

The exchange between metal ions and protons was the major binding mechanism in biosorption by protonated biomass. Experiments showed the relevance of two specific biomass binding sites in metal ion sequestering. One weakly acidic site, with an apparent pK_a around 4.8, was responsible for the main part of the binding, and a strongly acidic site was present to a smaller extent. The contribution of the strongly acidic group to metal ion binding was significant at low pH. A model that considers reversible binding of metal ions and protons to two types of binding sites was used to describe metal ion - proton exchange. The binding of metal ions and protons could be predicted as a function of metal ion concentration and pH. It was possible to use the same model for both adsorption and desorption.

It is recommended to use the two-site model instead of Langmuir or Freundlich isotherm models in order to accommodate the significance of ion exchange in biosorption. Although the version of the multi-component Langmuir model presented here (equations (4.1.5) and (4.1.6)) applies for the sorption of divalent ions or protons onto sites which are free or occupied by the other respective ion, the model can be easily modified to account for different competing ions. Furthermore, in that form it can be appropriate for other than protonated biosorbents where ion exchange is predominant.

4.2 Multi-Metal Systems at different pH values

Practical attempts to apply biosorption in the purification of industrial wastewaters will rarely encounter a wastewater which contains only one type of metal ion. Therefore, it is desirable to be able to predict the binding of one type of ion in the presence of several different metal ion types. Also of interest is the recovery of one specific metal ion after sorption in a multi-metal system. One possibility for recovery is selective desorption where one metal may be released while another one remains bound to the biomass.

It has been demonstrated for other biosorption systems that there is competition between different metal ions for the same binding sites (Chong and Volesky, 1995). This section presents experimental data on the extent to which metal ions interfere with each other in binding to *Sargassum* biomass. An appropriate mathematical treatment that reflects this type of interaction will also be presented. The sorption model from Section 4.1 is extended so that ion exchange in multi-metal systems involving multiple binding sites can be described. The sorption performance prediction by the extended sorption model is examined for a specific typical multi-metal system.

The results presented in this section have in modified form been published in Schiewer and Volesky (1996).

4.2 Results and Discussion: Multi-Metal Systems at different pH values

4.2.1 Multi-Component Sorption Isotherm Model

Multi-component Langmuir isotherms for one binding site and formation of 1:1 sorbate/sorbent complexes have been described by Hill (1977, pp. 173-177). A case including one gaseous species that occupies two sites after dissociation was also considered by that author.

These multi-component isotherms were adapted for the case of multi-site and multi-ion biosorption for different ion-valences. Since biosorption by seaweed biomass is largely an ion-exchange phenomenon, it was assumed that each cationic species sorbs to the number of monovalent ionized groups which is equal to the charge of the cation, such that the overall charge is preserved. The equation for a cation ${}^j\text{M}$ of charge z_j sorbing to a binding site ${}^i\text{B}$ is, for ideal behavior (all activity coefficients equal to unity):



$${}_{ij}\text{K} = \frac{[{}^i\text{B} {}^j\text{M}_{1/z_j}]^{z_j}}{[{}^i\text{B}]^{z_j} [{}^j\text{M}]} \quad (1/\text{mM}) \quad (4.2.1b)$$

The first character of the upper left index of the equilibrium constant refers to the binding site, the following to the sorbed ion. Protons are treated as one of the monovalent species with $z_j = 1$. Divalent ions form ${}^i\text{B}{}_2\text{M}_{0.5}$ complexes.

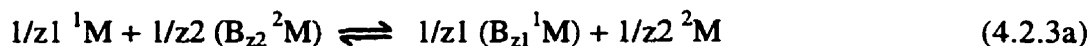
Note that the term $z_j {}^i\text{B} {}^j\text{M}_{1/z_j}$ has been chosen instead of ${}^i\text{B}_{z_j} {}^j\text{M}$ because it implies that z_j bonds have to be broken for the release of a z_j -valent ion, i.e. the dissociation reaction is of the order z_j and not of the order one as would be the case for the dissociation of a ${}^i\text{B}_{z_j} {}^j\text{M}$ species. According to Buffle (1988, pp. 278-286), the former version should be preferred over the latter when specific complexation instead of non-specific electrostatic attraction is the binding mechanism. In biosorption, selectivity for specific ions is high (see preceding section) and therefore ${}^i\text{B} {}^j\text{M}_{1/z_j}$ complexes were assumed. This choice is in agreement with the experimental data (see discussion of Figure 4.2.1 and 4.2.5).

Although equation (4.2.1) expresses sorption to free sites, ion exchange can be modeled when the corresponding equations for all exchanged ions are included because the ion exchange constant is obtained by simply dividing the z_j^{th} root of the binding constant (equation (4.2.1)) for one ion by the respective root for the other ion:

$$\text{K}_{\text{exch}} = \frac{{}^{\text{B}1}\text{K}^{1/z_1}}{{}^{\text{B}2}\text{K}^{1/z_2}} = \frac{[{}^{\text{B}1}\text{M}_{1/z_1}] [{}^2\text{M}]^{1/z_2}}{[{}^{\text{B}2}\text{M}_{1/z_2}] [{}^1\text{M}]^{1/z_1}} \quad (\text{mM}^{z_1/z_2}) \quad (4.2.2)$$

4.2 Results and Discussion: Multi-Metal Systems at different pH values

If the term $B_{z_j}^j M$ were chosen (i.e. $B_{z_j}^j M$ complexes form for divalent ions), the exchange constant for the reaction



would be:

$$K_{\text{exch}} = \frac{[B_{z_1} {}^1M]^{1/z_1} [{}^2M]^{1/z_2}}{[B_{z_2} {}^2M]^{1/z_2} [{}^1M]^{1/z_1}} \quad (-) \quad (4.2.3b)$$

This corresponds to the commonly known ion exchange constant in the literature (Marcus and Kertes, 1969, pp. 277; Reddy, 1977, pp. 185) which has also been used for the description of biosorption of multivalent ions (Crist et al., 1994; Haug and Smidsrod, 1970).

Instead of using ion exchange constants where the binding of each metal ion can only be obtained by repeated iterations, it is useful to have an explicit isotherm expression which relates the binding of a species to the concentrations of all species such that the binding can be calculated directly. It is assumed that secondary interactions are negligible and that there is no other influence of the other cation than competition for the same binding sites. For the reaction of the ion jM in a system with n cations and m binding sites it follows then from equation (4.2.1):

$${}^j q = \sum_{k=1}^m [{}^k B {}^j M]_{1/z_j} = \sum_{k=1}^m K^t B \frac{({}^k j K [{}^j M])^{1/z_j}}{1 + \sum_{h=1}^n ({}^k h K [{}^h M])^{1/z_h}} \quad (\text{mequiv/g}) \quad (4.2.4)$$

4.2.1.1 Comparison to Other Isotherms

If only one site is present (i.e. $m = 1$) equation (4.2.4) can be regarded as a specific case of the Fritz - Schluender isotherm (Fritz and Schluender, 1974) which, however, needs $n(2n + 3)$ parameters in order to describe a n -solute system (i.e. 14 for a 2-solute system). The model presented here needs only $(n+1)$ parameters (i.e. 3 for a 2-solute system) for the one-site case and $(2n+2)$ for the two-site case. Since the exponents $1/z_j$ are related to the ion valence, they do not constitute adjustable parameters. Since the Fritz-Schluender isotherm needs such a high number of constants, it has frequently been used in different simplified forms (Crittenden and Weber, 1978; Liapis and Rippin, 1977) which include the so called Langmuir-Freundlich isotherm (Ruthven, 1984, pp. 108).

Timewise parallel to the work presented here, a multi-component isotherm was recently developed by Koopal et al. (1994) and used by Benedetti et al. (1995). The model

4.2 Results and Discussion: Multi-Metal Systems at different pH values

was able to predict metal binding at different pH quite well, the amount of protons released per metal bound was, however, underestimated in some cases because the model assumed a 1:1 stoichiometry between metal ions and binding sites.

Koopal's two-site isotherm model differs from classical multi-component isotherms in that it includes exponents in order to account for non-ideal behavior and site heterogeneity. These exponents constitute additional fitting parameters. Consequently, it is necessary to determine many parameters in order to apply the model. The authors recognize that this may not always be easy and therefore propose different simplifications which can lead to a two-site Freundlich isotherm.

Parallels to this work exist in the structure of the resulting isotherm. The model case for discrete sites (i.e. Koopal's exponent "p" = 1) closely resembles equation (4.2.4). However, while the exponents $1/z_j$ in equation (4.2.4) are fixed values related to the charge and number of sites occupied by an ion, the "non-ideality" parameters "n" in Koopal's isotherm have to be obtained through curve fitting. It is interesting to note, that the resulting parameters obtained for binding of Cu, Cd, Ca and H to a humic acid containing carboxyl and phenolic groups averaged 0.81 for proton binding (0.91 for H binding to carboxyl sites) and 0.56 for the divalent ions (Benedetti et al., 1995). This resembles the exponents 1.0 for H and 0.5 for divalent ions used in this work. It would be interesting to investigate how well the exponents "n", which are supposed to account for non-ideality, may reflect the charge or stoichiometry as they do in this work.

The other exponent in Koopal's isotherm is supposed to account for the site heterogeneity, reflecting decreasing binding strength with an increasing degree of site occupation. Instead of assuming site heterogeneity, the effect of decreasing binding strength can also be interpreted as the result of electrostatic effects. This avenue was chosen in this work and further described in Sections 4.4 and 4.5. The fact that the heterogeneity parameter was significantly smaller than 1.0 does not necessarily indicate that site heterogeneity is an important factor.

4.2.1.2 Two Site Version Applied for *Sargassum*

The binding sites in *Sargassum* biomass are believed to be mostly the carboxyl groups of alginate (signified by C) and the sulfate groups of fucoidan (referred to as S sites) (see Sections 2.2 and 4.1). Therefore, the model case including these two sites, C and S groups, was chosen for the sorption system presently considered. In a system of two divalent metal ions 1M and 2M as well as protons (H) equation (4.2.4) is reduced to

4.2 Results and Discussion: Multi-Metal Systems at different pH values

$${}^i q = {}^i C \frac{(C^1 K [^1 M])^{1/2}}{1 + C^H K [H] + (C^1 K [^1 M])^{1/2} + (C^2 K [^2 M])^{1/2}} + {}^i S \frac{(S^1 K [^1 M])^{1/2}}{1 + S^H K [H] + (S^1 K [^1 M])^{1/2} + (S^2 K [^2 M])^{1/2}} \quad (\text{mequiv/g}) \quad (4.2.5)$$

$${}^H q = {}^i C \frac{C^H K [H]}{1 + C^H K [H] + (C^1 K [^1 M])^{1/2} + (C^2 K [^2 M])^{1/2}} + {}^i S \frac{S^H K [H]}{1 + S^H K [H] + (S^1 K [^1 M])^{1/2} + (S^2 K [^2 M])^{1/2}} \quad (\text{mequiv/g}) \quad (4.2.6)$$

In order to predict final concentrations and binding from the initial conditions, the equilibrium program MINEQL+ was used (for a review of different equilibrium programs see (Nordstrom and Ball, 1984)). As input parameters it is necessary to specify the total concentrations of all species and the equilibrium constants. The model iteratively computes the final speciation of each component in solution as well as the formation of solid compounds.

4.2.2 Reaction Stoichiometry

Fogler (1986, pp. 238-244) recommends plotting $[M]^{0.5} / M_q$ versus $[M]^{0.5}$ in order to confirm sorption according to the equation $2B + M \rightleftharpoons 2BM_{0.5}$. This can be applied to the system under investigation. Although protons are always present, the system may be treated as a one-ion system when pH is constant because the presence of protons reduces the number of free sites by a constant factor (because $BH / B = {}^{BH}K [H] = \text{const}$). Additionally, it is assumed that Na, which was introduced into the system by pH adjustment, has (at the concentration levels employed here) no influence on heavy metal ion binding because it is only bound by weak electrostatic forces. For one site, equation (4.2.5) is reduced to

$$M_q = {}^i B ({}^{BM} K [M])^{0.5} / (1 + {}^{BH} K [H] + ({}^{BM} K [M])^{0.5}) \quad (\text{mequiv/g}) \quad (4.2.7a)$$

4.2 Results and Discussion: Multi-Metal Systems at different pH values

This can be linearized as

$$\frac{[M]^{0.5}}{M_q} = \frac{1 + {}^B H K [H]}{{}^B M K^{0.5} [B]} + \frac{[M]^{0.5}}{[B]} \quad (\text{mol g / mequiv L}) \quad (4.2.7b)$$

If $BM_{0.5}$ complexes are formed, the plotting of $[M]^{0.5} / M_q$ versus $[M]^{0.5}$ should yield a straight line. The results for sorption of all three metals at pH 4.5 are plotted in Figure 4.2.1a. A straight line describes the data well (Cd: R = 0.99, Cu: R = 0.98, Zn: R = 0.96). On the other hand for the reaction



$${}^B M K = [B_2M]^{0.5} / ([M]^{0.5}[B]) \quad (\text{mol g / mequiv L})^{0.5} \quad (4.2.8b)$$

it follows that

$$\frac{[M]^{0.5}}{M_q^{0.5}} = \frac{\frac{[B]}{[B]} + \frac{[BH]}{[B]} + \frac{2[B_2M]}{[B]}}{\sqrt{2} {}^B M K [B]} \quad (\text{mol g / mequiv L})^{0.5} \quad (4.2.9a)$$

This can be written as:

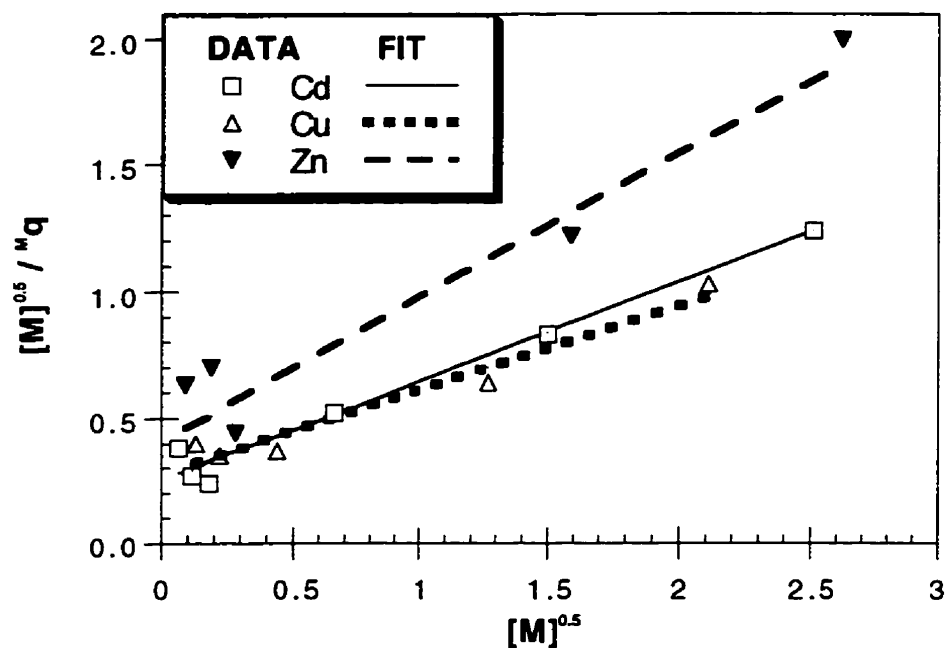
$$\frac{[M]^{0.5}}{M_q^{0.5}} = \frac{1 + {}^B H K [H]}{\sqrt{2} {}^B M K [B]} + \frac{2 {}^B M K [M]^{0.5} [B_2M]^{0.5}}{\sqrt{2} {}^B M K [B]} \quad (\text{mol g / mequiv L})^{0.5} \quad (4.2.9b)$$

Therefore, the following linearized uptake relationship is proposed in this work:

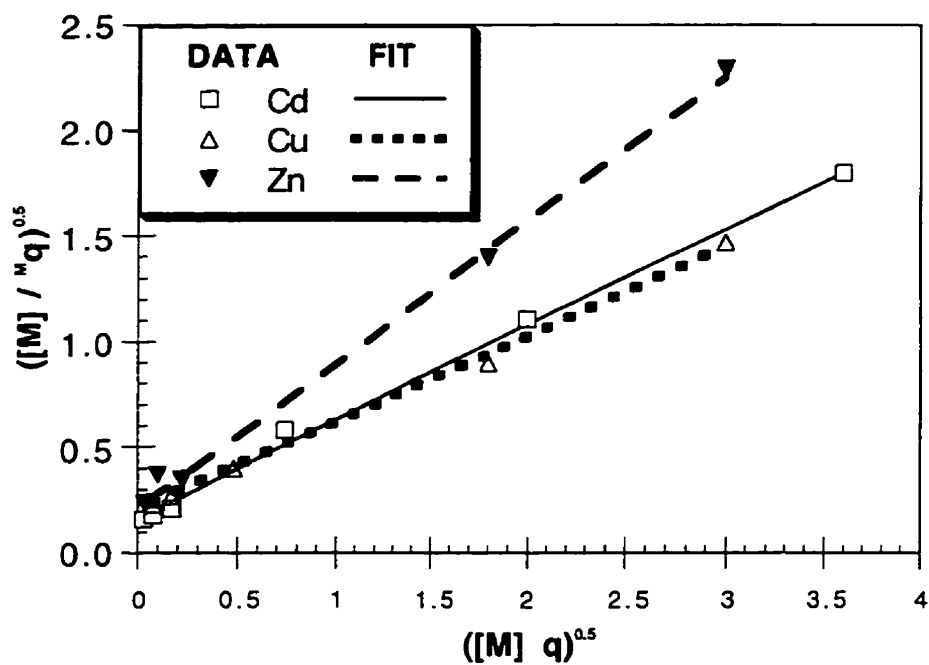
$$\frac{[M]^{0.5}}{M_q^{0.5}} = \frac{1 + {}^B H K [H]}{\sqrt{2} {}^B M K [B]} + \frac{[M]^{0.5} q^{0.5}}{[B]} \quad (\text{mol g / mequiv L})^{0.5} \quad (4.2.10)$$

A plot of $[M]^{0.5} / M_q^{0.5}$ versus $[M]^{0.5} M_q^{0.5}$ should yield a straight line if B_2M complexes are formed. This representation of the same data is shown in Figure 4.2.1b. Similarly to Figure 4.2.1a, the data for each ion fall into a straight line (all metal ions: R ≥ 0.99).

For both representations of the metal binding reaction stoichiometry (Figures 4.2.1a and b), a straight line fits the experimental data quite well. At low concentrations, however, the fit for B_2M complexes is better, whereas some results of section 4.2.6 below favor $BM_{0.5}$ complexes. Either stoichiometric assumption ($BM_{0.5}$ or B_2M complexes) could be justified by the data. This shows that a good straight line fit for any proposed model is not unequivocal evidence for the correctness of the underlying assumptions.



a



b

Figure 4.2.1: Investigation of the reaction order for binding of divalent ions by *Sargassum fluitans* biomass at pH 4.5

a) Linear representation for formation of $BM_{0.5}$ complexes

b) Linear representation for formation of B_2M complexes

4.2.3 Equilibrium Constants

For each of the two-metal systems Cd-Cu, Cd-Zn and Cu-Zn experiments were performed at pH 2.5, 3 and 4.5. In order to quantify the effect of one metal ion on the binding of the other, the constants ${}^{C1}K$ and ${}^{S1}K$ as well as ${}^{C2}K$ and ${}^{S2}K$ for equations (4.2.5) and (4.2.6) were determined by minimizing the average absolute deviations between the model predictions and experimental data points for the metal ion binding using the computer program MATLAB 4.2c. The values ${}^C = 2$ mequiv/g, ${}^S = 0.25$ mequiv/g, ${}^{CH}K = 10^{4.8}$ L/mol and ${}^{SH}K = 10^{2.5}$ L/mol were derived in Section 4.1. As mentioned above, the competitive effect of Na which was added during pH adjustment was assumed to be negligible. The concentration of Na was of the same order of magnitude (< 5 mM) as those of the other ions, but its binding was much weaker because it is monovalent and can be expected to bind only electrostatically as has been confirmed for humic acids (Van Den Hoop and Van Leeuwen, 1990) which also contain carboxyl groups as one of the main binding groups (Buffle, 1988, pp. 166).

The determined constants for binding site - metal complexes are summarized in Table 4.2.1. Parameter set 1 consists of the values determined in Section 4.1 from one-metal systems. Parameter set 2 are the constants determined for true two-metal systems. Parameter set 3 was obtained using data from both the one-metal and the two-metal systems. It can be observed that, in most cases, the magnitude of the constants determined from one-metal systems is similar to those determined from two-metal systems.

4.2.3.1 Modeling Errors

Table 4.2.1 also lists the average discrepancies between the data points and the model predictions. For the modeling of one-metal systems, the error was smallest for parameter set 1 and largest for set 2. For the two-metal system data, set 2 fit better than set 1. Set 3 was intermediate in both cases. When both one- and two-metal systems were considered, the error for each metal species in each system (metal combination and pH) was weighed equally to form an average. Thus, for all the data, set 3 gave the best fit. This means that the experimental data were in each case (one-metal system, two-metal system or all data) best described by the parameter set derived from these data (set 1, 2, 3 respectively). In general, however, the absolute deviations between model predictions and experiments were similar for all data sets, averaging around 6 % of the total binding capacity.

4.2 Results and Discussion: Multi-Metal Systems at different pH values

Table 4.2.1 Model parameters and deviations between model predictions and experimentally determined metal ion binding

parameter set	Equilibrium constants (L/mmol)						(%) ave. absolute errors* predicting systems with		
	CCd _K	CCu _K	CZn _K	SCd _K	SCu _K	SZn _K	1 metal	2 metals	1 or 2 met.
1	80	200	10	0.8	3.7	0.5	5.4	6.4	6.1
2	40	210	7.6	0.5	5.2	0.1	6.3	6.1	6.1
3	65	190	10	0.5	6.3	0.1	5.6	6.2	6.0

* expressed in % of total binding capacity

Parameter set 1 was derived from one-metal systems,
set 2 from two-metal systems and set 3 from all data.

For all parameter sets the amounts of binding sites were ${}^tC = 2$ mequiv/g,
 ${}^tS = 0.25$ mequiv/g, with the apparent proton binding constants
 ${}^{CH}K = 10^{4.8}$ L/mol, ${}^{SH}K = 10^{2.5}$ L/mol

4.2.3.2 Comparison between Constants from One- and Two-Metal Systems

In general, the constants determined in two-metal systems (set 2) and one-metal systems (set 1, from Section 4.1) are similar to the ones determined for all the data (set 3). The latter set of constants (set 3) may be regarded as the most reliable because it is based on the largest number of data points.

The largest differences between sets 1 or 2 in comparison to set 3 were observed for ${}^{SCd}K$ and ${}^{SZn}K$. However, this difference may not be physicochemically relevant but only a random variation since the relative error in the determination of these two constants is rather large. This is due to the fact that S sites only contribute significantly to binding when the pH is low. At low pH, however, the binding of Cd and Zn is low which results in a large relative error in the determination of the metal binding as described in Section 4.3. Additionally, the optimization procedure for the equilibrium constants which is based on a minimization of the absolute errors in binding was not very sensitive to these constants whose magnitude does not strongly influence the absolute binding.

4.2 Results and Discussion: Multi-Metal Systems at different pH values

As Table 4.2.1 indicates, the data in two-metal systems are described best by parameter set 2 which was derived exactly from these data. However, the error in the prediction of two-metal system sorption behavior increased only by 5 % (from 6.2 to 6.4% of the maximum binding) when the constants derived from one-metal systems (set 1) were used. This means that the prediction of the two-metal system behavior by using results from one-metal systems is possible. Therefore, the amount of experimental work needed to provide a basis for modeling multi-metal systems can be greatly reduced. Instead of a systematic investigation of the influence of each metal ion only spot-checks may be necessary in order to confirm the applicability of the constants derived from one-metal systems. For those spot-checks, the modeling may already help to design the experiments in such a way that the desired final concentrations are reached and that the experimental error is kept low (see Section 4.3).

From a theoretical modeling perspective, this similarity in the different sets of constants indicates that secondary interactions in the ion exchange based metal biosorption systems are probably weak. The influence of the presence of one metal on the binding of another one is mainly due to competition for sorption sites.

4.2.3.3 Number of Constants, Predictive Power

A major advantage of the presented model, as compared to earlier multi-metal isotherms (Chong and Volesky, 1995), is that only two constants ^{SM}K and ^{CM}K were necessary to predict the binding of each metal ion at different pH values and in the presence of different concentrations of either of the two other competing ions. Previously, it was necessary to determine a new set of constants for each pH and each combination of metal ions. The presented model reduces the amount of experimental work since, for example, the prediction of binding at other pH values is possible.

4.2.4 Influence of Metal Ion Concentrations on Binding: 3D plots

As an example of one of the nine systems investigated, the binding of metal ions in the Cd-Zn system at pH 4.5 was plotted in a 3D graph (Figure 4.2.2). This way the metal binding can be plotted as a function of both metal concentrations. The grid surface is simply an interpolation between the individual points. The computer program MATLAB 4.2c was used in order to calculate an interpolated surface through the experimental data points after a grid had been specified. The same program was used for creating the 3D plots.

4.2 Results and Discussion: Multi-Metal Systems at different pH values

4.2.4.1 Affinity Sequence

It can be seen that the binding of Cd (Figure 4.2.2a) is less affected by the presence of Zn than vice versa (Figure 4.2.2b). In general, a preference of sorption $\text{Cu} > \text{Cd} > \text{Zn}$ was observed at all pH values and for all metal combinations.

The affinity sequence $\text{Cu} > \text{Cd} > \text{Zn}$ derived in this work is the same as observed for biosorption of these metals by other algal biomass (Chong and Volesky, 1995; Crist et al., 1994). The number of protons displaced per mol of metal ion bound for pure alginate also decreased in the order $\text{Cu} > \text{Cd} > \text{Zn}$ (Haug and Smidsrod, 1970). This has been explained by a transition from probably more covalent bonding for Cu to ionic charge bonding.

These observations can be viewed in a wider context: Zn is classified as predominately hard, especially in aqueous solution but not necessarily in vivo (Moore and Ramamoorthy, 1984, pp. 187). Cd and Cu share characteristics of both classes (Bell, 1977, pp. 39). Some characteristics of the three ions are listed in Table 2.3.1. It can be seen that according to the (z^2 / r_{hyd}) criterion the strength of ionic bonds is $\text{Cu} > \text{Cd} > \text{Zn}$ but the differences among the metals are small. Using the Δx or the $1 - \exp(-\Delta x^2/4)$ criteria, it is indicated that the binding of Zn is more ionic (electrostatic) than the binding of Cd or Cu. The binding of Cu, on the opposite, is to a larger degree covalent than for the other two metals. The $x^2 (r_{\text{cryst}} + 0.85)$ criterion confirms that the relative contribution of covalent bonding is $\text{Cu} > \text{Cd} > \text{Zn}$. All criteria indicate that Zn should be the cation with the least tendency to covalent binding, and its ionic binding is of similar strength to Cd and Cu. This can explain its weaker binding as reflected in the parameter for the total binding strength ξ .

4.2.4.2 Plateau Phenomenon

At low concentrations of both metals, the total binding of Cd and Zn (Figure 4.2.2c) increases with the concentrations of either metal. When the concentration of one of the metals reaches about 3 mM or higher, the experimentally determined total binding did not show any large increase with metal concentration, but reached a plateau value of $q \sim 2$ mequiv/g. Although the proportion of the binding of the two metal ions may vary with the concentrations, the total metal ion binding stays more or less constant.

The occurrence of a plateau value for high metal ion concentrations where the total binding is independent of the concentration indicated that both metal ions compete for the same limited number of sites: with an increased concentration of one metal ion the increase in the binding of this metal is accompanied by a corresponding decrease in binding of the other metal such that the total binding is constant when it is at its maximum value.

4.2 Results and Discussion: Multi-Metal Systems at different pH values

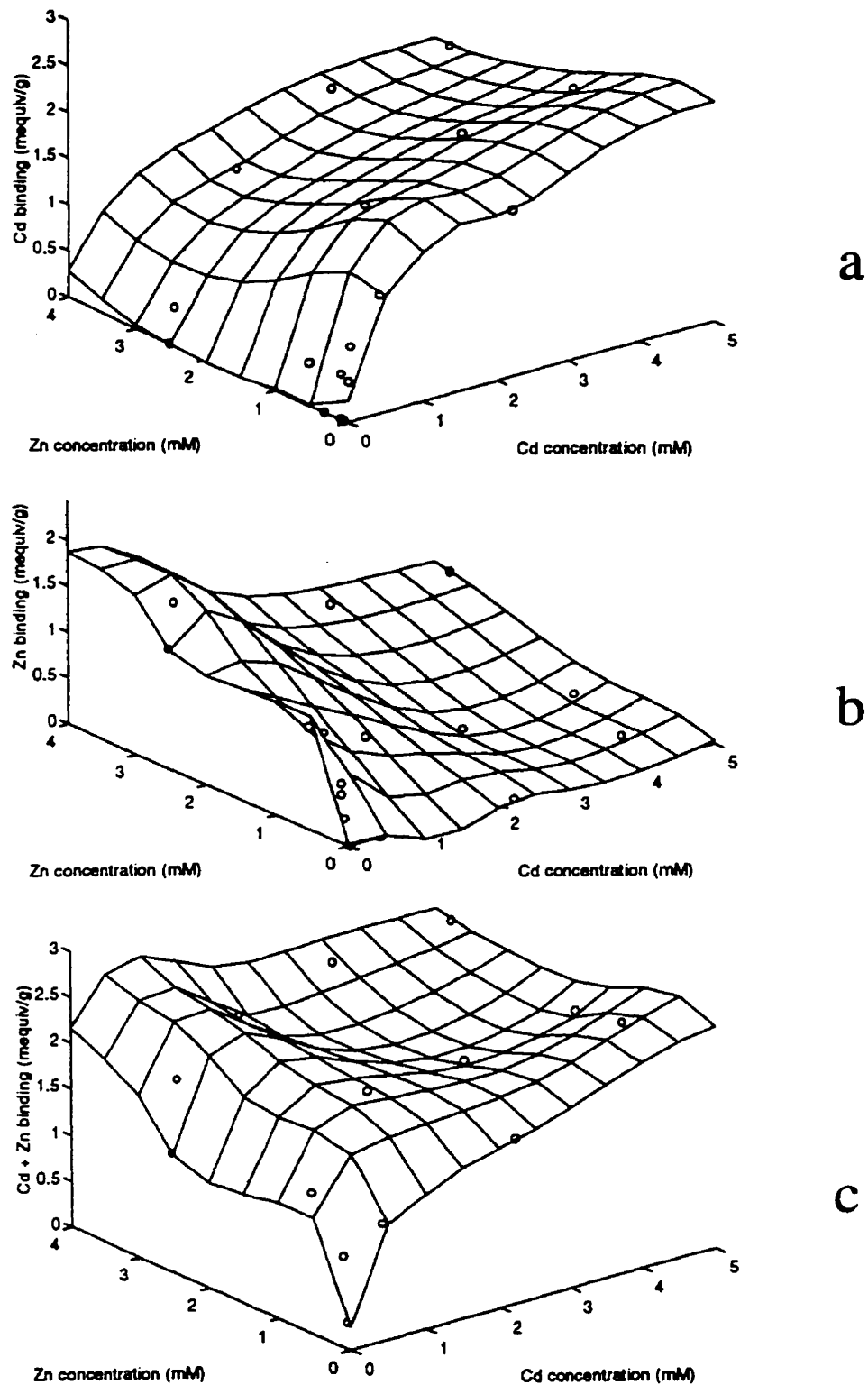


Figure 4.2.2:

Two-metal (Cd+Zn) biosorption by *Sargassum fluitans* biomass at pH 4.5.

Experimental binding in the interpolated sorption isotherm surface;

a) Cd binding;

b) Zn binding;

c) Total metal ion binding.

4.2 Results and Discussion: Multi-Metal Systems at different pH values

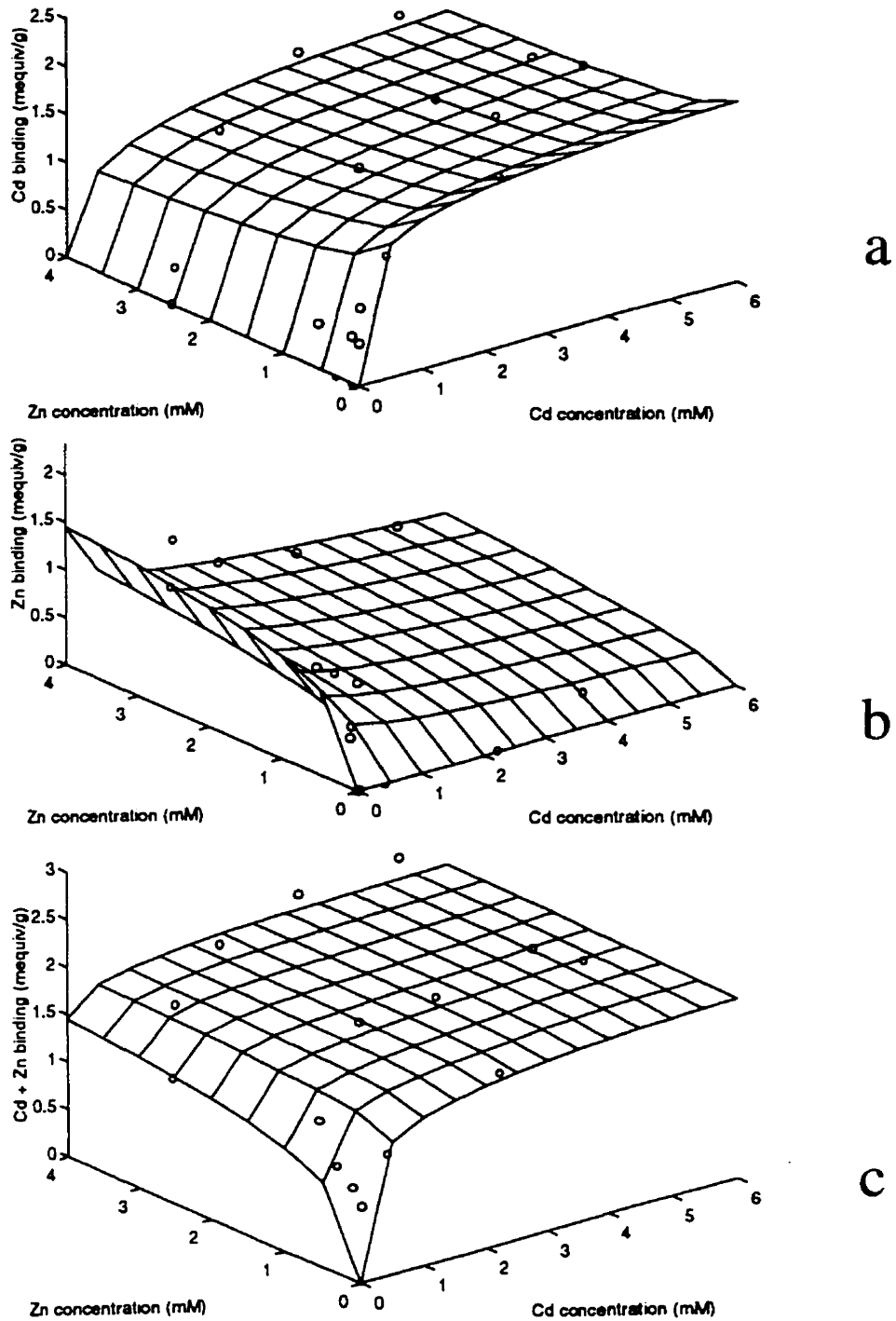


Figure 4.2.3:

Two-metal (Cd+Zn) biosorption by *Sargassum fluitans* biomass at pH 4.5.

Experimental data and the model-predicted sorption isotherm surface

a) Cd binding; b) Zn binding; c) Total metal ion binding

4.2 Results and Discussion: Multi-Metal Systems at different pH values

This is in accordance with the model which assumes competition of all ions for the same binding sites.

Using the constants from parameter set 3, the model predictions and experimental data for the total metal ion binding in the Cd-Zn system at pH 4.5 are plotted in Figure 4.2.3, again using the computer program MATLAB 4.2c. The plateau phenomenon is reflected in the model.

4.2.4.3 Dominant Site Speciation

In general, larger amounts of free sites exist only at high pH and low metal concentrations. Protons occupy the majority of sites at low pH. At high pH and medium or high metal concentrations most sites are complexed with metal ions. Metal ions alone occupy between 0 and ~ 100 % of the sites, metal ions and protons together between 50 and ~ 100 %. Since the ratio of binding of the two metal ions changes when a plateau value for the total binding (Figures 4.2.2c and 4.2.3c) is reached, data near the saturation level are interesting for competition modeling although there is no effect of the concentrations on the total binding.

4.2.5 Influence of Metal Ion Concentrations on Binding: 2D Plot

Since the quantitative interpretation of 3D graphs is difficult, it is recommendable to evolve them into a series of 2D graphs which represent iso-concentration cuts of the 3D plot (Chong and Volesky, 1995). Figure 4.2.4 shows the binding of Cd and Cu at pH 4.5 as a function of both concentrations. In general, the experimental methodology used does not allow for the adjustment of the final concentration as an independent variable. This concentration is dependent on the initial concentration and cannot be predicted beforehand unless the equilibrium constants are already known. Therefore, a direct comparison between the measurements and the model predictions for the binding of one metal ion at a specific concentration of the competing ion is not feasible. In order to render such a comparison possible, a limited number of experiments was performed in a liquid volume large enough so that the concentration of metal ions in the liquid phase remained constant (and known) throughout the experiment. With this approach, however, the binding cannot be determined from the concentration difference in the solution (initial-final) but was determined by metal ion elution from the sorbent instead (equation (3.3.1)).

Some experimental data obtained by this methodology are included in Figure 4.2.4. The model predicts the trends displayed by these additional data which had not been used in the determination of the model parameters. A tendency of the experimental binding to be

4.2 Results and Discussion: Multi-Metal Systems at different pH values

lower than the modeled binding can, however, be observed for both metals. This may be due to the experimental methodology: specifically for the data points in Figure 4.2.4, desorption was used in order to determine the binding. This elution of the metal ions may not have been 100 % complete, resulting in an underestimation of the binding.

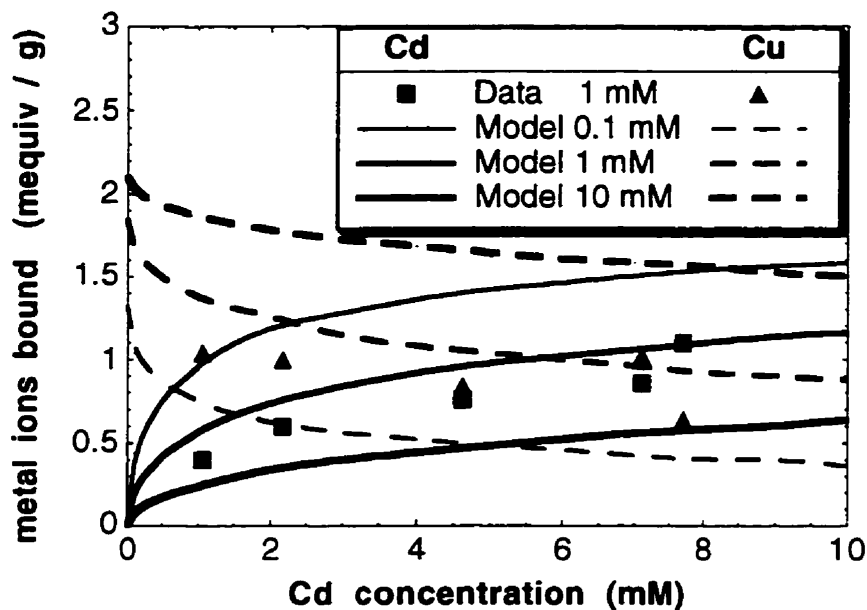


Figure 4.2.4: Biosorption of Cd and Cu by *Sargassum fluitans* biomass at pH 4.5 for different Cu concentrations: Binding data and model predictions.

4.2.6 Influence of Metal Concentration Ratio on Metal Binding

While Figure 4.2.4 represents cuts of the sorption isotherm “surface” at constant Cu concentrations, Figure 4.2.5 is composed of diagonal cuts at constant total metal ion concentration and pH. The ratio of the Cd / Cu binding as well as their sum are depicted as a function of the concentration ratio $[Cd] / [Cu]$.

4.2 Results and Discussion: Multi-Metal Systems at different pH values

4.2.6.1 Effect on Total Metal Binding

Although the total binding is almost independent of the concentration ratio at pH 4.5 for $[Cd]+[Cu] = 5$ mM, it decreases with increasing Cd portion when the total metal concentration or pH are lower.

As seen in Figure 4.2.5, the effect of the concentration ratio on the total metal ion binding is most pronounced at low pH or low total metal ion concentrations. Under these conditions the presence of the more strongly binding Cu instead of Cd can contribute to increased total metal ion binding by competing more effectively for sites occupied by protons (at low pH) or by occupying additional free sites (at low metal concentrations). At high pH and metal ion concentrations this is not possible because even Cd can occupy almost all sites and nearly no protonated or free sites remain.

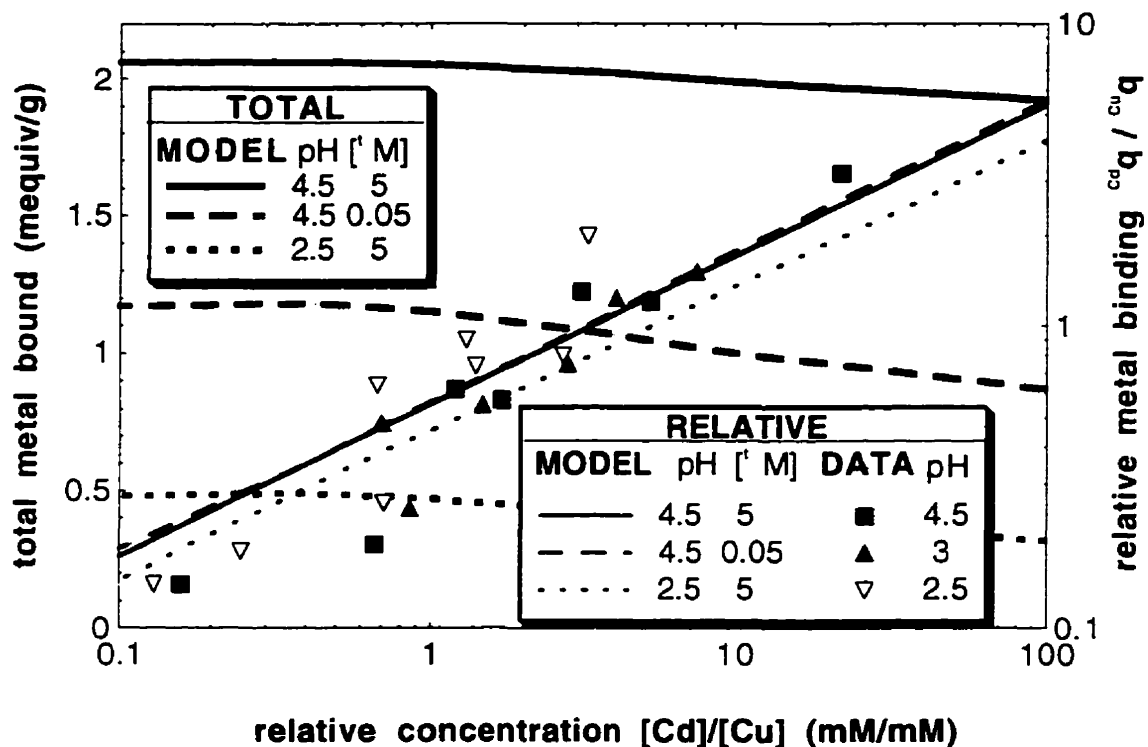


Figure 4.2.5: Metal binding by *Sargassum fluitans* biomass for different total metal concentrations and pH values: Model predictions and experimental data.

4.2 Results and Discussion: Multi-Metal Systems at different pH values

4.2.6.2 Effect on Relative Metal Binding

The model-predicted ratio between the Cd and Cu bindings also varied with pH but not significantly with the total metal concentration (Figure 4.2.5). The theoretical relationship between the relative binding and the relative concentration is linear with a slope of 0.5. This slope corresponds to the exponent of the metal ion concentration ratio in equation (4.2.2) which, expressed in logarithmic terms, becomes for $z_1 = z_2 = 2$:

$$\log ({}^1q / {}^2q) = \log ([B {}^1M_{0.5}] / [B {}^2M_{0.5}]) = \log K_{\text{exch}} + 0.5 \log ([{}^1M] / [{}^2M]) \quad (-) \quad (4.2.11)$$

A similar slope is also visible in the experimental data for which the line of the best fit has a slope of 0.65 ($R = 0.93$, line not shown in the figure). Since the total concentration has no significant influence on the relative binding (when the pH is constant and both metal ions have the same valence), the data points were obtained at different total concentrations.

Consequently, the $BM_{0.5}$ assumption which yields a slope of 0.5 fits the Cd-Cu data better than the B_2M assumption which would predict a slope of 1.0. For the other two-metal systems (Cd-Zn and Cu-Zn), however, the experimentally observed slope of 0.97 and 0.77, respectively, (data not shown) was larger, favoring the B_2M assumption (which is also favored by the data in Figure 4.2.1 for low concentrations). It can be concluded that both electrostatic attraction (corresponding to a slope of 1.0) and covalent bonds may contribute to biosorption, since the observed behavior is between the one expected for $BM_{0.5}$ and B_2M complexes. Their relative importance appears to depend on the softness of the ions involved. The results indicate that for Cd and Cu, mostly $BM_{0.5}$ complexes may be formed. However, there is an advantage in assuming $BM_{0.5}$ complexes for all divalent metal ions since it facilitates the easy representation in an isotherm (equations (4.2.4 - 4.2.6)). This is not possible for B_2M or mixed complexes.

When both concentrations are equal, the binding of Cd is about half of that of Cu. In order to obtain equal binding of both metals, the concentration ratio has to be between 3 and 6, depending on pH. The lower the pH, the higher the necessary concentration ratio $[Cd]/[Cu]$ required for equal binding of both metal ions.

From equation (4.2.11) it can also be seen that the exchange constant reflects the vertical position of the line describing the relative binding. At equal concentrations of both metals, the exchange constant corresponds to the ratio between ${}^{\text{Cd}}q$ and ${}^{\text{Cu}}q$ which is in this case close to 0.6. Similarly, the exchange constant is reflected in the ratio $[Cu]^{0.5} / [Cd]^{0.5}$ for equal binding of both metals. This means that for equal binding a concentration ratio $[Cd] / [Cu] = {}^{\text{Cd}}K / {}^{\text{Cu}}K \sim 3$ is necessary.

In a two-site system, however, it is not possible to define one overall exchange constant jK for the relative binding of two ions. This is seen in the different position of the

4.2 Results and Discussion: Multi-Metal Systems at different pH values

line for relative binding at pH 2.5. When binding is dominated by C sites (i.e. at high pH values), the value of the apparent exchange "constant" is close to $(\frac{^{CCd}K}{^{CCu}K})^{0.5} = (65 / 190)^{0.5} = 0.58$. The exchange "constant" for lower pH is smaller, however. With increasing importance of S groups in binding, the influence of the smaller ratio $\frac{^{SCd}K}{^{SCu}K} = 0.46 / 6.3 = 0.073$ in the overall exchange "constant" gains importance, resulting in its lower values.

4.2.7 pH Titration in the Presence of Two Metals

Figure 4.2.6 demonstrates the sorption behavior of a Cu-Zn system at changing pH values for a constant total concentration (solid + liquid phase) of each metal. At a higher pH, the binding of the two metals is similar. With decreasing pH, however, Zn gets released much more readily than Cu. At pH 3.6 the Zn binding is already reduced to less than half of its maximum value, while the binding of Cu is still almost unchanged.

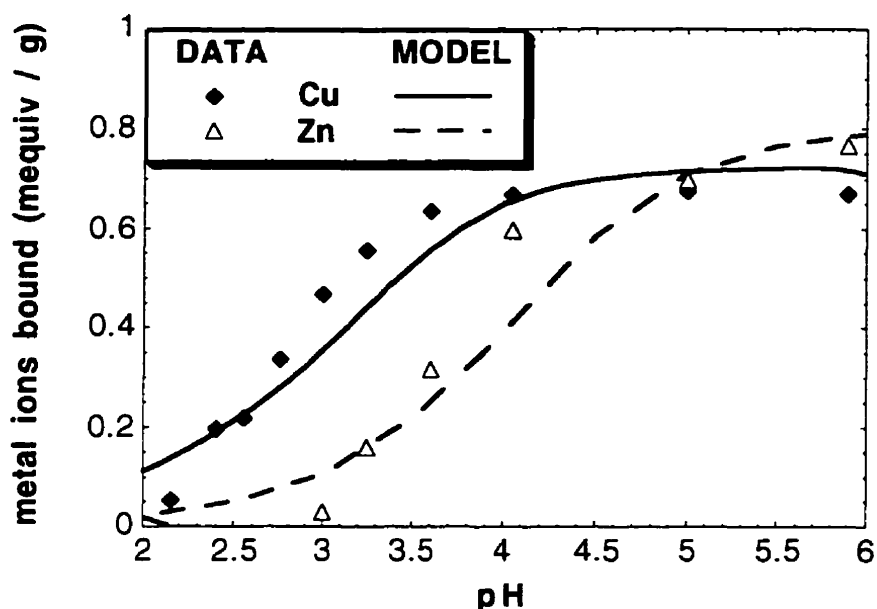


Figure 4.2.6: Titration of *Sargassum fluitans* biomass in the presence of Cu and Zn at constant total concentrations of each metal: Biosorption binding data and MINEQL⁺ model predictions.

4.2 Results and Discussion: Multi-Metal Systems at different pH values

The system was modeled by incorporating the equilibrium constants into the chemical equilibrium program MINEQL⁺. The complete final state (concentrations in solution and binding values) was predicted from the known initial conditions. The model predicted a similar trend as observed from the experimental data.

In Figure 4.2.6, the difference between the inflection points of the curves for Cu and Zn binding is due to the fact that the more strongly binding Cu can better resist the competition from protons than the weakly binding Zn. This effect can be used in practice for selective metal ion desorption. Desorption with acids is a promising technique for the regeneration of the sorbent material (Aldor et al., 1995). When the difference between the binding constants of the sorbed metal ions is large enough, not only can the biomass be regenerated by acidic desorption but partially selective recovery of the sorbed metal may also be possible.

4.2.8 Using the Model if some Metals have Different q_{\max} Values

The model generally assumes that all cations bind to the same sites. Therefore, the maximum binding capacity q_{\max} (in mequiv/g) attained at high concentrations of the respective ion is generally the same for all metals, it is equal to the total number of binding sites. If the experimentally determined binding of metal ions shows different q_{\max} values, the model can nevertheless still describe these data. There are three different ways of modeling data with different q_{\max} values.

First, it is possible that the apparent q_{\max} of a data set does not reflect the total number of binding sites that this ion could bind to. This may occur especially for weakly binding ions like Zn or at low pH values. In those cases, the maximum binding reached (for metal concentrations of several mM) and, consequently, the value of q_{\max} determined by fitting a Langmuir model to these data (see Figure 4.1.2a-c and Table 4.1.2) is much lower than the total number of binding sites according to the two-site model. This occurs because competition by protons can be strong enough to prevent the metal from occupying all sites even at concentrations of several mM. Even though the two-site model assumes ${}^1B = 2.25$ mequiv/g (Table 4.1.1), the binding in those cases where q_{\max} is much lower than 1B is not greatly over-predicted because the binding constants for metals such as Zn are low (Table 4.1.1) and/or the proton binding constant is of a magnitude that, according to the two-site model, protons occupy a significant part of the sites at the respective pH. The fact that the Langmuir model approximates some of the data in Figure 4.1.2 more closely than the 2-site model is to be expected since the parameters K and q_{\max} for the Langmuir model were determined individually to fit each isotherm for a specific metal and a specific pH

4.2 Results and Discussion: Multi-Metal Systems at different pH values

while in the 2-site model the same number of binding sites is assumed for 4 cations at any pH and the metal binding constants are independent of pH. Since competition by protons for sorption sites can never be completely avoided when the total number of binding sites is determined from metal binding experiments, the most reliable estimate of the number of binding sites may be obtained from pH titrations. As a second step, metal binding experiments can serve to confirm that the acidic groups are used for metal binding.

Second, if the apparent q_{\max} values for different ions deviate quite strongly from each other, it is possible to go one step further and assume that the ion which binds to a smaller extent does not bind to one of the binding sites at all. Accordingly, the binding constant with respect to that site is set equal to zero. In deciding which binding site may not be effective in sequestering the particular ion, it is necessary to consider both the site quantity in relation to the observed difference in q_{\max} and also the variations of binding with pH. For example, if the differences in binding capacity are most pronounced at high pH, the binding constant with respect to a site with a high pK_a should be set equal to zero. If the occurrence of this site is much higher than the observed differences in q_{\max} , then it may also be taken into account that groups which have a similar pK_a may differ in their metal binding behavior. For example, the carboxyl groups of mannuronic and guluronic acids in alginate have very similar pK_a and may therefore be considered as one type of site. However, it is known that guluronic acid has a higher selectivity for metal binding than mannuronic acid. Theoretically, the metal binding constants for these two uronic acids can differ substantially, even to the extent that one metal may not be specifically bound to one of these groups. For the other metals, different binding constants relative to mannuronic and guluronic acid residues *can* be assumed but it is a question of "modeling economy" and one may choose to avoid the introduction of additional fitting parameters for distinguishing between these sites.

Third, the opposite case, where the binding of one metal ion exceeds the number of binding sites determined in pH titration (on a mequiv basis), may occur. In that case, it is advisable to verify whether complex formation with ligands in the solution occurs for the respective ion. If so, it could be possible that a metal-ligand complex is bound to the biomass. A divalent ion that usually binds to two sites, could require only one site if it is bound as a metal-ligand complex. This way, twice as much of that metal can be bound. For confirmation of this possibility, the change of ligand concentration in the course of the experiment should be determined. It is quite possible that the free metal ion M^{2+} and the complex ML^+ may compete for the same binding sites. The competitive sorption model (equation 4.2.4) can be applied without further modification just by treating the ML^+ complex as a separate monovalent species with distinct binding constants. In order to

4.2 Results and Discussion: Multi-Metal Systems at different pH values

obtain the total metal binding, the binding of M^{2+} and ML^+ are simply added (for conversion to a molar basis, the binding as $BM_{0.5}$ in mequiv has to be multiplied by 0.5). As an example, the total binding of M^{2+} and ML^+ to one binding site with protons as the only competing species is:

$$M_q = \frac{B \left((BMK [M])^{1/2} + (BMLK [ML]) \right)}{1 + B^H K [H] + (BMK [M])^{1/2} + (BMLK [ML])} \quad (\text{mequiv/g}) \quad (4.2.12)$$

Figure 4.2.7 illustrates that according to this model, the binding of ML^+ complexes becomes increasingly important with increasing metal concentration. The model calculations were performed for a hypothetical case at pH 4.5 where the concentrations in solution $[M^{2+}] = [ML^+]$ with binding constants $B^H K = 10^{4.8}$ L/mol, $BMK = 10$ L/mmol, $BMLK = 1$ L/mmol and a site quantity of 2 mequiv/g. The increasing importance of the binding of metal-ligand complexes is in agreement with observations of (Chen et al., 1990).

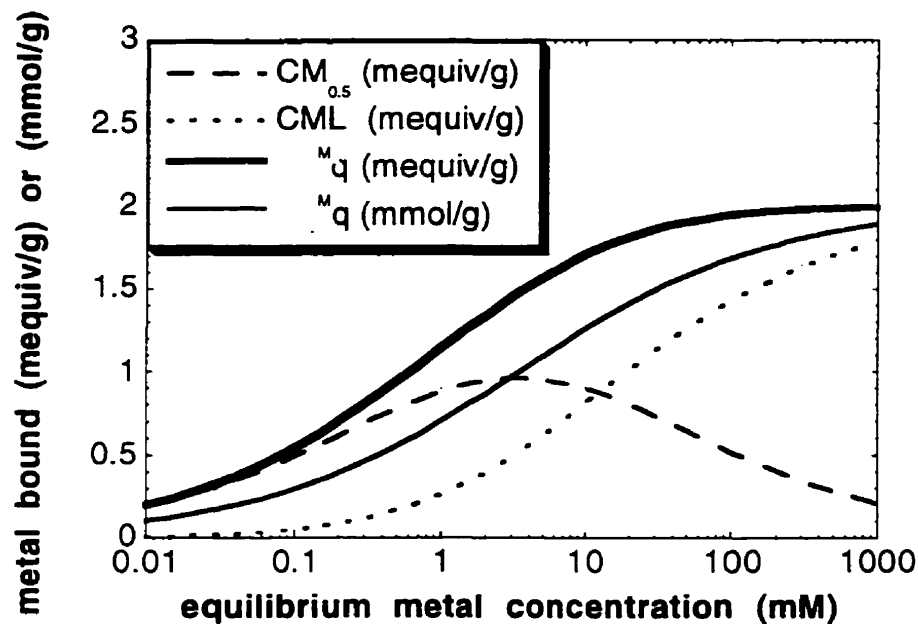


Figure 4.2.7

Competitive binding of metal ions and metal-ligand complexes
Model predictions for a hypothetical case

4.2.9 Section Summary

A general model for biosorption involving multiple ions competing for multiple sites was developed. The model case for one monovalent and two divalent ions sorbing to two binding sites was successful in describing sorption by protonated biomass of *Sargassum fluitans* in two-metal systems (involving Cd, Cu and Zn) at different pH values. The equilibrium constants determined from one-metal systems were similar to those determined from two-metal systems, indicating little secondary interaction between the metals and rendering the prediction of multi-metal systems using constants from one-metal systems possible. Only two constants were needed for each ion to describe its sorption behavior at different pH values and in the presence of different competing ions.

The stoichiometry of the actual biosorption behavior fell between the one expected for $BM_{0.5}$ and B_2M complexes. Therefore, either stoichiometric assumption may be used for modeling.

Prediction of the complete final state of the biosorption system from its initial state using the MINEQL⁺ equilibrium program was possible for a pH titration in the presence of Cu and Zn, demonstrating the predictive power of the model presented in this work. The results also show that partially selective desorption, eventually leading to the recovery of the selected metal, is possible when the equilibrium constants for metal ions present on the biosorbent are sufficiently different.

4.3 Experimental and Modeling Errors

Although experimental work in biosorption has been carried out for more than a decade now, no systematic study of the experimental error involved in the determination of metal uptake has been available. The present work aims to close that gap. The purpose of this section is to investigate the error in the experimental determination of metal uptake during the batch equilibrium biosorption process. The objective is to quantify the inaccuracies in mass and volume measurement as well as calibration, drift and fluctuation of the Atomic Absorption Spectrophotometer readings for an example of Cd, Cu or Zn sorption by protonated *Sargassum fluitans* biomass.

The results presented in this section have in modified form been published in Schiewer and Volesky (1995c)

4.3.1 Determination of the Error in Metal Binding

The absolute error Δ^{Mq} for the metal uptake is calculated by taking the derivative of the uptake function (equation (3.3.11) with $M_{qi} = 0$ and $V_i \sim V$) with respect to each independent variable, multiplying the respective derivative with the error in the determination of the independent variable and summing the products. Applying this approach to equation (3.3.11) and multiplying with $100 / M_q$ yields the relative error:

$$\% \Delta^{Mq} = 100 \frac{\Delta^{Mq}}{M_q} = 100 \left(\frac{\Delta [M]_i + \Delta [M]_f}{[M]_i - [M]_f} + \frac{\Delta V}{V} + \frac{\Delta m}{m} \right) \quad (-) \quad (4.3.1)$$

ΔV and Δm are constant under the conditions studied and can be determined directly. The error in determining the concentration, however, is composed of errors in dilution of the sample as well as errors associated with the calibration of the atomic absorption spectrometer (AA) and drift and fluctuation of its readings.

4.3.2 Evaluation of the Calibration Error

Directly after calibrating the AA with standard solutions of known concentrations, the AA-readings of these standards were taken. The difference between the actual known concentrations and those determined by using the AA were taken as the calibration error $\Delta[M]_{cal}$. For each standard solution, the average calibration error of about six calibrations was calculated. This average is represented by one data point in Figure 4.3.1.

For the calibration of the Cd analysis at a wavelength of 326 nm the absolute error increases with the concentration from about 0.9 mg/L for $[M] = 20$ mg/L to about 4 mg/L for $[M] = 800$ mg/L. The relative error in this concentration range falls from 4.3 to 0.5 % (Figure 4.3.1). In order to describe this concentration dependency mathematically, a hyperbolic function was chosen to represent the Cd data (calibration at 326 nm) since it fitted the data best.

$$\Delta[M] = a + \frac{b [M]}{1 + d [M]} \quad (mg/L) \quad (4.3.2)$$

A linear fit was sufficient for the Cu analysis or for the Cd analysis at 229 nm. For Zn the concentration range was rather small, and no significant difference in the absolute errors was noticed. Consequently, a constant absolute error was assumed. Equation (4.3.2) was linearized as $1/(\Delta[M]-a) = d/b + 1/(b [M])$. The constants were determined using the linear fit resulting in the least square deviations, except for constant "a" for Cd which was assumed to be half of the sensitivity of the AA instrument. The values for the respective constants are listed in Table 4.3.1.

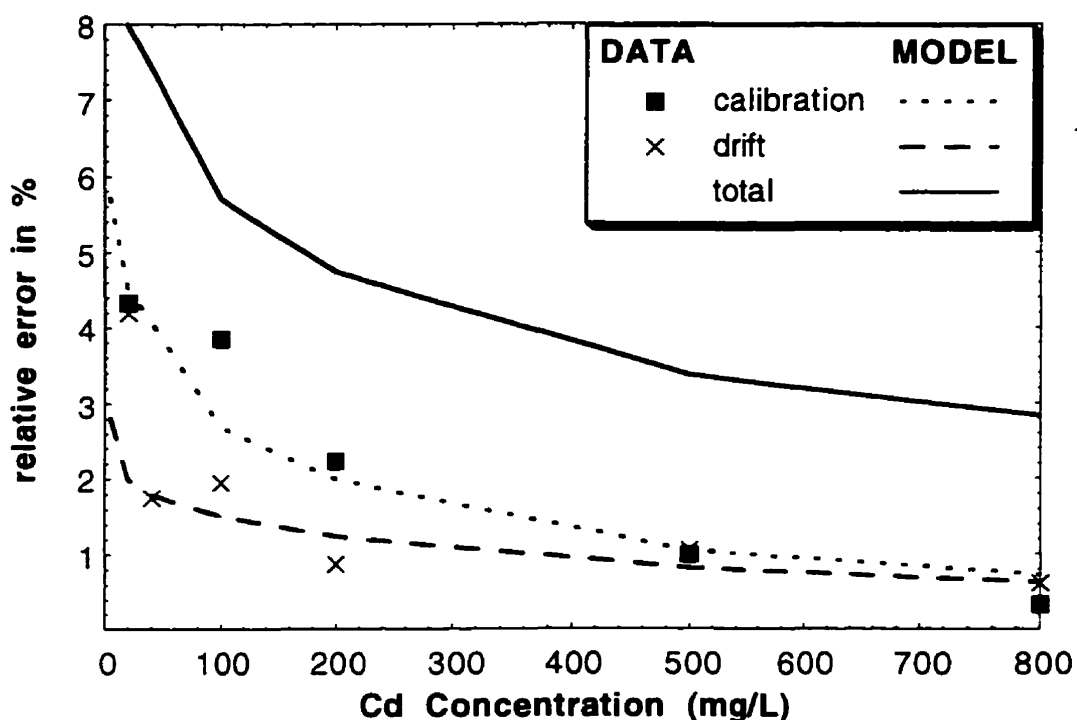


Figure 4.3.1: Components of error in Cd concentration determination

Table 4.3.1:

Parameters for the function describing the error in the determination of [M]

	WAVELENGTH [nm]	CALIBRATION				DRIFT and FLUCTUATION			
		a [mg/L]	b [-]	d [L/g]	R	a [mg/L]	b [-]	d [L/g]	R
Cd	326 ℓ	0.05	0.049	7.4	0.95	0.05	0.018	2.5	0.97
	229 s	0.02	0.005	0	0.98	0.05	0.008	0	0.98
Cu	249 ℓ	0.9	0.016	0	0.97	0.037	0.013	0	0.98
	218 ℓ	0.15	0.042	0	0.98	0.037	0.013	0	0.98
Zn	214 s	0.09	0	0	-	0.045	0.022	0	0.98

Note: ℓ : long way for AA burner head

s: short way for AA burner head

R is the regression coefficient for linear or linearized representation

4.3.3 Drift and Fluctuation

The cumulative error $\Delta[M]_{dr}$ for drift and fluctuation of the AA readings was obtained as the difference between the readings of the same sample directly after calibration and the reading about one hour later. The behavior resembles the one for the calibration error. Figure 4.3.1 shows the results for Cd determination at 326 nm. The best fit for Cd at 326 nm was again obtained with a hyperbolic function, while a linear fit was used for Cd at 229 nm as well as for Cu and Zn. The values of constants for equation (4.3.2) are listed in Table 4.3.1.

4.3.4 Dilution

In order to evaluate the error induced by dilution, a solution of 500 mg Cd/L was diluted 1:10, 1: 100 and 1:1000, with 10 samples prepared for each dilution factor. For each dilution factor (DF), the average reading and the deviation of the individual readings from that average were compared with the respective values for the undiluted sample. After subtracting the error due to calibration as well as drift and fluctuation, the remaining error for the dilution procedure used in this study was expressed as a function of dilution factor and concentration as:

$$\Delta[M]_{dil} = 0.01 \cdot [M] \log(DF) \quad (\text{mg/L}) \quad (4.3.3)$$

This means a one percent error occurs for a dilution factor of 10, a two percent error for DF = 100. This dilution error corresponds to the error of the pipetted volumes during dilution.

4.3.5 Total Error for the Concentration

The total error for the original concentration before dilution is calculated from the sum of the individual errors evaluated at the concentration after dilution multiplied by the dilution factor:

$$\Delta[M] = DF (\Delta [M]_{cal} + \Delta [M]_{dr} + \Delta [M]_{dil}) [M]_{after dil} \quad (\text{mg/L}) \quad (4.3.4)$$

Figure 4.3.2 compares the absolute and relative errors in the determination of the metal concentration for undiluted samples ("1:1") as well as for a dilution factor of 10. In the latter case, the distinction is made between the error in determining the concentration after dilution ("1:10 after dil") and the concentration of the original sample before dilution ("1:10 original") as evaluated from equation (4.3.4). The absolute error in all three cases increases with the concentration while the relative error decreases. Although the dilution by a factor

of 10 increases the error for the concentration after dilution by only one percentage point (compared to an undiluted sample at the same concentration), the dilution error is rather large when the original concentration before dilution is considered because the absolute error (though smaller at the lower concentrations after dilution) is multiplied by the dilution factor.

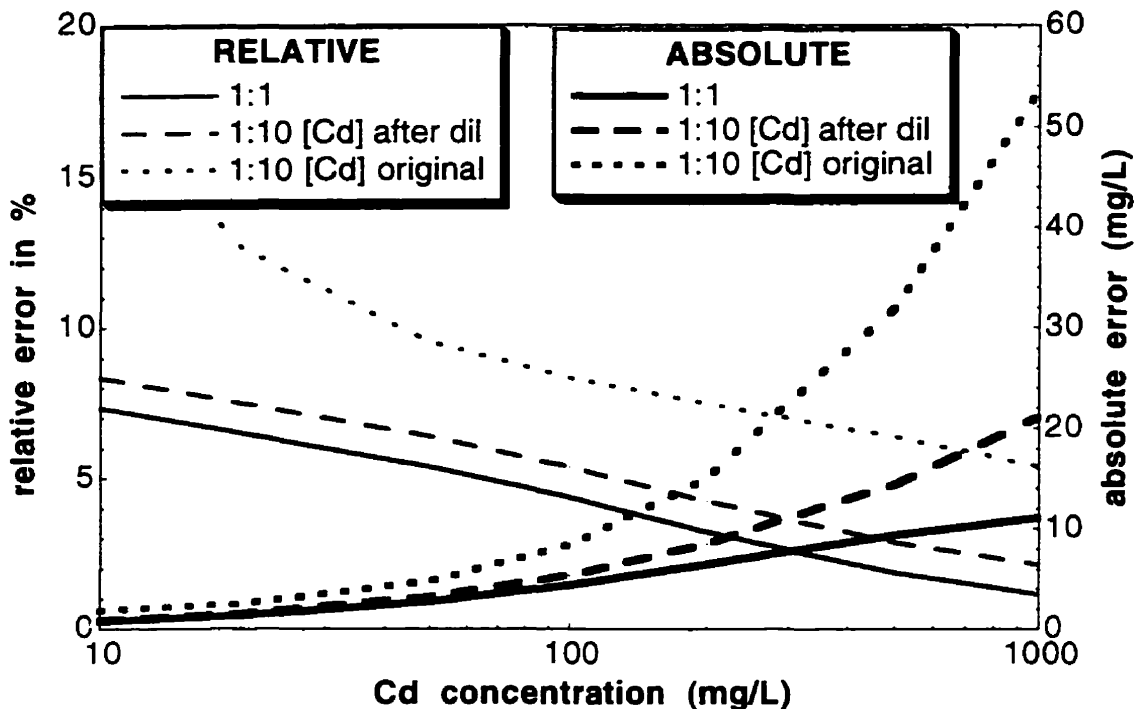


Figure 4.3.2: Influence of sample dilution on error in determining [Cd]

4.3.6 Total Error for the Metal Uptake

With one percent error in measuring the mass of the sorbent and a half percent error in measuring the solution volume, the total error for the uptake was calculated according to equation (4.3.1) and plotted in Figure 4.3.3. For a given initial concentration, the total absolute error depends only slightly on the final concentration. This is due to the fact that the total error is determined mainly by the larger initial concentration. Consequently, the total absolute error increases with the initial concentration. Although the absolute error is almost constant, the relative error increases sharply with $[M]_f$ and decreases with $[M]_i$ because the difference between the initial and final concentrations in the denominator of equation (4.3.1) decreases or increases respectively.

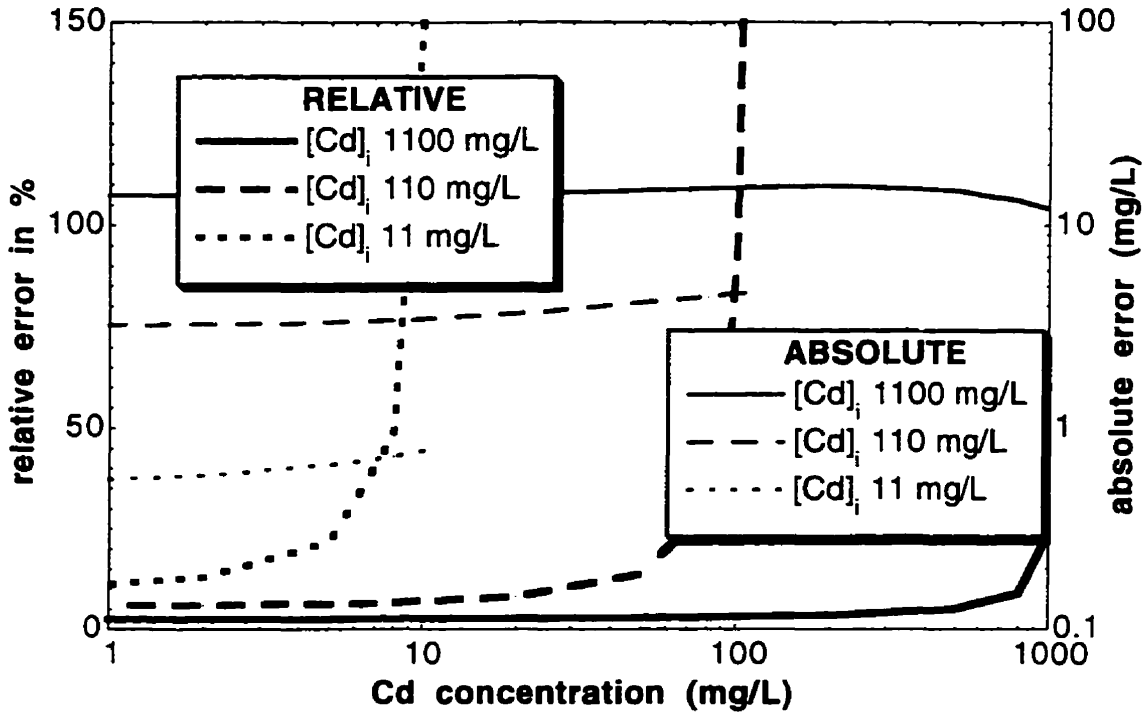


Figure 4.3.3: Influence of $[Cd]_f$ and $[Cd]_i$ on the error in determining M_q

4.3.7 Error Limitation through Choice of the Initial Concentration

The minimum initial concentration $[M]_{i,min}$ which yields an error smaller than the maximum tolerable error Δq_{max} can be calculated iteratively for a given $[M]_f$ by solving equation (4.3.1) for $[M]_i$.

The resulting necessary initial concentrations for 5 and 10 % maximum errors, respectively, are plotted in Figure 4.3.4 for the sorption of Cd and the calibration at 326 nm.

In order to obtain a desired final concentration from the necessary initial concentration, it is necessary to adjust the solid (biomass) to liquid (solution volume) ratio (S/L) correspondingly because for any given S/L ratio, the initial and final concentrations are coupled through the mass balance (equation (3.3.11)) and an isotherm equation. The required S/L ratio is obtained by solving equation (3.3.11) for m/V :

$$S/L = m/V = ([M]_i - [M]_f) / M_q \quad (\text{g/L}) \quad (4.3.5)$$

4.3 Results and Discussion: Experimental and Modeling Errors

The metal uptake $^m q$ as a function of $[M]_f$ has to be estimated by available sorption isotherms for similar conditions. The calculated minimum S/L ratios are plotted in Figure 4.3.4 using the isotherm determined in Section 4.1 for the sorption of Cd by protonated *Sargassum natans* biomass at pH 2.5 and pH 4.5 as examples. Generally, higher S/L ratios are necessary when the uptake is low (for example low pH) or when the concentration is so high that, due to the limited uptake capacity of the biomass, the concentration difference (although high in absolute terms) is relatively small compared to the higher error ΔC at these high concentrations. Thus, S/L = 2 is sufficient for Cd sorption at pH 4.5 in order to keep the error to less than 10 %. At pH 2.5, however, S/L ratios >10 are necessary.

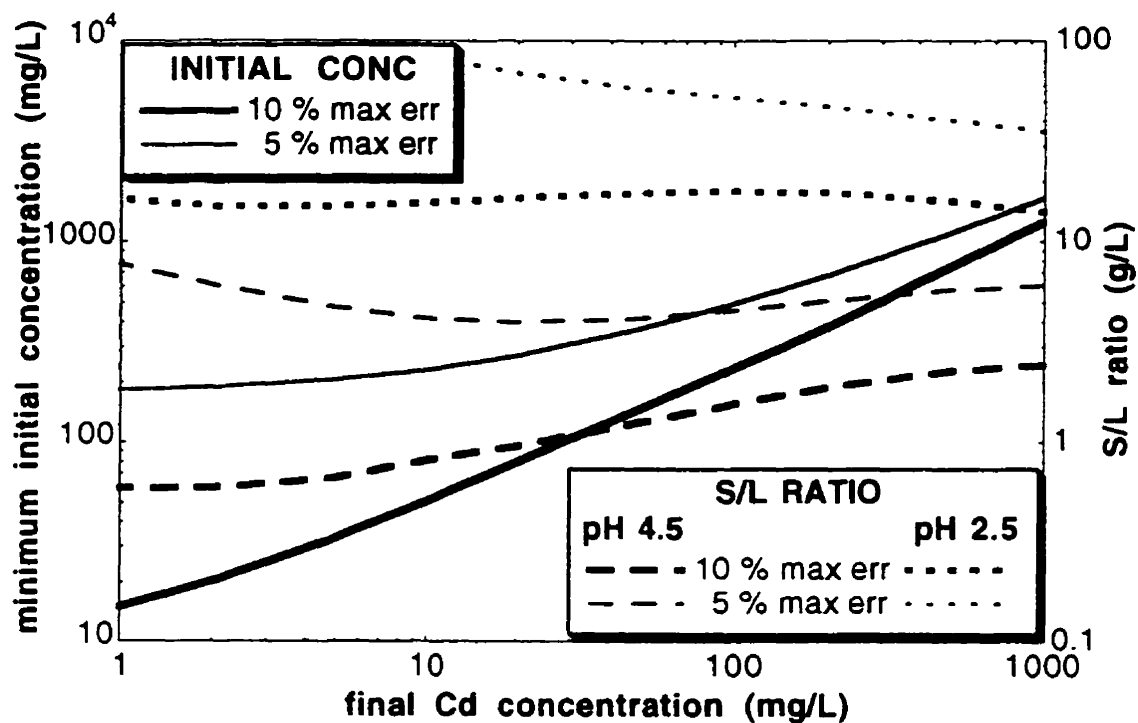


Figure 4.3.4: Necessary $[Cd]_i$ and S/L ratio for the limitation of errors

In contrast to Figure 4.3.3 which applies to Cd sorption by any biomass at any pH, Figure 4.3.5 is based on isotherms derived for protonated *Sargassum natans* biomass in Section 4.1. As shown in Figure 4.3.5, the experimental errors at pH 2.5 can be as high as 70 % if a low solid-to-liquid ratio (S/L = 2) is used.

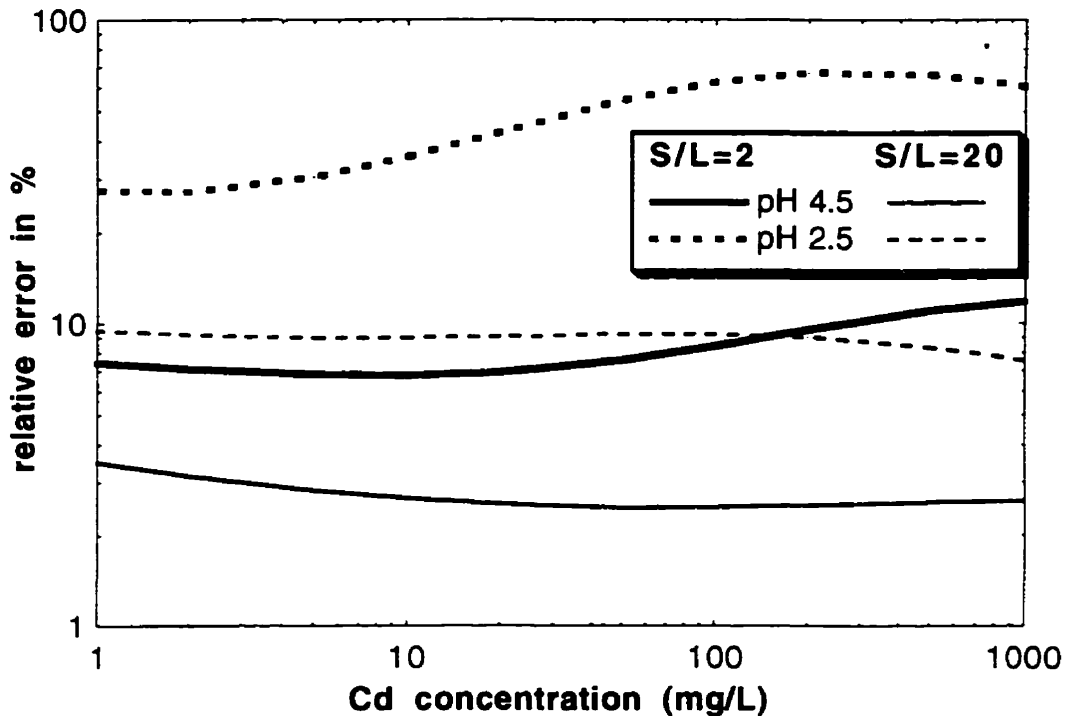


Figure 4.3.5: Influence of pH and S/L on error in determining Cd uptake

4.3.8 Comparison of the Experimental Error against the Model Error

The accuracy of the model does not only depend on the mathematical formulae used and on the determined constants but also on the reliability of the independent variables that are fed into the model. For the 2-site model (sites "C" and "S") which considers ion exchange reactions in multi-ion systems these input parameters also include the concentrations of other competing ions.

For a sorption system with one metal M and H⁺ the isotherm for the metal uptake is given by equation (4.1.6). The modeling error $\Delta^M q_{pH} = (dq^M / d[H]) \Delta[H]$ induced by an inaccurate determination of the pH value (with $\Delta pH = 0.05$, $\Delta[H] = 10^{-pH} - 10^{-pH-0.05}$) is:

$$\Delta^M q_{pH} = \left(C \frac{CHK \sqrt{CMK [M]}}{(1 + CHK [H] + \sqrt{CMK [M]})^2} + S \frac{SHK \sqrt{SMK [M]}}{(1 + SHK [H] + \sqrt{SMK [M]})^2} \right) \Delta[H] \quad (\text{mequiv/g}) \quad (4.3.6)$$

Since this part of the modeling error is due to an experimental error, it was added to the estimated experimental error.

4.3 Results and Discussion: Experimental and Modeling Errors

In Figure 4.3.6 the total error between data points and model predictions according to equation (4.3.6) (or the respective equation for systems which contain 2 metals and protons) are plotted against the experimental error.

The data points were obtained at different pH values (2.5, 3, 4.5) and with different combinations of the three metals Cd, Cu and Zn for sorption by protonated *Sargassum natans* biomass. Each point in Figure 4.3.6 corresponds to the arithmetic mean (i.e. most error values in one set can be significantly lower than this average) of a set of data points (between 6 and 12 points) derived for similar conditions (the same pH, the same combination of metals).

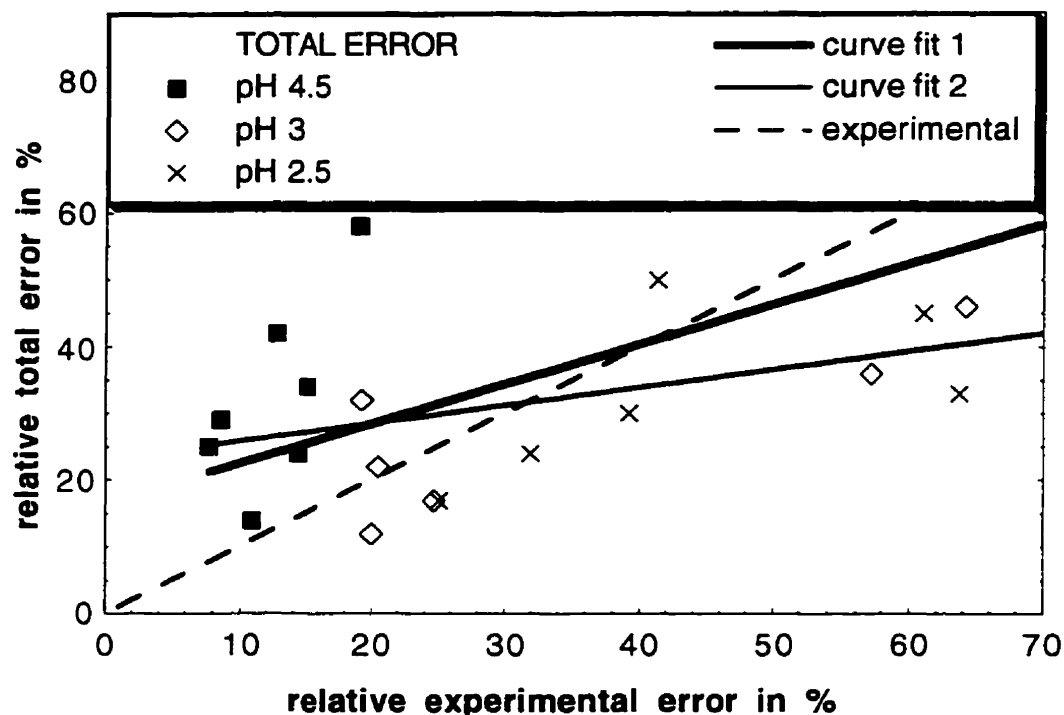


Figure 4.3.6:
Comparison of experimental errors and deviations data points - model

The highest relative errors occurred when the metal binding was low due to low pH and the low value of the ratio $S/L = 2$, resulting in a small difference between $[M]_f$ and $[M]_i$. It should be noted that absolute errors under these conditions were low, however.

The total errors are of a similar magnitude than the experimental errors whose actual value may, of course, vary from the estimated value (the diagonal in the plot). This can be

4.3 Results and Discussion: Experimental and Modeling Errors

due to different calibrations for different sets. Nine of the 19 total error points fall within a 10 % range of the estimated experimental error (dashed line in Figure 4.3.6). For the same points, the modeling error, which corresponds to the difference between the total and experimental errors, is thus less than $\pm 10\%$. For 16 of 19 points it is less than $\pm 25\%$. This means that overall there is no noticeable modeling error.

For smaller estimated experimental errors, however, there is a tendency for positive modeling errors (i.e. the difference between the best fit for the total error and the estimated experimental error) which constitutes up to 15 %. However, more experiments under conditions where low experimental error is expected would be necessary to quantify the modeling error more precisely.

The average experimental errors in the determination of the binding of each metal ion are summarized in Table 4.3.2. Most of the errors result from inaccuracies of the determination of the initial and final metal concentration using the Atomic Absorption Spectrophotometer. While calibration error affects the accuracy of the measurement, the drift and fluctuation errors affect the precision of the measurement. The error of the metal uptake modeling that occurred due to errors in the determination of the final pH (estimated 0.05 pH units) are also listed. Overall, the experimental errors in Table 4.3.2 are of a similar magnitude to the modeling errors (Table 4.2.1).

Table 4.3.2 Experimental errors in the determination of metal ion binding: average absolute errors in % of the total binding capacity

Metal	pH	Calibration	Drift & Fluct.	pH reading	Total
Cd	4.5	0.64	0.45	0.50	1.91
	3.0	0.73	0.51	0.75	2.12
	2.5	0.75	0.52	0.51	1.83
Cu	4.5	0.91	0.62	0.82	2.87
	3.0	0.81	0.69	0.74	2.68
	2.5	0.77	0.67	0.44	2.31
Zn	4.5	1.21	1.94	0.05	3.45
	3.0	1.79	2.61	0.35	4.85
	2.5	2.00	2.71	0.12	4.86

4.3.9 Section Summary

In the determination of the metal concentration in solution, errors in calibration were of similar magnitude as the ones for drift and fluctuation of the AA. Absolute errors increased with the increasing metal concentration while relative errors decreased from about 5 to 1 %.

Although errors in the sample dilution were small, dilution magnified the error substantially due to the fact that the larger relative errors at low concentrations were "scaled up" to higher concentrations. Therefore, dilution should be avoided when possible, for example by choosing the appropriate AA wavelength and burner orientation.

In determining the metal uptake, the errors in mass and volume measurements are rather negligible compared to the error in determining the metal concentration. When the latter one is of the same magnitude as the difference between the initial and final concentrations, the total error for the uptake is large. In order to minimize the source of the errors, it is necessary to obtain a large difference between the initial and final concentrations which can only be achieved by adjusting the solid to liquid ratio.

The calculated experimental errors were of a similar magnitude as deviations between data points and model predictions. This means that no significant modeling error could be detected, except possibly at low experimental errors where the modeling error may be about 15 %.

4.4 Proton Binding at Different Ionic Strengths

Although it is known that sodium only binds weakly, through electrostatic attraction (van den Hoop and van Leeuwen, 1990), a significant ionic strength effect may be observed if the Na concentration is varied over a wide range. Therefore, a mathematical model of the biosorption equilibrium should include the influence of ionic strength. Additionally, an electrostatic model accounting for ionic strength effects may eventually prove useful in the estimation of the extent to which electrostatic effects contribute to heavy metal sorption (see Section 4.5).

Previous results from titrations of *Sargassum* biomass which involved the measurement of its electrophoretic mobility (Section 4.1.5) showed that it bears a significant negative charge when the concentration (and therefore the binding) of protons or covalently bound divalent metal ions is low. Obviously, this charge must lead to electrostatic attraction of cations. Until now, however, biosorption of metal ions has only been modeled using chemical binding constants (Sections 4.1 and 4.2), disregarding the effects of electrostatic attraction.

The purpose of this section is to provide a model that includes ionic strength effects in biosorption modeling for charged and heterogeneous sorbent materials such as *Sargassum* biomass or alginic acid, occurring as particles which are large in comparison to the double layer thickness. The metal ion or proton binding sites in *Sargassum* biomass are predominantly the carboxyl groups of alginate and, to a smaller extent, also the sulfate groups of fucoïdan. Since alginate is a macromolecule of about 80 monomers (Chapman, 1980, pp. 194-196), the focus in this work is on *poly*-electrolyte models.

The results presented in this section have, in modified form, been submitted for publication as Schiewer and Volesky (1997a and b).

4.4 Results and Discussion: Proton Binding at Different Ionic Strengths

4.4.1 General Model Equations

The equations for charge neutrality in solution and in the particle or gel are for $[L] \gg [OH]$:

$$[L] = [H] + [Na] \quad (\text{mmol/L}) \quad (4.4.1)$$

$$B/V_m + [L_p] = [H_p] + [Na_p] \quad (\text{mmol/g}) \quad (4.4.2)$$

where B is the total number of charged groups in the biomass. Assuming that only one binding site C contributes to the surface charge one can write:

$$B = C = {}^cC - CH \quad (\text{mmol/g}) \quad (4.4.3)$$

The ionic strength in solution is defined as:

$$I = 0.5 \sum z_j^2 [X_j] = 0.5 ([H] + [Na] + [L] + [OH]) \quad (\text{mmol/L}) \quad (4.4.4)$$

For $[OH] \ll [L]$ this can be simplified by substituting equation (4.4.1) into equation (4.4.4):

$$I = [L] \quad (\text{mmol/L}) \quad (4.4.5)$$

The apparent C-site proton binding constant is:

$${}^{CH}K_{app} = \frac{CH}{C \gamma [H]} \quad (\text{L/mmol}) \quad (4.4.6)$$

with γ as the activity coefficient which is estimated using the extended Debye-Hückel equation with the coefficients determined by Robinson and Stokes (1959, pp. 231, 236) for NaCl:

$$\log \gamma = \frac{-0.51 \sqrt{I (\text{mol/L})}}{1 + 1.32 \sqrt{I (\text{mol/L})}} + 0.055 I (\text{mol/L}) \quad (-) \quad (4.4.7)$$

The degree of dissociation of the acidic group C is defined as:

$$f = \frac{C}{{}^cC} = \frac{{}^cC - CH}{{}^cC} \quad (-) \quad (4.4.8)$$

4.4 Results and Discussion: Proton Binding at Different Ionic Strengths

In the first approximation, assuming $CH \sim H_q$, this is equal to

$$f = \frac{C}{C} = \frac{C - H_q}{C} \quad (-) \quad (4.4.9)$$

Since no equation for calculating the experimentally obtained CH is mentioned in the available literature, it appears that most if not all other researchers assume that $CH \sim H_q$, thus using (4.4.9). As pointed out below, however, the assumption $CH \sim H_q$ results in marked differences in the calculated $^{CH}K_{app}$ at low f, from which the intrinsic ^{CH}K is estimated. Therefore, this work makes a point in distinguishing between the amount of protons that are bound covalently (i.e. as CH) and electrostatically (i.e. as $[H_p] - [H]$). This requires the derivation of equations for CH (equation (4.4.20)) and $[H_p]$ (equation (4.4.16)) that reflect this situation.

Substituting (4.4.8) into (4.4.6) and taking the logarithm yields:

$$-p^{CH}K_{app} = pH + \log\left(\frac{L-f}{f}\right) + p\gamma \quad (-) \quad (4.4.10)$$

The algorithm for the calculation of the variables H_q , CH, B, f and $p^{CH}K_{app}$ from raw experimental data (i.e. final pH) is given in Figure 4.4.1. Starting with the calculation of the amount of ligand in solution (L) and the amount of protons bound (H_q), the other variables are calculated. The last terms to be evaluated are B (useful to know as a starting value for the model calculations, see Figures 4.4.2 and 4.4.3) and $p^{CH}K_{app}$ which is plotted in some of the graphs.

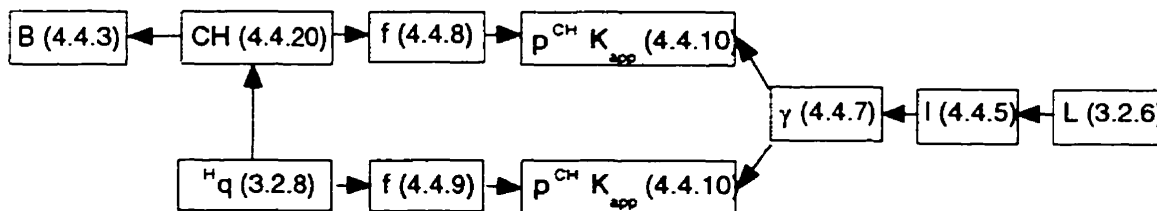


Figure 4.4.1:
Calculation algorithm for experimentally determined variables

4.4.2 Equations for Donnan Model (DO)

Since ions can easily diffuse into the algal cell wall, it might be appropriate to treat *Sargassum* biosorbent as a Donnan type gel. Consequently, the Donnan model is considered in this work. This model reflects that for negatively charged *Sargassum* biomass, the intra-particle concentrations of cations can be higher than the bulk concentrations. The particle is treated as a separate phase with a homogenous concentration throughout this phase. The remaining question concerning the use of the Donnan model is whether *Sargassum* particles are too heterogeneous to be described with a model that assumes a uniform concentration of ions throughout the gel. Therefore, a Gouy-Chapman model which does not assume a uniform ion concentration will also be considered in this study (Section 4.4.3 below).

The commonly known equation for the concentration factor λ in an electrolytic gel according to the Donnan theory (Donnan, 1911) is:

$$\lambda_p^{z_x} = \frac{[X_p]}{[X]} \quad (-) \quad (4.4.11)$$

$$\frac{[Na_p]}{[Na]} = \frac{[H_p]}{[H]} \quad (-) \quad (4.4.12)$$

$$\frac{[H_p]}{[H]} = \frac{[L]}{[L_p]} \quad (-) \quad (4.4.13)$$

with $[X_p]$ being the concentration of any ionic species X with a charge z_x in the gel. Substituting $[Na_p]$ according to equation (4.4.2) into (4.4.12), solving the resulting equation for $[H_p]$ and replacing $[H] + [Na]$ with I (equations (4.4.1) and (4.4.5)) and λ according to equation (4.4.11) yields:

$$\lambda_p = \frac{[H_p]}{[H]} = \frac{(B/V_m + [L_p])}{I} \quad (-) \quad (4.4.14)$$

Solving (4.4.13) for $[L_p]$ and substituting into (4.4.14) yields with L according to equation (4.4.5):

$$\lambda_p = \frac{[H_p]}{[H]} = \frac{B/V_m}{I} + \frac{[H]}{[H_p]} = \frac{B/V_m}{I} + \frac{1}{\lambda_p} \quad (-) \quad (4.4.15)$$

The recurring dimensionless group $B / (V_m I)$ which indicates the magnitude of intra-particle accumulation of ions as compared to the bulk ionic strength will henceforth be

4.4 Results and Discussion: Proton Binding at Different Ionic Strengths

called Q. The solution of the quadratic equation for $[H_p]$ which can be obtained from (4.4.15) is

$$\lambda_p = \frac{[H_p]}{[H]} = \frac{B/V_m}{2I} + \sqrt{\frac{(B/V_m)^2}{4I^2} + 1} = \frac{Q}{2} + \sqrt{\frac{Q^2}{4} + 1} \quad (-) \quad (4.4.16)$$

For conditions where $Q \gg 1$ (4.4.16) can be simplified as:

$$\lambda_p = \frac{[H_p]}{[H]} = \frac{B/V_m}{I} = Q \quad (-) \quad (4.4.17)$$

In the literature this same equation (4.4.17) is obtained from equations (4.4.12) and (4.4.2) by implicitly assuming high concentration factors λ or Q values (so that $[L_p] \ll B/V_m$) and $[Na] \gg [H]$ (such that $[Na] = I$ and $[Na_p] = B/V_m$) (Marinsky and Ephraim, 1986; Marinsky, 1987).

If, on the other hand, $Q \ll 1$ equation (4.4.16) can be simplified as:

$$\lambda_p = \frac{[H_p]}{[H]} = \frac{B/V_m}{2I} + 1 = \frac{Q}{2} + 1 \sim 1 \quad (-) \quad (4.4.18)$$

In order to obtain a more general Donnan model that applies for any Q value and also under conditions where $[Na] \gg [H]$ is not fulfilled, this work does not follow the Marinsky equations (4.4.17) but uses equation (4.4.16) instead.

Substituting equations (4.4.17) or (4.4.18), respectively, into equation (4.4.13) yields that $[L_p]$ approaches 0 for $Q \gg 1$ and L for $Q \ll 1$.

A generalized version of equations (4.4.17) and (4.4.18) is:

$$\lambda_p = \frac{[H_p]}{[H]} = \frac{B/V_m}{nI} + 1 = \frac{Q}{n} + 1 \quad (-) \quad (4.4.19)$$

with n varying between 1.0 ($Q \gg 1$) and 2.0 ($Q \ll 1$). Substituting (4.4.3) and (3.3.7) into (4.4.19) yields for $V_m \ll H_q/[H]$ (which is always fulfilled for the data in this work since the minimum value of $H_q/[H]$ reached is $\sim 2 \text{ mequiv/g} / 10^{-2} \text{ mol/L} = 200 \text{ mL/g}$ which is much larger than V_m at low pH):

$$CH = H_q \frac{nI}{nI - [H]} - {}^t C \frac{[H]}{nI - [H]} \quad (\text{mmol/g}) \quad (4.4.20)$$

For the data in this study a value of n significantly larger than 1.0 ($n > 1.1$) is only obtained when $nI \gg [H]$ or when $H_q \sim {}^t C$. In these cases, however, the value of n cancels out and

4.4 Results and Discussion: Proton Binding at Different Ionic Strengths

equation (4.4.20) reduces to $CH = Hq$. Therefore it was possible to calculate CH using equation (4.4.20) with $n = 1$ for all data in this study. Without this simplification, CH and $[H_p]$ or n have to be calculated iteratively. The above equation is useful in order to determine the CH value in the experiments which is necessary for calculating f (equation (4.4.8)) and thereby $(p^{CH}K_{app})$ (equation (4.4.10)).

In the modeling, the intrinsic proton binding constant is defined as:

$${}^{CH}K = \frac{CH}{C \gamma_p [H_p]} \quad (\text{L/mmol}) \quad (4.4.21)$$

Substituting C using equation (3.3.2) into (4.4.21), CH according to the Donnan model can be calculated as:

$$CH = \frac{{}^tC \ {}^{CH}K \ \gamma_p [H_p]}{1 + {}^{CH}K \ \gamma_p [H_p]} \quad (\text{mmol/g}) \quad (4.4.22)$$

where γ_p is evaluated at the local ionic strength I_p . It is proposed in this work to calculate I_p by substituting equations (4.4.1), (4.4.5) and (4.4.11) into (4.4.4), where (4.4.4) is evaluated at the average concentration $[X_p]$ of each species in the particle.

$$I_p = 0.5 I (([H] + [Na]) \lambda_p + [L] / \lambda_p) = 0.5 I (\lambda_p + 1 / \lambda_p) \quad (\text{mmol/L}) \quad (4.4.23)$$

The particle volume V_m is the fitting parameter which takes care of electrostatic effects for the rigid Donnan (DORI) model. Swelling changes the concentration of charged sites per volume and therefore also the concentrations of ions in the gel. Since it was observed (see Section 4.4.8 below) that swelling of both *Sargassum* and alginate increased with pH, the following simple linear relationship between the specific particle volume and pH was assumed:

$$V_m = Y_v \text{ pH} \quad (\text{L/g}) \quad (4.4.24)$$

Y_v is a constant that has to be determined from the experimental data (for the DO model with swelling). Two versions of the Donnan model are considered in the following: one which assumes a rigid particle (DORI), and one which accounts for swelling (DOSW). The method of using the Donnan model in the study presented here was different from that by Lin and Marinsky (1993): instead of using the binding data in order to calculate the gel volume, a simple estimate of the gel volume (equation 4.4.24) was used in order to predict the proton binding. These predictions were then compared with the experimental results.

4.4 Results and Discussion: Proton Binding at Different Ionic Strengths

The algorithm for the calculation of the proton binding and other variables is shown in Figure 4.4.2. It is necessary to perform the calculations iteratively. A reliable, stable method has been to start the iteration by assuming that the concentration of free sites is equal to the experimentally determined value (equations (4.4.3) and (4.4.20)). Additionally to B , V_m is the other starting value which, however, does not have to be calculated iteratively since it is constant for a given pH value. In each loop of the iteration, H_p , I_p , γ , CH and B have to be evaluated. When stable values are reached, the remaining variables H_q , f and ultimately $p^{CH}K_{app}$ are calculated without further iteration.

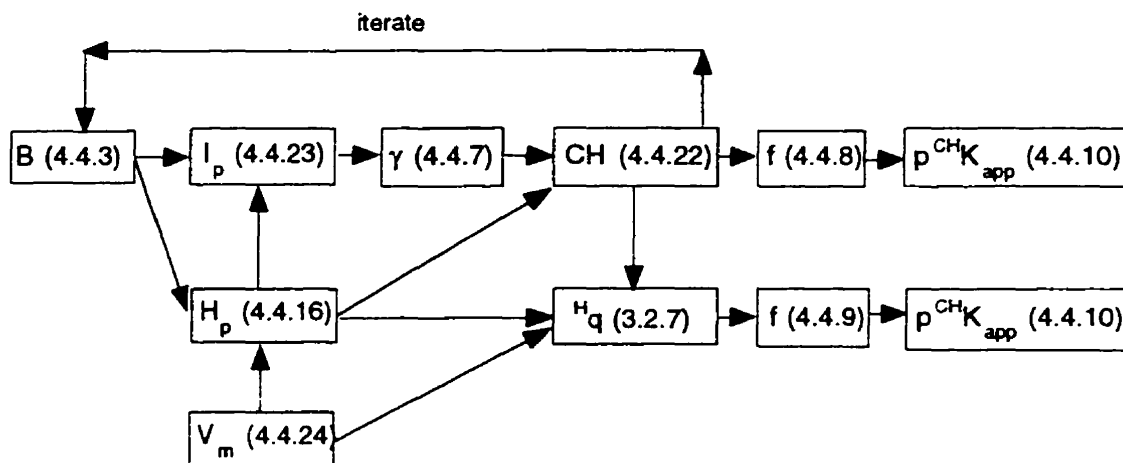


Figure 4.4.2: Calculation algorithm for the Donnan model

Variables not mentioned in this figure are taken to be the same as in Figure 4.4.1

4.4.3 Equations for the Gouy-Chapman (GC) Model

Descriptions of the classical Poisson-Boltzmann equation as applied to counter ion concentration near a charged surface according to the Gouy-Chapman (GC) theory (including derivations and explanations for equations 4.4.25; 4.4.26; 4.4.27 and 4.4.29) are given by Stumm and Morgan (1992, pp. 43-49, 79-81) and Rieger (1994, pp. 59-68). The advantage of the Gouy-Chapman theory as compared to the earlier Helmholtz theory is that while the latter assumes a constant capacitance, the former one considers changes in capacitance with changing ionic strength. Therefore, the GC equation is chosen as a double layer model to be used in this work. The Gouy-Chapman theory is based on the consideration that a diffuse counter ion layer forms near the charged surface such that thermal motion and electrostatic attraction are balanced. Since ion-ion interactions in

4.4 Results and Discussion: Proton Binding at Different Ionic Strengths

solution, discontinuous charge density variations and changes of the dielectric constant due to changing orientation of the water molecules are not accounted for, the equations should be used for low to moderate ionic strength, surface charge density and potential (Rieger, 1994, pp. 67-68).

Most studies reported in the literature concerning double layers in natural materials use models that either cannot predict ionic strength effects (Bartschat et al., 1992; Xue et al., 1988) or that are based on empirical correlations (Tipping et al., 1988; Tipping, 1993). Of the available literature only De Wit et al. (1993) uses the GC model. The latter, however, deal with small humic molecules having an average diameter of 0.31 nm, which is smaller or about equal to the double layer thickness (for water at 25 °C the double layer thickness $1/\kappa \sim 0.3$ nm for $I = 1000$ mM, $1/\kappa \sim 10$ nm for $I = 1$ mM, see equation 4.4.29 for a definition of the double layer thickness). The biosorbent materials considered in the present work are much larger than the double layer thickness even at the lowest imaginable ionic strength (the double layer thickness decreases with increasing ionic strength), therefore the charge must be balanced inside the particle, i.e. equation (4.4.2) is valid for the particle as a whole. Consequently, it is not necessary to know the local concentrations at each distance from the interface according to equation (4.4.25) but it is sufficient to calculate the average concentrations to which equation (4.4.2) refers. Therefore, for $[H_p]$ the same equation (4.4.16) as for the DO model is used, which is then required in the calculation of H_q (equation (3.3.7)). The chemical reaction equilibrium, different than in the Donnan model, is calculated for the local concentration at the charged interface $[X_s]$. This means that the GC model which is presented really is a combination of the Gouy-Chapman and Donnan models.

The Poisson equation for the concentration $[X_d]$ of a species X with the charge z_x at a distance d from the charged interface is

$$[X_d] = [X] \lambda_d^{z_x} \quad (\text{mmol/L}) \quad (4.4.25)$$

$$\lambda_d = \exp\left(\frac{-F \phi_d}{R T}\right) \quad (-) \quad (4.4.26)$$

where λ_d is the concentration factor at distance d . The surface potential ϕ_s (at $d = 0$, index: s) according to the Gouy-Chapman equation for small ϕ_s (< 25 mV) is calculated as:

$$\phi_s = \frac{\sigma_s}{\epsilon \kappa} \quad (\text{V}) \quad (4.4.27)$$

4.4 Results and Discussion: Proton Binding at Different Ionic Strengths

with ϵ being the dielectric constant and $1/\kappa$ the double layer thickness. The surface charge density σ_s , assuming uniform charge distribution over a hypothetical surface A_m , is for a number of free binding sites B with F being the Faraday constant:

$$\sigma_s = \frac{-BF}{A_m} \quad (\text{coul/m}^2) \quad (4.4.28)$$

The double layer thickness $1/\kappa$ is defined as:

$$\frac{1}{\kappa} = \sqrt{\frac{\epsilon RT}{2 F^2 I}} \quad (\text{m}) \quad (4.4.29)$$

with R being the ideal gas constant and T the temperature. The concentration factor at the interface is:

$$\lambda_s = \left(\frac{[X_s]}{[X]} \right)^{1/z_x} \quad (-) \quad (4.4.30)$$

From these equations the following were derived in this work by substituting (4.4.27; 4.4.28) and (4.4.29) into (4.4.26), yielding:

$$\lambda_s = \exp\left(\frac{BP}{\sqrt{I}}\right) \quad (-) \quad (4.4.31)$$

Factor P must be determined empirically from the experimental data, and is defined as:

$$P = \frac{F}{A_m \sqrt{2 \epsilon R T}} \quad (\text{g mmol}^{-0.5} \text{ L}^{-0.5}) \quad (4.4.32)$$

If it is assumed that the surface area per dry mass increases when the particle swells then this has an effect on the factor P which is related to the charge density per surface area (equation (4.4.32)). Assuming a linear relationship between surface area and volume

$$P = \text{const} / A_m = Y_p / V_m \quad (\text{g mmol}^{-0.5} \text{ L}^{-0.5}) \quad (4.4.33)$$

and using equation (4.4.24) for the specific volume we obtain:

$$P = Y_p / (Y_v \text{ pH}) = Y_{pv} / \text{pH} \quad (\text{g mmol}^{-0.5} \text{ L}^{-0.5}) \quad (4.4.34)$$

where Y_p (if Y_v is known) or $Y_{pv} = Y_p / Y_v$ (if Y_v is unknown) are constant fitting parameters. Similar to the Donnan model, two model versions, one which assumes rigid particles (GCRI) and one which accounts for swelling (GCSW), are considered in the following.

4.4 Results and Discussion: Proton Binding at Different Ionic Strengths

The intrinsic proton binding constant for the Gouy-Chapman model (GC) is defined as:

$${}^{\text{CH}}K = \frac{\text{CH}}{C \gamma_s [\text{H}_s]} \quad (\text{L/mmol}) \quad (4.4.35)$$

Hence, substituting (4.4.3) into (4.4.35), CH according to the GC model can be calculated as:

$$\text{CH} = \frac{{}^{\text{C}}\text{CH} \gamma_s [\text{H}_s]}{1 + {}^{\text{CH}}K \gamma_s [\text{H}_s]} \quad (\text{mmol/g}) \quad (4.4.36)$$

Where γ has to be evaluated at the local ionic strength. This work proposes to calculate the ionic strength at the surface by substituting equations 4.4.1, 4.4.5 and 4.4.30 into (4.4.4) where (4.4.4) applies to the concentrations at the surface.

$$I_s = 0.5 ([\text{H}_s] + [\text{Na}_s] + [\text{L}_s]) = 0.5 I (\lambda_s + 1/\lambda_s) \quad (\text{mmol/L}) \quad (4.4.37)$$

The relationship between the apparent and the intrinsic binding constant can be derived from equations 4.4.6, 4.4.30 and 4.4.35:

$${}^{\text{CH}}K_{\text{app}} = {}^{\text{CH}}K \frac{\gamma_s [\text{H}_s]}{\gamma [\text{H}]} = {}^{\text{CH}}K \frac{\gamma_s}{\gamma} \lambda_s \quad (\text{L/mmol}) \quad (4.4.38)$$

The calculation algorithm is shown in Figure 4.4.3. One can see that this model is similar in structure but slightly more complex than the Donnan model: P , λ_s and $[\text{H}_s]$ (which takes the place of $[\text{H}_p]$ in calculating CH) are introduced as additional variables while V_m is no longer necessary. Again, the iteration is started with P and B (initially assumed to be equal to the experimentally determined value). The variables λ_s , I_s , γ , H_s , CH and B are calculated in each loop of the iteration. H_a , H_q , f and ${}^{\text{CH}}K_{\text{app}}$ are evaluated after the iteration yields stable results.

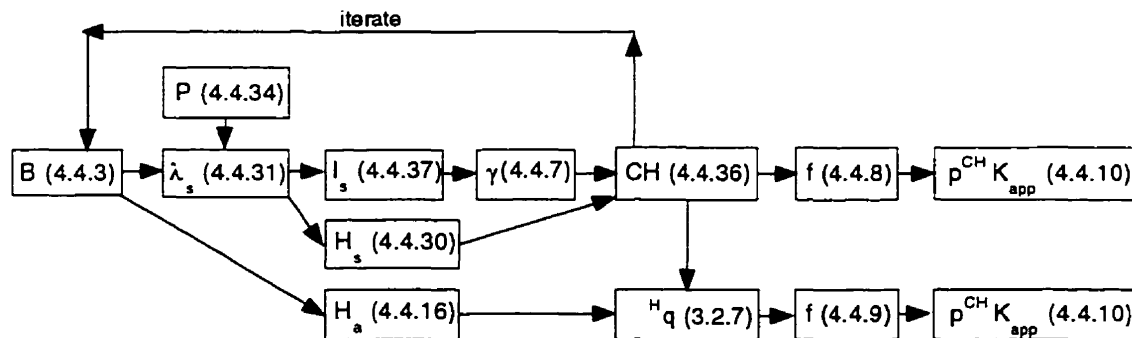


Figure 4.4.3: Calculation algorithm for the Gouy-Chapman model

Variables not mentioned in this figure are taken to be the same as in Figure 4.4.1

4.4.4 Equations for the Plot of f versus $(\text{pH}-\text{pNa})$

In the earlier work of the Marinsky research group (Marinsky and Ephraim 1986; Marinsky, 1987), it was recommended to plot $\text{p}^{\text{CHK}}_{\text{app}}$ versus $(\text{pH} + \text{pL})$ or versus pH . No influence of ionic strength should be noticed if, in the former case, the particle is rigid and permeable, or, as in the latter case, if it is rigid and impermeable. As Cabaniss and Morel (1989) point out, however, these plots are not reliable. They recommend using a plot of f versus $(\text{pH}-\text{pNa})$. This type of plot was then employed in the later work of the Marinsky research group (Lin and Marinsky, 1993). Neither of these authors give a mathematical justification of the use of this plot that indicates when it is valid. This will be undertaken in the present work. From equations 4.4.8 and 4.4.21 one can derive:

$$-\text{p}^{\text{CHK}} = \text{pH}_p + \log\left(\frac{1-f}{f}\right) + \text{p}\gamma \quad (-) \quad (4.4.39)$$

For $Q \gg 1$ (that yields $[\text{H}_p] \gg [\text{H}]$) and substituting $[\text{H}_p] = [\text{H}] B / (V_m I)$ (4.4.17) into (4.4.39) yields after expressing B in terms of f using equations 4.4.3 and 4.4.8:

$$-\text{p}^{\text{CHK}} = \text{pH} - \text{pI} + \text{p}^{\text{tB}/V_m} + \text{p}f + \text{p}\left(\frac{f}{1-f}\right) + \text{p}\gamma \quad (-) \quad (4.4.40)$$

This equation is the justification for the plot of f versus $(\text{pH}-\text{pNa})$ if $[\text{Na}] \gg [\text{H}]$ (i.e. $[\text{Na}] \sim I$) is assumed: since p^{CHK} and p^{tB/V_m} are constant for a rigid particle, f is only a function of $(\text{pH}-\text{pNa})$, not additionally a function of I (assuming γ does not change much). However, it would be more appropriate to plot f versus $(\text{pH}-\text{pI})$ which avoids making the additional assumption that $[\text{Na}] \gg [\text{H}]$. Additionally, I is a more easily accessible variable: while Na has to be measured or calculated as a function of H_q , I can usually be assumed to be constant throughout the experiment (if only monovalent species are present) and calculated from equations 4.4.5 and 3.3.6, assuming $[\text{L}_p] \sim L$.

If the opposite assumption is made, i.e. $Q \ll 1$ (or $[\text{H}] \sim [\text{H}_p]$), it can easily be shown from equation (4.4.39) that:

$$-\text{p}^{\text{CHK}} = \text{pH} + \text{p}\left(\frac{f}{1-f}\right) + \text{p}\gamma = \text{pH} - \text{pI} + \text{p}^{\text{tB}/V_m} + \text{p}f + \text{p}\left(\frac{f}{1-f}\right) + \text{p}\gamma - \text{p}Q \quad (-) \quad (4.4.41)$$

This means that compared to the above equation (4.4.40) the curves of f versus $(\text{pH}-\text{pNa})$ are shifted by $\text{p}Q$ to the right. Whether the one or the other equation may be used now depends on which assumption is more appropriate. This will be discussed in Section 4.4.13.

4.4.5 Titration Curves

Figure 4.4.4 shows the proton binding (H_q) by *Sargassum* biomass at different ionic strengths (I) of the solution as a function of pH. It should be noted that in this and in all other figures the I values that are given in the figure's legend refer to I at $f = 0.5$ of the respective series. Since different amounts of acid or base were added to each sample, the actual final ionic strength varies from point to point. The proton binding was calculated from equation (3.3.9) with $B + [H_p]_i$; $V_m = 2.6$ mmol/g. This value was chosen such that the inflection that signifies the endpoint of the titration occurs at $H_q = 0$. It can be noticed that the maximum proton binding and therefore the number of binding sites (assuming one type of binding site C only) C is equal to 2.1 mmol/g for any ionic strength. This means that 0.5 mmol/g of extra protons in the pores or in the cell would have been present due to incomplete washing.

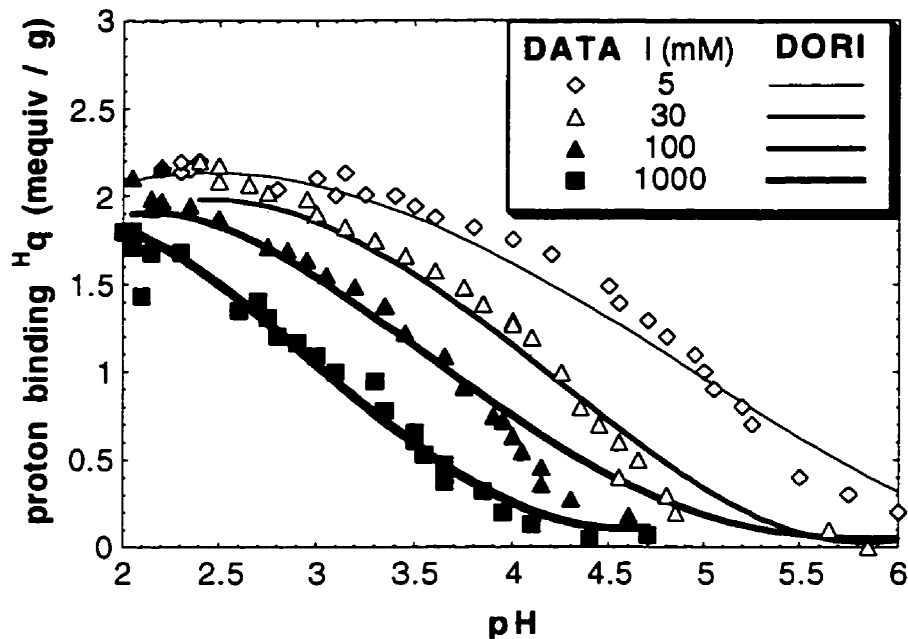


Figure 4.4.4: Titration of protonated *Sargassum* biomass at different ionic strengths:

Experimental data and predictions of the Donnan model for rigid particles (DORI)

The apparent proton binding constant ($^{CHK}_{app}$) changes drastically with ionic strength: while the $-p^{CHK}_{app}$ (p^{CHK} at half-dissociation of the acidic group) for low I is close to 5, it decreases to about 3 for high ionic strength. This corresponds to a change in the proton binding constants by a factor of 100. The observed shift in p^{CHK}_{app} values is a

4.4 Results and Discussion: Proton Binding at Different Ionic Strengths

common phenomenon in titrations of polyelectrolytes (Lin and Marinsky, 1993; Marinsky and Ephraim, 1986; Tipping et al., 1988). The reason for this is that, due to electrostatic effects, the local proton concentration at the solid-solution interface $[H_s]$ is higher than the bulk concentration $[H]$. The half-dissociation for low ionic strength then does not really occur at pH 5 but at a local, lower pH (equation (4.4.38)). The concentration factor λ_s , by which the local concentration exceeds the bulk concentration, decreases with the ionic strength (4.4.31). Consequently, the electrostatic effects are low at high ionic strength such that the p^{CHK}_{app} at high ionic strength approaches the intrinsic p^{CHK} .

The proton binding for alginate is shown in Figure 4.4.5. Equation (3.3.8) was evaluated with $CH_i + SH_i + [H_p]_i V_m = 0$ because Na-alginate was used. Since the determination of proton accumulation becomes rather inaccurate at $pH < 2$, it is not possible to reliably calculate the proton binding at such low pH values. At $pH > 2$, however, the maximum proton binding is not yet achieved. Therefore, the total number of binding sites cannot be determined graphically. Consequently, it is also not possible to read the half-dissociation pH from the graph.

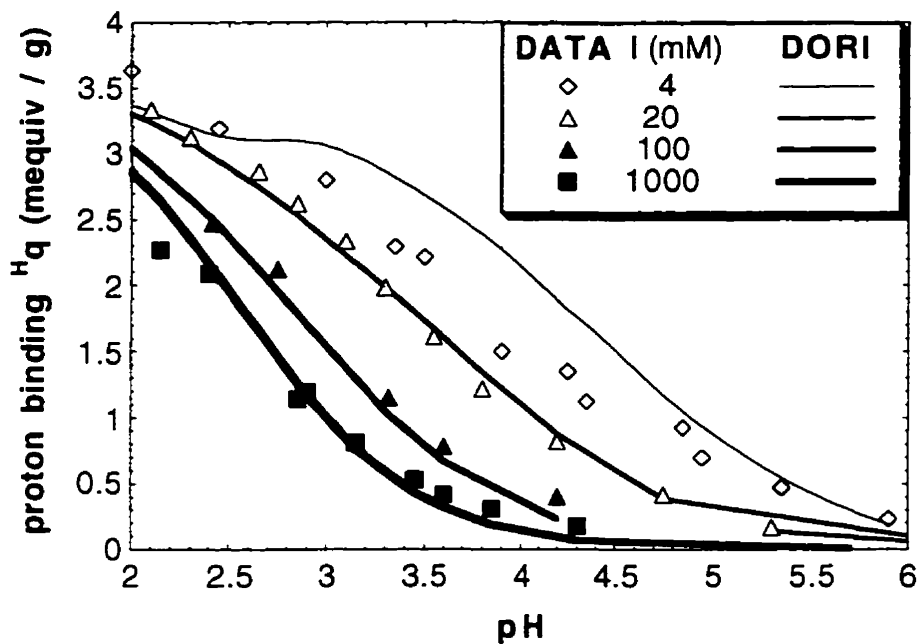


Figure 4.4.5: Titration of Na-alginate at different ionic strengths:
Experimental data and predictions of the Donnan model for rigid particles (DORI)

4.4 Results and Discussion: Proton Binding at Different Ionic Strengths

However, it is obvious that the p^{CHK} values for alginate are generally lower than for *Sargassum*. Also, one can see that the p^{CHK} values for high and low ionic strength (the values of I are similar for both materials) differ only by one pH unit as opposed to two pH units for *Sargassum*. This may indicate less pronounced electrostatic effects in the case of alginate.

The modeling results both for the titrations of *Sargassum* and alginate are discussed in section 4.4.11.

4.4.6 Variation of Apparent p^{CHK}

Figures 4.4.6 and 4.4.7 show the influence of the degree of dissociation (f) and the ionic strength on p^{CHK}_{app} for *Sargassum* and alginate, respectively. The apparent p^{CHK} is calculated according to equation (4.4.10). The degree of dissociation, f , of the acidic group C is defined in equation (4.4.8). As a first approximation, assuming $CH \sim H_q$, this is equal to (4.4.9). While the definition of f according to equation (4.4.9) renders the direct calculation of f from H_q possible, it is necessary to estimate CH with equation (4.4.20) for the more correct calculation of f using equation (4.4.8).

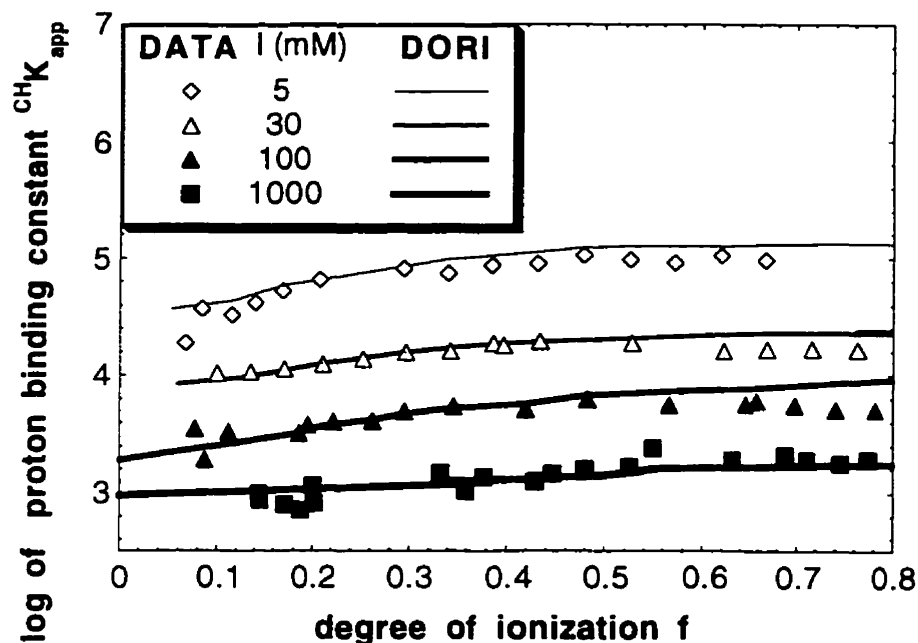


Figure 4.4.6: Variations of apparent p^{CHK} for titration of protonated *Sargassum* biomass at different ionic strengths: Experimental data and predictions of the Donnan model for rigid particles (DORI)

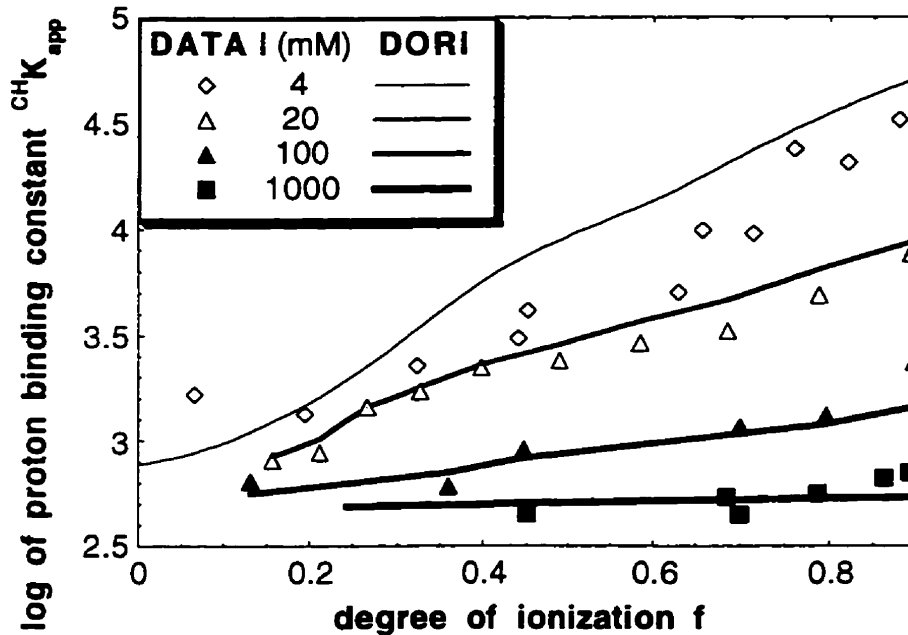


Figure 4.4.7: Variations of apparent $p^{\text{CHK}}_{\text{app}}$ for titration of Na-alginate at different ionic strengths:

Experimental data and predictions of the Donnan model for rigid particles (DORI)

The values of f obtained from these two methods do not differ widely and, consequently, the values for $p^{\text{CHK}}_{\text{app}}$ are also quite similar for most data points. At low f and low I , however, even a small difference in f has a significant effect on $p^{\text{CHK}}_{\text{app}}$. The $p^{\text{CHK}}_{\text{app}}$ values calculated with (4.4.9) are up to 0.25 units higher than the ones calculated with (4.4.8) for the same data points (data not shown). As shown below, the value of $p^{\text{CHK}}_{\text{app}}$ for low f is of special importance for the extrapolation of the intrinsic $^{\text{CHK}}K_{\text{app}}$. Therefore, the calculation of f should be based on CH and not on H_q .

In general, it can be seen that the $p^{\text{CHK}}_{\text{app}}$ values for low I are generally higher and more strongly dependent on f . The apparent p^{CHK} decreases with decreasing degree of dissociation. As f goes towards zero, $p^{\text{CHK}}_{\text{app}}$ (using f from equation (4.4.8)) for the alginate approaches a value of about 2.6 for any ionic strength, while for *Sargassum* $p^{\text{CHK}}_{\text{app}} = 3 - 4.5$ (depending on the ionic strength) is approached. The decrease of $p^{\text{CHK}}_{\text{app}}$ with decreasing f can be explained as the result of a decreasing concentration factor with a decreasing charge (equations (4.4.38) and (4.4.31)) when the degree of dissociation decreases. For increasing ionic strength or decreasing degree of dissociation,

4.4 Results and Discussion: Proton Binding at Different Ionic Strengths

the concentration factor approaches unity since the exponent in equation (4.4.31) approaches zero. Consequently, the p^{CHK}_{app} value is expected to approach the intrinsic p^{CHK} under these conditions, and electrostatic effects are no longer relevant. The fact that the curves for *Sargassum* do not appear to converge toward a common value for all ionic strengths may be due to the fact that electrostatic effects are stronger in *Sargassum* such that they only become negligible at very low degrees of dissociation for which no data points exist.

The modeling of the variation of the apparent p^{CHK} for *Sargassum* and alginate is discussed in section 4.4.12.

4.4.7 Plot of f versus (pH-pNa)

According to Cabaniss and Morel (1989) a plot of the degree of dissociation versus (pH-pNa) reveals whether a polyelectrolyte gel is rigid or flexible (equation (4.4.40)): for a given degree of dissociation the value of (pH-pNa) should not vary with ionic strength if the gel is rigid whereas it may vary for flexible gels. Figures 4.4.8 and 4.4.9 show this type of plot for *Sargassum* and alginate, respectively.

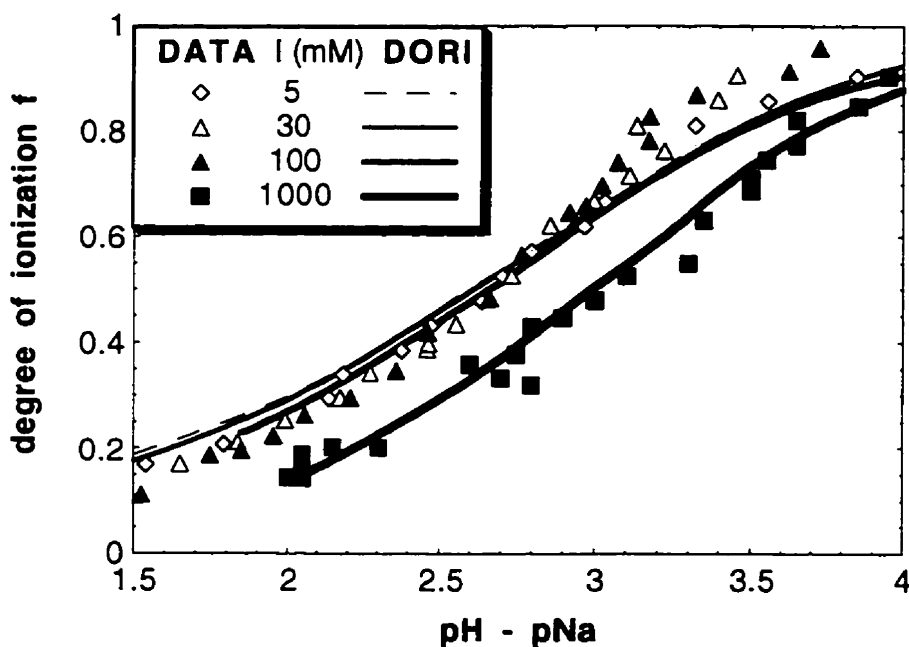


Figure 4.4.8: Plot of f versus (pH-pNa) for titration of protonated *Sargassum* biomass at different ionic strengths: Experimental data and predictions of the Donnan model for rigid particles (DORI)

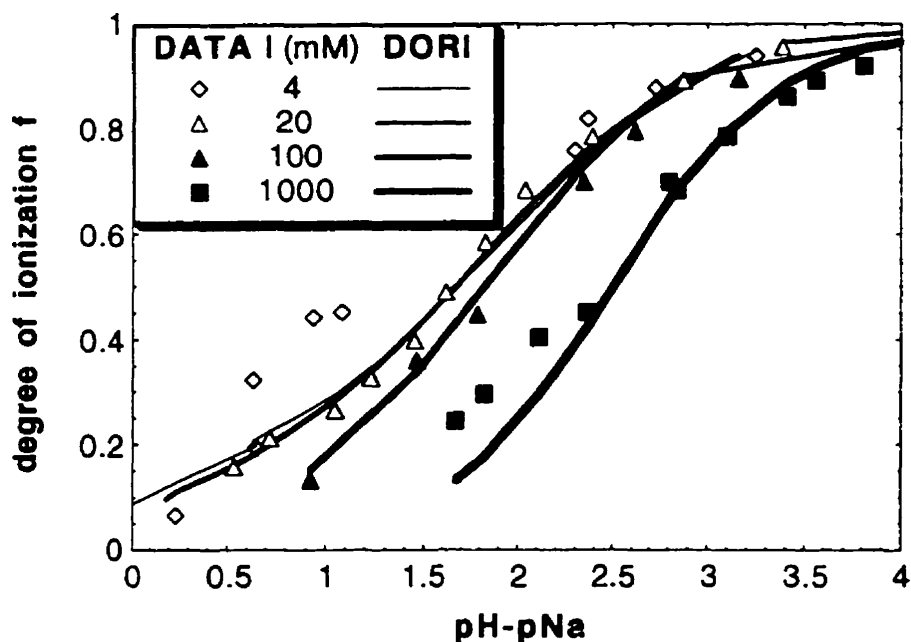


Figure 4.4.9:
Plot of f versus $(\text{pH}-\text{pNa})$ for titration Na-alginate at different ionic strengths:
 Experimental data and predictions of the Donnan model for rigid particles (DORI)

It appears that *Sargassum* behaves as a rigid particle since little ionic strength effect is observed in this plot. Only for $I = 1000$, there seems to be some flexibility of the particle. In contrast, alginate obviously swells since the curves for different ionic strength deviate strongly from each other. This result is intuitively appealing because the fact that alginate swells is known from the literature (Lin and Marinsky, 1993), (Moe et al., 1993), and less swelling can be expected for *Sargassum* because its alginate is constrained in the cellulose matrix of the cell wall.

4.4.8 Physical Behavior of Biosorbents

Swelling experiments were performed in order to test the hypothesis that alginate is flexible while *Sargassum* is not, and also to obtain information about the relationship between swelling and experimental conditions such as pH and ionic strength. The bed volume of *Sargassum* biomass particles in the graduated cylinders was constant (data not

4.4 Results and Discussion: Proton Binding at Different Ionic Strengths

shown) and did not depend on either pH or ionic strength. This would tend to support the hypothesis that *Sargassum* does not swell.

When the dry weight of the biomass after the swelling experiment was measured, however, it was observed (data not shown) that the biomass had lost 30 % of its initial weight at high pH, while it lost less than 20 % at low pH. The weight loss increased with pH but was not related to the ionic strength. Since at high pH the same bed volume was taken in by a smaller mass than at low pH, this would indicate that swelling could have occurred to a small extent.

In a further attempt to investigate swelling, the ratio between the wet weight of the biomass after swelling and its dry weight after swelling and oven drying was calculated. This ratio was proportional to the specific volume V_m of the biomass. The specific volume V_m increased from 5 to 10 mL/g when the pH was raised from 2 to 4.5. No influence of ionic strength was noticeable (data not shown). Since the specific volume changed by as much as a factor of 2, swelling appears to be relevant in *Sargassum*, contrary to the above mentioned observations. A reason why the bed volume remained unchanged may be that the bed porosity (void space) decreased with increased particle swelling and pH. It has to be mentioned, however, that only volume changes in the volume that is active in proton binding (i.e. the alginate zone) of the biomass are of importance for the protonation behavior. These volume changes may not necessarily correspond to overall volume changes of the particle. Therefore, the results from the swelling experiments cannot be used for modeling purposes in a quantitative way.

For alginate, the amount of mass recovered decreased more significantly with increasing pH (no data shown) as compared with *Sargassum* biomass. Already at pH 3 very little alginate was recovered. This can be explained by the fact that sodium alginate is soluble. For the remaining recovered mass, the ratio between wet gel mass and dry mass was calculated analogous to *Sargassum*. The specific volume V_m increased from about 20 to about 200 mL/g when pH rose from 1.5 to 3.5 (data not shown). Although these values are not to be taken quantitatively (because it is difficult to estimate how much excess liquid remained in the gel), from the measured volume change by a factor of 10 it can be concluded that alginate swelling strongly increases with pH. This corresponds to experimental results of Moe et al. (1993) for alginate swelling where the volume was observed to increase with pH. Whether alginate swelling in this study also increased with decreasing salt concentration as observed by Moe et al. was not clearly discernible.

4.4.9 Model Parameters and Errors

4.4.9.1 Types of Models

The work presented here makes an effort to represent the system in the simplest possible way that is physico-chemically plausible and that gives reasonably low modeling errors, stating the assumptions and limitations of its validity. This way the observed behavior in the experiments and the fitting parameters can be interpreted in a meaningful way that contributes to the understanding of biosorption. In addition, the closer a model reflects the real processes, the better it can be expected to predict experimental conditions under which it was not originally derived. Purely empirical models usually fit for limited conditions only. In order to evaluate the validity of a model, a broad range of conditions has to be considered. Therefore, multiple independent variables were widely varied (proton concentration: five orders of magnitude, Na concentration: about four orders of magnitude, two materials) in a range which produced pronounced variations of the dependent variable H_q . A high ratio between the number of experimental data points and the number of fitting parameters was achieved.

Three general ways of modeling the influence of ionic strength were considered. The simplest one is a model based on chemical equilibrium constants (in the following referred to as the CHEM model) which assumes that intra-particle concentrations are equal to bulk concentrations and that the effect of Na in the solution simply consists of competition for the binding sites of the sorbent. This type of model has been used by, amongst others, Westall et al. (1995). It is known that Na does not bind covalently but only electrostatically and, therefore, that this model does not reflect the physical reality. It is, however, attractive due to its mathematical simplicity and the fact that it can easily be used with computer programs, such as MINEQL+ (Schecher, 1991), for computation of chemical solution equilibria. With this type of model (CHEM) the equilibrium does not depend on the particle volume, i.e. swelling has no effect on proton binding. Proton binding can be calculated using a multi-component Langmuir isotherm model. From equation (4.2.4) we obtain for one site ($m = 1$) and two monovalent cations ($n = 2$, $z_j, z_h = 1$):

$$H_q = \frac{C_{CHK} [H]}{1 + CHK [H] + C_{NaK} [Na]} \quad (\text{mmol/g}) \quad (4.4.42)$$

The second one is a Donnan type model (DO) as described in Section 4.4.2. It is based on the assumption that the intra-particle concentration may be different from the bulk concentration. The intra-particle concentration is assumed to be homogeneous throughout

4.4 Results and Discussion: Proton Binding at Different Ionic Strengths

the reactive gel volume. Two versions of the Donnan model are considered in the following: one which assumes a rigid particle (DORI), and one which accounts for swelling (DOSW).

The third type of model makes use of the Gouy-Chapman equation (GC) (see Section 4.4.3). In this case, the concentrations in the particle are not only different from the bulk concentrations but are also not homogeneous throughout the particle. At the solid/liquid interface the concentrations of ions differ more strongly from the ones in the bulk solution than the average intra-particle concentrations. However, it is not necessary to know the concentrations at each point: since the particle size is much larger than the double-layer thickness, the charge must always be balanced within the particle. Therefore, only the surface concentration (at which the chemical equilibrium is evaluated) and the average concentration to which the charge balance (equation (4.4.2)) refers must be known. Similarly to the Donnan model, two model versions, one which assumes rigid particles (GCRI) and one which accounts for swelling (GCSW), are considered in the following.

4.4.9.2 Determination of Model Parameters

For all types of models it was found that three parameters were necessary and sufficient. Apart from the total number of binding sites tC and the equilibrium constant for proton binding CHK , which are already necessary for modeling a single titration curve, only one more parameter was necessary in order to account for the effect of ionic strength. The third parameter for the CHEM, DORI, DOSW, GCRI, and GCSW models were CNaK , V_m , Y_v , P and Y_{pv} , respectively.

Alternatively to $V_m = Y_v$ pH, another swelling correlation $V_m = Y_x + Y_v$ pH, which involves one more fitting parameter (Y_x), was used. In this case, however, the optimization procedure (for which the computer program MATLAB 4.2c was used in order to minimize the deviations between modeled and experimentally determined H_q) did not yield stable results. Therefore this alternative swelling correlation was not considered any further.

For *Sargassum* biomass the value ${}^tC = 2.1$ mmol/g for the total number of binding sites was read directly from Figure 4.4.4. This is the maximum binding achieved at low pH values. It was assumed that all sites were initially occupied by protons. The value $[H_p]_i$; $V_m = 0.5$ mmol/g was chosen so that H_q at high pH values, where the curves level out, approaches zero. This value of $[H_p]_i$; $V_m = 0.5$ mmol/g also corresponds to the amount of protons released when the protonated biomass is equilibrated in distilled water where no exchangeable ions are present (0.46 mmol/g was the average of 4 samples). Since the charge of the biomass must remain balanced by counter ions, the protons released

4.4 Results and Discussion: Proton Binding at Different Ionic Strengths

must have been excess HCl from the protonation which had not been removed during previous washing with distilled water. The value for ${}^{\circ}C = 2.1$ mmol/g is in accordance with previous results for *Sargassum* biosorption (Section 4.1 and 4.2). ${}^{\circ}C$ for the alginate (see Table 4.4.1) was obtained from the fitting procedure. When the value obtained is compared with 4.74 mmol/g, the theoretical number of binding sites in pure Na-alginate, it appears that about 20 weight % of the material used may not have been alginate but, for example, excess sodium salt.

Table 4.4.1: Parameters for polyelectrolyte models

MODEL TYPE	<i>Sargassum</i> biomass			Alginate		
	${}^{\circ}C$ mmol/g	$-p^{CHK}$ -	3rd parameter L/mmol	${}^{\circ}C$	$-p^{CHK}$	3rd parameter mmol/g L/mmol
CHEM	2.1	5.6	$C_{NaK} = 0.8$ L / mmol	3.1	3.9	$C_{NaK} = 0.022$ L/mmol
DORI	2.1	2.9	$V_m = 1.4$ mL / g	3.7	2.7	$V_m = 17$ mL / g
DOSW	2.1	2.8	$Y_v = 0.22$ mL / g	3.6	2.7	$Y_v = 4.2$ mL / g
GCRI	2.1	3.0	$P = 11.7$ g (mmol L) $^{-0.5}$	4.1	2.7	$P = 2.0$ g mmol $^{-0.5}$ L $^{-0.5}$
GCSW	2.1	3.1	$Y_{pv} = 47$ L $^{0.5}$ mmol $^{-0.5}$	3.8	2.6	$Y_{pv} = 11$ L $^{0.5}$ mmol $^{-0.5}$

For both *Sargassum* and alginate the p^{CHK} values obtained from the fitting procedure are similar for all models except the CHEM model. For the CHEM model the fitted p^{CHK} value was even higher than the half-dissociation pH at low ionic strength, especially for *Sargassum* where some Na was added for pH adjustment. Since Na is treated as a competitor, the curve for $Na = 0$ would have a half-dissociation pH equal to the value of p^{CHK} in the model. For the other models, the p^{CHK} values were about equal to the pH of half dissociation for high ionic strength (Figures 4.4.4 and 4.4.5). This means that for all but the CHEM model one could obtain the intrinsic p^{CHK} easily by reading it from the titration curve at $I = 1000$ mM. The only problem is that estimation of the activity coefficient for protons is less reliable for such high values of I . It may, therefore, be

4.4 Results and Discussion: Proton Binding at Different Ionic Strengths

desirable to use, for example, the titration curve for $I = 100$ mM (more established relations for the activity coefficient) in order to obtain a graphical estimate of p^{CHK} . This can be done using Figures 4.4.6 and 4.4.7: for alginate at $I = 20$ or 100 mM, the lines of p^{CHK}_{app} for f approaching zero are close to the fitted value of 2.6 - 2.7. The value of p^{CHK} determined by Lin and Marinsky (1993) for alginate using the Donnan model was 2.95. It has to be mentioned, however, that this was only a rough and somewhat arbitrary estimate since no points for $f < 0.2$ were given by that author. For *Sargassum* the fitted value of about 3 is between the p^{CHK}_{app} values for f approaching 0 at $I = 100$ (~3.2) and at $I = 1000$ mM (~2.8).

For both *Sargassum* and alginate the volume in the DORI model corresponded to that in the DOSW model at high pH, which is reasonable because electrostatic effects are especially noticeable at high pH (i.e. at high pH the volume has the strongest effect on binding). The model predicts that both *Sargassum* and alginate swell by a factor of two when the pH rises from pH 2 to pH 4. This corresponds to the swelling behavior observed in *Sargassum* but it is less pronounced than the swelling observed in alginate. While on the one hand additional water retained after filtering may produce seemingly high values of V_m in the experiments, one may, on the other hand, consider using a different swelling correlation, for example one where V_m is proportional to $(pH)^2$.

When the absolute values of the proton binding volume V_m in the model and the total particle volume tV_m determined in the experiment are compared, it is obvious that the specific volume determined experimentally from the fraction of wet / dry weight after swelling is consistently larger than the one from the model (by a factor of about 6 for alginate and by a factor of about 4 for *Sargassum* for an average value at $f = 0.5$). This could be explained, for example, by assuming that only a fraction of the particle volume is active in proton binding. This assumption certainly does not hold for alginate because all of it should be an active volume. Also for *Sargassum* it can be expected that the alginate volume makes up more than 1/4 of the total volume since it constitutes about 40 % of the mass. Therefore, this can be at best only a partial explanation. Another plausible explanation could be that the concentration at the binding site is indeed higher than the average concentration in the particle but that the Donnan model, because it cannot predict a concentration profile, predicts a "step function" of the concentration instead. This would assume that all the ions that are accumulated in the particle because of electrostatic effects are concentrated in a smaller volume where the concentration is equal to the one at the interface. However, one should not place too large emphasis on these differences between the proton binding volume V_m and the total particle volume tV_m since especially for alginate in the transition between gel state and solubilized state the determination of the gel

4.4 Results and Discussion: Proton Binding at Different Ionic Strengths

volume is unreliable and excess liquid can produce seemingly high values of V_m . It can be regarded as encouraging and supporting of the model assumptions that the proton binding volume determined for the model is of the same order of magnitude than the total particle volume and smaller than the latter.

Since the only unknown variable in the determination of the P value (equation (4.4.32)) is A_m , a rough estimate of the specific surface A_m of *Sargassum* can be obtained by solving (4.4.32) for A_m . For a typical $P = 7 \text{ g mmol}^{-0.5} \text{ L}^{-0.5}$ we obtain $A_m = 7.4 \cdot 10^3 \text{ m}^2/\text{g}$ (water, 25 °C). In order to understand the order of magnitude of geometrical structures having this A_m , one may assume that the surface area is that of little spheres completely filling the volume V_m . For a typical V_m of 1 mL/g these spheres would then have a radius $r = 3 V_m / A_m = 3 \cdot 10^{-6} \text{ m}^3/\text{g} / (7.4 \cdot 10^3 \text{ m}^2/\text{g}) = 4.3 \text{ nm}$. This is in the order of magnitude of molecular (but not cellular) dimensions: the repetition distance (2 uronic acids) in alginate is about 1 nm (Mackie and Preston, 1974, pp. 60).

4.4.10 Modeling the Effect of Ionic Strength

Figure 4.4.10 shows the effect of ionic strength on proton binding for the CHEM model (simplest model in this study) as compared to the DORI model.

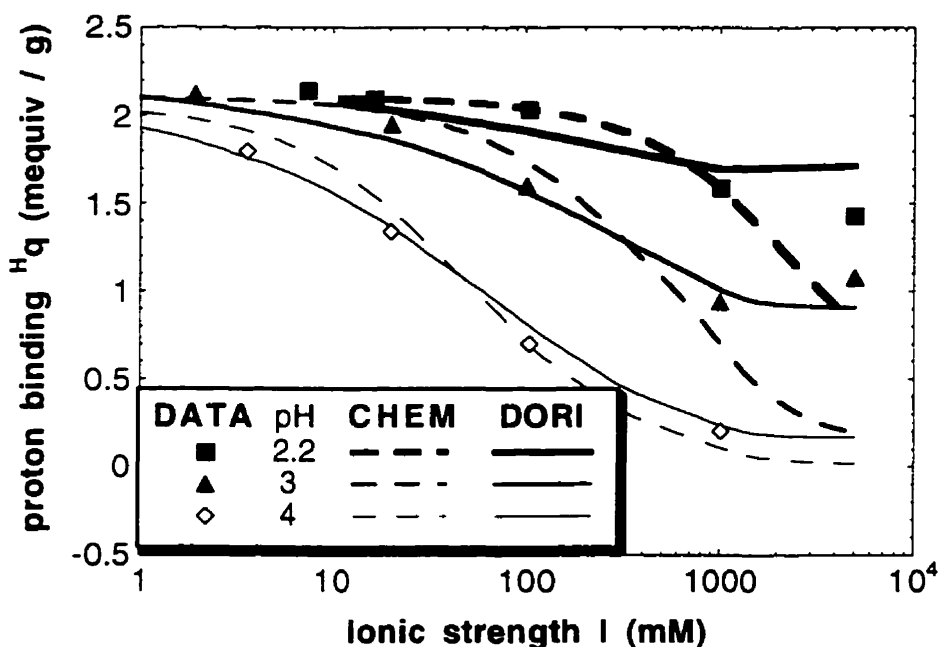


Figure 4.4.10: Proton binding by protonated *Sargassum* biomass as a function of ionic strength:

Experimental data and predictions according to the CHEM and DORI models

4.4 Results and Discussion: Proton Binding at Different Ionic Strengths

One can see that for both models $H_q = {}^tC$ at low I, even up to pH 4. This occurs in spite of the fact that the p^{CHK} for the DO model is smaller than 4 because, due to electrostatic effects, the local proton concentration for the DO model is (regardless of the proton concentration in solution) high enough for occupation of most binding sites. With increasing I, H_q decreases because of competing Na in the case of the CHEM model, and because of decreased concentration factors in the case of the DO model. It is apparent that, in spite of different underlying principles, both models behave in a similar way for low I. At high I, the Donnan model predicts that the proton binding reaches a constant value for each pH, where the ionic strength has no further influence because the local proton concentration is equal to the proton concentration in the solution. For the CHEM model, however, any increase in I leads to a further reduction in proton binding until all sites are deprotonated. The experimental data points clearly support the DORI model. Consequently, the CHEM model has to be ruled out at this point because it is not valid at high I and because it does not reflect the physical reality of Na accumulation being an electrostatic process. The GC models (not shown) predict even slightly lower effect of I on H_q than the DO model.

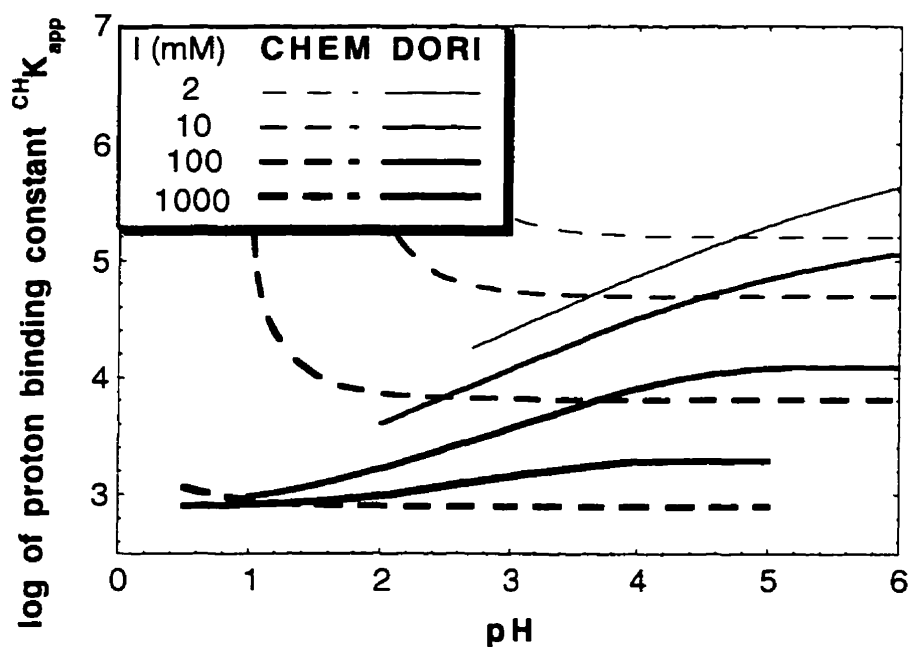


Figure 4.4.11: Variation of the apparent proton binding constant with pH for protonated *Sargassum* biomass at different ionic strengths: Model predictions of the CHEM and DORI models

4.4 Results and Discussion: Proton Binding at Different Ionic Strengths

An additional indication that the CHEM model is inappropriate is the predicted variation of the apparent p^{CHK} with pH for *Sargassum* (Figure 4.4.11): the decrease of the apparent p^{CHK} with increasing pH is contrary to the experimentally observed trend that the apparent p^{CHK} increases with f (which, of course, increases with pH) as shown in Figure 4.4.6.

4.4.11 Modeling Titration Curves

The model fits for the remaining 4 models are compared in Table 4.4.2. The mean square of the absolute deviations (mmol/g) of the model from the experimental data is for convenience expressed in percent of the total binding capacity tC . The GCRI model represents the worst fits for both the *Sargassum* and alginate titrations (average absolute error: 7.2 % of the total binding capacity). It should be therefore ruled out. The DOSW model has the smallest average errors (average error: 4.6 %), closely followed by the DORI model (4.9 %) which has the advantage of being simpler. The GCSW model has an intermediate average error (6.0 %) but it has the advantage of having the most equally distributed errors for all 8 series (the mean deviation of error for each series from the average error for all series = 1.1 %). In order to avoid too many or too cluttered figures, only the modeling using the DORI model is presented in the figures. This model was chosen for the figures because it is the simplest one that represents the data reasonably well. The only series where the model predictions substantially deviate from the experimental data is the one for alginate at the lowest ionic strength. An explanation for these deviations could be the fact that swelling was most pronounced for this series. The model which assumes a rigid particle underestimates the particle volume and therefore yields too high predictions of the intra-particle concentrations and correspondingly the proton binding.

Since the concentration factor λ both for *Sargassum* and for alginate is close to unity for any of the models at high I 's, the predictions of all models at high I 's are similar. The largest differences between the different models occur at low I 's where electrostatic effects are particularly pronounced: for *Sargassum* the GC models, especially the rigid one, predict too low H_q at low pH and too high H_q at high pH. This may indicate that P changes more strongly with pH than the model assumes. This would be the case if, for example, V_m is proportional to $(\text{pH})^2$ (see above) instead of being constant or proportional to pH. Another possibility is that the model does not fit well because the assumption $\phi_s < 25$ mV (on which equation (4.4.27) is based) is not fulfilled at low I 's or at high values of f .

4.4 Results and Discussion: Proton Binding at Different Ionic Strengths

Table 4.4.2 Absolute mean square errors of model in % of ϵ^c

MODEL TYPE	<i>Sargassum</i> at different I^a (mmol/L)					Alginate at different I^a (mmol/L)					Both	
	5	30	100	1000	ave	4	20	100	1000	ave	ave	dev ^b
DORI	3.0	6.1	6.8	3.1	4.8	10.3	2.0	3.6	3.8	4.9	4.9	2.2
DOSW	2.7	5.5	7.5	3.8	4.9	8.0	2.2	3.4	3.4	4.3	4.6	1.9
GCRI	11.7	11.9	8.8	3.6	9.0	2.4	7.3	4.5	7.0	5.3	7.2	2.8
GCSW	6.2	8.8	6.1	7.2	7.1	5.0	5.0	3.8	5.6	4.9	6.0	1.1

^a since I varies from point to point the value at $f = 0.5$ is given here

^b mean deviation of the errors in the eight series from the average error for all eight series

4.4.12 Modeling the Variation of Apparent p^{CHK}

The predictions of the Donnan model for rigid particles match the data in Figures 4.4.6 and 4.4.7 well, except for the lowest ionic strength series in Figure 4.4.7. Again, as explained in the preceding section, this is probably due to the fact that the model for rigid particles assumes a too low value of the particle volume for those conditions where swelling is most pronounced.

For all models the apparent p^{CHK} at $I = 1000$ mM is approximately constant and equal to the intrinsic one. For lower values of I , the extrapolation of p^{CHK}_{app} (for f approaching zero) yields the intrinsic p^{CHK} . Since the ionic strength in the experiments was not completely uniform for each series (because of the addition of HNO_3 or $NaOH$ for pH adjustment), the model predictions in Figure 4.4.11 which are for a specific fixed I give a better picture of this behavior than the model predictions in Figure 4.4.6 and 4.4.7 which were calculated at the exact I that was present at each experimental data point.

For *Sargassum*, extrapolation of the intrinsic p^{CHK} from curves of p^{CHK}_{app} for f approaching zero is difficult at a moderate ionic strength. This may be due to a continuing importance of electrostatic effects even at low degrees of ionization, which may be caused either by a higher charge density (i.e. higher Y_p or lower Y_v) or by the presence of additional acidic groups that are still ionized at low pH (for example sulfate groups). Model predictions at a specific ionic strength (Figure 4.4.11) show that for the low ionic strength,

4.4 Results and Discussion: Proton Binding at Different Ionic Strengths

still be larger than p^{CHK} . This plot of p^{CHK}_{app} versus pH shows, however, that all series converge to p^{CHK} when they are extrapolated to low pH values. Since the model (which assumes that only one binding site exists) successfully predicts that even at low f the experimental $p^{CHK}_{app} > p^{CHK}$ (Figure 4.4.6), one can conclude that it is not necessary to postulate the presence of a second site in order to explain this phenomenon.

4.4.13 Modeling the Plot of f versus (pH-pNa)

For *Sargassum*, all models except GCRI predict the data points well (DORI modeling shown in Figure 4.4.8). The curves for $I \leq 100$ are very close together, only the one for $I = 1000$ is shifted toward the right. For alginate, the GC models predict the data best, the DO models under-predict f at low (pH-pNa) values but otherwise they are also appropriate (DORI modeling shown in Figure 4.4.9).

An interesting observation is that even the *rigid* Donnan model (DORI) predicts an effect of ionic strength in this type of plot. This is contrary to the theory (Lin and Marinsky, 1993),(Cabaniss and Morel, 1989) according to which the curves for all I values should coincide for rigid polymers. A closer look at the underlying equation (4.4.40) reveals that the assumption that the intra-particle accumulation of H or Na is much larger than the bulk concentration (Q or $\lambda_p \gg 1$) does not hold. In Table 4.4.3, the values of $\lambda_p - 1 = Q / n$ (this follows from equation (4.4.19)) are given as predicted by the DORI model.

Table 4.4.3

The concentration factor $\lambda_p - 1 = Q / n$ ($n = 1 - 2$)

according to the DORI model for *Sargassum* at different I (mmol/L)

I (mM)	<i>Sargassum</i>			Alginate		
	10	100	1000	10	100	1000
pH 2	4.0	1.1	0.21	1.7	0.33	0.05
pH 4	39	9.3	1.4	13	1.95	0.21

It can be seen in Table 4.4.3 that the assumption (i.e. $\lambda_p - 1 \gg 1$) for the present data set is only valid at low ionic strengths and high pH. Both H_p and H can be of a comparable magnitude already for $I = 100$. For $I = 1000$ and low pH, the relationship is even reversed: Q or $\lambda_p - 1 \ll 1$, i.e. the average intra-particle concentration $[H_p]$ is similar to the bulk concentration $[H]$.

4.4 Results and Discussion: Proton Binding at Different Ionic Strengths

When $Q \gg 1$ is assumed, it is to be expected, as pointed out by Cabaniss and Morel (1989), that the curves for different values of I coincide. Therefore, only one curve which is valid for any I is plotted in Figure 4.4.12 for representing this assumption (equation (4.4.40)). When the opposite assumption $Q \ll 1$ is made, the curves according to equation (4.4.41) shift by pQ to the right in relation to the curve corresponding to equation (4.4.40). Consequently, the curves shift most strongly to the right for high I and low f (where Q is < 1 and pQ therefore positive). The curves shift towards the left for low I (where $Q > 1$ and therefore pQ negative). These trends are shown in Figure 4.4.12.

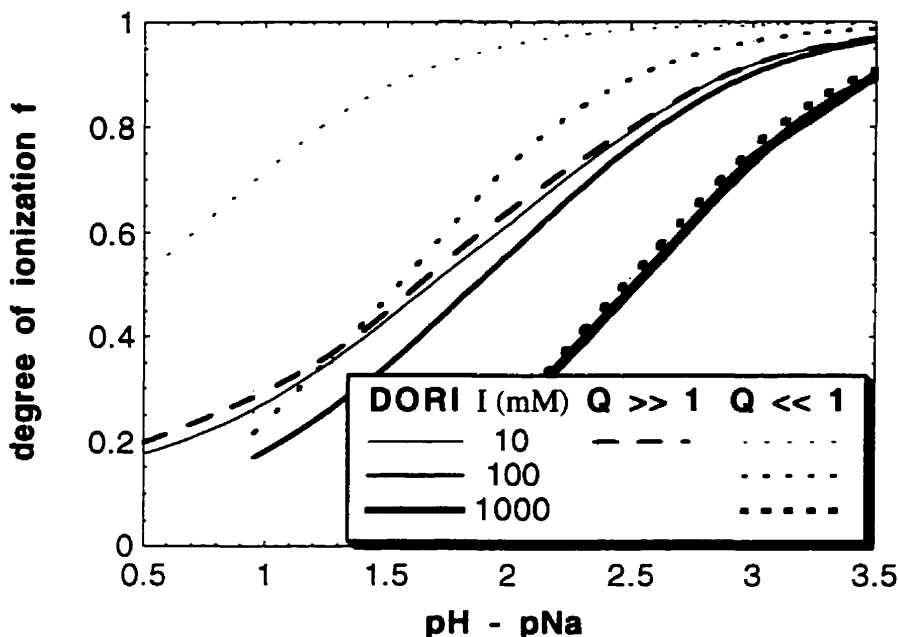


Figure 4.4.12: Modeling f as a function of $(pH-pNa)$ for titration of Na-alginate at different ionic strengths:

Predictions of the Donnan model for rigid particles (DORI) and simplified equations derived by assuming $Q \ll 1$ or $Q \gg 1$ (yielding the model used by Cabaniss and Morel as well as by the Marinsky research group).

Comparing both limiting cases with the more general DORI model, one can see that the assumption $Q \gg 1$ is justified for low I : at low I , the DORI model is closely approximated when $Q \gg 1$ is assumed and but not when $Q \ll 1$ is assumed. For high I , the situation is the opposite: the assumption $Q \ll 1$ is appropriate, assuming $Q \gg 1$ is unreasonable. At intermediate ionic strength of 100 mM, either assumption fits moderately

4.4 Results and Discussion: Proton Binding at Different Ionic Strengths

well. For most data points the real behavior according to the DORI model is, as shown in Figure 4.4.9, intermediate between the two limiting cases. Consequently, for the DORI model a smaller shift to the right (relative to the curve obtained when assuming $Q \gg 1$) occurs as shown in Figure 4.4.12. This is supported by the experimental data shown in Figure 4.4.9. Thus, the use of this type of plot as a criterion for rigidity is not recommended unless it is known that the criterion $Q \gg 1$ is fulfilled. Unfortunately, no evidence for fulfilling these conditions was given in most publications where this plot has been used and neither has this assumption been explicitly stated.

Another implication of Table 4.4.3 relates to the derivation of equation (4.4.17) from equation (4.4.16): Is the assumption $Q \gg 1$ (for which (4.4.16) reduces to (4.4.17)) which is implicitly made by those who use this equation (for example (Lin and Marinsky, 1993),(Cabaniss and Morel, 1989)) justified? The assumption $Q \gg 1$ is, as can be seen from Table 4.4.3, only fulfilled for a fraction of the data points. This means that the rigorous equation (4.4.16) should be used instead of the simplified one (4.4.17). These two equations predict markedly different values for $[H_p]$ at high I, resulting in different values for H_q . For example, for $Q = 0.5$, the correct value for $[H_p]$ (4.4.16) is ~ 2.5 times higher than the one according to (4.4.17), which is even smaller than $[H]$. The resulting reduction in the calculated proton binding at pH 2 is ~ 15 %.

4.4.14 Section Summary

A strong effect of ionic strength on proton binding by both *Sargassum* and alginate was noted. Marked variations of apparent p^{CHK} occurred due to electrostatic effects. Therefore, it is necessary to account for electrostatic effects in biosorption modeling. Three general types of models which use either chemical equilibrium constants for Na (CHEM), or the Donnan (DO) or Gouy-Chapman (GC) equations were considered for modeling the ionic strength effect. Each of the models required only three parameters: the total number of binding sites, the equilibrium constant CHK for proton binding, and one additional parameter to model the influence of ionic strength. The total number of binding sites in *Sargassum* was determined as 2.1 mmol/g. The intrinsic $-p^{CHK}$ for protons was around 3 for *Sargassum* and 2.7 for alginate.

The CHEM model appeared less suitable because it still predicted a high sensitivity of proton binding to ionic strength even at high ionic strength values. In addition, it predicted a behavior of the apparent p^{CHK} which was contrary to the observed one. The DO and GC models were found to be appropriate: the average absolute square deviations between the model predictions and experiments were only about 5% of the total binding capacity. Experiments indicated that some swelling of the sorbent materials occurred: the volume of both *Sargassum* and alginate increased with pH. In the modeling, the fit was better when swelling was taken into account (by assuming a linear relationship between the sorbent volume and pH) but even the model versions which assumed rigid particles gave reasonably good predictions in most cases.

The plot of the degree of ionization f versus $pH-pNa$ showed even for the rigid model a behavior which should, according to theories in the literature, only occur with a flexible material. This was the case because the assumption of these theories, that the intra-particle concentration was much larger than the bulk concentration, was not valid in the system investigated in this study. This means that the plots of f versus $(pH-pNa)$, which have been generally recommended until now as an indicator for rigidity, are shown to be valid only under conditions where λ is high.

4.5 Metal and Proton Binding at Different Ionic Strengths

Though Na as a typical "hard" ion is not expected to form strong covalent bonds but rather to be electrostatically attracted to the negatively charged biomass particle, the presence of Na can reduce the amount of other electrostatically bound counter-ions that balance the negative charge of the biomass. By affecting the intra-particle concentration of other ions it can reduce their binding. Calcium, which may form specific, covalent bonds (see section 2.2.6.3), might have an even stronger influence on heavy metal ion binding. In modeling biosorption of protons, the effect of ionic strength was taken into account in Section 4.4. The influence of light metal ions in heavy metal binding is investigated in this section and the model is modified in order to account for this phenomenon.

In the modeling of electrostatic effects on cation binding to humic and fulvic acids, double layer models and Donnan models have been applied. Biosorption by algal particles is different from humic and fulvic acids in that the particles are large and heterogeneous. This work investigates how far similar concepts as those used in humic and fulvic acid modeling can be applied for biosorption.

The results presented in this section have, in modified form, been submitted for publication as Schiewer and Volesky (1997c).

4.5 Results & Discussion: Metal & Proton Binding at Diff. Ionic Strengths

4.5.1 Model

4.5.1.1 Reactions and Isotherms

Since this work is an extension of Section 4.4, only the equations relating to metal ion binding which have not yet been given in other sections will be listed here. As in Section 4.4, it is assumed that most of the cation binding is dominated by one site "C". The reaction for the complexation of divalent metal ions M to a binding site C is:



$${}^{CM}K = \frac{CM_{0.5}^2}{C^2 \gamma_p [M_p]} \quad (\text{L / mmol}) \quad (4.5.1b)$$

The equation for proton-metal ion exchange can be written as



$${}^{CHM}K_{\text{exch}} = \frac{CM_{0.5}^2 \gamma_p^2 [H_p]^2}{CH^2 \gamma_p [M_p]} \quad (\text{mM}) \quad (4.5.2b)$$

Correspondingly, a plot of $CM_{0.5} / CH$ versus $[M]^{0.5} / [H]$ should yield a straight line passing through the origin, with a slope $({}^{CHM}K_{\text{exch}} / \gamma_p)^{0.5}$. If, on the other hand, C_2M complexes are formed the exchange reaction is:



$${}^{CHM}K_{\text{exch}}^* = \frac{C_2M \gamma_p^2 [H_p]^2}{CH^2 \gamma_p [M_p]} \quad (\text{g / L}) \quad (4.5.3b)$$

In this case, plotting $(C_2M)^{0.5} / CH$ versus $[M]^{0.5} / [H]$ should yield a straight line passing through the origin, with a slope $({}^{CHM}K_{\text{exch}}^* / \gamma_p)^{0.5}$.

The total number of binding sites stays constant

$${}^tC = C + CH + C Cd_{0.5} + C Ca_{0.5} \quad (\text{mequiv/g}) \quad (4.5.4)$$

The isotherm for the proton and metal ion binding can be derived from the binding constants for metal ions (equation (4.5.1)) and protons (equation (4.4.21)) by substituting ${}^tC/C$ using equation (4.5.4). Then:

4.5 Results & Discussion: Metal & Proton Binding at Diff. Ionic Strengths

$$CH = \frac{C \text{ } ^{CH}K \gamma_p [H_p]}{1 + \text{ } ^{CH}K \gamma_p [H_p] + \sqrt{C \text{ } ^{Cd}K \gamma_p [Cd_p]} + \sqrt{C \text{ } ^{Ca}K \gamma_p [Ca_p]}} \quad (\text{mequiv / g}) \quad (4.5.5)$$

$$CM_{0.5} = \frac{C \sqrt{C \text{ } ^{M}K \gamma_p [M_p]}}{1 + \text{ } ^{CH}K \gamma_p [H_p] + \sqrt{C \text{ } ^{Cd}K \gamma_p [Cd_p]} + \sqrt{C \text{ } ^{Ca}K \gamma_p [Ca_p]}} \quad (\text{mequiv / g}) \quad (4.5.6)$$

This isotherm is a specific case of the general multi-component isotherm equation (4.2.4) for any number of bound ions and several sites. M refers to either Cd or Ca and γ_p is the activity coefficient which is estimated using equation (4.4.7) evaluated at the local intra-particle ionic strength I_p .

4.5.1.2 Donnan Model

The equations for charge neutrality in the particle are for $[L] \gg [OH]$ when one site C is dominating so that $B \sim C$:

$$C - B = V_m \Sigma (z_x [X_p]) = V_m ([H_p] + 2[Cd_p] + 2[Ca_p] + [Na_p] - [L_p]) \quad (\text{mmol / g}) \quad (4.5.7)$$

For a divalent ion M, the equation (4.4.11) for the concentration factor λ in an electrolytic gel, according to the Donnan theory (Donnan, 1911), is:

$$\lambda = \frac{[X_p]^{1/z_x}}{[X]^{1/z_x}} = \sqrt{\frac{[M_p]}{[M]}} \quad (-) \quad (4.5.8)$$

with $[X_p]$ being the concentration of any ionic species X with a charge z_x in the gel. Since only the Donnan model is used in this section, it is not necessary to distinguish between λ_p and λ_s . Therefore, the concentration factor λ_p in the Donnan model is for simplicity called λ .

According to equations (4.5.8) and (4.4.11) $[M_p]^{0.5} / [H_p] = (\lambda^2 [M])^{0.5} / (\lambda [H]) = [M]^{0.5} / [H]$. Therefore, the bulk values $[M]$ and $[H]$ can be used for the stoichiometry plots based on Equations 4.5.2 and 4.5.2.

Expressing all intra-particle concentrations in terms of λ (equations (4.5.8) and (4.4.11)) and substituting into the charge balance of the particle (4.5.7) yields after

4.5 Results & Discussion: Metal & Proton Binding at Diff. Ionic Strengths

replacing $([Cd] + [Ca])$ by $[\Sigma M]$ and $([H] + [Na])$ by $(I - 3 [\Sigma M])$ (using the charge balance in solution and the definition of the ionic strength):

$$\lambda = \frac{[H_p]}{[H]} = -\frac{I - 3 [\Sigma M]}{4 [\Sigma M]} + \sqrt{\frac{(I - 3 [\Sigma M])^2}{16 [\Sigma M]^2} + \frac{C/V_m + I - [\Sigma M]}{2 [\Sigma M]}}$$

(mmol / L) (4.5.9)

The equation is also valid if more than two divalent and/or more than two monovalent ions are present. $[\Sigma M]$ generally stands for the sum of the concentrations of all divalent ions, $(I - 3 [\Sigma M])$ for the sum of the concentrations of all monovalent ions. In the derivation of (4.5.9) it was assumed that $C/V_m + L/\lambda \sim C/V_m + L$ since at high ionic strength values, λ approaches 1.0 and at low ionic strength (i.e. low L and $\lambda > 1$) $\lambda C/V_m \gg L$.

The intra-particle ionic strength is calculated by the usual definition of I (4.4.4) applied to the intra-particle concentrations which are expressed in terms of λ according to equations (4.5.8) and (4.4.11):

$$I_p = 2 [\Sigma M] \lambda^2 + 0.5 (I - 3 [\Sigma M]) \lambda + 0.5 (I - [\Sigma M]) / \lambda \quad (\text{mmol / L}) \quad (4.5.10)$$

The apparent C-site metal ion binding constant is:

$${}^{CM}K_{app} = \frac{(CM_{0.5})^2}{C^2 \gamma [M]} = {}^{CM}K \frac{\gamma_p \lambda^2}{\gamma} \quad (\text{L / mmol}) \quad (4.5.11)$$

Or, if C is unknown, the apparent binding constant can be defined as:

$${}^{CM}K_{app}^* = \frac{Mq^2}{C_{app}^2 \gamma [M]} = {}^{CM}K \lambda^2 \frac{\gamma_p}{\gamma} \frac{Mq^2}{CM_{0.5}^2} \frac{C^2}{C_{app}^2} \quad (\text{L / mmol}) \quad (4.5.12)$$

with $C_{app} = {}^tC - {}^Hq - {}^{Cd}q - {}^{Ca}q$.

4.5.1.3 Swelling of *Sargassum* Particles

The particle volume V_m is the fitting parameter which takes care of electrostatic effects for the rigid Donnan (DORI) model. Swelling changes the concentration of charged sites per volume and therefore also the concentrations of ions in the gel. Since it will be observed (see Sections 4.5.2 and 4.5.3) that swelling of *Sargassum* increased with the

4.5 Results & Discussion: Metal & Proton Binding at Diff. Ionic Strengths

number of free sites C , the following simple linear relationship between the specific particle volume and C was assumed:

$$V_m = Y_v C \quad (L / g) \quad (4.5.13)$$

Y_v is a constant that has to be determined from the experimental data. For C approaching zero (i.e. all sites are occupied), electrostatic effects and therefore the volume are irrelevant (i.e. it does not matter that the value calculated for V_m approaches zero). Equation (4.5.13) expresses that the charge density per volume is constant, independent of the degree of site occupation.

Since, however, the swelling not only strongly increased with C but *additionally* decreased with M_q , the following alternative swelling correlation was considered:

$$V_m = 1 + 0.5 (C^2 - M_q) \quad (L / g) \quad (4.5.14)$$

Three versions of the Donnan model are considered in the following: one which assumes a rigid particle (DORI), one (DOSWa) which accounts for swelling by a linear correlation (4.5.13) and one (DOSWb) which accounts for swelling by a more complex relation (4.5.14).

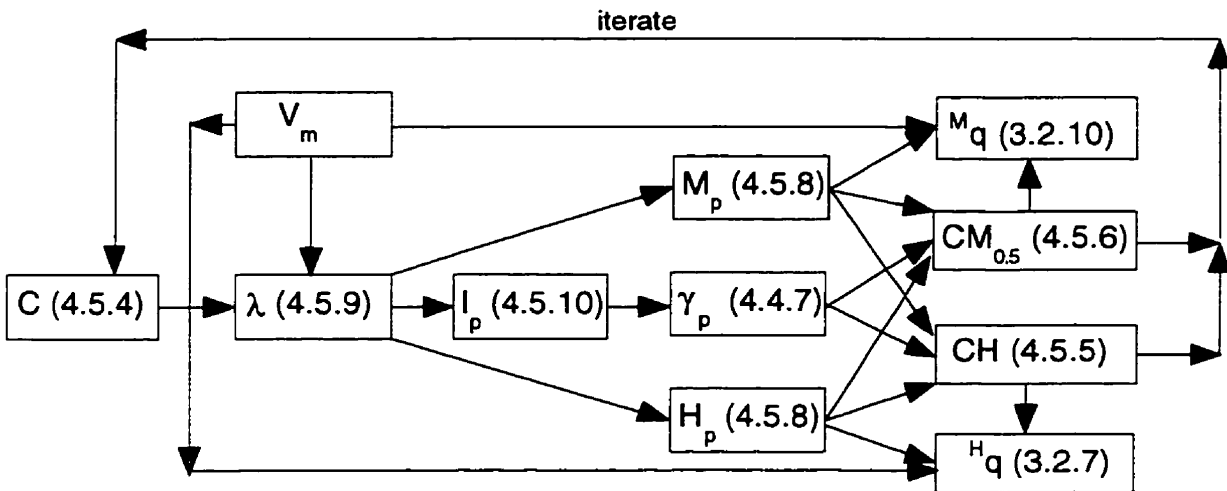


Figure 4.5.1 Calculation algorithm for the extended Donnan model.

Depending on the assumption made for particle swelling, V_m is defined in different ways:

The figure shows the algorithm for the DORI model where V_m is constant.

For the DOSWa model, no iteration is necessary and λ is the first variable calculated.

For the DOSWb model, V_m is a function of C and M_q (equation (4.5.14)).

4.5 Results & Discussion: Metal & Proton Binding at Diff. Ionic Strengths

The algorithm for the calculation of the cation binding and other variables is shown in Figure 4.5.1. It is necessary to perform the calculations iteratively unless one of the equations (4.5.17) - (4.5.22) is used, which is only possible for the DOSWa model. It has proven a reliable, stable method to start the iteration by assuming that the concentration of free sites is equal to the experimentally determined value of apparently free sites $C \sim C_{app} = C - H_q - Cd_q - Ca_q$. The other starting value is V_m , which remains constant for the rigid Donnan model. All other values have to be calculated iteratively except for H_q and M_q which are calculated after the iteration is completed.

4.5.1.4 Combination of the Isotherm and Donnan Models

The general calculation algorithm shown in Figure 4.5.1 can be used in conjunction with any type of sorption isotherm. Specifically for the isotherm model used here, the calculation process can be further simplified. The amount of covalently bound metal (equation (4.5.6)) is substituted into (3.3.10). Then, $[X_p]$ is replaced in terms of $[X]$ and λ (4.5.8) and (4.4.11). Finally, the denominator and numerator are divided by λ , yielding the following relationship:

$$M_q = \frac{C \sqrt{C^M K \gamma_p [M]}}{\frac{1}{\lambda} + \frac{C^H K \gamma_p [H]}{\lambda} + \sqrt{\frac{C^{Cd} K \gamma_p [Cd]}{\lambda}} + \sqrt{\frac{C^{Ca} K \gamma_p [Ca]}{\lambda}}} + 2 [M] (\lambda^2 - 1) V_m \quad (\text{mequiv / g}) \quad (4.5.15)$$

Though this equation is already more "compact" it still requires iterative calculation of λ and V_m . For the specific case that swelling linearly increases with the number of free sites (i.e. for the DOSWa model), the isotherm can be further simplified so that M_q can be calculated directly without iterations. Substituting V_m according to equation (4.5.13) into (4.5.15) yields:

$$M_q = \frac{C \sqrt{C^M K \gamma_p [M]}}{\frac{1}{\lambda} + \frac{C^H K \gamma_p [H]}{\lambda} + \sqrt{\frac{C^{Cd} K \gamma_p [Cd]}{\lambda}} + \sqrt{\frac{C^{Ca} K \gamma_p [Ca]}{\lambda}}} + \frac{2 [M] (\lambda^2 - 1) Y_v C / \lambda}{C / (\lambda C)} \quad (\text{mequiv / g}) \quad (4.5.16)$$

The second term was expressed in such a way that it's denominator equals the denominator of the first term. This way the two numerators can easily be added:

4.5 Results & Discussion: Metal & Proton Binding at Diff. Ionic Strengths

$$M_q = \frac{C \left(\sqrt{C_M K \gamma_p [M]} + 2 [M] Y_v (\lambda - 1/\lambda) \right)}{\frac{1}{\lambda} + C_H K \gamma_p [H] + \sqrt{C_{Cd} K \gamma_p [Cd]} + \sqrt{C_{Ca} K \gamma_p [Ca]}} \quad (\text{mequiv / g}) \quad (4.5.17)$$

Analogously, an equation for proton binding can be derived as:

$$H_q = \frac{C \left(C_H K \gamma_p [H] + [H] Y_v (1 - 1/\lambda) \right)}{\frac{1}{\lambda} + C_H K \gamma_p [H] + \sqrt{C_{Cd} K \gamma_p [Cd]} + \sqrt{C_{Ca} K \gamma_p [Ca]}} \quad (\text{mequiv / g}) \quad (4.5.18)$$

Now it is possible to calculate the binding of both metal ions and protons *without iteration*. First, λ is calculated according to equation (4.5.9), with the constant $1/Y_v$ substituted for the term C/V_m . Then, I_p (4.5.10), γ (4.4.7), M_q (4.5.17) and H_q (4.5.18) are calculated. Theoretically, equations (4.5.9; 4.5.10), and (4.4.7) could be substituted into (4.5.17) and (4.5.18) so that only one equation is necessary, but the resulting equation would be rather complicated and "inelegant".

If the ionic strength both in the bulk solution and in the particle (though this is rarely the case since divalent ions are preferably accumulated near the charged interface) is dominated by monovalent ions, then the more simple equation (4.4.19) can be used for λ . For V_m according to (4.5.13) it is:

$$\lambda = \frac{1}{Y_v n I} + 1 \quad (-) \quad (4.5.19)$$

where n is dimensionless and approaches 1.0 for $I Y_v \ll 1$ and it approaches 2.0 for $I Y_v \gg 1$. For intermediate $I Y_v$ equation (4.4.16) has to be used. Substituting (4.5.19) into (4.5.17) we obtain:

$$M_q = \frac{C \left(\sqrt{C_M K \gamma_p [M]} + 2 [M] \left(\frac{Y_v}{1 + n I Y_v} + \frac{1}{n I} \right) \right)}{\frac{n I Y_v}{1 + n I Y_v} + C_H K \gamma_p [H] + \sqrt{C_{Cd} K \gamma_p [Cd]} + \sqrt{C_{Ca} K \gamma_p [Ca]}} \quad (\text{mequiv/g}) \quad (4.5.20)$$

When high concentration factors λ are to be expected $n = 1$ can be assumed and λ (equation (4.5.19)) approaches $1/(I Y_v)$. Substituting this term for λ into (4.5.17) yields:

$$M_q = \frac{C \left(\sqrt{C_M K \gamma_p [M]} + 2 [M] / I \right)}{I Y_v + C_H K \gamma_p [H] + \sqrt{C_{Cd} K \gamma_p [Cd]} + \sqrt{C_{Ca} K \gamma_p [Ca]}} \quad (\text{mequiv/g}) \quad (4.5.21)$$

4.5 Results & Discussion: Metal & Proton Binding at Diff. Ionic Strengths

The corresponding equation for protons is

$$H_q = \frac{C ({}^{CH}K \gamma_p [H] + [H] Y_v)}{I Y_v + {}^{CH}K \gamma_p [H] + \sqrt{{}^{CCd}K \gamma_p [Cd]} + \sqrt{{}^{CCa}K \gamma_p [Ca]}} \quad (\text{mequiv/g}) \quad (4.5.22)$$

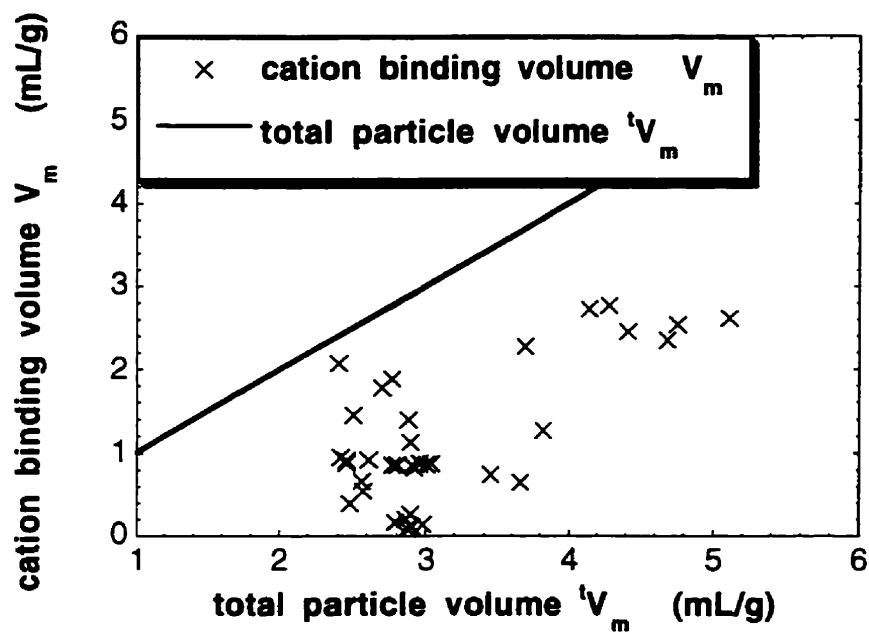
In this case, the metal or proton binding can be directly calculated from *one* equation each, for different metal concentrations, pH values, ionic strength and concentrations of a competing ion like Ca.

4.5.2 Specific Particle Volume

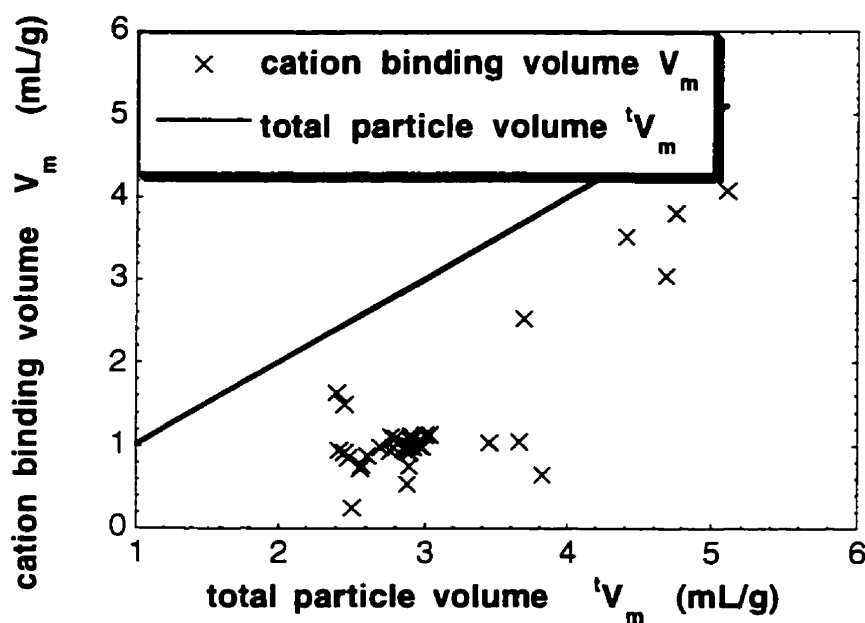
For all selected experimental series (different pH, I, combination of divalent ions) it was observed that the specific particle volume per dry biomass (the ratio between wet and dry weight of the particle, assuming a density ~ 1 g/mL for wet biomass) decreased with increasing M^{2+} concentration, approaching a value of 2.5 - 3 mL/g for $[Cd] \geq 1$ mM, $[Ca] \geq 5$ mM (data not shown). At low metal concentrations, the different series diverge from each other. For low pH and low I the specific particle volume remains about constant (at 2.5 - 3 mL/g). For high pH and high I, on the other hand, the particle swells considerably, and a specific volume of up to 4.5 - 5 mL / g is reached for $[M] < 0.3$ mM. This volume change by a factor of two means that swelling can still be significant in the presence of heavy metals at low to intermediate concentration. The observation that swelling is most pronounced at high pH and I can be explained by the fact that under these conditions the number of free sites is high. It was noticed in Section 4.4 that swelling increased with pH because protonated alginic acid has a smaller volume than dissociated alginic acid. The fact that swelling does not only decrease with pH but also with the increasing Cd or Ca concentration indicates that Cd-alginate or Ca-alginate also has a smaller volume than dissociated alginic acid (Na-alginate). This phenomenon may be enhanced by the possibility that divalent ions may cross-link alginate when bound to it (Mackie and Preston, 1974, pp. 59; Kohn, 1975).

4.5.3 Modeling the Swelling of the Particle

Unfortunately, the determined values of the total specific particle volume V_m can not be used in a quantitative way for modeling. Alginate makes up only a fraction of the total particle volume V_m and only the alginate layers of the cell wall constitute the active, cation binding volume V_m of the particle (Chapman, 1980, pp. 196; Fourest and Volesky, 1996). Therefore, the cation binding volume is smaller than the total particle volume.



a



b

Figure 4.5.2 Swelling of the *Sargassum* particle.

Model predictions of the cation binding volume V_m as a function of the experimentally determined total particle volume $'V_m$:

- a) cation binding volume calculated with the DOSWa model;
- b) cation binding volume calculated with the DOSWb model.

4.5 Results & Discussion: Metal & Proton Binding at Diff. Ionic Strengths

Additionally, the cation binding volume may swell to a different extent than the average particle. Nevertheless, it may be reasonable to assume that the active volume V_m increases when the total volume tV_m increases. Especially since changes in the overall volume appear to be related to binding (in the active volume), it might be expected that the active volume swells more strongly than the total volume.

Using the swelling correlation (4.5.13) with $Y_v = 1.5$ mL/mequiv, Figure 4.5.2a shows a plot of V_m over a linear interpolation of the experimentally determined total particle volume tV_m . The diagonal $V_m = {}^tV_m$ is also drawn in for reference. When the magnitudes of V_m and tV_m are compared, the calculated value of the active volume appears plausible: it makes up about 1/2 of the total volume.

This corresponds to the fact that about half of the dry weight of the *Sargassum* particle consists of alginate (Fourest and Volesky, 1996). The concurrent trend of the increasing total volume with the modeled active volume (which is proportional to the number of free binding sites) confirms the hypothesis that swelling increases with the number of free sites. However, the relationship is not perfect: although an overall trend relating tV_m and C is recognizable, the data points are rather scattered.

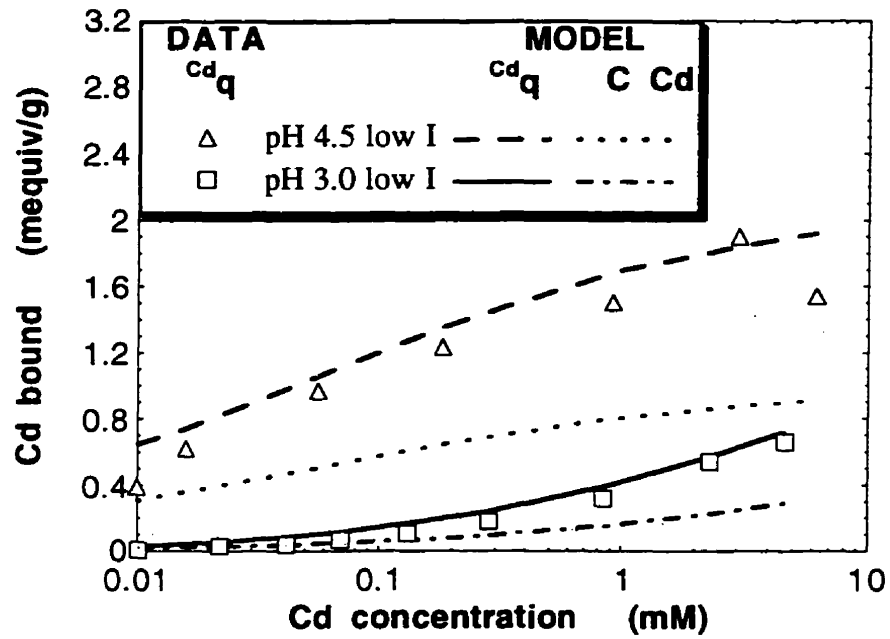
Ideally, a good correlation between V_m and tV_m should be an unambiguous one (i.e. that the data points for different pH and I do not deviate from each other) and one where V_m monotonously increases with tV_m . This is much better achieved ($R = 0.7$ for linear correlation between V_m and tV_m) when the swelling correlation (4.5.14) is used (Figure 4.5.2b), which assumes that swelling strongly increases with the amount of free sites and, *in addition*, decreases with increasing amount of Cd bound (possibly due to crosslinking effects). It also becomes apparent that when this model is used, swelling in the active volume is stronger than swelling of the whole particle: the fraction of the active volume increases with increasing tV_m from ~ 30 to ~ 90 % of the total volume.

4.5.4 Cadmium and Proton Binding

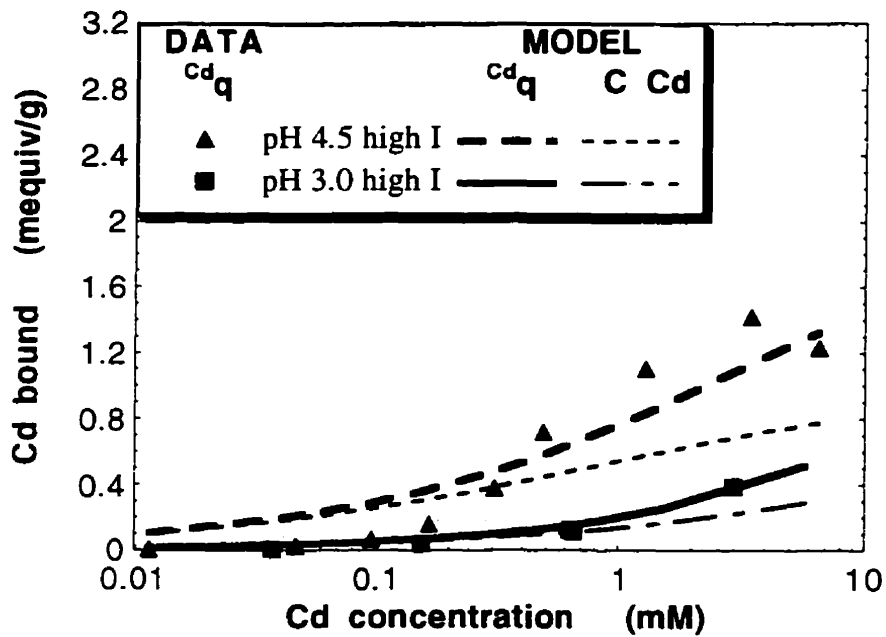
As shown in Figures 4.5.3a-b Cd binding increases with increasing pH and Cd concentration. H binding on the other hand decreases with increasing pH and Cd concentration (Figures 4.5.3c-d). This once again illustrates the competition of heavy metal ions and protons for the same binding sites which is described in Section 4.1.

The binding of Cd and H decreases with increasing ionic strength (I). This can be explained by lower intra-particle concentrations of Cd and H at high I , because Na contributes to balancing the negative charge of the free sites of the biomass.

4.5 Results & Discussion: Metal & Proton Binding at Diff. Ionic Strengths



a



b

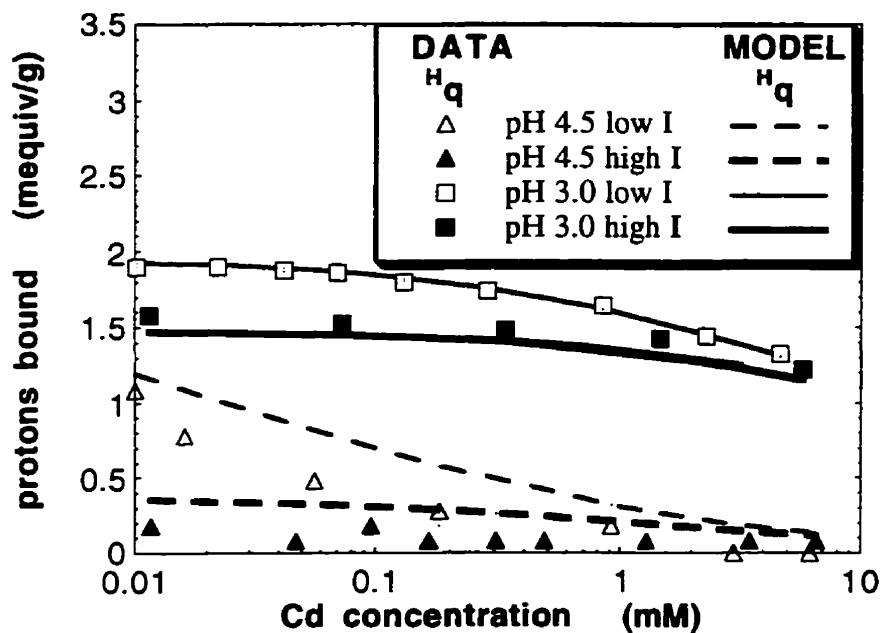
Figure 4.5.3 Cadmium and proton binding by *Sargassum* biomass at different ionic strength I and pH:

(experimental data and predictions by the Donnan model DOSWa for swelling particles).

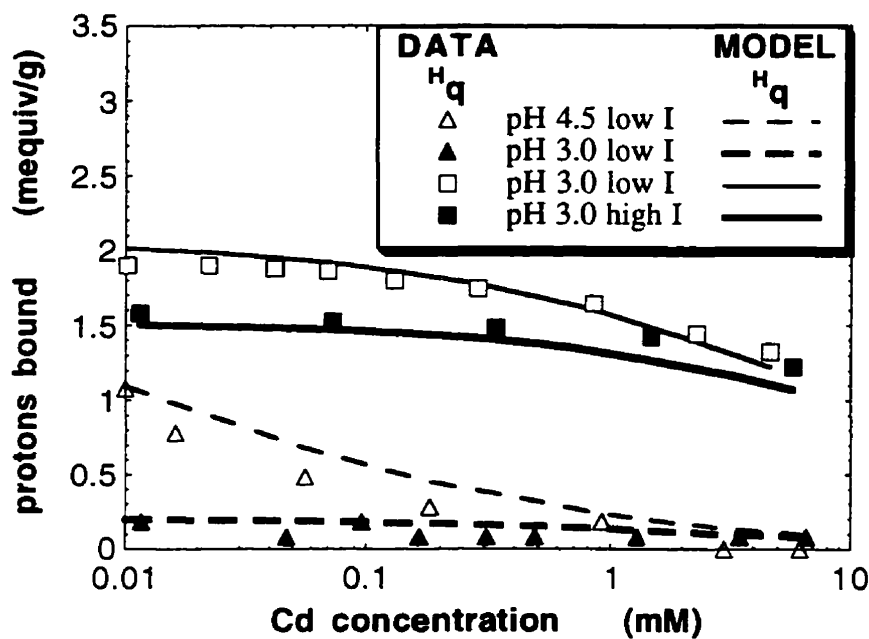
a) total (Cd_q) and covalent (CCd) cadmium binding at low ionic strength

b) total (Cd_q) and covalent (CCd) cadmium binding at high ionic strength

4.5 Results & Discussion: Metal & Proton Binding at Diff. Ionic Strengths



c



d

Figure 4.5.3 Cadmium and proton binding by *Sargassum* biomass at different ionic strength I and pH:

c) total (H_q) proton binding (experimental data and predictions by the Donnan model DORIA for rigid particles);

d) total (H_q) proton binding (experimental data and predictions by the Donnan model DOSWa for swelling particles).

4.5 Results & Discussion: Metal & Proton Binding at Diff. Ionic Strengths

At low I, the intra-particle concentrations are much larger than the bulk concentration because of electrostatic attraction of cations by the negatively charged biomass. Since binding of each ion obviously increases with its concentration near the binding site, these elevated concentrations also contribute to a higher amount of covalently bound H or Cd. The effect of I is most pronounced at high pH and low [Cd]. Under these conditions the binding of both ions at low I is several times higher than the binding at high I (Figure 4.5.3a-d). This observation can be explained by the large charge due to a larger number of free sites at high pH and low [Cd].

4.5.5 Stoichiometry Plot

Figure 4.5.4 shows that for both stoichiometric assumptions ($CM_{0.5}$ or C_2M complexes formed) good linear correlations between the ratios $M_q^{0.5} / H_q$ or M_q / H_q and $[M]^{0.5} / [H]$ are achieved.

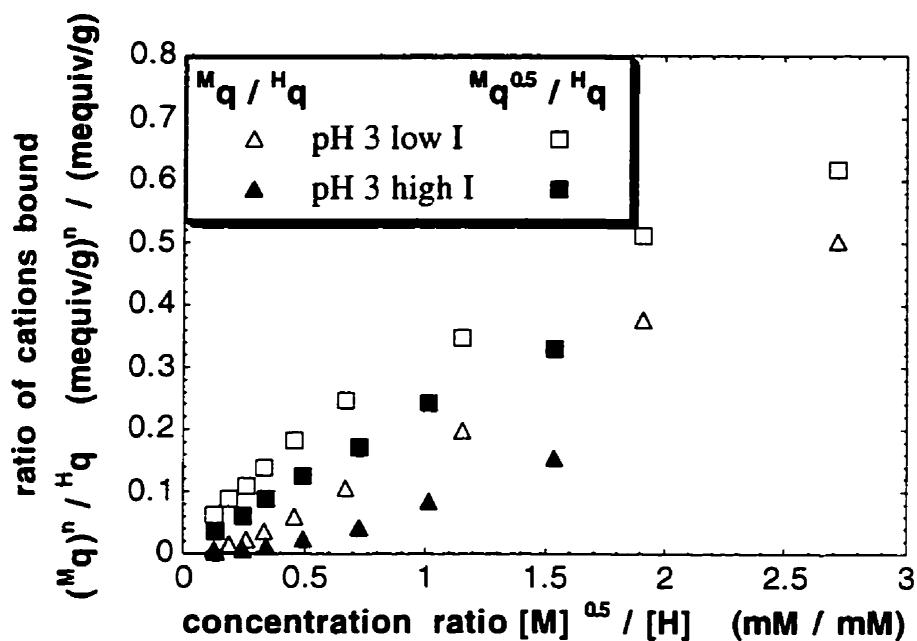


Figure 4.5.4 Investigation of the reaction stoichiometry for divalent metal binding (experimental data for Cd and H binding by *Sargassum* biomass).

Formation of $CM_{0.5}$ complexes:

linear correlation of M_q / H_q and $[M]^{0.5} / [H]$ expected.

Formation of C_2M complexes:

linear correlation of $M_q^{0.5} / H_q$ and $[M]^{0.5} / [H]$ expected.

4.5 Results & Discussion: Metal & Proton Binding at Diff. Ionic Strengths

Theoretically, the amounts of covalently bound Cd and H should be known in order to employ the stoichiometry plot. These values, however, cannot be determined directly but only calculated from the total binding of each ion by employing one or the other of the hypotheses to be verified. Nevertheless, when the ratio between the total and the covalent binding of an ion is approximately constant within a series, the plot should still be linear, but with a different slope than $^{CHM}K_{exch}^{0.5}$. This is the case for most data points on which the regressions in Table 4.5.1 are based (Figure 4.5.4). In each case only the data points where $[M] > 0.005$ mM, $M_q > 0.05$ mequiv/g and $H_q > 0.1$ mequiv/g were used. Points that did not fulfill these criteria were eliminated because their relative experimental error in the binding and therefore in the binding ratio was high. This led to an elimination of the series pH 4.5, I = 100 mM because for all except one point at least one of the three criteria was not fulfilled. The correlation coefficients for straight lines through the origin and their slopes are listed in Table 4.5.1. Similarly good fits were obtained using both stoichiometric assumptions.

Table 4.5.1: Regressions for stoichiometry test

Stoich. Assumpt.	for estimating the linearity (R^2)								for estimating k	
	pH 4.5, low I (6 points)		pH 3, low I (6 points)		pH 3, high I (5 points)		all 3 series (17 points)		all data with $CM_{0.5} > 0.7 M_q$ (9 points)	
	R^2	k^*	R^2	k^*	R^2	k^*	R^2	k^*	R^2	k^*
BM _{0.5}	0.98	0.27	0.99	0.19	0.90	0.16	0.981	0.27	0.83	0.12
B ₂ M	0.97	0.23	0.88	0.26	0.90	0.28	0.979	0.23	0.96	0.32

* slope of line of best fit $\sim ^{CHM}K_{exch}^{0.5}$

The last column in Table 4.5.1 is based on points where Cd binding is predominantly covalent (> 70 %). Unfortunately, this is only the case for low [Cd] and low pH or high I where the relative experimental error is high. If the above criteria were applied, only 3 points would meet them. In order to have more points in this category, the criterion for the minimum metal binding was relaxed: $M_q > 0.01$ mequiv/g was allowed. Though the precision of the data is lower, the estimate of $^{CHM}K_{exch}$ obtained for these data

4.5 Results & Discussion: Metal & Proton Binding at Diff. Ionic Strengths

set can be regarded as the most accurate because with a high contribution of electrostatic binding ${}^{\text{CHMK}}K_{\text{exch}}$ appears higher than it really is.

The slope k is equal to the square root of ${}^{\text{CHMK}}K_{\text{exch}}$ (4.5.2). Thus one can calculate ${}^{\text{CMK}}$ for known values of ${}^{\text{CHMK}}K_{\text{exch}}$ and ${}^{\text{CHK}}$: ${}^{\text{CMK}} / \gamma_p = {}^{\text{CHMK}}K_{\text{exch}} {}^{\text{CHK}}^2 = k^2 {}^{\text{CHK}}^2$. The proton binding constant was determined in section 4.4 (Table 4.4.1) as ${}^{\text{CHK}} = 2.9$ for the rigid Donnan model and ${}^{\text{CHK}} = 2.8$ for the Donnan model when swelling was assumed. The same values are used in this section (4.5) as listed in Table 4.5.2. With the slope $k = 0.12$ for the $\text{BM}_{0.5}$ assumption and $\text{p}^{\text{CHK}} = 2.9$ or 2.8 , we obtain ${}^{\text{CMK}} / \gamma_p = 9.1$ L/mol or 5.7 L/mol for the DORI and DOSW models, respectively. The latter is close to the optimum ${}^{\text{CMK}} / \gamma_p = 4.9$ L/mmol / $0.7 = 7$ L/mmol for the DOSWa model (see Table 4.5.2).

For both stoichiometric assumptions good correlations were obtained for all series. In general, it is not possible to discern which assumption is the more appropriate one. The formulation of explicit sorption isotherm models (including the combined Donnan-isotherm) which allows the direct calculation of cation binding from the concentrations is only possible when $\text{CM}_{0.5}$ complexes are assumed. Therefore, this formulation will be chosen in the following sections.

4.5.6 Model Parameters and Fit

After initially also applying a version of the Gouy-Chapman model (which was used in Section 4.4 for modeling the proton binding at different ionic strengths) for metal ion binding, the use of this model was discontinued because it did not lead to better predictions than the simpler Donnan model on which this work subsequently focused. In each modeling case, the values for the total number of binding sites (${}^{\text{C}} = 2.1$ mequiv / g) and the binding constant for protons (for the Donnan model for rigid particles: $-\text{p}^{\text{CHK}} = 2.9$, for the Donnan model with swelling $-\text{p}^{\text{CHK}} = 2.8$) were adopted from Section 4.4.

For the rigid Donnan model (DORI) the following cases were distinguished:

- a) Only ${}^{\text{CMK}}$ was optimized.

The value for V_m was adopted from Section 4.4.

- b) Both V_m and ${}^{\text{CMK}}$ were optimized simultaneously.

For the Donnan model with swelling (DOSW) two alternative swelling correlations were considered:

- a) A linear relation between active volume and number of free binding sites (equation (4.5.13)) where the parameter Y_v was optimized in addition to ${}^{\text{CMK}}$. With this model version, equations (4.5.17) and (4.5.18) can be used;

4.5 Results & Discussion: Metal & Proton Binding at Diff. Ionic Strengths

b) A more complex correlation (equation (4.5.14)) which in itself can already be regarded as an optimization for V_m (see section 'Modeling the Particle Volume') so that only CMK was optimized.

The model parameters for systems without Ca are all listed in Table 4.5.2; those which have been optimized in this work are marked with an asterisk (*).

Table 4.5.2: Model parameters for mono-metal systems with Cd

Model type	Parameters			
	$\%C$ mequiv / g	$-p^{CHK}$ -	CCdK L / mol	V_m mL / g
DOR Ia	2.1	2.9	2.8*	1.4
DOR Ia	2.1	2.9	3.0**	1.4
DOR Ib	2.1	2.9	2.8*	1.4*
DOS Wa	2.1	2.8	4.9*	1.5 C mL/mequiv *
DOS Wb	2.1	2.8	4.4*	1 + 0.5 (C ² - M _q)*

* parameters optimized in this Section (4.5)

** determined only from selected data at pH 4.5, low I, $M_q < 0.75 \%C$

The average absolute deviations of model predictions from experimental data, expressed in percent of the total binding capacity $\%C$, range from 5.8 to 6.5 %. They can be considered rather similar so that it is not necessary to include swelling in the modeling for obtaining a good fit of the experimental data.

Additionally, it is possible to use V_m determined in Section 4.4. As shown in Table 4.5.2, the value obtained for V_m when both CCdK and V_m were optimized is identical to the one obtained earlier in pH titrations (Section 4.4). This means that the effect of electrostatic attraction in metal binding can be predicted from results obtained from proton binding experiments. For that reason the DOR Ia model may be considered the best model because it is conceptually the simplest one and requires a minimum number of fitting parameters to be determined (i.e. the relation between the model complexity and results is most advantageous).

When V_m from pH titrations can be used (i.e. for the DOR Ia model) it is not necessary to perform experiments at different pH and different I for determining CMK because the effect of pH and I on metal binding can already be predicted. It is sufficient to

4.5 Results & Discussion: Metal & Proton Binding at Diff. Ionic Strengths

experimentally determine the metal binding at different metal concentrations (i.e. to establish one isotherm without varying pH or I). For optimal choice of the conditions of that experiment, the sensitivity of metal binding to the metal binding constant as opposed to other parameters (C^{HK} and V_m) should be as high as possible. At low pH, the binding is dominated by protons and the determined C^{MK} significantly depends on the choice of C^{HK} . Therefore, it is more appropriate to choose experiments at high pH for determining C^{MK} . While on the one hand the metal binding had a very nice steep increase (i.e. is highly sensitive to C^{MK}) at $I = 100$ mM, the binding at this I is strongly affected by the volume change of the particle. If a rigid model is used, this swelling phenomenon is not accounted for, and inappropriate estimates of C^{MK} may result from that. It is therefore recommendable to use the data for high pH, low I and low to intermediate metal concentration ($[M] = 0.005-1$ mM, $M_q < 75$ % of tC) for determining C^{MK} . At high concentrations the metal binding approaches the total binding capacity and is therefore insensitive to C^{MK} and at very low metal concentrations the relative error in determining M_q is high and swelling occurs. The binding constant determined from only these data was $C^{MK} = 3.0$ L / mol. This is only 7 % higher than C^{MK} determined from all data and, accordingly, the fit for the data was similarly good. This means that a single isotherm at pH 4.5 and low I can provide all the data needed for determining C^{MK} . Using this C^{MK} and the values for C^{HK} and V_m from pH titrations, Cd and H binding at different $[Cd]$, pH and I can be predicted quite well.

The results of the DORIA model application are depicted in Figures 4.5.3, 4.5.5, 4.5.6 and 4.5.7, using C^{CdK} determined only from the data at pH 4.5 and low ionic strength. In order to also show the performance of the combined Donnan isotherm for the DOSWa model which is conceptually a little more complicated but which, on the other hand, has the advantage of being the most user-friendly, equation (4.5.17) was used for calculating the metal binding presented in Figures 4.5.8 and 4.5.9.

4.5.7 Modeling the Cadmium and Proton Binding

Using the DORIA model, which was the simplest model tested, the metal binding (Figure 4.5.3a) was very well predicted for all but the pH 4.5, $I = 100$ mM series. For the latter conditions swelling is of major importance and therefore a "rigid model" yields worse predictions than the "swelling models". Especially for DOSWb the predictions of this series are much better than for DORIA. The proton binding (Figure 4.5.3b) is reasonably well predicted, though with a tendency of overestimation. This again improves when using the DOSW models for which C^{HK} is lower (Figure 4.5.3c). The competition of protons and cadmium for the same binding sites is well reflected in the model.

4.5 Results & Discussion: Metal & Proton Binding at Diff. Ionic Strengths

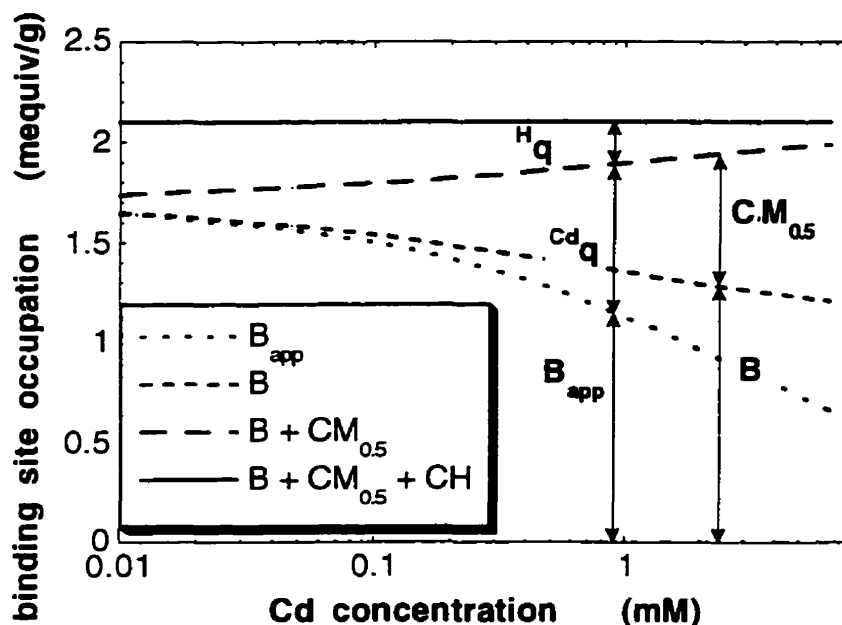


Figure 4.5.5 Change of *Sargassum* biomass binding sites occupation with increasing metal concentration
for pH 4.5 and $I = 100$ mM (predictions by the Donnan model (DOR1a) for rigid particles).

However, not only does ion exchange between these two cations occur, but the sum of the binding of both ions changes, indicating that a variable amount of free sites is present (Figure 4.5.5).

Additionally to the total binding of Cd, the extent to which it is covalently bound is also shown in Figures 4.5.3a - b. The covalent binding of protons (CH) is not plotted because it is practically identical to the total proton binding H_q . One can see that for protons the two lines coincide ($CH \sim H_q$), i.e. practically all binding is covalent. This is the case because for the DOSWa model $Y_v \ll CHK$. Therefore the right hand term in the numerator of equation (4.5.18) is negligible. For Cd, however, a significant portion of the binding is electrostatic: especially at low I , $\sim 50\%$ of Cd_q is bound electrostatically. The increasing amount of electrostatic binding with an increasing Cd concentration for the high ionic strength data is due to the fact that the intra-particle ionic strength becomes dominated by Cd, i.e. $[Cd_p] \gg [H_p] + [Na_p]$. That means that the charge of the biomass particles is mostly balanced by Cd. If, however, the Cd concentration were to be increased further, all sites would eventually be occupied by Cd until "no" free sites are left and then, of course, the Cd binding would be exclusively covalent and not electrostatic.

4.5 Results & Discussion: Metal & Proton Binding at Diff. Ionic Strengths

The generally higher direct contribution of electrostatic binding to M_q as compared to H_q is due to the fact that divalent ions are preferably accumulated near the charged interface. But apart from the direct contribution of electrostatic effects to binding (as $[M_p]$ or $[H_p]$) there is an indirect contribution: $CM_{0.5}$ or CH are increased because of intra-particle concentrations that are higher than the bulk concentrations. This is also very strongly visible for protons: the change of CH with changing I is a consequence of elevated intra-particle concentrations for low I ; with increasing I electrostatic effects become diminished. This indirect contribution to cation binding shows in the change of the apparent binding constant which will be discussed in the next section. It is possible to conclude that, while electrostatic effects contribute to H binding mainly in an *indirect* way, a significant *direct* contribution ($\sim 50\%$) exists for Cd binding.

4.5.8 Change of Apparent Binding Constant

The apparent binding constant for Cd as defined in equations (4.5.11) and (4.5.12) is plotted in Figure 4.5.6 (since apparent proton binding constants have been discussed in Section 4.4 they are not depicted). It can be observed that $^{CM}K_{app}$ may be several orders of magnitude higher than the intrinsic constant. Inspection of equation (4.5.11) reveals that the factor by which $^{CX}K_{app}$ exceeds ^{CX}K is equal to λ^{Zx} . Consequently, $^{CM}K_{app}$ is more strongly affected than $^{CH}K_{app}$ and both are the highest at low I and high B , i.e. at high pH and low $[Cd]$. This change in $^{CH}K_{app}$ indicates the large importance of the *indirect* contribution of electrostatic effects.

If $^{CM}K_{app}^*$ is defined according to equation (4.5.12) the behavior is similar as for $^{CM}K_{app}$ except that $^{CM}K_{app}^*$ increases with $[Cd]$ because of the increasing *direct* contribution of electrostatic binding with increasing $[Cd]$, yielding higher $M_q / CM_{0.5}$ and especially higher C/C_{app} with ($C_{app} = {}^tC - H_q - M_q$). In this case, the difference between intrinsic and apparent binding reflects the contributions of electrostatic attraction both in a direct and in an indirect way.

4.5.9 Importance of the Na Concentration for Cd Binding

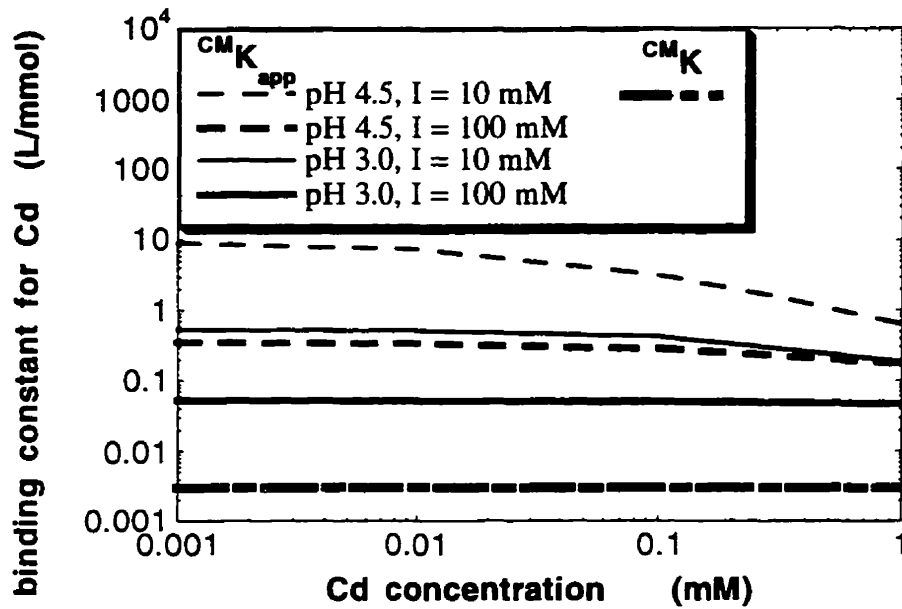
First of all, it is necessary to make a distinction between conditions where

a) electrostatic effects are important

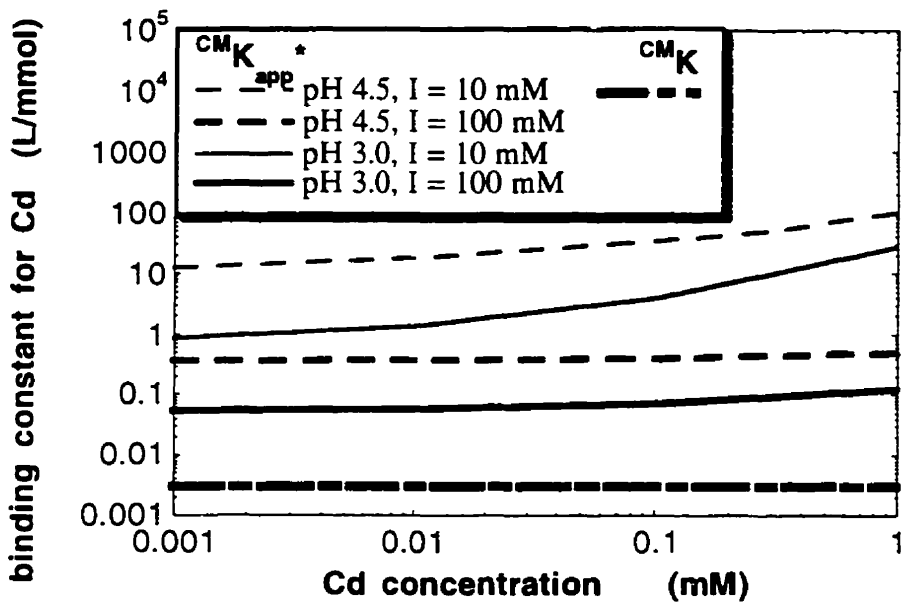
or b) the influence of changes in the Na concentration on Cd binding is noticeable.

Electrostatic effects are only negligible at a very high ionic strength, i.e. at a high concentration of Na or other ions. The Na concentration has no influence on Cd binding either if electrostatic effects are negligible (i.e. if I is very high) or if the Na concentration is very low.

4.5 Results & Discussion: Metal & Proton Binding at Diff. Ionic Strengths



a



b

Figure 4.5.6 Change of apparent binding constants for Cd binding by *Sargassum* biomass

(predictions by the Donnan model DOR1a assuming rigid particles).

a $CM_{K_{app}}$ refers to the amount of covalently bound Cd (CCd) and the true number of free sites;

b $CM_{K_{app}}^*$ refers to the total amount of bound Cd (C^{dq}) and the apparent number of free sites;

The intrinsic binding constant CM_K (thick line at bottom) is of course always constant.

4.5 Results & Discussion: Metal & Proton Binding at Diff. Ionic Strengths

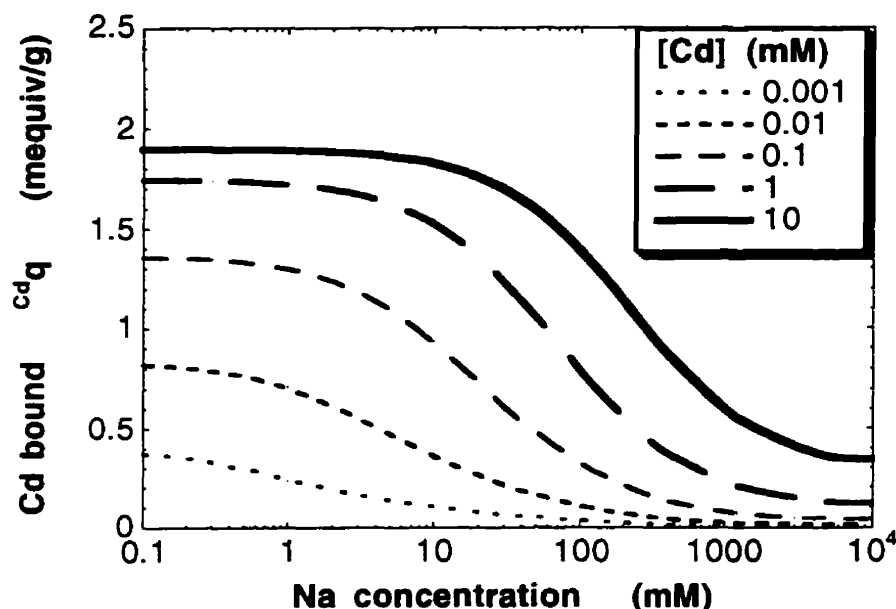


Figure 4.5.7 Importance of Na in Cd binding by *Sargassum* biomass (predictions by the Donnan model DOR1a assuming rigid particles).

An example of how the Na concentration affects Cd binding is given in Figure 4.5.7. The metal uptake at pH 4.5 predicted by the DOR1a model is plotted for different final Cd concentrations as a function of the Na concentration. A noticeable effect of the presence of Na (10 % reduction in Cd binding as compared to Cd binding in Na-free system) is for example observed at Na = 0.6 mM for [Cd] = 0.01 mM (1 ppm) or at Na = 2.5 mM for [Cd] = 0.1 mM (10 ppm). These or even lower final metal concentrations can be regarded as typical for practical applications of biosorption as a 'polishing' step in the treatment of industrial wastewaters. Although in each of those cases [Na] \gg [Cd] was necessary to exert a noticeable effect, significant amounts of Na are usually present in wastewater. In the experiments performed in this study, for example, the final Na concentration resulting from pH adjustment (no additional NaL added) was already > 4 mmol / L for M = 0.01 or 0.1 mM. This means that even without a deliberate salt addition the effect of Na is already noticeable.

A complete elimination of electrostatic effects (i.e. a leveling out of the curves, so that any further increase of Na does not reduce the Cd binding) only occurs at Na ~ 1000 mM. As a consequence, ionic strength effects should always be considered in the modeling of biosorption unless it is ensured that either

4.5 Results & Discussion: Metal & Proton Binding at Diff. Ionic Strengths

- a) I is constant in all experiments
- or b) [Na] is not too much larger than [M], for example
[Na] < 0.1 mM for [Cd] = 0.001 mM, [Na] < 10 mM for [Cd] = 1 mM
- or c) I > 1000 mM.

Only at a very high I is the use of a purely chemical binding model theoretically justified. In cases a) and b) electrostatic effects still affect the binding but it is possible to model the binding as a function of the pH and Cd concentration alone. However, if the data points were obtained for different amounts of biomass added per solution volume (i.e. different "S/L" ratios) then the ionic strength in the samples may (even at identical amounts of Na salt added, final pH and concentration of divalent metal ions) vary substantially as a consequence of pronounced differences in the amount of base added for pH adjustment. In conclusion, it is recommended to use a model that incorporates the influence of I due to electrostatic effects for most practically relevant conditions (i.e. [M] << [Na] < 1000 mM).

4.5.10 Binding of Calcium in Mono-Metal Systems

The binding of Ca and H in systems with Ca as the only divalent ion is depicted in Figure 4.5.8. The general behavior is similar to the Cd system (Figure 4.5.3) except that Ca binding is lower and to a lesser degree covalent. This is reflected in the binding constant ^{CCa}K for Ca which is much lower than the one for Cd (Table 4.5.2). The constant $^{CCa}K = 1.2$ L/mol was determined from Ca binding data at pH 4.5 and I ~ 100 mM only. Though this value is different from the one determined from all Ca binding data in mono-metal system $^{CCa}K = 0.28$ L/mol, the average absolute errors for both constants in modeling all data, being 9.7 and 9.6 % of the total binding capacity, respectively, do not differ widely. Since all models fitted the Cd binding data similarly well, only the DOSWa model which is the most user-friendly one was used for predicting Ca systems, including the two-metal system Cd-Ca (see below).

Though a significant portion (~ 40 % for low I, > 60 % for high I) of the Ca binding is covalent, the total Ca binding at pH 4.5 and low I according to the DOR1a model would only be reduced by ~ 15-20 % if $^{CCa}K = 0$ (i.e. purely electrostatic binding) was assumed (data not shown). This means that for obtaining a preliminary estimate of light metal binding before any experiments are conducted one can assume that it binds only electrostatically and use the data from pH titrations at different I in order to predict the Ca binding. Also, this was the reason for choosing the high I data for determining ^{CCa}K , since the binding at low I is very insensitive to changes in ^{CCa}K .

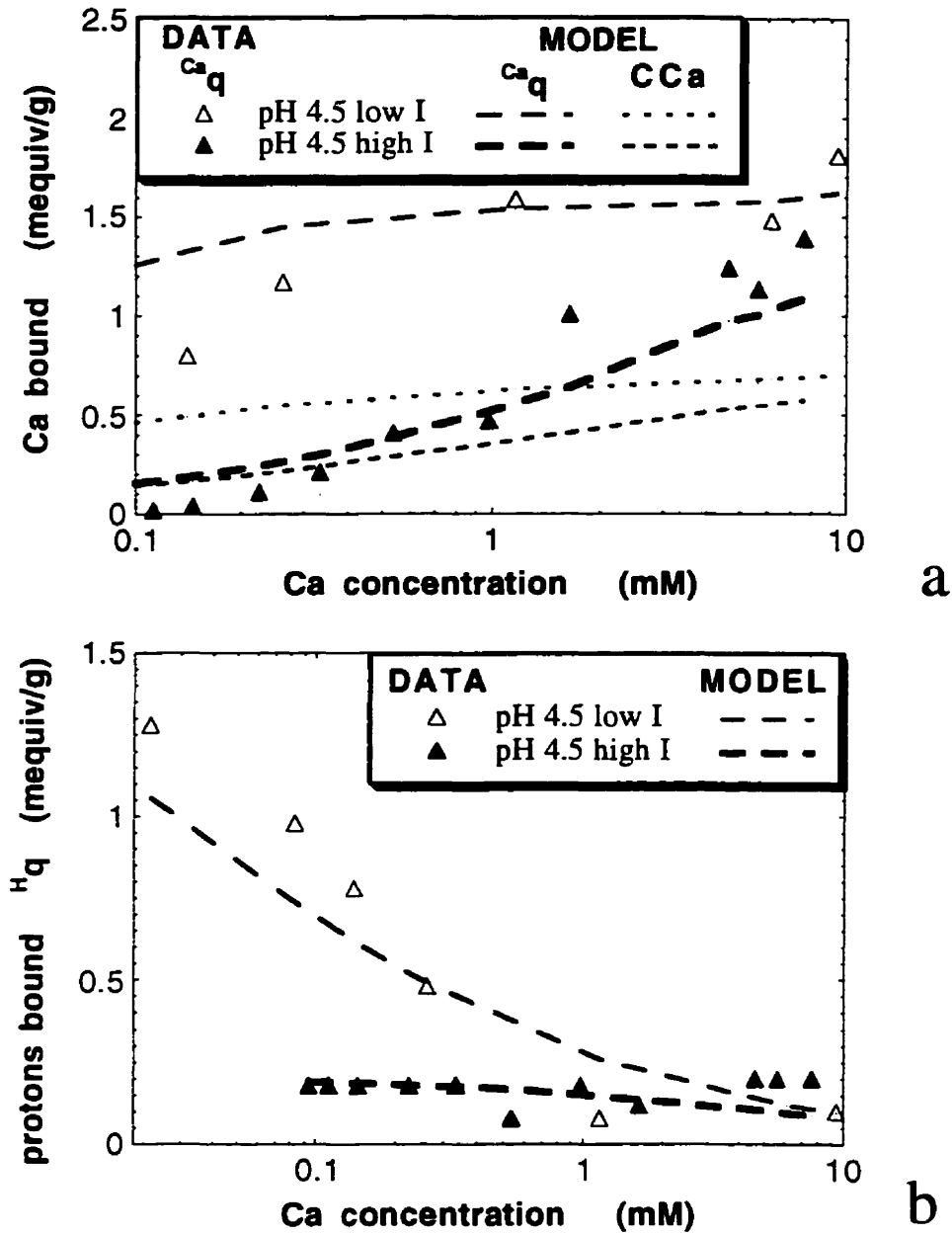


Figure 4.5.8 Calcium and proton binding by *Sargassum* biomass at different ionic strength levels and pH 4.5

(experimental data and predictions by the combined Donnan isotherm model):

- a) total (Ca_q) and covalent (CCa) calcium binding;
- b) total (H_q) and covalent (CH) proton binding.

4.5 Results & Discussion: Metal & Proton Binding at Diff. Ionic Strengths

4.5.11 Influence of Ca on Cd Binding in Di-Metal Systems

The combined Donnan-isotherm (4.5.17) and (4.5.18) with the parameters $Y_v = 1.5 \text{ mL / mequiv}$, ${}^{CCd}K = 4.9 \text{ L / mol}$ (determined for the DOSWa model in systems with Cd alone) and ${}^{CCa}K = 1.2 \text{ L/mol}$ (determined only from the data at $I \sim 100 \text{ mM}$ for Ca mono-metal systems) was used in order to predict the Cd binding in the two-metal system Ca-Cd at different ionic strength levels. The modeling errors were similar to the ones determined in the modeling of Cd binding in mono-metal systems (5.8 - 6.5 % of tC , depending on the model used): the average absolute error of Cd binding in the two-metal system was 5.8 % of the total binding capacity tC for low I and 6.7 % for $I \sim 100 \text{ mM}$. This means that the behavior of two metal systems can be predicted from one-metal systems without losing precision. Similar prediction possibilities have been shown to exist for the competition among heavy metals in Section 4.2.

As an example, Figure 4.5.9 shows the Cd binding at pH 4.5 and low I as a function of both Ca and Cd concentrations. The experimental data and an interpolated surface are depicted as a 3D plot in Figure 4.5.9a. One can see that the Cd binding is visibly reduced with the increasing Ca concentration. The same trend is reflected in Figure 4.5.9b which shows the model predictions with the DOSWa model, using the convenient combined Donnan isotherm (equation (4.5.17)). For easier quantitative evaluation of the Ca influence on the Cd binding, Figure 4.5.9c shows a series of 2D "cuts" through the 3D surface of Figure 4.5.9b at constant $[Cd]$'s. It can be seen that a 10 % reduction of the Cd binding is reached when $[Ca]$ is $\sim 5\text{-}10 \%$ of the $[Cd]$. For a 50 % reduction, $[Ca]$ has to be between 2 (for $[Cd] = 10 \text{ mM}$) and 100 (for $[Cd] = 0.001 \text{ mM}$) times higher than $[Cd]$.

Comparing the influence of Ca and Na on the Cd binding (Figures 4.5.9c and 4.5.7) one can see that a Ca concentration of $\sim 0.4 \text{ mM}$ has a similar effect as a Na concentration of $\sim 20 \text{ mM}$, for example by reducing the Cd binding at $[Cd] = 0.1 \text{ mM}$ by 50 %. As expected, the divalent ion Ca has a higher effect on the Cd binding both due to its higher electrostatic accumulation and because it partially binds covalently. Given a fixed ratio of light metal per heavy metal in solution, the influence of the light metals is more pronounced at higher concentrations because fewer free binding sites are available and ion competition is therefore more severe.

4.5 Results & Discussion: Metal & Proton Binding at Diff. Ionic Strengths

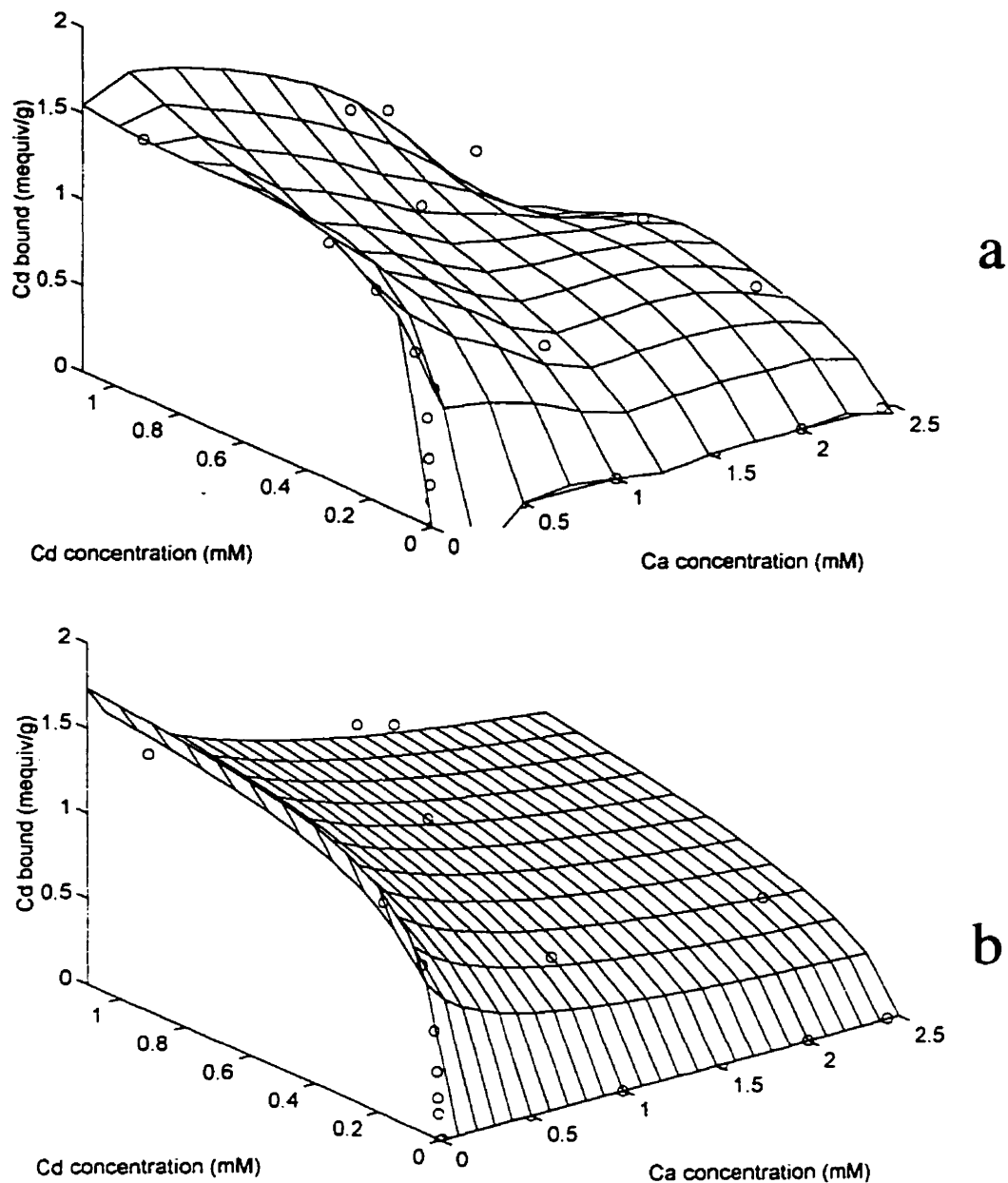


Figure 4.5.9 Cadmium binding by *Sargassum* biomass in the two-metal system Cd-Ca as a function of both metal concentrations at pH 4.5 and low ionic strength:

- a) 3D plot of metal uptake: experimental data;
- b) 3D plot of the metal binding predictions by the combined Donnan isotherm model;

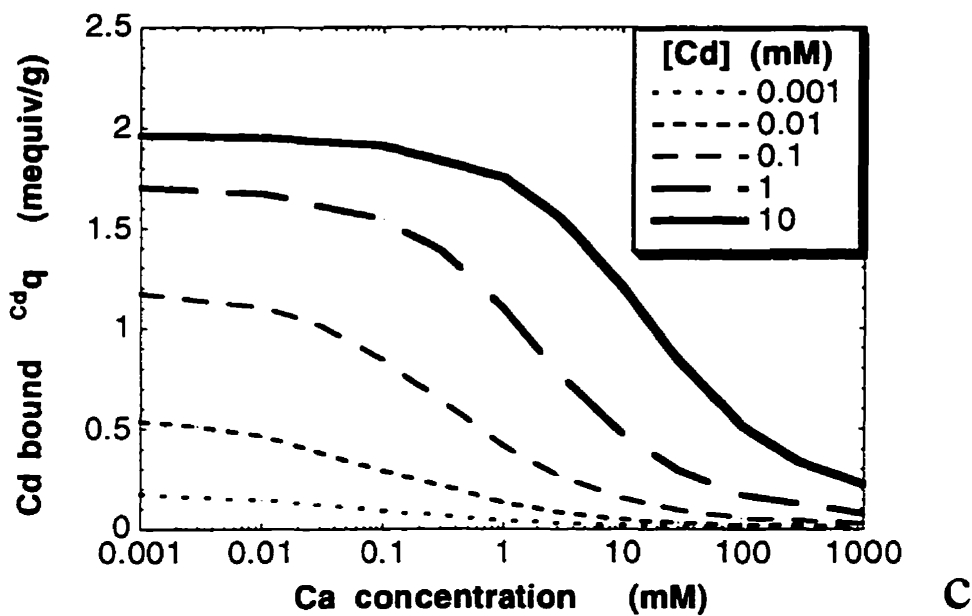


Figure 4.5.9 Cadmium binding by *Sargassum* biomass in the two-metal system Cd-Ca as a function of both metal concentrations at pH 4.5 and low ionic strength:

c) reduction of Cd binding with increasing Ca concentration; predicted by the combined Donnan isotherm model.

4.5.12 Comparison with Ca Competition Results in the Literature

Several other researchers report decreased heavy metal binding in the presence of Ca and explain this by competition for the same sorption sites (Cabaniss and Shuman, 1988; Ferguson and Bubela, 1974; Kinniburgh et al., 1996; Tipping, 1993). However, some results that differ from this observation have been described. Hering and Morel (1988) noticed practically no influence of Ca (even in large excess) on Cu binding by humic acids. Probably, the Ca concentration was still not high enough to displace Cu which is a very strongly binding ion. The Ca concentration used by these authors was just high enough to achieve occupation of all sites in mono-metal systems with Ca alone.

This corresponds to the observations of Kinniburgh et al. (1996) who noticed a significant effect of Ca and Cd binding and a smaller effect on Cu binding which corresponded to the predictions of his competitive binding model in which the constant for binding of Cu to carboxyl groups was more than 100 times larger than the respective

4.5 Results & Discussion: Metal & Proton Binding at Diff. Ionic Strengths

constant for Ca. The binding constants with respect to phenolic groups differed even more strongly.

A system with simultaneous presence of Ca and Cd (or Zn) was recently studied by Plette et al (1996) for sorption to the soil bacterium *Rhodococcus erythropolis*. The effect of Ca was opposite to that in this work: heavy metal binding was enhanced in the presence of Ca. This is all the more surprising since the Ca binding was as strong as Zn binding and even a charge reversal to a positive charge may have occurred at high Ca concentrations. The explanation given was that Ca binding to active metal binding sites may *reduce* crosslinking among those and thereby render more sites accessible. This is opposite to the effect of Ca in alginate where it is known to *increase* crosslinking. Again (see Section 4.2.1), the NICA sorption isotherm model used by those authors proved adequate at predicting metal binding at different pH values but under-predicted the proton release, probably due to the 1:1 stoichiometry assumed.

4.5.13 Comparison with Donnan Models in the Literature

Donnan models have been used extensively by the Marinsky research group (Marinsky, 1987). The focus of these works was, however, interpretation rather than prediction of proton binding at different ionic strengths.

Recently, a Donnan model has been applied for actual modeling of the ionic strength influence on proton binding to humic acids (Benedetti et al., 1996). Also very recently, an extended version of this Donnan model, including metal ion binding, was used by Kinniburgh et al. (1996). Since the model of these authors parallels the work presented here more closely than any other study, the two models are compared below.

One parallel to this work, for example, is that the total binding of a metal ion is calculated in the same way. The amount of covalent binding is added to the electrostatically bound metal, i.e. the difference between the intra-particle and bulk concentrations multiplied by the specific particle volume (equation (3.3.10)). The correlation for estimating the swelling of this particle volume was, however, the opposite: the gel volume assumed by Kinniburgh et al. (1996) and Benedetti et al. (1996) in order to achieve the best fit of the data decreased with increasing ionic strength. This is a common phenomenon in non-crosslinked polyelectrolytes: in order to equalize the osmotic potential, the gel (in which the ionic strength is higher than in the bulk) swells. This effect is more pronounced when the bulk ionic strength is low. In *Sargassum*, however, the effect is opposite to that. It was noticed in this work that, in the presence of divalent cations, swelling decreased with decreasing ionic strength. This is likely due to an increasing amount of metal ions bound which crosslink between alginate chains. Higher ionic strength leads to reduced metal

4.5 Results & Discussion: Metal & Proton Binding at Diff. Ionic Strengths

binding and consequently increased swelling. In the pH titrations described in Section 4.4 no effect of I on swelling of *Sargassum* particles was noticed. This could be caused by a mutual compensation of two opposing effects: high ionic strength reduces on the one hand the driving force for swelling (for equalization of the osmotic potential) but on the other hand raises the local pH so that more alginic acid is solubilized as Na-alginate such that the particle swells (swelling was noticed to increase with pH).

Another major difference lies in the isotherm models used for calculating the amount of covalently bound metal. The isotherm used by Kinniburgh et al. (1996) was developed by Koopal et al. (1994). In Section 4.2.1 it is compared to the isotherm model developed here. The principal difference is that Koopal's isotherm includes exponents in order to account for non-ideal behavior and site heterogeneity. This is an advantage of the isotherm used by Kinniburgh et al. (1996). But, on the other hand, it is necessary to determine many parameters in order to apply the model.

It is interesting that the intrinsic pK values for the carboxyl group protonation (2.5-3.4) determined by Benedetti et al. (1996) are close to the ones determined in Section 4.4. The model used by Kinniburgh et al. was able to predict metal binding at different pH values quite well, the amount of protons released per metal bound was, however, underestimated in some cases because the model assumed a 1:1 stoichiometry between metal ions and binding sites.

The third main difference between the models lies in how the concentration factor λ was calculated. A disadvantage of Benedetti's model is that it assumes $[Na_p] \gg [H_p]$ which makes the model less suitable for determining the actual degree of dissociation at low pH and low ionic strength. Kinniburgh's model is more comprehensive but its major drawback is the computational effort it requires: no simple iteration algorithm was developed (this is given in Figure 4.5.1 for the work presented here), let alone explicit equations like (4.5.17)-(4.5.22) and (4.5.9) in this work. Instead, for an n-metal system, it is necessary to solve $5+2n$ equations simultaneously, that is 9 equations for a two metal system. Especially when the equilibrium model is expected to be incorporated in packed bed flow through sorption models, it is of importance that the equilibrium model is simple enough in order to facilitate the necessary calculations and to save computer time.

4.5.14 Section Summary

Increasing ionic strength (as added NaNO_3) lead to a marked reduction of the binding of cadmium, calcium and protons by protonated *Sargassum* biomass. This effect was modeled by applying the Donnan theory in order to account for elevated intra-particle concentrations in the polyelectrolytic biomass particle.

It was assumed that divalent ions bind to two mono-protic acidic sites. Since the assumptions of $\text{CM}_{0.5}$ or C_2M complexes being formed agreed equally well with the experimental data it was decided to model the metal binding as $\text{CM}_{0.5}$ complexes, which rendered the formulation of an explicit multi-metal sorption isotherm model possible. The amount of covalently bound cations calculated with this isotherm was higher at a low ionic strength due to the higher intra-particle concentrations. For Ca and Cd the high concentrations of free mobile counter-ions in the particle contributed significantly to the total binding of these ions.

It was observed that *Sargassum* particle swelling was correlated with the number of free, ionized sites. The presence of heavy metal ions lead to a reduction of swelling, probably due to crosslinking effects. Different swelling correlations were used in modeling the data but a simple Donnan model which assumed a rigid, non-swelling particle yielded similarly good fit of the data as those models that incorporated swelling. The specific particle volume and the proton binding constant derived earlier from pH titrations were used to predict the binding of Cd at different ionic strength and pH levels after the binding constant for Cd was determined at one pH and one ionic strength. Similarly, the effect of ionic strength on the Ca binding was predicted. An advantage of using a linear correlation between particle swelling and the number of free sites (i.e. assuming constant volumetric charge density) is that this allowed for the derivation of an explicit sorption isotherm model that already included the Donnan model. With this combined isotherm equation, the cation binding can be calculated directly, without iterations. This model was successfully applied to predict the binding of Cd in the presence of Ca using constants that were determined in mono-metal biosorption systems.

5

SUMMARY, ORIGINAL CONTRIBUTIONS AND RECOMMENDATIONS FOR FUTURE RESEARCH

5.1 Summary

Ion exchange was established as the major mechanism in binding and desorption of metal ions on the brown alga *Sargassum*. Titrations revealed the presence of 2.1 mequiv/g of weakly acidic (carboxylic) sites which were responsible for the major part of metal binding by the biomass. Their apparent pK_a was 4.8. A strong acidic group (sulfate, apparent pK_a 2.5, 0.25 mequiv/g) contributed significantly to metal binding only at low pH. The increase of metal binding with increasing pH can be explained and modeled as decreasing competition of protons for the same binding sites.

The novel biosorption isotherm model which was derived, based on chemical equilibrium constants, considers two types of binding sites. It assumes that protons bind to one site, divalent metal ions to two sites. Both ion exchange and binding to free sites were taken into consideration. The number of constants used for each type of site is equal to the number of sorbed cation types plus one for the amount of binding sites. In order to predict both metal binding and desorption by a two site model, only two constants were necessary for each type of cation considered. The binding strength was found to decrease in the order $Cu > Cd > Zn$.

An extended version of this sorption model allowed for describing biosorption in multi-metal systems. The metal binding in two-metal systems could be predicted using the constants determined from one-metal (plus protons) systems. This means that one metal interferes with the binding of another only in so far as both ions compete for the same type of sites. It was also possible to predict binding of Cu and Zn in a pH titration where two metals were simultaneously present. The results indicated that partially selective desorption is possible when the equilibrium constants for metal ions are sufficiently different.

It was observed that increasing ionic strength (as NaNO_3) lead to a reduction of binding for H, Cd and Ca, yielding a change in apparent binding constants for these ions. In order to describe the effect of ionic strength, three different types of mathematical models were applied. A multi-component biosorption model of the type described above including one term for Na sorption, could be employed under limited conditions (for example small range of ionic strength) only, otherwise it yielded unreasonable results.

A Donnan model was coupled with the above model which was then evaluated for the local, intra-particle concentration (which is higher than the bulk concentration for cations). This lead to the determination of intrinsic binding constants that are several orders of magnitude lower than the apparent ones. The Donnan model used here is more general (does not make certain simplifying assumptions) than other Donnan models in the literature used to describe metal ion binding to organic polyelectrolytes.

Different mathematical relationships were discussed in this work in order to account for biosorption particle swelling. However, though particle swelling increased with increasing number of free sites (i.e. decreasing metal concentration, increasing pH, increasing ionic strength) it was not necessary to include swelling in the model in order to achieve a good representation of the experimental data. The advantage of adopting a linear correlation between swelling and the number of free sites is, however, that a new type of explicit multi-metal sorption isotherm model could be derived that *includes* the Donnan effect. This way it is possible to avoid iterations and calculate the metal binding directly, which makes this approach very simple and user-friendly.

Using the Gouy-Chapman model to calculate the concentrations at the interface, coupled with the Donnan model to account for charge neutrality of the particle, again in conjunction with the same isotherm, yielded as good fits as the Donnan model. However, since it is more complex than the latter one its use cannot be justified.

It was possible to use the Donnan model calibrated by pH titrations at different solution ionic strengths in order to predict the effect of ionic strength on Cd and Ca binding. The effect of Ca on Cd binding was predicted from the mono-metal systems for both ions, assuming competition for the same sites. Predictions matched well with experimental data.

5.2 Original Contributions

Biosorption Mechanism

- It was demonstrated that the biosorption mechanism in *Sargassum* is ion exchange
- Amounts and pK_a values of the two main binding sites were determined

Multi-component Biosorption Model

- A novel type of explicit multi-metal sorption isotherm model was derived, featuring ion exchange and binding to free sites, and 2 :1 stoichiometry of sites per divalent metal ion bound
- Equilibrium constants for Cd, Cu and Zn binding to the two sites were determined
- Experimental and modeling errors were quantified
- Binding of protons was modeled
- Influence of pH on metal binding (mono- and di-metal systems) was predicted
- Desorption equilibrium was predicted for various initial conditions

Polyelectrolyte Cation Binding Models

- A set of equations for using the Donnan (DO) model was derived
- A set of equations for using the Gouy - Chapman (GC) model was derived
- Explicit multi-metal sorption isotherm model including the Donnan model was derived
- Charge density of the biomass was characterized (including swelling)
- Intrinsic binding constants for biosorption of H, Cd and Ca were determined
- Contribution of electrostatic effects in cation biosorption was quantified
- Ionic strength effect on H binding was modeled (with DO and GC model)
- Effect of ionic strength on Cd and Ca binding was predicted (by DO model)
- Influence of Ca on Cd binding was predicted

5.3 Recommendations for Future Research

- biosorption of metal ions of different binding character like Ag (weak electrostatic, strong covalent binding), Al (strong electrostatic, weak covalent binding), Pb (medium electrostatic, strong covalent binding) or Au (strong electrostatic, strong covalent binding) should be considered
- it would be useful to investigate the binding stoichiometry for trivalent cations and to modify the sorption model(s) accordingly
- the model should be tested for the description of metal - ligand complex binding
- the binding mechanism(s) and the binding sites for positively charged complexes have to be elucidated
- the possible involvement of other binding groups (R-OH) at high pH may be investigated

6 REFERENCES

- Ahrland, S., Chatt, J. and Davis, N.R.** (1958) The relative affinities of ligand atoms for acceptor molecules and ions. *Quart. Revs. Chem.* 12, pp. 265-276.
- Aldor, I., Fourest, E. and Volesky, B.** (1995) Desorption of cadmium from algal biosorbent. *Can. J. Chem. Eng.* 73, pp. 516-522.
- Avery, S.V. and Tobin, J.M.** (1993) Mechanism of adsorption of hard and soft metal ions to *Saccharomyces cerevisiae* and influence of hard and soft anions. *Appl. Environ. Microbiol.* 59, pp. 2851-2856.
- Baes, C.F.J. and Mesmer, R.E.** (1976) *The Hydrolysis of Cations*. Wiley-Interscience, John Wiley & Sons, New York, pp. 1-7, 174-310, 397-419.
- Bartschat, B.M., Cabaniss, S.E. and Morel, F.M.M.** (1992) Oligoelectrolyte model for cation binding by humic substances. *Environ. Sci. Technol.* 26, pp. 284-294.
- Bell, C.F.** (1977) *Principles and Applications of Metal Chelation*. Clarendon, Oxford, UK, pp. 30-50.
- Benedetti, M.F., Milne, C.J., Kinniburgh, D.G., Van Riemsdijk, W.H. and Koopal, L.K.** (1995) Metal ion binding to humic substances: applications of the non-ideal competitive adsorption model. *Environ. Sci. Technol.* 29, pp. 446-457.
- Benedetti, M.F., Van Riemsdijk, W.H. and Koopal, L.K.** (1996) Humic substances considered as a heterogeneous Donnan gel phase. *Environ. Sci. Technol.* 30, pp. 1805-1813.
- Black, W.A.P. and Mitchell, R.L.** (1952) Trace elements in the common brown algae and in sea water. *J. Marine Biol. Assoc.* 30, pp. 575-584.

- Bold, H.C. and Wynne, M.J.** (1985) *Introduction to the Algae*. Prentice-Hall, Englewood Cliffs, N.J., pp. 389-391.
- Bower, V.E. and Bates, R.G.** (1963) Equilibrium constants for proton-transfer reactions. In: Meites, L. (Ed.), *Handbook of Analytical Chemistry*, McGraw-Hill, New York, pp. 1.20-1.27.
- Buffle, J.** (1988) *Complexation Reactions in Aquatic Systems: An Analytical Approach*. Ellis Horwood Ltd., Chichester, UK, pp. 47-72, 154-330.
- Cabaniss, S.E. and Shuman, M.S.** (1988) Copper binding by dissolved organic matter: I. Suwannee river fulvic acid equilibria. *Geochim. Cosmochim. Acta* 52, pp. 185-193.
- Cabaniss, S.E. and Morel, F.M.M.** (1989) Comment on Marinsky, J.A. and Ephraim, J. (1986): A unified physicochemical description of the protonation and metal ion complexation equilibria of natural organic acids (humic and fulvic acids). *Environ. Sci. Technol.* 23, pp. 746-747.
- Cahn, R.S. and Dermer, O.L.** (1979) *Introduction to Chemical Nomenclature*. Butterworths, London, UK, pp. 17-18.
- Chapman, V.J.** (1963) *The Marine Algae of Jamaica*. The Institute of Jamaica Science Series, No 12, Kingston, Jamaica, pp. 38-41.
- Chapman, V.J.** (1980) *Seaweeds and their Uses*. Chapman and Hall, London, UK, pp. 194-240.
- Chen, X.H., Gosset, T. and Thevenot, D.R.** (1990) Batch copper ion binding and exchange properties of peat. *Wat. Res.* 24, pp. 1463-1471.
- Chong, K.H. and Volesky, B.** (1995) Description of two-metal biosorption equilibria by Langmuir-type models. *Biotechnol. Bioeng.* 47, pp. 451-460.

- Collins, Y.E. and Stotzky, G.** (1992) Heavy metals alter the electrokinetic properties of bacteria, yeasts and clay minerals. *Appl. Environ. Microbiol.* 58, pp. 1592-1600.
- Crist, R.H., Oberholser, K., Shank, N. and Nguyen, M.** (1981) Nature of bonding between metallic ions and algal cell walls. *Environ. Sci. Technol.* 15, pp. 1212-1217.
- Crist, R.H., Oberholser, K., Schwartz, D., Marzoff, J., Ryder, D. and Crist, D.R.** (1988) Interactions of metals and protons with algae. *Environ. Sci. Technol.* 22, pp. 755-760.
- Crist, R.H., Martin, J.R., Guptill, P.W., Eslinger, J.M. and Crist, D.R.** (1990) Interactions of metals and protons with algae. 2. Ion exchange in adsorption and metal displacement by protons. *Environ. Sci. Technol.* 24, pp. 337-342.
- Crist, R.H., Oberholser, K., McGarrity, J., Crist, D.R., Johnson, J.K. and Brittsan, J.M.** (1992) Interaction of metals and protons with algae. 3. Marine algae, with emphasis on lead and aluminum. *Environ. Sci. Technol.* 26, pp. 496-502.
- Crist, R.H., Martin, J.R., Carr, D., Watson, J.R., Clarke, H.J. and Crist, D.R.** (1994) Interaction of metals and protons with algae. 4. Ion exchange vs adsorption models and a reassessment of Scatchard plots; ion-exchange rates and equilibria compared with calcium alginate. *Environ. Sci. Technol.* 28, pp. 1859-1866.
- Crittenden, J.C. and Weber, W.J.Jr.** (1978) Model for design of multicomponent adsorption systems. *J. Envir. Eng. Div. ASCE* 104, pp. 1175-1195.
- Darnall, D.W., Greene, B., Henzl, M.T., Hosea, J.M., McPherson, R.A., Sneddon, J. and Alexander, M.D.** (1986) Selective recovery of gold and other metal ions from an algal biomass. *Environ. Sci. Technol.* 20, pp. 206-208.
- Davis, J.A. and Leckie, J.O.** (1978) Effect of adsorbed complexing ligands on trace metal uptake by hydrous oxides. *Environ. Sci. Technol.* 12, pp. 1309-1315.

- de Wit, J.C.M., van Riemsdijk, W.H. and Koopal, L.K.** (1993) Proton binding to humic substances. I. Electrostatic effects. *Environ. Sci. Technol.* 27, pp. 2005-2014.
- Dean, J.A.** (1985) *Lange's Handbook of Chemistry*, McGraw-Hill, New York, pp. 3.11-3.12, 7.476-7.477.
- Dodge, J.D.** (1973) *The Fine Structure of Algal Cells*. Academic Press, London, U.K., pp. 14-45.
- Donnan, F.G.** (1911) Theorie der Membrangleichgewichte und Membranpotentiale bei Vorhandensein von nicht dialysierenden Elektrolyten. *Z. Elektroch.* 17, pp. 572-581.
- Ephraim, J., Alegret, S., Mathuthu, A., Bicking, M., Malcolm, R.L. and Marinsky, J.A.** (1986a) A united physicochemical description of the protonation and metal ion complexation equilibria of natural organic acids (humic and fulvic acids). 2. Influence of polyelectrolyte properties and functional group heterogeneity on the protonation equilibria of fulvic acid. *Environ. Sci. Technol.* 20, pp. 354-366.
- Ephraim, J. and Marinsky, J.A.** (1986b) A unified physicochemical description of the protonation and metal ion complexation equilibria of natural organic acids (humic and fulvic acids). 3. Influence of polyelectrolyte properties and functional heterogeneity on the copper ion binding equilibria in an Armandale horizons Bh fulvic acid sample. *Environ. Sci. Technol.* 20, pp. 367-376.
- EPS** (1977) *Metal Finishing Liquid Effluent Guidelines. Report EPS 1-WP-77-5*. Water Pollution Control Directorate, Environmental Protection Service, Fisheries and Environment Canada, pp. 5958-5960.
- Evans, H.T.** (1993) Ionic radii in crystals. In: Lide, D.R. (Ed.), *CRC Handbook of Chemistry and Physics*, CRC press, Boca Raton, FL, pp. 12.8-12.9.
- Evans, L.J.** (1989) Chemistry of metal retention by soils. *Environ. Sci. Technol.* 23, pp. 1046-1056.

- Ferguson, J. and Bubela, B.** (1974) The concentration of Cu (II), Pb (II), and Zn (II) from aqueous solutions by particulate algal matter. *Chem. Geol.* 13, pp. 163-186.
- Fernelius, W.C.** (1953) Nomenclature of coordination compounds and its relation to general inorganic nomenclature. In: ACS (Ed.), *Chemical Nomenclature*, American Chemical Society, Washington, DC, pp. 9-15.
- Fogler, H.S.** (1986) *Elements of Chemical Reaction Engineering*. Prentice-Hall, Englewood Cliffs, NJ, pp. 238-244.
- Fourest, E. and Volesky, B.** (1996) Contribution of sulphonate groups and alginate to heavy metal biosorption by the dry biomass of *Sargassum fluitans*. *Environ. Sci. Technol.* 30, pp. 277-282.
- Fourest, E. and Volesky, B.** (1997) Alginate properties and heavy metal biosorption by marine algae. (*personal communication*)
- Freundlich, H.** (1907) Ueber die Adsorption in Loesungen. *Z. physik. Chem.* 57, pp. 385-470.
- Fritz, W. and Schluender, E.-U.** (1974) Simultaneous adsorption equilibria of organic solutes in dilute aqueous solutions on activated carbon. *Chem. Eng. Sci.* 29, pp. 1279-1282.
- Gamble, D.S. and Schnitzer, M.** (1974) The chemistry of fulvic acid and its reactions with metal ions. In: Singer, P.C. (Ed.), *Trace Metals and Metal-Organic Interactions in Natural Waters*, Ann Arbor Science, Ann Arbor, MI, pp. 265-302.
- Gardea-Torresdey, J.L., Becker-Hapak, M.K., Hosea, J.M. and Darnall, D.W.** (1990) Effect of chemical modification of algal carboxyl groups on metal ion binding. *Environ. Sci. Technol.* 24, pp. 1372-1378.
- Glaus, M.A., Hummel, W. and Van Loon, L.R.** (1995) Stability of mixed-ligand complexes of metal ions with humic substances and low molecular weight ligands. *Environ. Sci. Technol.* 29, pp. 2150-2153.

- Gonzales-Davila, M., Santana-Casiano, J.M., Perez-Pena, J. and Millero, F.J.** (1995) Binding of Cu (II) to the surface and exudates of the alga *Dunaliella tertiolecta* in seawater. *Environ. Sci. Technol.* 29, pp. 288-301.
- Grant, G.T., Morris, E.R., Rees, D.A., Smith, P.J.C. and Thom, D.** (1973) Biological interactions between polysaccharides and divalent cations: The egg-box model. *FEBS Lett* 32, pp. 195-198.
- Greene, B., Hosea, M., McPherson, R., Henzl, M., Alexander, M.D. and Darnall, D.W.** (1986a) Interaction of Gold(I) and Gold(III) complexes with algal biomass. *Environ. Sci. Technol.* 20, pp. 627-632.
- Greene, B., Henzl, M.T., Hosea, J.M. and Darnall, D.W.** (1986b) Elimination of bicarbonate interference in the binding of U(VI) in mill-waters to freeze-dried *Chlorella vulgaris*. *Biotechnol. Bioeng.* 28, pp. 764.
- Greene, B., McPherson, R. and Darnall, D.** (1987) Algal sorbents for selective metal ion recovery. In: Patterson, J.W. and Pasino, R. (Eds.), *Metals Speciation, Separation and Recovery*, Lewis, Chelsea, MI, pp. 315-338.
- Greene, B. and Darnall, D.W.** (1988) Temperature dependence of metal ion sorption by *Spirulina*. *Biorecovery* 1, pp. 27-41.
- Haug, A.** (1961a) Dissociation of alginic acid. *Acta Chem. Scand.* 15, pp. 950-952.
- Haug, A.** (1961b) The affinity of some divalent metals to different types of alginates. *Acta Chem. Scand.* 15, pp. 1794-1795.
- Haug, A. and Smidsrod, O.** (1965) The effect of divalent metals on the properties of alginate solutions. II. Comparison of different metal ions. *Acta Chem. Scand.* 19, pp. 341-351.
- Haug, A. and Smidsrod, O.** (1970) Selectivity of some anionic polymers for divalent metal ions. *Acta Chem. Scand.* 24, pp. 843-854.

- Haug, A., Larsen, B. and Smidsrod, O.** (1974) Uronic acid sequence in alginate from different sources. *Carbohyd. Res.* 32, pp. 217-225.
- Helfferich, F.** (1962) *Ion Exchange*. McGraw-Hill, New York, pp. 72-94.
- Hering, J.G. and Morel, F.M.M.** (1988) Humic acid complexation of calcium and copper. *Environ. Sci. Technol.* 22, pp. 1234-1237.
- Hering, J.G. and Morel, F.M.M.** (1990) The kinetics of trace metal complexation: implications for metal reactivity in natural waters. In: Stumm, W. (Ed.), *Aquatic Chemical Kinetics*, Wiley Interscience, John Wiley & Sons, New York, pp. 145-171.
- Hill, C.G.Jr.** (1977) *An Introduction to Chemical Engineering Kinetics and Reactor Design*. John Wiley & Sons, New York, pp. 167-204.
- Ho, Y.S., Wase, D.A.J. and Forster, C.F.** (1995) Batch nickel removal from aqueous solution by sphagnum moss peat. *Wat. Res.* 29, pp. 1327-1332.
- Holan, Z.R., Volesky, B. and Prasetyo, I.** (1993) Biosorption of cadmium by biomass of marine algae. *Biotechnol. Bioeng.* 41, pp. 819-825.
- Holan, Z.R. and Volesky, B.** (1994) Biosorption of lead and nickel by biomass of marine algae. *Biotechnol. Bioeng.* 43, pp. 1001-1009.
- Huang, J.-P., Huang, C.P. and Morehart, A.L.** (1991a) Removal of heavy metals by fungal (*Aspergillus oryzae*) adsorption. In: Vernet, J.P. (Ed.), *Heavy Metals in the Environment*, Elsevier Science Publishers, Amsterdam, The Netherlands, pp. 329-349.
- Huang, C., Huang, C.P. and Morehart, A.L.** (1991b) Proton competition in Cu (II) adsorption by fungal mycelia. *Wat. Res.* 25, pp. 1365-1375.
- Jain, M.K. and Wagner, R.C.** (1980) *Introduction to Biological Membranes*. John Wiley & Sons, New York, pp. 196-201.

- Jang, L.K., Harpt, N., Grasmick, D., Vuong, L.N. and Geesey, G.** (1990) A two-phase model for determining the stability constants for interactions between copper and alginic acid. *J. Phys. Chem.* 94, pp. 482-488.
- Jang, L.K., Nguyen, D. and Geesey, G.G.** (1995a) Selectivity of alginate gel for Cu vs. Co. *Wat. Res.* 29, pp. 307-313.
- Jang, L.K., Nguyen, D. and Geesey, G.G.** (1995b) Effect of pH on the absorption of Cu (II) by alginate gel. *Wat. Res.* 29, pp. 315-321.
- Kaplan, D., Christiaen, D. and Arad, S.** (1987) Chelating properties of extracellular polysaccharides from *Chlorella* spp. *Appl. Env. Microbiol.* 53, pp. 2953-2956.
- Kapoor, A. and Viraraghavan, T.** (1995) Fungal biosorption - an alternative treatment option for heavy metal bearing wastewaters: A review. *Biores. Technol.* 53, pp. 195-206.
- Katchalsky, A., Cooper, R.E., Upadhyay, J. and Wassermann, A.** (1961) Counter-ion fixation in alginates. *J. Am. Chem. Soc.* 83, pp. 5198-5204.
- Kinniburgh, D.G., Milne, C.J., Benedetti, M.F., Pinheiro, J.P., Filius, J., Koopal, L.K. and Van Riemsdijk, W.H.** (1996) Metal ion binding by humic acid: Application of the NICA-Donnan model. *Environ. Sci. Technol.* 30, pp. 1687-1698.
- Kloareg, B., Demarty, M. and Mabeau, S.** (1986) Polyanionic characteristics of purified sulphated homofucans from brown algae. *Int. J. Biol. Macromol.* 8, pp. 380-386.
- Kohn, R.** (1975) Ion binding on polyuronates - alginate and pectin. *Pure Appl. Chem.* 42, pp. 371-397.
- Koopal, L.K., Van Riemsdijk, W.H., De Wit, J.C.M. and Benedetti, M.F.** (1994) Analytical isotherm equations for multicomponent adsorption to heterogeneous surfaces. *J. Coll. Int. Sci.* 166, pp. 51-60.

- Kratochvil, D., Fourest, E. and Volesky, B.** (1995) Biosorption of copper by *Sargassum fluitans* biomass in fixed-bed column. *Biotechnol. Lett.* 17, pp. 777-782.
- Kreger, D.R.** (1962) Cell Walls. In: Lewin, R.A. (Ed.), *Physiology and Biochemistry of Algae*, Academic Press, New York, pp. 315-335.
- Kuyucak, N. and Volesky, B.** (1989a) Accumulation of cobalt by marine alga. *Biotechnol. Bioeng.* 33, pp. 809-814.
- Kuyucak, N. and Volesky, B.** (1989b) Desorption of cobalt-laden algal biosorbent. *Biotechnol. Bioeng.* 33, pp. 815-822.
- Kuyucak, N. and Volesky, B.** (1989c) The mechanism of cobalt biosorption. *Biotechnol. Bioeng.* 33, pp. 823-831.
- Kuyucak, N. and Volesky, B.** (1989d) Accumulation of gold by algal biosorbent. *Biorecovery* 1, pp. 189-204.
- Kuyucak, N. and Volesky, B.** (1990a) Biosorption by algal biomass. In: Volesky, B. (Ed.), *Biosorption of Heavy Metals*, CRC Press, Boca Raton, FL, pp. 173-198.
- Kuyucak, N.** (1990b) Feasibility of biosorbents application. In: Volesky, B. (Ed.), *Biosorption of Heavy Metals*, CRC Press, Boca Raton, FL, pp. 371-378.
- Langmuir, I.** (1918) The adsorption of gases on plane surfaces of glass, mica and platinum. *J. Am. Chem. Soc.* 40, pp. 1361-1403.
- Lee, R.E.** (1989) *Phycology*. Cambridge University Press, Cambridge, UK, pp. 10-13, 34-37, 534-539, 584-599.
- Leusch, A., Holan, Z.R. and Volesky, B.** (1995) Biosorption of heavy metals (Cd, Cu, Ni, Pb, Zn) by chemically-reinforced biomass of marine algae. *J. Chem. Tech. Biotechnol.* 62, pp. 279-288.
- Leusch, A., Holan, Z.R. and Volesky, B.** (1996) Solution and particle effects on the biosorption of heavy metals by seaweed biomass. *Appl. Biochem. Biotechnol.* (in press).

- Lewin, R.A.** (1974) Biochemical Taxonomy. In: Stewart, W.D.P. (Ed.), *Algal Physiology and Biochemistry*, Blackwell Scientific Publications, Oxford, UK, pp. 1-25.
- Liapis, A.I. and Rippin, D.W.T.** (1977) A general model for the simulation of multi-component adsorption from a finite bath. *Chem. Eng. Sci.* 32, pp. 619-627.
- Lin, F.G.** (1981) *Studies of hydrogen and metal ion equilibria in polysaccharide systems - alginic acid and chondroitin sulfate*, Ph.D. thesis, SUNY Buffalo, NY.
- Lin, F.G. and Marinsky, J.A.** (1993) A Gibbs-Donnan-based interpretation of the effect of medium counterion concentration levels on the acid dissociation properties of alginic acid and chondroitin sulfate. *React. Polymers* 19, pp. 27-45.
- Lobban, C.S., Harrison, P.J. and Duncan, M.J.** (1985) *The Physiological Ecology of Seaweeds*. Cambridge University Press, Cambridge, UK, pp. 123-131.
- Macaskie, L.E., Dean, A.C.R., Cheetham, A.K., Jakeman, R.J.B. and Skarnulis, A.J.** (1987) Cadmium accumulation by a *Citrobacter* sp.: the chemical nature of the accumulated metal precipitate and its location on the bacterial cells. *J. Gen. Microbiol.* 133, pp. 539-544.
- Macaskie, L.E., Empson, R.M., Cheetham, A.K., Grey, C.P. and Skarnulis, A.J.** (1992) Uranium bioaccumulation by a *Citrobacter* sp. as a result of enzymatically mediated growth of polycrystalline HUO_2PO_4 . *Science* 257, pp. 782-784.
- Mackie, W. and Preston, R.D.** (1974) Cell wall and intercellular region polysaccharides. In: Stewart, W.D.P. (Ed.), *Algal Physiology and Biochemistry*, Blackwell Scientific Publications, Oxford, UK, pp. 40-85.
- Mann, H.** (1990) Biosorption of heavy metals by bacterial biomass. In: Volesky, B. (Ed.), *Biosorption of Heavy Metals*, CRC Press, Inc., Boca Raton, FL, pp. 93-137.
- Marcus, Y. and Kertes, A.S.** (1969) *Ion Exchange and Solvent Extraction of Metal Complexes*. Wiley Interscience, John Wiley & Sons, London, UK, pp. 10-33, 277-298, 345-351.

- Marinsky, J.A., Gupta, S. and Schindler, P.** (1982a) The interaction of Cu(II) ion with humic acid. *J. Coll. Int. Sci.* 89, pp. 401-411.
- Marinsky, J.A., Gupta, S. and Schindler, P.** (1982b) A unified physicochemical description of the equilibria encountered in humic acid gels. *J. Coll. Int. Sci.* 89, pp. 412-426.
- Marinsky, J.A. and Ephraim, J.** (1986) A unified physicochemical description of the protonation and metal ion complexation equilibria of natural organic acids (humic and fulvic acids). I. Analysis of the influence of polyelectrolyte properties on protonation equilibria in ionic media: Fundamental concepts. *Environ. Sci. Technol.* 20, pp. 349-354.
- Marinsky, J.A.** (1987) A two-phase model for the interpretation of proton and metal ion interaction with charged polyelectrolyte gels and their linear analogs. In: Stumm, W. (Ed.), *Aquatic Surface Chemistry*, Wiley Interscience, John Wiley & Sons, New York, pp. 49-81.
- May, H.** (1984) *Biosorption by Industrial Microbial Biomass*, M.Eng. thesis, McGill University, Montreal, Canada.
- Mayers, I.T. and Beveridge, T.J.** (1989) The sorption of metals to *Bacillus subtilis* walls from dilute solutions and simulated Hamilton harbour (Lake Ontario) water. *Can. J. Microbiol.* 35, pp. 764-770.
- Moe, S.T., Skjak-Braek, G., Elgsaeter, A. and Smidsrod, O.** (1993) Swelling of covalently crosslinked alginate gels: Influence of ionic solutes and nonpolar solvents. *Macromolecules* 26, pp. 3589-3597.
- Moore, J.W. and Ramamoorthy, S.** (1984) *Heavy Metals in Natural Waters*. Springer-Verlag, New York, pp. 28-57, 77-99, 182-204.
- Morel, F.M.M.** (1983) *Principles of Aquatic Chemistry*. John Wiley & Sons, New York, pp. 237-266.

- Morris, E.R., Rees, D.A. and Thom, D.** (1978) Chiroptical and stoichiometric evidence of a specific, primary dimerization process in alginate gelation. *Carbohydr. Res.* 66, pp. 145-154.
- Myers, D.** (1991) *Surfaces, Interfaces, Colloids. Principles and Applications.* VCH, Weinheim, Germany, pp. 39-67.
- Nieboer, E. and McBryde, W.A.E.** (1973) Free-energy relationships in coordination chemistry. III. A comprehensive index to complex stability. *Can. J. Chem.* 51, pp. 2512-2524.
- Nieboer, E. and Richardson, D.H.S.** (1980) The replacement of the nondescript term 'heavy metals' by a biologically and chemically significant classification of metal ions. *Environ. Poll.* 1B, pp. 3-26.
- Nordstrom, D.K. and Ball, J.W.** (1984) Chemical models, computer programs and metal complexation in natural waters. In: Kramer, C.J.M. and Duinker, J.C. (Eds.), *Complexation of Trace Metals in Natural Waters*, Nijhof/Junk, The Hague, The Netherlands, pp. 149-164.
- Nowack, B., Luetzenkirchen, J., Behra, P. and Sigg, L.** (1996) Modeling the adsorption of metal-EDTA complexes onto oxides. *Environ. Sci. Technol.* 30, pp. 2397-2405.
- O'Colla, P.S.** (1962) Mucilages. In: Lewin, R.A. (Ed.), *Physiology and Biochemistry of Algae*, Academic Press, New York, pp. 348-351.
- Pagenkopf, G.K.** (1978) *Introduction to Natural Water Chemistry.* Marcel Dekker, New York, pp. 161-167, 214-216, 220-230.
- Paskins-Hurlburt, A.J., Tanaka, Y. and Skoryna, S.C.** (1976) Isolation and metal binding properties of fucoidan. *Bot. Mar.* 19, pp. 327-328.
- Pauling, L.** (1967) *Nature of the Chemical Bond.* Cornell University Press, Ithaca, NY, pp. 49-73.

- Pearson, R.G.** (1963) Hard and soft acids and bases. *J. Am. Chem. Soc.* 85, pp. 3533-3539.
- Percival, E. and McDowell, R.H.** (1967) *Chemistry and Enzymology of Marine Algal Polysaccharides*. Academic Press, London, U.K., pp. 1-25, 53-72, 83-86, 99-126, 157-176.
- Phillips, C.S.G. and Williams, R.J.P.** (1965) *Inorganic Chemistry. Principles and Non-Metals*. Oxford University Press, New York, pp. 142-164.
- Plette, A.C.C., Benedetti, M.F. and Van Riemsdijk, W.H.** (1996) Competitive binding of protons, calcium, cadmium and zinc to isolated cell walls of a gram-positive soil bacterium. *Environ. Sci. Technol.* 30, pp. 1902-1910.
- Prasetyo, I.** (1992) *Removal of toxic metals from aqueous solutions by biosorption*, M. Eng. thesis, McGill University.
- Ramelow, G.J., Fralick, D. and Zhao, Y.** (1992) Factors affecting the uptake of aqueous metal ions by dried seaweed biomass. *Microbios* 72, pp. 81-93.
- Reddy, M.M.** (1977) Ion exchange materials in natural water systems. In: Marinsky, J.A. and Marcus, Y. (Eds.), *Ion Exchange and Solvent Extraction*, Volume 7, Marcel Dekker, New York, pp. 165-219.
- Rieger, P.H.** (1994) *Electrochemistry*, 2nd ed. Chapman & Hall, New York, pp. 59-105.
- Robinson, R.A. and Stokes, R.H.** (1959) *Electrolyte Solutions*, 2nd ed.. Butterworths, London, UK, pp. 223-252.
- Russell, J.B.** (1980) *General Chemistry*. McGraw-Hill, New York, pp. 314-316, 340-341.
- Ruthven, D.M.** (1984) *Principles of Adsorption and Adsorption Processes*. John Wiley & Sons, New York, pp. 86-123, 278-279, 124-282.

- Schecher, W.D.** (1991) *MINEQL+ : A Chemical Equilibrium Program for Personal Computers, Users Manual Version 2.22*. Environmental Research Software, Inc., Hallowell, ME.
- Schiewer, S. and Volesky, B.** (1995a) Modeling of the proton-metal ion exchange in biosorption. *Environ. Sci. Technol.* 29, pp. 3049-3058.
- Schiewer, S.; Fourest, E.; Chong, K.H. and Volesky, B.** (1995b) Ion exchange in biosorption by dried seaweed: Experiments and model predictions. In Jerez, C.A., Vargas, T., Toledo, H., Wiertz, J.T. (Eds.): *Biohydrometallurgical Processing*. Proceedings of the International Biohydrometallurgy Symposium, Vina del Mar, Chile, pp. 219-228.
- Schiewer, S. and Volesky, B.** (1995c) Mathematical evaluation of the experimental and modeling errors in biosorption. *Biotechnol. Techniques* 9, pp. 843-848.
- Schiewer, S. and Volesky, B.** (1996) Modeling of the multi-metal ion-exchange in biosorption. *Environ. Sci. Technol.* 30, pp. 2921-2927.
- Schiewer, S. and Volesky, B.** (1997a) Ionic strength and electrostatic effects in biosorption. Part 1: Proton binding models. *Environ. Sci. Technol.* (submitted May 1996).
- Schiewer, S. and Volesky, B.** (1997b) Ionic strength and electrostatic effects in biosorption. Part 2: Proton binding in *Sargassum* and Alginate. *Environ. Sci. Technol.* (submitted May 1996).
- Schiewer, S. and Volesky, B.** (1997c) Ionic strength and electrostatic effects in biosorption. Part 3: Binding of divalent cations and protons. *Environ. Sci. Technol.* (submitted August 1996).
- Schweiger, R.G.** (1962) Acetylation of alginic acid. 2: Reaction of algin acetates with calcium and other divalent ions. *J. Org. Chem.* 27, pp. 1789-1791.
- Schweiger, R.G.** (1964) Complexing of alginic acid with metal ions. *Kolloid Z.* 196, pp. 47-53.

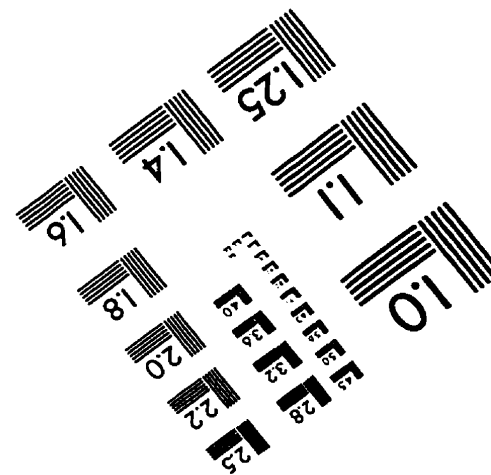
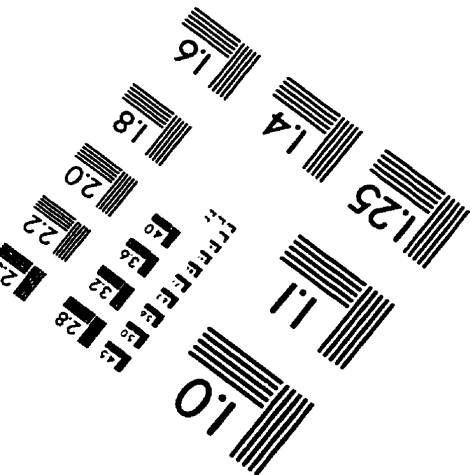
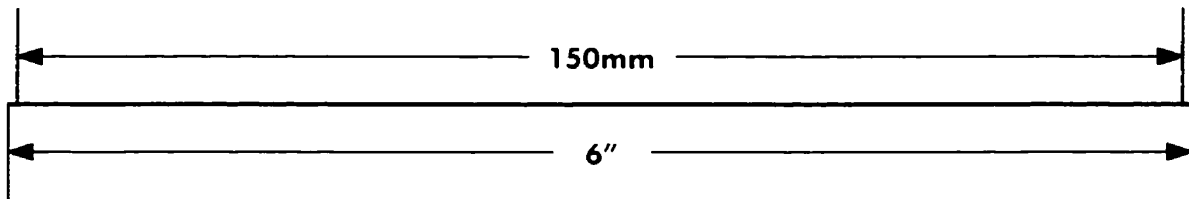
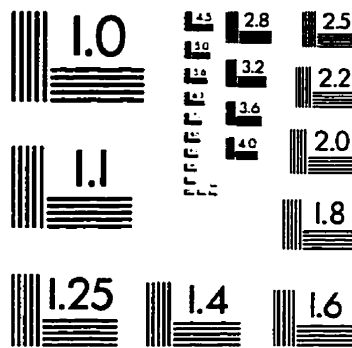
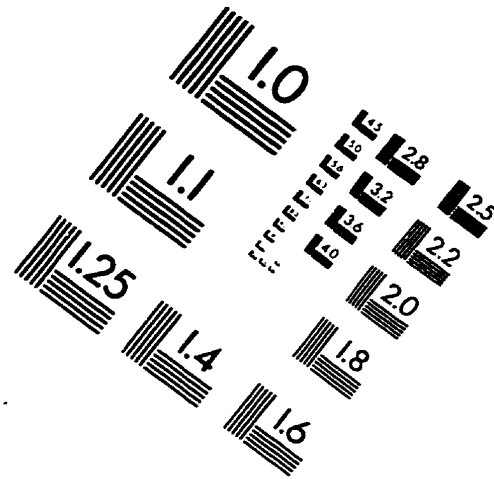
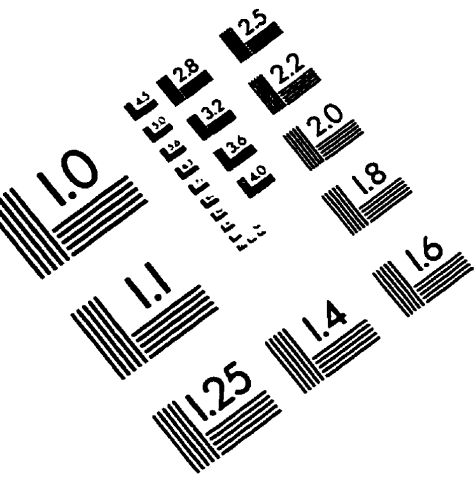
- Sears, M.E.** (1986) *Propagation and Characterization of Rhizopus Biosorbents*, Ph.D. thesis, McGill University, Montreal, Canada.
- Seki, H., Suzuki, A. and Kashiki, I.** (1990) Adsorption of lead ions on immobilized humic acid. *J. Coll. Int. Sci.* 134, pp. 59-65.
- Smidsrod, O. and Haug, A.** (1965) The effect of divalent metals on the properties of alginate solutions. I. Calcium ions. *Acta Chem. Scand.* 19, pp. 329-340.
- Smith, J.M.** (1981) *Chemical Engineering Kinetics*. McGraw-Hill, New York, pp. 310-322.
- South, G.R. and Whittick, A.** (1987) *Introduction to Phycology*. Blackwell Scientific Publications, Oxford, UK, pp. 27-28, 61-62.
- Stumm, W. and Morgan, J.J.** (1970) *Aquatic Chemistry*. John Wiley & Sons, New York, pp. 238-299, 445-513.
- Stumm, W.** (1992) *Chemistry of the Solid-Water Interface*. John Wiley & Sons, New York, pp. 43-81, 87-97.
- Stumm, W., Sigg, L. and Sulzberger, B.** (1994) The role of coordination at the surface of aquatic particles. In: Buffle, J. and De Vitre, R.R. (Eds.), *Chemical and Biological Regulation of Aquatic Systems*, Lewis Publishers, Boca Raton, FL, pp. 45-89.
- Taylor, W.R.** (1960) *Marine Algae of the Eastern Tropical and Subtropical Coasts of the Americas*. University of Michigan Press, Ann Arbor, MI, pp. 736.
- Thom, D., Grant, G.T., Morris, E.R. and Rees, D.A.** (1982) Characterisation of cation binding and gelation of polyuronates by circular dichroism. *Carbohydr. Res.* 100, pp. 29-42.

- Tien, C.T. and Huang, C.P.** (1991) Formation of surface complexes between heavy metals and sludge particles. In: Vernet, J.P. (Ed.), *Heavy metals in the environment*, Elsevier, Amsterdam, The Netherlands, pp. 295-311.
- Tipping, E., Backes, C.A. and Hurley, M.A.** (1988) The complexation of protons, aluminum and calcium by aquatic humic substances: A model incorporating binding-site heterogeneity and macroionic effects. *Wat. Res.* 22, pp. 597-611.
- Tipping, E.** (1993) Modeling the competition between alkaline earth cations and trace metal species for binding by humic substances. *Environ. Sci. Technol.* 27, pp. 520-529.
- Tobin, J.M., Cooper, D.G. and Neufeld, R.J.** (1984) Uptake of metal ions by *Rhizopus arrhizus* biomass. *Appl. Envir. Microbiol.* 47, pp. 821-824.
- Tobin, J.M.** (1986) *The Uptake of Metals by Rhizopus arrhizus Biomass*, Ph.D. thesis, McGill University, Montreal, Canada.
- Tobin, J.M., Cooper, D.G. and Neufeld, R.J.** (1987) Influence of anions on metal adsorption by *Rhizopus arrhizus* biomass. *Biotechnol. Bioeng.* 30, pp. 882-886.
- Tobin, J.M., Cooper, D.G., Neufeld, R.J.** (1988) The effects of cation competition on metal adsorption by *Rhizopus arrhizus* biomass. *Biotechnol. Bioeng.* 31, pp. 282-286.
- Treen-Sears, M.E., Volesky, B. and Neufeld, R.J.** (1984) Ion exchange / complexation of the uranyl ion by *Rhizopus* biosorbent. *Biotechnol. Bioeng.* 26, pp. 1323-1329.
- Trujillo, E.M., Jeffers, T.H., Ferguson, C. and Stevenson, H.Q.** (1991) Mathematically modeling the removal of heavy metals from wastewater using immobilized biomass. *Environ. Sci. Technol.* 25, pp. 1559-1565.
- Tsezos, M. and Volesky, B.** (1981) Biosorption of Uranium and Thorium. *Biotechnol. Bioeng.* 23, pp. 583-604.

- Tsezos, M.** (1990) Engineering aspects of metal binding by biomass. In: Ehrlich, H.L. and Brierley, C.L. (Eds.), *Microbial Mineral Recovery*, McGraw-Hill, New York, pp. 325-340.
- Turner, D.R., Whitfield, M. and Dickson, A.G.** (1981) The equilibrium speciation of dissolved components in freshwater and seawater at 25°C and 1 atm pressure. *Geochim. Cosmochim. Acta* 45, pp. 855-881.
- UNEP** (1989) *Environmental Aspects of the Metal Finishing Industry: A Technical Guide*. United Nations Environment Programme, Industry and Environment Office, Paris, pp. 19-39, 53-57.
- Van Den Hoop, M.A.G.T. and Van Leeuwen, H.P.** (1990) Study of the polyelectrolyte properties of humic acids by conductimetric titration. *Anal. Chim. Acta* 232, pp. 141-148.
- Veroy, R.L., Montano, N., Guzman, M.L.B., Laserna, E.C. and Cajipe, G.J.B.** (1980) Studies of the binding of heavy metals to algal polysaccharides from Phillipine seaweeds. I. Carrageenan and the binding of lead and cadmium. *Bot. Marina* 23, pp. 59-62.
- Volesky, B.** (1970) Algal Products. In: Zajic, J.E. (Ed.), *Properties and Products of Algae*, Plenum Press, New York, pp. 49-82.
- Volesky, B.** (1990) Removal and recovery of heavy metals by biosorption. In: Volesky, B. (Ed.), *Biosorption of Heavy Metals*, CRC Press, Boca Raton, FL, pp. 7-43.
- Volesky, B. and Prasetyo, I.** (1994) Cadmium removal in a biosorption column. *Biotechnol. Bioeng.* 43, pp. 1010-1015.
- Volesky, B. and Holan, Z.R.** (1995) Biosorption of heavy metals. *Biotechnol. Prog.* 11, pp. 235-250.
- Votruba, J.** (1994) Modeling the pH effect on biosorption of lead and cadmium. *Proceedings of IUMS Congress*, Prague, Czech Republic.

- Weber, W.J.Jr.** (1985) Adsorption theory, concepts and models. In: Slejko, F.L. (Ed.), *Adsorption technology: a step by step approach to process evaluation and application*, Marcel Dekker, New York, pp. 9-17.
- Weppen, P. and Hornburg, A.** (1995) Calorimetric studies on interactions of divalent cations and microorganisms or microbial envelopes. *Thermochim. Acta* 269/270, pp. 393-404.
- Westall, J.C.** (1987) Adsorption mechanisms in aquatic surface chemistry. In: Stumm, W. (Ed.), *Aquatic Surface Chemistry*, John Wiley & Sons, New York, pp. 3-32.
- Westall, J.C., Jones, J.D., Turner, G.D. and Zachara, J.M.** (1995) Models for association of metal ions with heterogeneous environmental sorbents: I. Complexation of Co(II) by leonardite humic acid as a function of pH and NaClO₄ concentration. *Environ. Sci. Technol.* 29, pp. 951-959.
- WHO** (1993) *Guidelines for drinking water-quality*. World Health Organization, Geneva, pp. 174-181.
- Williams, R.J.P.** (1960) The complexes of B-sub-group metals. *Proc. Chem. Soc.* pp. 20-21.
- Williams, R.J.P. and Hale, J.D.** (1966) The classification of acceptors and donors in inorganic reactions. *Structure and Bonding* 1, pp. 249-281.
- Xue, H.-B., Stumm, W. and Sigg, L.** (1988) The binding of heavy metals to algal surfaces. *Wat. Res.* 22, pp. 917-926.
- Xue, H.B. and Sigg, L.** (1990) Binding of Cu(II) to algae in a metal buffer. *Wat. Res.* 24, pp. 1129-1136.
- Yang, J. and Volesky, B.** (1996) Intraparticle diffusivity of Cd ions in a new biosorbent material. *J. Chem. Technol. Biotechnol.* (submitted)
- Yu, J.-W. and Neretnieks, I.** (1990) Single-component and multicomponent adsorption equilibria on activated carbon of methylcyclohexane, toluene and isobutyl methyl ketone. *Ind. Eng. Chem. Res.* 29, pp. 220-231.

IMAGE EVALUATION TEST TARGET (QA-3)



APPLIED IMAGE, Inc
 1653 East Main Street
 Rochester, NY 14609 USA
 Phone: 716/482-0300
 Fax: 716/288-5989

© 1993, Applied Image, Inc., All Rights Reserved